# Role of Hox Genes in Sub-circuit Diversification During Cortico-Ponto-Cerebellar Map Formation

**Inauguraldissertation**

Zur

Erlangung der Würde eines Doktors der Philosophie
vorgelegt der
Philosophisch-NaturwissenschaftlichenFakultät
der Universität Basel

Von

Upasana Maheshwari
aus Indien

2020

Genehmigt von der Philosophisch-Naturwissenschaftlichen Fakultät

auf Antrag von:

**Prof. Dr. Filippo Rijli**
(Dissertationsleiter)

**Prof. Dr. Peter Scheiffele**
(Koreferent)

Basel, 17 September, 2019

**Prof. Dr. Martin Spiess**
(Dekan)

# Table of contents

# SUMMARY

Cortical input is relayed to the cerebellum mainly via precerebellar pontine nuclei. The pontine nuclei (PN), which include pontine gray and reticulotegmental nuclei (RTN), are largest of the precerebellar nuclei providing principal input to the cerebellum. PN are hypothesized to serve as an integrator of cortical information before sending these signals to the cerebellum (Schwarz and Their, 1999). The pathway from the cerebral cortex to pontine to the cerebellum is crucial for cerebellar function and learning. It is due to their critical role in the cortico-cerebellar pathway, the pontine nuclei have received much attention. Even though the projection of cortical afferents in the PN is well established (reviewed in Kratochwil et al., 2017), the molecular mechanisms underlying this complex circuitry are poorly understood. During my Ph.D., I studied the role of Hoxa5 transcription factor in the development of pontine neurons and in formation of their input-output projections.

Cortical afferents, arising in layer V of the cerebral cortex, are mapped onto the pontine nuclei in a topographic manner (Leergaard and Bjaalie, 2007). It has been proposed that cortical afferents in the PN are organized in an inside-out fashion, matching the birthdate of PN neurons (Altman and Bayer, 1987, 1997). Earliest arriving cortico-pontine fibers grow in the core of PN where the earliest born PN neurons have settled (reviewed in Kratochwil et al., 2017). A rostro-caudal organization of cortico-pontine afferents is also suggested such that afferents arising in the visual cortical area project to the anterior, while afferents arising in the somatosensory areas are mapped to the posterior pontine nuclei (Leergaard and Bjaalie, 2007). A previous study from our lab has shown that the PN neurons born from the lower rhombic lip (lRL) of rhombomere 6 (r6) settle in anterior PN while neurons born from

rhombomere 8 settle in posterior PN (Di Meglio et al., 2013). As a result, PN neurons can be sub-divided in clusters based on their Hox expression pattern. Anterior PN neurons express *Hox2-3* genes while *Hox5* genes are expressed only in posterior PN neurons. This suggests presence of an intrinsic topographic organization in the PN based on the rostro-caudal origin or *Hox* expression of PN neurons. *Hox* genes are known to influence the topographic organization as well as input-output connectivity of several nuclei in the hindbrain and spinal cord (Bechara et al., 2016; Karmakar et al., 2017; Philippidou and Dasen, 2013). In my thesis, I therefore focused on investigating the role of *Hox5* genes, expressed in posterior PN neurons, in the formation of topographic cortico-pontine circuits.

We have identified role of *Hoxa5* gene in defining the position of PN neurons and orchestrating somatosensory specific input connectivity of the PN neurons. Using mouse genetics and *in-utero* electroporation as a tool for embryonic gene manipulation, we show that *Hoxa5* overexpression leads to change in position of PN neuron towards posterior PN. This is a result of downregulation of *Unc5B*, a repulsive cue to Netrin, upon ectopic expression of Hoxa5 in migrating PN neurons. The positioning of PN neurons toward posterior PN enables them to receive somatosensory specific cortical input. By using trans-synaptic rabies virus tracing technique, we could also show that *Hoxa5* enables PN neuron to receive or attract somatosensory input and avoid visual input from the cerebral cortex irrespective of the PN neuron position.

In this thesis, I have also investigated the molecular basis of PN connectivity with the cerebellum. While cortical inputs are mapped onto PN in a topographic manner, the projections from pontine to the cerebellum are present in a fractured map (Leergaard et al.,

2006). How continuous cortical maps are transformed to fractured maps in the cerebellum remains unanswered. We hypothesize that the combinatorial expression of Hox genes in PN neurons underlies their ability to project to different parts of the cerebellum. A PN neuron is more likely to express a combination of several *Hox* genes as we move from the rostral to the caudal part of the PN. To address this question, we used mouse genetics to identify neurons in anterior PN neuron subsets and found that these neurons primarily project to the paraflocculus, a lobule known for its role in the visual system (reviewed in Kheradmand and Zee, 2011), while *Hoxa5* positive posterior PN neurons project to several lobules of cerebellum concerned with processing of somatosensory information (Leergaard et al., 2006). Thus, the output connectivity of PN neurons also matches their input connectivity. However, we still do not understand the role of individual Hox genes in shaping the ponto-cerebellar projections. The findings presented in this thesis will serve as a basis to understand involvement of Hox genes in fracturing of the information between cortex and the cerebellum.

As a whole, this thesis highlights the role of *Hoxa5* gene in orchestrating the topographic input connectivity of pontine nuclei by defining the position of pontine neurons as well as by providing cues to somatosensory cortical afferents for targeting the PN. It also provides basis to understand the role of Hox genes in ponto-cerebellar connectivity.

# ABBREVIATIONS

| | |
|---|---|
| 3-D | 3-Dimensional |
| 4C | Circular chromosome conformation capture |
| IV | Tochlear nerve |
| V | Trigeminal nerve |
| VI | Abducens nerve |
| VII | Facial nerve |
| IX | Glossopharyngeal nerve |
| X | Vagus nerve |
| XI | Accessory nerve |
| XII | Hypoglossal nerve |
| A-P | Antero-Posterior |
| AES | anterior extramural stream |
| ANT-C | Antennapedia complex |
| AVCN | Antero-Ventral cochlear nucleus |
| bHLH | basic helix-loop-helix |
| BMP | Bone morphogenetic protein |
| BPN | Basal pontine nucleus |
| BX-C | Bithorax complex |
| ChIP | Chromatin Immunoprecipitation |
| CNS | central nervous system |
| COP | Copula |
| CRABP | Cellular retinoic acid binding protein |
| CST | cortico-spinal tract |
| CVA | Contralateral vestibuloacoustic |
| D-V | Dorso-Ventral |
| DCC | Deleted in colorectal cancer |
| dPrV | dorsal Principal trigeminal nucleus |
| E | embryonic day |
| ECN | External Cuneate Nuclei |
| FACS | Fluorescence Activated Cell Sorting |
| FC | fold change |
| FDR | false discovery rate corrected |
| FGF | fibroblast growth factor |
| FISH | fluorescent *in situ* hybridization |
| FL | Floculus |
| FN | Facial nucleus |
| GDNF | Glial-derived neurotrophic factor |
| GFP | green fluorescent protein |
| GO | gene ontology |
| HGF | Hepatocyte growth factor |

| | |
|---|---|
| IO | inferior olivary complex |
| IRES | internal ribosome entry site |
| lRL | lower Rhombic Lip |
| LRN | Lateral Reticular Nuclei |
| M-L | medio-lateral |
| MHB | midbrain-hindbrain boundary |
| MN | Motor neurons |
| miRNA | micro-RNA |
| NA | numerical aperture |
| nls | nuclear localisation sequence |
| P | postnatal day |
| PcG | polycomb group |
| PES | posterior extramural stream |
| PF | Paraflocculus |
| RALDH2 | Retinaldehyde dehydrogenase 2 |
| RFP | red fluorescent protein |
| PG | Paralogous Group |
| PGN | pontine gray nucleus |
| PML | paramedian lobule |
| PN | Pontine nuclei |
| PVCN | posterior-ventral cochlear nucleus |
| qPCR | quantitative PCR |
| r | rhombomere |
| RA | retinoic acid |
| RARE | retinoic acid responsive element |
| RAR | Retinoic acid receptor |
| Rbp4 | retinol binding protein 4 |
| RL | rhombic lip |
| RT | reverse transcription |
| RTN | Reticulotegmental nuclei |
| RXR | Retinoid receptor |
| S1 | primary somatosensory cortex |
| SL | simple lobule |
| SHH | sonic hedgehog |
| Tcf | T cell factor |
| TGF | transforming growth factor |
| TrxG | trithorax |
| V1 | primary visual cortex |
| vPrV | ventral principal trigeminal nucleus |
| vs | versus |

# CHAPTER 1: INTRODUCTION

## 1.1 Development of the Mammalian Nervous System

The mammalian nervous system is derived from monolayer of uniform neuroepithelial cells, the neural plate. Through a process called neurulation, the cells in the neural plate give rise to the neural tube. The caudal region of the neural tube gives rise to the spinal cord, while the rostral region becomes the brain (Figure 1A-C). Early development of the nervous system is coupled with rapid cell proliferation. Proliferation in the anterior part of the neural tube results in a series of constrictions, subdividing the anterior part in three brain vesicles, the forebrain (prosencephalic), the midbrain (mesencephalic) and the hindbrain (rhombencephalic) vesicle. Later, further subdivisions occur mostly in the hindbrain, where a series of segment like swelling or the rhombomeres are formed, playing an important role in the further development of hindbrain (Principles of neural science, V edition).

Secreted signals or morphogens from tissues flanking the neural tube, are among the first factors involved in the establishment of the antero-posterior axis of the neural tube. Wnt, FGF and RA constitutes the main signaling pathways in this category. The anterior neural tube is exposed to low Wnt signaling activity, while the caudal region is exposed to higher Wnt activity giving an initial rostro-caudal identity to the neural tube (Kiecker and Niehrs, 2001). Later, FGF secreted by specialized anterior cells patterns the telencephalon, while RA together with FGF, patterns the hindbrain and spinal cord. Together with these factors, signals originating within the neural tube, especially Shh, direct cells in neural compartments to acquire diverse neuronal fates and identities across the rostro-caudal axis. Expression of transcription factors such as Otx2 in the forebrain and midbrain, and Gbx2 in the hindbrain

is also instrumental in establishing the positional identity in the developing nervous system (Figure 1D). Wnt, BMPs and Shh also play a critical role in establishment of the dorso-ventral axis, especially in the spinal cord.

The neural tube generates a large number of distinct neurons and non-neuronal cell types or glia. All neurons and glia are generated from a proliferative layer of cells lining the lumen of the neural tube, the ventricular zone (Davis and Temple, 1994). Cellular diversity is a remarkable feature of the nervous system structure. There are thousands of distinct neuronal and glial cell types. This complexity excludes the existence of a single "master gene" responsible for the entire gene expression program leading to the many differentiated phenotypes. Rather, the combinatorial action of numerous transcription factors is required for the development and function of the nervous system. The development of the nervous system requires tightly controlled expression of transcription factors and their target genes.

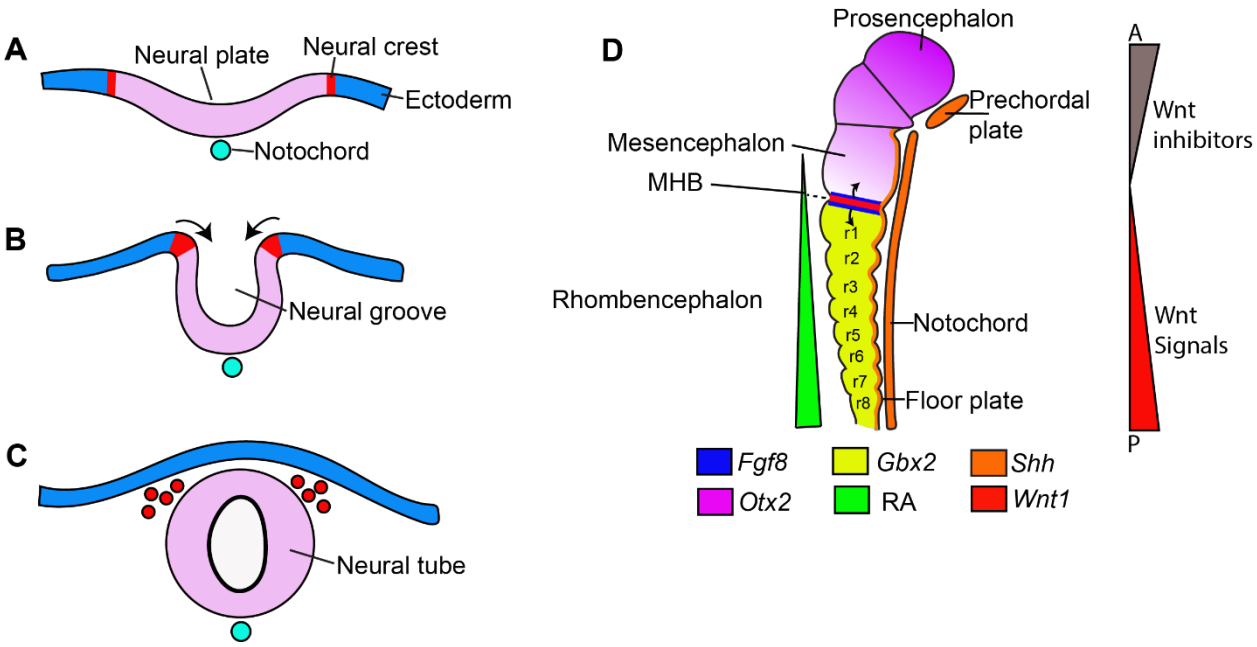


**Figure 1: Development of the nervous system**. Schematic illustrations to show the formation of neural tube early in embryogenesis. (A) Ectoderm gives rise to the neural plate (pink), which is separated from the ectodermal tissue (blue) by neural place border or future

neural crest (red). (B) The neural plate bends at its midline, with the two ends converging together to form the neural groove. (C) The closure of neural tube disconnects the neural crest from the ectodermal tissue. Neural tube lies over notochord (cyan). (D) Schematic illustration to show the expression pattern of various signaling molecules involved in early development of the anterior neural tube. MHB – midbrain-hindbrain boundary, A – anterior, P – posterior. (Figure adapted from Principles of neural science, V edition, Molecular and Developmental Biology (BIOL3530), Frank and Donenfeld, 2019).

A remarkable feature of the CNS development is a timely switch from neurogenesis to gliogenesis. Progenitors in CNS gives rise to neurons and then later during development, switch their fate to then generate glia (Alvarez-Buylla, 2001; Fishell and Kriegstein, 2003; Götz and Huttner, 2005). A timely switch from neurogenesis to gliogenesis is important for normal neural circuit formation and brain development. Several transcription factors, including basic-Helix-Loop-Helix (bHLH) factors, have been identified as key determinants of neural progenitor fate. Neural fate is controlled by proneural bHLH genes like *Ascl1* and *Neurog 2*, whereas oligodentrocyte and astrocytic fate is determined by *Olig2* and *Hes1* respectively (Reviewed in Kageyama et al., 2018). Defects in proliferation have also been reported in mice mutant for transcription factor Pax6 (Arai et al., 2005), Lhx2 (Porter et al., 1997), and Foxg1 (Hanashima et al., 2002). Apart from these, several other transcription factors have also been identified for their roles in maintaining neural proliferation, promoting neurogenesis or astrogliogenesis. However, the molecular mechanism underlying the activity or spatial-temporal regulation of expression of these factors is still not completely understood.

## 1.2 Development of Mammalian Hindbrain

Hindbrain is a key centre in the CNS comprising of several neural assemblies that control physiological processes like respiration, circulation, and motor coordination. Hindbrain also gives rise to different streams of cranial neural crest cells giving rise to cranial sensory ganglia, schwann cells and most of the cranial skeleton (Koentges and Matsuoka, 2002; Le Douaris and Kalcheim, 1999). The embryonic hindbrain is divided into eight segmented regions called the rhombomeres (r) (Lumsden and Krumlauf, 1996). The most rostral rhombomere, r1, shares a border with the midbrain in a region called the midbrain-hindbrain boundary (MHB) while the most posterior rhombomere, r8, shares a boundary with the anterior spinal cord. Each rhombomere has a unique gene expression pattern, critical for determining region-specific cell fates. Rhombomeres can be observed as early as neural tube closure, with r4 territory appearing first (Maves et al., 2002). The presumptive r4 then acts as a local organizing centre, signaling to adjacent territories and initiating a molecular cascade leading to specification of adjacent rhombomeric segments (Figure 3A). During the process of rhombomere specification, distinct physical boundaries appear to separate molecularly and neuroanatomically distinct segments. Cells from one rhombomeric origin rarely crosses the boundary to mingle with cells of other adjacent rhombomeres (Fraser et al., 1990; Guthrie et al., 1991). The process of boundary formation is regulated by repulsive interactions between cells of adjacent compartments, based on the expression of respective cell adhesion molecules (Wizenmann and Lumsden, 1997; Xu et al., 1999; Cooke et al., 2001; Cooke et al., 2005). Interactions between adjacent segments induces the establishment of boundary cells (Guthrie and Lumsden, 1991). These are specialized cells, distinguishable from other non-boundary cells of rhombomeres based on their morphology and gene

expression (Heyman et al., 1995). Unlike non-boundary cells, these cells have reduced proliferative capacity (Guthrie et al., 1991). The segment-restricted expression of some Notch pathway components in the hindbrain (Pasini et al. 2001, Prince et al. 2001) raises the possibility that Notch activation has roles in segmental patterning. Sustained expression of the Notch pathway is required to maintain boundary cells by inhibiting premature neuronal differentiation (Cheng et al., 2004). Finally, boundary cells are required to inhibit the mixing of cells between adjacent rhombomeres and to act as local signaling centers aiding to establish segmental neuronal organization of the hindbrain. The segmentation of the hindbrain is relevant for the formation of distinct structures as it enables every rhombomere to respond to environmental stimuli in a unique manner. Individual rhombomeres also act as signaling centers that influence their neighboring rhombomeres. Furthermore, proper development of other structures like cranial neural crest cells, which are relevant for head development, are critically dependent on rhombomere formation (Tumpel et al., 2009).

### 1.2.1 Hox Transcription factors and their role in hindbrain development

*Hox* genes are a subset of homeobox genes that code for homeodomain transcription factors well known for their conserved role in regionalization of the body plan along the antero-posterior axis. Hox genes are early players in initiating a cascade of interactions that enable the development of morphologically distinct regions in a segmented animal. *Hox* genes were first identified in Drosophila (Bridges and Morgan, 1923), following observation of two mutations: mutation in the *Antennapedia* gene resulting in the transformation of antenna to limbs and the *Bithorax* mutation resulting in the transformation of haltere to wing. These transformations were called homeotic transformations due to the change of one body structure to another (Bateson, 1984). Subsequently, *Hox* genes were identified as “homeotic

selector gene" for their critical role in identity specification of each segment in Drosophila. In Drosophila, *Hox* genes are present in two clusters, the Antennapedia complex with 5 homeobox genes (*lab* – Labial, *Pb* – Proboscipedia, *Dfd* – Deformed, *Scr* – Sex combs reduced, and *Antp* – Antennapedia), and the Bithorax complex with 3 homeobox genes (*Ubx* – Ultrabithorax, *Abd-A* – Abdominal-A, and *Abd-B* – Abdominal-B) (Kaufman et al., 1980; Lewis, 1978; Lewis et al., 1980). Hox genes follow colinear expression patterns, whereby the expression domains along the antero-posterior axis mirror the order of the genes within the Hox cluster (Figure 2) (Lewis, 1978; Akam, 1987; Harding et al., 1985).

Following genome duplication events during evolution, *Hox* genes are present in 4 clusters in most vertebrates (reviewed in Duboule, 1992), except teleost fishes that have seven or eight Hox clusters (Hurley et al., 2005). The Hox genes are further arranged in 13 paralog groups, with no one cluster retaining all 13 paralogs (Figure 2). Basic genome organization of mouse and Drosophila Hox genes share some common features, particularly the principle of spatial collinearity, which is followed by mouse Hox genes as well (Graham et al., 1989). The paralog groups 1-8 are closely related to the Antennapedia complex, while groups 9-13 are related to the Bithorax complex. However, the presence of overlapping sets of Hox genes, or the paralogue groups in vertebrates suggest that complex morphological features in vertebrates could be a product of combinatorial expression of genes in the four Hox clusters. Presence of multiple Hox genes in each segment in vertebrates also suggests the possibility of redundancy.

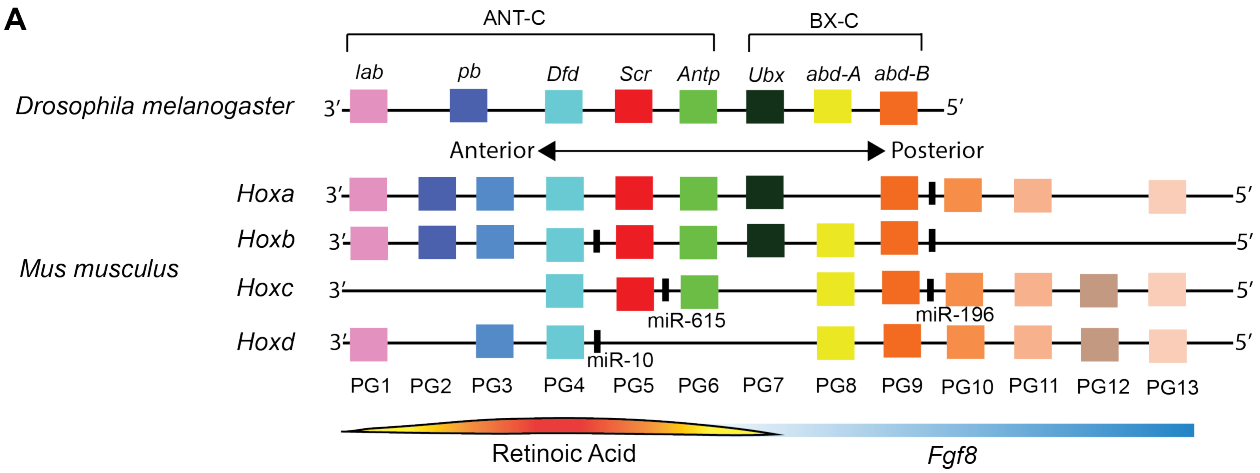


**Figure 2: Organization and regulation of *Hox* genes**. (A) Expression domains of the individual *Hox* genes within the Antennapedia (ANT-C) and Bithorax cluster (BX-C) along the anteroposterior axis of the *Drosophila* (top). Expression domains of individual *Hox* genes in the 4 Hox clusters present along the anteroposterior axis of the mouse (Bottom). The *Hox* gene organization along the chromosome, as well as their order of expression along the anteroposterior axis display collinearity between mouse and *Drosophila*. Also depicted is the position of several miRNAs within the Hox cluster and gradients of the expression domain of retinoic acid and FGF, critical for establishing Hox gene expression during early development. (Figure adapted from Mallo and Alonso, 2013; Philippidou and Dasen, 2013)

In vertebrates, the identity of each rhombomeric segment is tightly linked to *Hox* gene expression (Keynes and Krumlauf, 1994; Lumsden and Krumlauf 1996). Apart from r1, all other rhombomeres show nested expression of Hox genes. Genes of paralogue groups 1-5 have anterior boundaries that map to junctions between rhombomeres (Figure 3) (Hunt et al., 1991; Wilkinson et al., 1989; Tümpel et al., 2009). Hox genes display dynamic expressions during development of the vertebrate hindbrain and their expression can also vary in a segment-specific manner. During the early stages of segment formation, both *Hoxa1* and *Hoxb1* are expressed up to the presumptive r3/r4 boundary. However, shortly afterwards, the expression of *Hoxa1* is downregulated while *Hoxb1* expression becomes restricted to r4. The A-P boundary of *Hoxb2* expression maps to the r2/r3 junction, *Hoxb3* maps to the r4/r5 junction, *Hoxb4* maps to the r6/r7 junction and *Hoxb5* maps to the r7/r8

junction. Genes within a paralogue group mostly have same boundaries of expression along the A-P axis. Unlike *Hoxb2*, the expression of *Hoxa2* extends to the r1/r2 boundary. Apart from providing an identity to a segment, Hox genes also control programs of cell-autonomous gene expression and morphogenesis characteristics of a rhombomere, well before rhombomere segmentation is complete (Guthrie et al., 1992; Krumlauf et al., 1993).

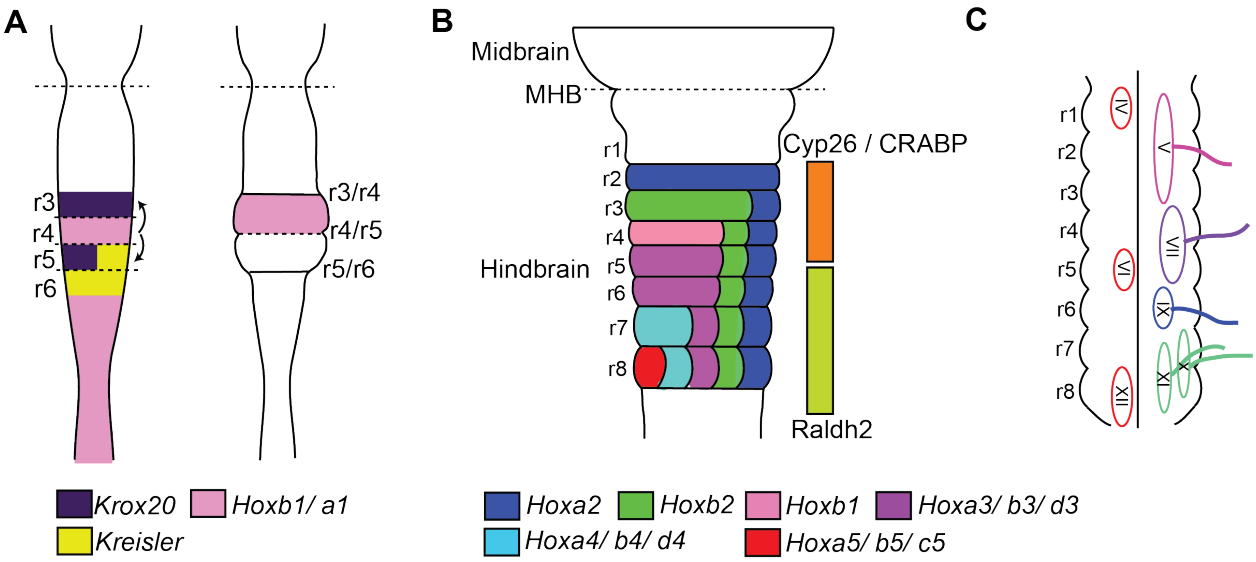


**Figure 3: Patterning the hindbrain**: (A) Schematic illustration to show the initial steps of rhombomere formation. Transient expression of Krox20 in r3, r5 and Kreisler in r5, r6 helps in establishing Hoxb1 expression in presumptive r4. The presumptive r4 then acts as a local organizing centre, signaling to adjacent territories and initiating a molecular cascade leading to specification of adjacent rhombomeric segments. (B) Schematic illustration to show nested expression of Hox genes in rhombomeres along the anteroposterior axis. Expression domains of Raldh2 and Cyp26 are also depicted. (C) Schematic illustration showing the rhombomeric origin of different hindbrain motor nuclei. IV- Trochlear, V- trigeminal, VI- abducens, VII- facial, IX- glossopharyngeal, X- vagus, XI- accessory, XII- hypoglossal. (Figure adapted from Guthrie, 1996; Glover et al., 2006; Philippidou and Dasen, 2013)

Analysis of phenotypes arising from loss- and gain-of-function of Hox genes in several species provided support for the function of Hox genes in regulating the segmental identity of rhombomeres. In *Hoxa1* mutant, r5 is lost and there is a fusion of r4 and r6, suggesting a

role of *Hoxa1* in maintaining r5 (Carpenter et al., 1993; Mark et al., 1993). In *Hoxb1* mutant, r4 adopts an r2 like identity (Studer et al., 1996). In *Hoxa1*/*Hoxb1* compound mutant, cells in the presumptive r4 fail to enter a segmental identity (Studer et al., 1998; Rossel and Capecchi, 1999). Ectopic expression of *Hoxa2* or *Hoxb2* leads to the transformation of r2 into an r4 identity (Zhang et al., 1994). *Hoxa2* is the only PG2 member expressed in r2 and is required for maintaining r2 identity, while *Hoxa2* and *Hoxb2* together are expressed in r3-r8. *Hoxa2* regulates the size of r3 and *Hoxb2* contributes towards maintaining r4 identity. To summarize, Hox genes are instrumental in specifying the segmental identity.

### 1.2.2 Establishing Hox expression in the hindbrain

It is important to precisely control the temporal and spatial expression of Hox genes to regulate the segmental identity of the vertebrate hindbrain. Several signaling pathways and transcription factors have been identified to regulate the expression of Hox genes throughout the hindbrain or more locally in some specific segments. Recently, Hox specific miRNAs have been identified adding another level to the regulation of Hox expression.

**Retinoic acid signaling**

Retinoic acid (RA) signaling is well known for its role in early Hox expression and hindbrain patterning (Gavalas and Krumlauf, 2000). Excess or reduced amounts of RA during early hindbrain patterning have severe consequences (Kessel and Gruss, 1991). Excessive RA during early embryogenesis results in the expansion of posterior hindbrain at the expense of anterior hindbrain which appears to be reduced. Conversely, lack of or reduced RA results in the expansion of anterior hindbrain at the expense of posterior hindbrain. In either case, abnormalities observed in the hindbrain patterning are a result of mis expressed 3' Hox genes (Morris-Kay et al., 1991; Marshall et al., 1992; Dupe and Lumsden, 2001). Cell culture

experiment demonstrated that genes in the 3' end of the Hox cluster respond rapidly to RA signaling while genes in the more 5' position respond slowly. Genes' response to RA can be directly mediated through retinoic acid response elements (RARE) (Gould et al., 1998; Marshall et al., 1994; Packer et al. 1998; Studer et al., 1998; Zhang et al., 2000). RAREs are bound by heterodimers of retinoid X receptor (RXR) and RA receptor (RAR). Mutations in RAREs can lead to diminished or complete absence of the neural expression of targeted Hox gene, suggesting that RAREs play a critical role in RA mediated expression in the CNS.

Spatial and temporal regulation of Hox expression by retinoic acid can be explained on the basis of synthesis and degradation of RA in the hindbrain (Figure 3B) (Neiderreither and Dollè, 2008). The relative levels of RA vary along the A-P axis of the hindbrain with higher RA levels in the posterior hindbrain. This is a result of the spatial availability of RA synthesis enzyme, Retinaldehyde dehydrogenase 2 (Raldh2) (Neiderreither et al., 1997). Raldh2 is expressed in somites flanking the posterior hindbrain. As the embryogenesis advances, the levels of RA in the hindbrain goes down. This is also regulated by members of the Cyp26 family, which degrade retinoids in the anterior hindbrain (Abu-abed et al., 2001; Sakai et al., 2001).

**Fibroblast growth factor signaling**

Fibroblast growth factor (FGF) signaling plays an important role in early segmentation of the hindbrain by initiating the expression of Hox genes. Exogenous FGF can lead to upregulation of posteriorly expressed *Hox* genes (Ruiz-i-Altaba and Melton, 1989). Conversely, reduced FGF signaling can result in the posteriorization of Hox gene expression (Godsave and Durston, 1997). In Zebrafish, *Fgf3* and *Fgf8* are transiently expressed in the hindbrain (Maves et al., 2002; Walshe et al., 2002). When the rhombomeres are formed, expression of *Fgf3* becomes restricted to the presumptive r4 territory while the expression of *Fgf8* is downregulated in this region. *Fgf8* expression is observed later at the midbrain-hindbrain boundary (Crossley and Martin, 1995) where it acts as a negative regulator of *Hoxa2*, thus establishing an anterior limit for *Hoxa2* at the r1/r2 border (Irving and Mason, 2000). Reduction in FGF signaling during early embryogenesis in zebra fish leads to the downregulation of *Hoxa2* expression while *Hoxb1* expression goes down (Walshe et al., 2002). During later stages of embryogenesis, FGF signaling is instrumental in establishing the expression of 5' Hox genes in the spinal cord (Bel-Vialar et al., 2002). This suggests that FGF signaling acts reciprocally to RA signaling by activating Hox expression in the spinal cord.

***Kreisler* (*Kr*)**

The *Kr* gene encodes for KRML1 protein, a member of MafB family. The gene is expressed transiently between E8.0 and E9.5. It is strongly expressed in r5 and r6 with a rostral limit at the r4/r5 boundary and a caudal limit close to the r6/r7 boundary (Cordes and Barsh, 1994). In *Kr* embryos, the caudal border of the *Hoxb1* expression, normally at r4/r5, extends posteriorly while anterior borders of *Hoxb3*, normally at r4/r5 and *Hoxb4*, normally at r6/r7, are poorly defined, suggesting that these rhombomeres fail to form and acquire an r4 like

identity (McKay et al., 1994; Frohman et al., 1993; Manzanares et al., 1999 and Giudicelli et al., 2003). Conversely, ectopic expression of *Kr* in r3 results in induced expression of *Hoxa3* and *Hoxb3* in r3, suggesting the transformation of r3 into an r5 like identity (Theil et al., 2002).

***Krox20***

*Krox20* is a Zinc-finger transcription factor expressed transiently in the presumptive r3 and r5. After rhombomeres are formed, *Krox20* is sequentially downregulated in r3 and then in r5 (Wilkinson et al., 1989; Nieto et al., 1991). In the absence of *Krox20*, the r3 and r5 cells are formed initially but they fail to maintain their identity (Schneider-Maunoury et al., 1997; Voiculescu et al., 2001). Krox20 can directly bind to the murine enhancers of *Hoxa2* (Nonchev et al., 1996), *Hoxb2* (Sham et al., 1993; Vesque et al., 1996) and *Hoxb3* (Manzanares et al., 2002). Krox20 dependent enhancers derive expression of *Hoxa2* and *Hoxb2* in r3 and r5. Regulation of *Hoxb3* in r5 requires both Krox20 and KRML1. *Krox20* was also found to regulate the expression of *EphA4* in r3 and r5 (Theil et al., 1998). It is possible that the cells of r3 and r5 in *Krox20* mutant switch their adhesive properties and therefore intermingle with the cells of adjacent rhombomeres. *Krox20* can also repress the expression of *Hoxb1* in r3 and r5, thereby helping in establishing *Hoxb1* expression in r4 (Garcia-Dominguez et al., 2006). All these studies suggest a critical role of *Krox20* in regulating *Hox* genes required for maintaining r3 and r5 identities.

**Auto and cross-regulatory interactions between *Hox* genes**

The early signaling pathways (RA, FGFs) and transcription factors (Kreisler, Krox20) regulating the expression of Hox genes are transiently present, suggesting that other mechanisms are required to maintain or stabilize the expression patterns of Hox genes.

Mechanisms involving Polycomb and trithorax mediated epigenetic changes in chromatin have been postulated to be important in vertebrate *Hox* regulation. Polycomb group (PcG) proteins are negative regulators of Hox gene expression that mediate their effect by deposition of the H3K27me3 mark (Margueron and Reinberg, 2011). Mutations in PcG lead to loss of spatial restriction of *Hox* gene expression with posterior *Hox* genes becoming active in more anterior parts of the embryo (Di Meglio et al., 2013; Moazed and O'Farrell, 1992). Trithorax group proteins methylate H3K4 leading to its trimethylation, a hallmark of active genes. This group therefore counteracts the repressive function of PcG, leading to stable activation of genes (Geisler and Paro, 2015). *Hox* genes can, however, show a surprising degree of auto and cross-regulation between themselves as an important mechanism for maintaining segmentally restricted expression (Pöpperl et al., 1995; Macanochie et al., 1997; Gould et al., 1997; Manzanares et al., 2001). During the establishment and maintenance of Hox expression, *Hox* genes can directly regulate the expression of other *Hox* genes or maintain their own expression by auto-regulation. One of the best-studied examples of auto and cross-regulation is of the maintenance of Hox expression in r4. Early retinoid signaling establishes both *Hoxa1* and *Hoxb1* expression directly via RAREs located in the 3' end of these genes. Along with cofactors Pbx and Meis, Hoxa1 and Hoxb1 bind to the auto-regulatory enhancer of *Hoxb1*. Hoxb1, in turn, regulates the expression of *Hoxa2* and *Hoxb2* in r4, Hoxb2 feedbacks on *Hoxb1*, thus maintaining its expression (Pöpperl et al., 1995; Macanochie et al., 1997; Ferretti et al., 2005). Analyses of single or compound mutants for players of this regulatory pathways provide functional support for their regulatory relationships (Studer et al., 1998; Davenne et al., 1999; Gavalas et al., 2003).

**Regulation of *Hox* genes via miRNAs**

miRNAs are short (22-mer) non-coding RNAs that repress gene expression by binding to a complementary sequence in 3'UTR of mRNA leading to mRNA degradation or repression (Bartel, 2009; Lee and Shin, 2012). Sevaral miRNAs have been identified that regulate the expression of Hox genes. Interestingly, most identified Hox-regulating miRNAs are encoded within the Hox clusters (Figure 2). This genomic arrangement suggests a mechanism guiding the production of miRNAs in spatial and temporal accordance with their Hox targets (Alonso, 2012). Well identified miRNAs in vertebrates include miR-196, miR-10 and miR-615. Three miR-196 gene paralogues are present in the mouse, namely miR-196b, miR-196-a1 and miR-196-a2, situated within the Hox clusters a, b, and c. The miR-196 genes are situated between Hox9 and Hox10 genes. For miR-10, two paralogues are identified in the mouse, miR-10a and miR-10b, situated within Hox clusters a and d. The miR-10 genes are situated between Hox4 and Hox5 genes. miR-615 is produced from an intron in Hoxc5.

## 1.3 Neural circuit formation

A distinct feature of the nervous system is the presence of intricate network of synaptic connections among neurons of diverse morphology as well as physiology. Neural networks are organized to enable efficient and stable processing of information across different brain regions. This requires a tight regulation between, the ability to learn and adapt to different environments, and the stability to ensure reliable execution of behavior. Initial connections are mainly formed through molecular mechanisms that depend on intrinsic developmental programs ranging from neural cell fate specification to proper matching between pre- and post-synaptic partners. The maintenance and maturation of neural connections is dependent on experience-driven activities. Initiation of a neural circuit happens when a neuron or a group of neurons extend their axons towards their target region. This process is called axon

guidance and is highly dependent on environmental cues, also known as guidance cues (Figure 4E,F). Guidance cues can work over long or short-range and can be both attractive and repulsive in nature. Long-range interactions mostly occur via diffusible factors that act as ligand and bind to a receptor present on extending axons, while short-range guidance cues are mediated by direct cell-to-cell contact (Chen and Cheng, 2009). A variety of guidance cues can work together to guide growing axons towards their targets (Kolodkin and Tessier-Lavigne, 2011). A growing axon usually interacts with intermediate targets, also known as guideposts that further guide the axon via several signaling molecules towards its target. Some of the well-known guidance cues are described below.

**Netrins**

Netrins are well known for their role in axon guidance in both vertebrates and invertebrates (Moore et al. 2007). In vertebrates, Netrins from the ventral midline floor plate cells mediate axon outgrowth and guidance of spinal commissural axons (Tessier-Lavigne et al., 1988; Kennedy et al., 1994; Serafini et al., 1994; Serafini et al., 1996). Netrins can function as both long-range and short-range cue (Kennedy et al., 1994; Kennedy et al., 2006; Deiner et al., 1997; Brankatschk and Dickson, 2006). Netrins are also bifunctional, capable of acting as both a chemoattractant and a chemorepellent (Colamarino and Tessier-Lavigne, 1995). The attractive effects of Netrin are mediated by members of the DCC (Deleted in Colorectal Carcinoma) family (Keino-Masu et al., 1996), while repulsive effects of Netrin are mediated by members of the Unc5 family (Leonardo et al., 1997; Hong et al., 1999; Kaleman and Disckson, 2001).

**Slits**

Slits are large secreted proteins that guide axons by repulsion (Brose et al., 1999; Kidd et al., 1999; Li et al., 1999) and are also involved in axon branching (Wang et al., 1999). The

repulsive action of Slits is mediated by members of the Robo family (Kidd et al., 1998; Zallen et al., 1998).

**Semaphorins**

Semaphorins are large proteins capable of functioning as both long-range and short-range guidance cues (Yazdani and Terman, 2006). Although most Semaphorins are repulsive in nature, depending on the receptor complex, Semaphorins can also function as an attractive cue. The major receptors of Semaphorins are members of the Plexin receptor family, but some Semaphorins can also bind with Neuropilins as a co-receptor. Neuropilins, together with Plexin receptors, form an active holoreceptor complex. Different combinations of Plexin and Neuropilins are required in various cell types for the proper functioning of Semaphorins (Tran et al., 2007). Semaphorin signaling via multiple receptors is capable of regulating axon pathfinding and fasciculation, pruning of projections, regulation of neuronal morphology, and synaptogenesis (Tran et al., 2007). Semaphorins can also serve as a receptors, participating in several events of nervous system development.

**Ephrins**

Ephrins are short-range guidance cues that play an important role in axon guidance (Klein et al., 2004). Ephrins bind receptor tyrosine kinases of the Eph family and participate in a variety of developmental events including topographic mapping, axonal growth and branching, pruning of axonal trajectories, regulation of dendritic morphology and synaptogenesis. Similar to several other guidance cues, Ephrins can also act as both chemoattractant and chemorepellent (Feldheim and O'Leary, 2010; Shen and Cowan, 2010). Similar to Semaphorins, Ephrins can also function as a receptors for axon pathfinding.

**Wnt**

Wnts participate in the formation of neural circuits at multiple levels as several Wnts have been identified in regulating the identity of neurons, neuronal migration, synapse formation, axon guidance and formation of topographic maps (Yoshikawa et al., 2003; Lyuksyutova et al., 2003; Salinas and Zou, 2008).

**Growth Factors**

A variety of growth factors, including hepatocyte growth factors (HGF), fibroblast growth factors (FGF), glial-derived neurotrophic factors (GDNF), and neuregulins, have been identified for their roles in guiding axons by attraction. Each growth factor has been associated with a certain set of axons.

The function of all guidance cues is dependent on transducing the extracellular signal to cytoskeletal changes (Dent and Gertler, 2003; Lowery and Van Vactor; 2009). Changes in the growth cone cytoskeletal components allows for the growth cone extension, steering or retraction. The guidance cues are indispensable for the initial establishment of axon path and selection of targets. However, sustenance of a circuit and its maturation is dependent on

activity. Both spontaneous activity during embryonic stages and experience-dependent activity during postnatal periods play an important role in circuit development (Penn and Shatz, 1999; Zhang and Poo, 2001). Both spontaneous and experience-dependent activity are involved in the refinement of neural circuits and consolidation of neural circuits in mature form.

Connections between different brain regions can be organized in several kinds. The most common neural circuit is a topographic kind, also known as continuous maps, maintaining the spatial relationship between the input and the output region (Figure 4A) (Kaas, 1997; Wandell and Winawer, 2011). These topographic neural maps are present in the somatosensory system (presence of a representation of different body parts in a spatial order in the somatosensory cortex, S1), the visual system (retinotopy), and the auditory system (tonotopy, representation of different sound frequencies, with tones close to each other being represented in neighboring cells of the nucleus). To establish topographic maps, morphogenetic gradients are used to sort the axons and form a spatial relationship. Another kind of neural map that can be identified is a discrete or fractured map (Figure 4B). In this kind of map, the spatial relation between projecting neurons is not preserved in the receiving brain region or cells. The olfactory system (Murthy, 2011) and the ponto-cerebellar maps (Leergaard et al., 2006; described later) are examples of such a neural organization. Projections can also have a divergent (projection from a small area to multiple regions) (Figure 4D) or a convergent feature (projection from multiple regions to a single area) (Figure 4C), thereby adding further complexity to the circuits.

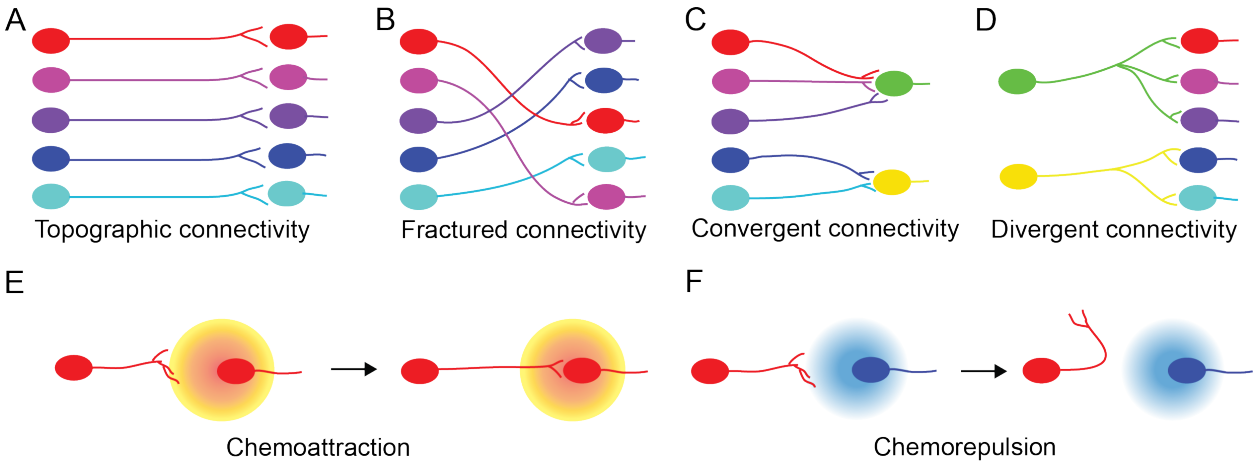


**Figure 4: Formation of neural circuits**. Schematic illustration of types of neural circuits (A) topographic connectivity, in which the spatial relationship between the input and output neurons is maintained. (B) Discontinuous or fractured map, in which the spatial relationship is fractured and the information is distributed in a random manner. (C) Continuous circuit, in which the projections from several neurons can converge onto few cells, or (D) divergent circuit, where information is distributed from a small number of neurons to multiple neurons. (E-F) Schematic illustration to show the response of a growing axon towards (E) attractive or (F) repulsive cues.

### 1.3.1 Role of *Hox* genes in neural circuit formation

Apart from their role in the segmentation of the hindbrain, *Hox* genes are also critical for neuronal specification and connectivity. Gain or loss-of-function experiments have suggested a role of *Hox* genes in forming functional connectivity between hindbrain neurons and their targets. For example, r4 is a source of two types of motor neurons (MNs): facial MNs that contribute to the cranial nerve VII (facial) and contralateral vestibuloacoustic (CVA) MNs of the cranial nerve VIII (Simon and Lumsden, 1993; Auclair et al., 1996; Jacob and Guthrie, 2000). Ectopic expression of *Hoxb1* in r2, anterior to its normal limit of expression, resulted in induction of r4 marker genes in r2 (Bell et al., 1999). Moreover, several MNs from r2 were observed to project contralaterally, similar to r4 CVA neurons

(Figure 5A). Conversely, in the absence of *Hoxb1*, the facial MNs acquire molecular marks of trigeminal MNs and fail to migrate caudally, leading to the loss of facial nerve (Figure 5B) (Gavalas et al., 1998; Gavalas et al., 2003; Goddard et al., 1996; Studer et al., 1996). MNs of the cranial nerve V (trigeminal) develop in r2-r3, where *Hoxa2* (r2) or *Hoxa2* and *Hoxb2* are expressed (r3). In the absence of *Hoxa2*, the trigeminal MNs are disorganized and their axons are misrouted (Figure 5C) (Gavalas et al., 1997). The generation of abducens (V1) MNs requires the collective activity of Hox PG3 genes. Ectopic expression of *Hoxa3* leads to the induction of these MNs, while in the absence of *Hoxa3* and *Hoxb3*, these MNs are completely lost (Gaufo et al., 2003; Guidato et al., 2003). *Hox3* genes are also required for the correct pathfinding of MNs of the glossopharyngeal nerve (IX), which are derived from r6 (Watari et al., 2001). To summarize, Hox genes are required for the generation of hindbrain MNs and a correct match between the Hox code of MNs and their peripheral target is required for axon pathfinding.

*Hox* genes have also been identified as players in the development of somatosensory circuits in the hindbrain. The ventral principal trigeminal nucleus (vPrV) is a central region of the whisker circuit (Erzurumlu et al., 2010). *Hoxa2* gene is expressed in vPrV neurons and is required to guide the axons to their targets (Figure 5G) (Oury et al., 2006). Ectopic expression of *Hoxa2* in dPrV is sufficient to transform the dPrV to a vPrV identity as well as connectivity (Figure 5H) (Bechara et al., 2015). Apart from this Hox PG2 genes are also involved in the refinement of tonotopic circuit in the anterior ventral cochlear nucleus (AVCN) (Figure 5F) (Karmakar et al., 2017). The AVCN and posteroventral cochlear nucleus (PVCN) are parts of the cochlear nucleus that have their origin in the hindbrain. The PVCN is derived from r4 while the AVCN is derived from r2/r3. In the absence of *Hoxb1* or *Hoxb2*, PVCN neurons acquire an AVCN like identity and project to AVCN targets

(Figure 5D) (Di Bonito et al., 2013). *Hox* genes are also required for the development of neural networks that control respiratory rhythm generation. The parafacial respiratory group (pFRG/RTN) derived from r3/r4 and the pre-Bötzinger complex (pre-BötC), derived from r6-r8, are the primary respiratory rhythm generators in the medulla, and defects in these nuclei can lead to perinatal death due to respiratory failure (Bouvier et al., 2010; Rose et al., 2009). The respiratory regions in the pons, derived from r1/r2, connect to the respiratory regulators in the medulla. Mutation in *Hoxa2*, lead to defects in the respiration with no fatality (Chatonnet et al., 2007). However, upon the loss of *Hoxa1*, the mice die shortly after birth from breathing defects (Carpenter et al., 1993; Chisaka et al., 1992; Lufkin et al., 1991; Mark et al., 1993). This is a result of changes in the r4 identity, where the pFRG is located.

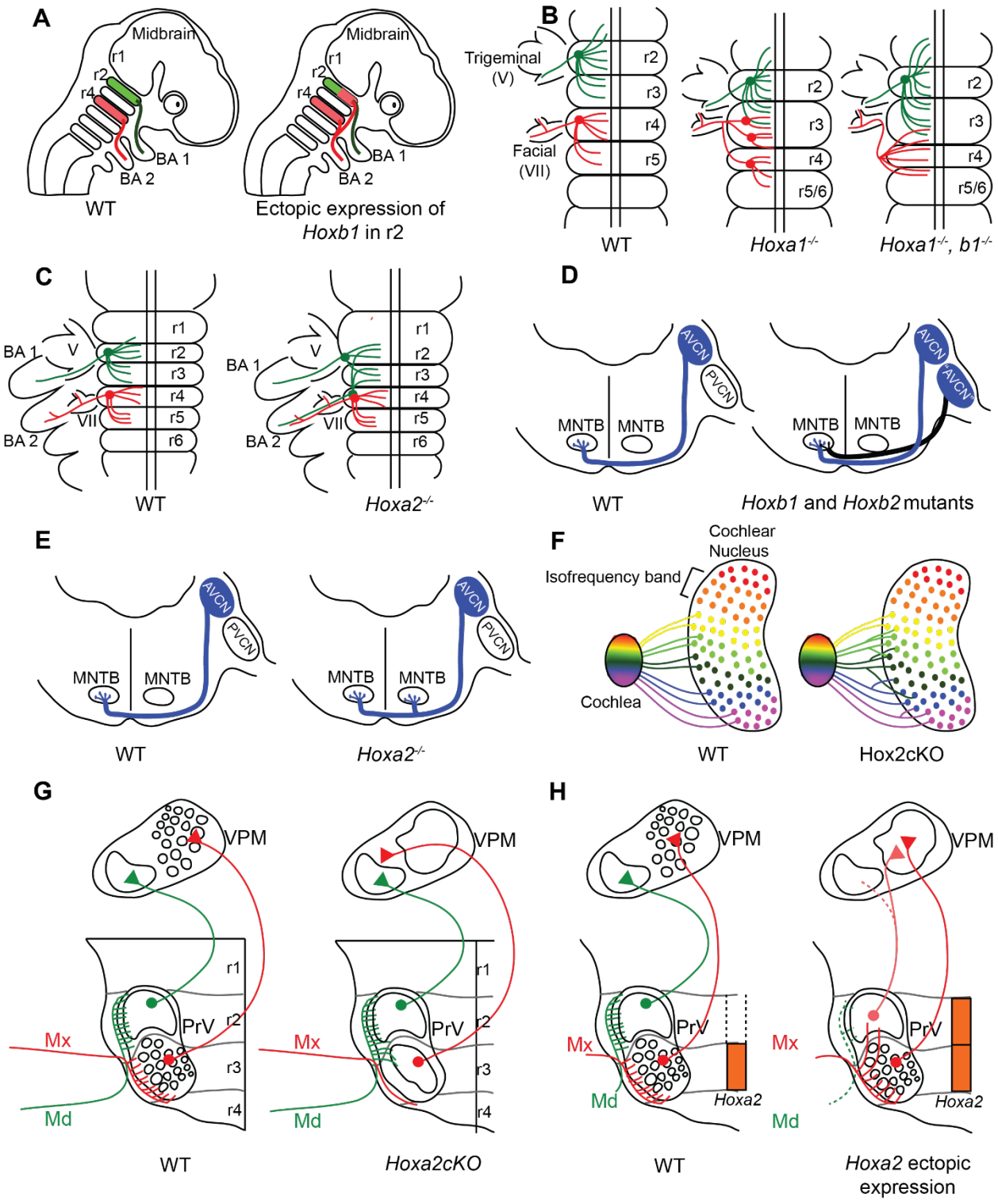


**Figure 5: Role of *Hox* genes in hindbrain neural circuit formation**. Schematic illustration to show various examples for the involvement of *Hox* genes in (A-C) regulation hindbrain motor neuron identity and connectivity, (D-H) hindbrain somatosensory circuit formation. Figure adapted from Bell et al.,1991 (A); Gavalas et al., 1998 (B); Gavalas et al., 1997 (C);

Di Bonito et al., 2013; Philippidou and Dasen, 2013 (D-E); Karmakar et al., 2017 (F); Oury et al., 2006 (G) and Bechara et al., 2015 (H).

### 1.3.2 Downstream effectors of Hox activities in the hindbrain

The role of *Hox* genes in neural cell specification and circuit development are well defined. However, the downstream pathways through which *Hox* genes contribute to circuit development are still poorly understood. Several transcription factors have been described to mediate parts of Hox functions. Expression of cell specification transcription factors such as Phoxb2, Nkx and Pax6 was affected in *Hox1* and *Hox2* mutants (Davenne et al., 1999; Gaufo et al., 2000; Pattyn et al., 2003). In r4, GATA2 and GATA3 are direct downstream targets of Hoxb1, controlling the migration of facial MNs and the projection of CVA neurons (Pata et al., 1999). Hox PG2 regulates the expression of interneuron determinant Envx1 and *Hox3* genes can confer somatic MN identity by regulating the expression of *Olig2* and *Hb9* (Davenne et al., 1999; Gaufo et al., 2003). *Hoxa2* and *Hoxb2* together regulate the expression of several synapse associated genes in the AVCN (Karmakar et al., 2017). Deletion of *Hoxa2* leads to defects in the AVCN axon guidance through downregulation of the guidance receptor Robo3 (Di Bonito et al., 2013). Hox genes also regulate expression of Eph receptors. EphA2 is under direct regulation of Hox PG1 (Chen and Ruley, 1998), while EphA4 and EphA7 could be downstream of Hoxa2 (Gavalas et al., 1997; Taneja et al., 1996; Oury et al., 2006).

## 1.4 Pontine nuclei: Development and Connectivity

**Accepted review in *Frontiers in Neural Circuits*, May 2017**

# The Long Journey of Pontine Nuclei Neurons: From Rhombic Lip to Cortico-Ponto-Cerebellar Circuitry

Claudius F. Kratochwil[1,2], Upasana Maheshwari[3,4] and Filippo M. Rijli[*3,4]

[1] Chair in Zoology and Evolutionary Biology, Department of Biology, University of Konstanz, Konstanz, Germany

[2] Zukunftskolleg, University of Konstanz, Konstanz, Germany

[3] Friedrich Miescher Institute for Biomedical Research, Basel, Switzerland

[4] University of Basel, Switzerland

**Correspondence:**

Filippo M. Rijli

Filippo.Rijli@fmi.ch

**Abstract**

The pontine nuclei (PN) are the largest of the precerebellar nuclei, neuronal assemblies in the hindbrain providing principal input to the cerebellum. The PN are predominantly innervated by the cerebral cortex and project as mossy fibers to the cerebellar hemispheres. Here, we comprehensively review the development of the PN from specification to migration, nucleogenesis, and circuit formation. PN neurons originate at the posterior rhombic lip and migrate tangentially crossing several rhombomere derived territories to reach their final position in ventral part of the pons. The developing PN provide a classical example of tangential neuronal migration and a study system for understanding its molecular underpinnings. We anticipate that understanding the mechanisms of PN migration and assembly will also help to learn the molecular and cellular basis of cortico-cerebellar circuit formation and function.

**Keywords: pontine gray nuclei, reticulotegmental nuclei, precerebellar system, Cortico-ponto-cerebellar circuitry, *Hox* genes**

## Introduction

The basal pontine nuclei (BPN) (also known as basilar pons, pontine gray nuclei or pontine nuclei (PN)) and the reticulotegmental nuclei (RTN) (also known as nucleus reticularis tegmenti pontis) are located within the ventral portion of the pons. Both nuclei (together referred to as PN) cannot be distinguished molecularly during development. The PN constitute the main mossy fiber input to the cerebellum carrying information from the cerebral cortex. The development of the PN has been intensively studied. Considerable progress has been made in understanding how the stereotypic tangential neuronal migration and positioning of the PN next to the ventral midline of the rhombomere (r) 3- and 4-derived

territory are orchestrated. Also, several studies addressed how the initial steps of axon guidance to the cerebellum and innervation from the cortex are organized. Yet, our understanding of the mechanisms that pattern the complex input-output circuitry of the PN is limited. Recent studies have shown that the PN are composed of a heterogeneous population of projection neurons and that this diversity might in turn contribute to the complex connectivity between neocortex, PN and cerebellum.

The aim of this review article is to provide an overview of our current understanding of the development of the PN and their circuitry. Moreover, we propose that developmental programs and protomaps established at the pre-migratory stage contribute in shaping the cortico-ponto- cerebellar circuitry. This is further influenced by environmental factors during migration and nucleogenesis. By summarizing the main literature that attempts to describe the complex input-output connectivity of the PN and their partially topographic organization, we describe emerging concepts on the logic behind the cortico-ponto-cerebellar connectivity. We also speculate about the evolution of PN and the cortico-ponto-cerebellar pathway. Lastly, we discuss outstanding questions and how they can be approached.

**Pontine nuclei as part of the precerebellar system: specification at the rhombic lip**

Precerebellar nuclei, including the inferior olivary nucleus (ION), external cuneate nucleus (ECN), lateral reticular nucleus (LRN), RTN and BPN (**Figure 1A**) originate from the posterior (lower) rhombic lip, an embryonic proliferative neuroepithelium that lies in the dorsal rhombencephalon and surrounds the alar recess of the fourth ventricle (Altman and Bayer, 1987a,b,c,d). Development of rhombic lip derivatives has been intensively studied (reviewed in Di Meglio and Rijli, 2013; Sotelo and Chedotal, 2013; Hatanaka et al., 2016). A hallmark of the rhombic lip is its dorsoventrally graded expression of *Wnt1* (Rodriguez

and Dymecki, 2000; **Figure 1B**). Precerebellar neuron progenitor pools within the *Wnt1* rhombic lip domain are molecularly and spatially defined, giving rise to distinct neuronal populations. All mossy fiber precerebellar neurons, i.e., those contributing to ECN, LRN, RTN and BPN, are derived from a defined dorsal domain of the rhombic lip specified by high *Wnt1* expression levels and the expression of the basic helix-loop-helix (bHLH) transcription factor *Atoh1* (*Math1*; Rodriguez and Dymecki, 2000; Machold and Fishell, 2005; Wang et al., 2005). Climbing fiber inferior olive neurons are instead derived from progenitors with low *Wnt1* levels that express *Ngn1* and *Pft1a* and are located ventral to the *Atoh1*-domain (**Figure 1B**). Consequently, *Atoh1* knockout mice lack all precerebellar nuclei except the ION (Wang et al., 2005), whereas *Pft1a* null mutants lack the ION, but not the other precerebellar nuclei (Yamada et al., 2007, 2014).

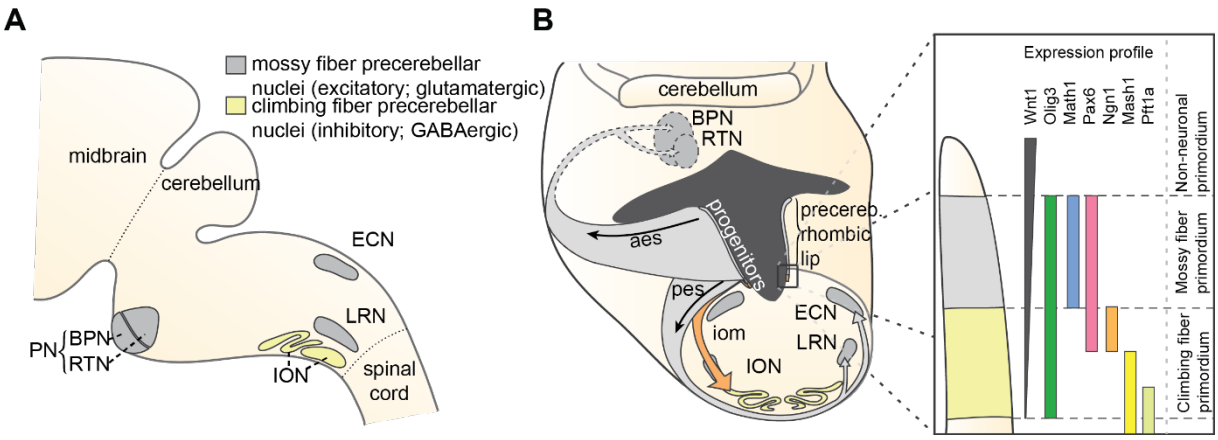


**Figure 1: The precerebellar nuclei and their specification**. (A) The pontine nuclei (PN) comprise the BPN and RTN. They are part of the mossy fiber precerebellar nuclei that also include ECN and LRN. The precerebellar ION is the source of the climbing fibers. (B) The PN are derived from progenitors at the rhombic lip. The rhombic lip is dorsoventrally patterned. The PN are derived from a domain that expresses *Wnt1*, *Olig3*, *Pax6* and *Atoh1*. Specified PN neurons migrate in the aes to their final position in the ventral pons. Abbreviations: aes: anterior extramural stream, BPN: Basal Pontine Nuclei, ECN: External Cuneate Nucleus, iom: inferior olivary migratory stream, ION: Inferior Olive Nucleus, LRN: Lateral Reticular Nucleus, pes: posterior extramural stream, PN: Pontine Nuclei (B modified from Altman and Bayer, 1987).

In mouse, the posterior lower rhombic lip (precerebellar lip) spans rhombomere (r)6 to pseudo-rhombomere (pr)8 (**Figures 2A,B**). These rostrocaudal progenitor domains are molecularly defined by the partially overlapping expression of *Hox* genes of the paralog group 2–5 (*Hox2–5*) whereas they lack *Hox6–11* expression (Di Meglio et al., 2013; Tomás-Roca et al., 2016). More anterior *Atoh1*-positive rhombic lip progenitors generate the granule neurons of the cerebellum (r1-derived) and the neurons of the brainstem cochlear complex (r2-r5- derived), respectively (Rodriguez and Dymecki, 2000; Machold and Fishell, 2005; Wang et al., 2005; Wingate, 2005; Farago et al., 2006; Ray and Dymecki, 2009). Hence, precerebellar nuclei neurons are generated from distinct intersections of dorso-ventral (DV; *Atoh1*$^{+}$/*Wnt1*$^{+}$) and anterior-posterior (AP; *Hox2–5*$^{+}$) progenitor pools, as assessed in several fate mapping studies using rhombomere- and DV progenitor-specific *Cre* and *FLP recombinase* expressing mouse lines, respectively (Rodriguez and Dymecki, 2000; Wingate, 2005; Fu et al., 2011; Di Meglio et al., 2013).

Several other transcription factors have been shown to affect the development of the PN and other precerebellar nuclei. The bHLH transcription factor *Olig3* is expressed in the rhombic lip and encompasses the *Atoh1*$^{+}$ domain. *Olig3*$^{-/-}$ mutants have significantly reduced levels of *Atoh1* expression and reduced PN size (Liu et al., 2008). Also, PAX6 has been shown to influence the specification of dorso-ventral domains in the rhombic lip by maintaining normal levels of BMP signaling. *Pax6* null mutants have a reduced *Atoh1* domain, but an increased *Ngn1* domain. Hence, *Pax6* mutants have strongly reduced PN, but larger ION (Engelkamp et al., 1999; Landsberg et al., 2005).

Finally, distinct precerebellar nuclei are generated during different ontogenetic periods, as shown initially by tritiated thymidine radiographic studies in the rat (Altman and Bayer,

1987d). This was confirmed by fate mapping with temporally inducible tamoxifen-dependent Atoh1*::CreER*$^{T2}$ lines (Machold and Fishell, 2005; Wang et al., 2005) and *in utero* electroporation in mice (Okada et al., 2007). The *Ptf1a*$^{+}$ ION neurons are the first ones to be generated and to migrate (E10.5–E11.5), followed by the *Atoh1*$^{+}$ LRN (E11.5–12.5), ECN (E11.5–12.5), RTN (E12.5–E13.5) and lastly the BPN (E13.5–E16.5) (Pierce, 1966; Altman and Bayer, 1987d; Machold and Fishell, 2005; Wang et al., 2005; Okada et al., 2007).

**A long way to go: the tangential migration of pontine nuclei**

Rhombic lip derivatives including the PN are amongst the best studied examples of tangential migration (Hatten, 1999; Nóbrega-Pereira and Marín, 2009; Di Meglio and Rijli, 2013; Sotelo and Chedotal, 2013; Hatanaka et al., 2016). From the rhombic lip, PN neurons undertake a long-distance tangential migration via the anterior extramural stream (AES). In contrast to radial migration, where neurons use radial glia as a scaffold, AES tangentially migrating neurons move orthogonally to the orientation of radial glia, just beneath the meninges.

PN neurons migrate rostroventrally (**Figures 1**–**4**), unlike other precerebellar neurons that directly take a ventral route from their dorsal progenitor zone (**Figures 1**, **2**). Migration of PN neurons can be subdivided into three phases (**Figure 4A**; Geisen et al., 2008). After leaving r6–pr8, PN neurons migrate ventrally (phase I). Next, they turn rostrally and migrate through r5 and r4, passing the vestibulocochlear and facial nerve roots (phase 2). The migratory stream then enters r3 and reaches the trigeminal nerve root in the caudal aspect of r2 where it turns again ventrally (phase 3) and finally settle on both sides of the floor plate in-between rostral r3 and rostral r5 derived territories (Farago et al., 2006; Geisen et al., 2008). Some PN neurons

cross the midline and contribute to the contralateral PN. In mice, the generation, migration, and settlement at final destination of PN neurons takes place between E13.5 and E18.5 (Okada et al., 2007; Hatanaka et al., 2016). The migration time of a single neuron from leaving the rhombic lip to reaching its final destination is approximately two days with the last neurons arriving at E18 (Okada et al., 2007; Hatanaka et al., 2016).

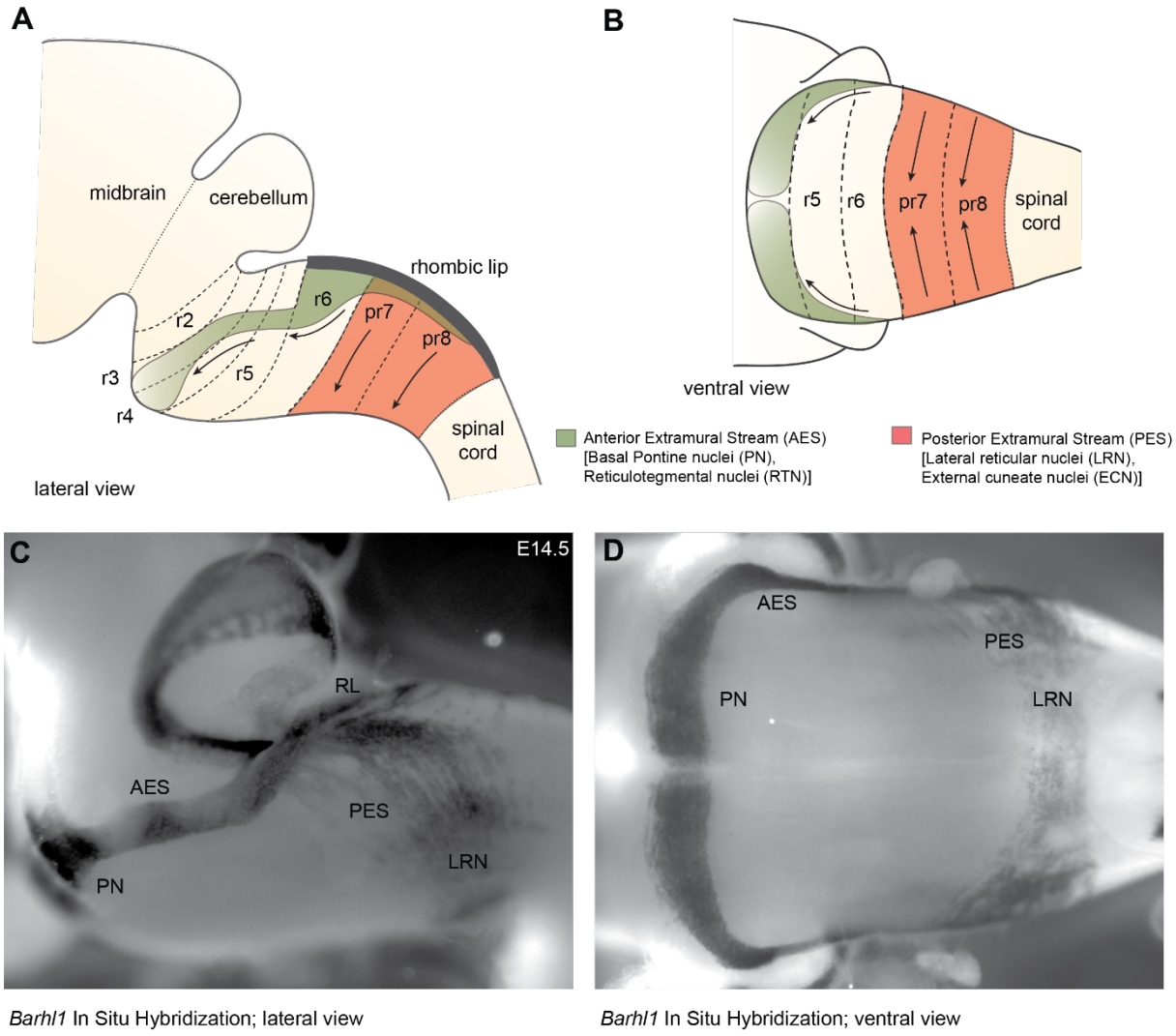


**Figure 2: The migration of the pontine nuclei (PN)**. (A-D) The PN derive from rhombomere (r)6-pr8 precerebellar rhombic lip and take a rostroventral path in the AES to finally settle ventrally in r3 partially and in r4 derived territories. Other precerebellar nuclei such as the LRN and ECN derive from pr7-pr8, migrate ventrally in the PES, cross the midline, and settle contralaterally at more dorsal positions. Migratory streams are shown from lateral (A,C) and ventral (B,D) views as schematic drawings (A-B) and as whole-mount in situ hybridization using as a probe the precerebellar neuron marker *Barhl1*. (C,D)

Abbreviations: AES: anterior extramural stream, LRN: Lateral Reticular Nucleus, PES: posterior extramural stream, PN: Pontine Nuclei, pr: pseudorhombomere, RL: Rhombic lip (C,D from Kratochwil, 2013)

Several reasons make the precerebellar system a suitable system for studying tangential migration. First, the subpial migratory streams can be easily visualized. Cells migrate directly underneath the meninges. Several markers allow to specifically distinguish migrating precerebellar cells from the surrounding tissue, including *Barhl1* (**Figures 2C,D**) (*Mbh2*) (Li et al., 2004), *Pax6* (Engelkamp et al., 1999), and *Tag1* (Backer et al., 2002) permitting the visualization of the complete migratory pathway on whole-mount preparations. Using this approach, it is also possible to efficiently screen for migratory defects in knockout mutant mice. Also, several *GFP* and *Cre* or *Flp* recombinase transgenic and knock-in mouse lines are available that target precerebellar neurons facilitating not only the analysis of the migration phenotypes but also allowing conditional knockout targeting of precerebellar neurons (Danielian et al., 1998; Dymecki and Tomasiewicz, 1998; Rodriguez and Dymecki, 2000; Machold and Fishell, 2005; Wang et al., 2010; Di Meglio et al., 2013; Lewis et al., 2013; Kratochwil and Rijli, 2014). More recently, *in utero* electroporation of precerebellar progenitors has become a powerful tool for analyzing the molecular mechanisms of tangential migration (Okada et al., 2007; Watanabe and Murakami, 2009; Di Meglio et al., 2013; Kratochwil, 2013; Zelina et al., 2014). Using this approach, not only can migrating neurons be effectively visualized at a single cell resolution by reporter gene expression, but they can also be co-electroporated with genes of interest or RNA interfering constructs for gain-of-function or knockdown experiments, respectively. This approach has the advantage that the behavior of the electroporated cells can be analyzed in a wild type environment (**Figure 3**).

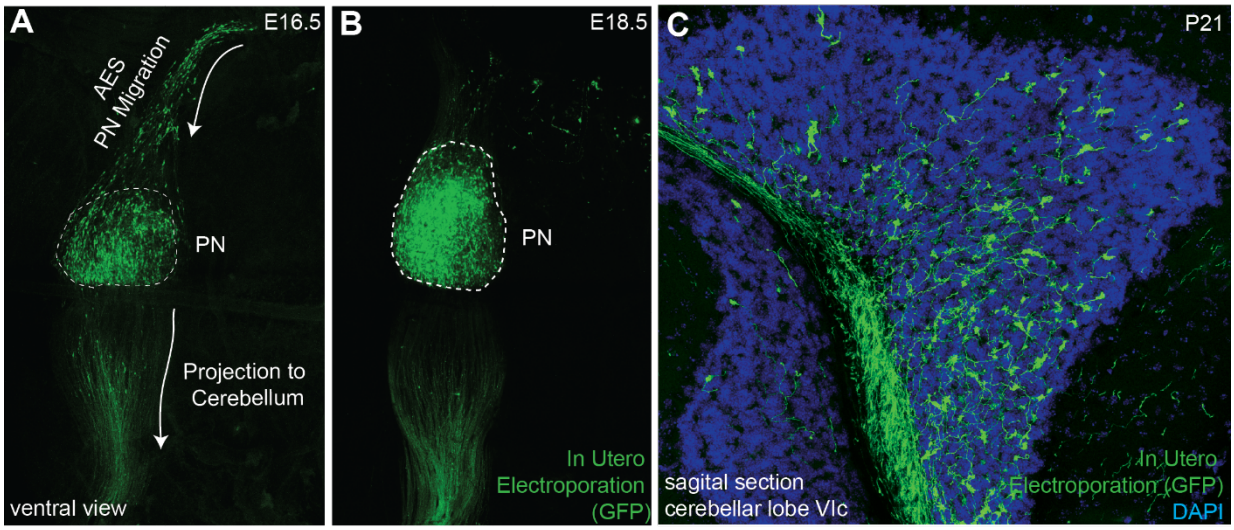


**Figure 3: *In utero* electroporation as a tool for analyzing pontine nuclei (PN) development**. (A-C) *In utero* electroporation at E14.5 lower rhombic lip with reporter genes (here expressing GFP) allows the visualization of the anterior extramural stream (AES) (A), PN assembly (A,B), axon projection to cerebellum (B,C) as well as target selection and circuitry (C). Also, it permits to analyze gene function *in vivo* through electroporation of overexpression constructs and RNA interference constructs. (A-C from Kratochwil, 2013)

### The molecular mechanisms controlling pontine nuclei migration

Several guidance factors and transcription factors have been shown to regulate the complex migratory pathway of PN neurons (**Figures 4**, **5**). PN neurons, as other migrating precerebellar nuclei neurons, are attracted by the floorplate. This attraction is mediated by NTN1/DCC signaling, with *Ntn1* being expressed in the floorplate and the *Dcc* receptor in migrating precerebellar neurons (Fazeli et al., 1997; Yee et al., 1999; Alcántara et al., 2000; Zelina et al., 2014). In *Dcc* and *Ntn1* null mutants, PN neurons do not reach the midline and are stalled in a medio-lateral position (**Figures 4E,H**; Yee et al., 1999; Zelina et al., 2014). Furthermore, cell number is decreased in both mutants, in accordance with the known role of NTN1/DCC as survival factors (Llambi et al., 2001).

But what makes PN neurons migrating rostrally? By the time the PN neurons migrate, most

other precerebellar nuclei have already reached their final destination or are in the last phases of migration. Also, other hindbrain nuclei including the facial motor nucleus (FN) have already formed. The FN is a source of the repulsive diffusive guidance molecules SLIT2 and SLIT3 (Geisen et al., 2008). The FN neurons are generated in r4 and migrate tangentially to ventral r6 (Garel et al., 2000). Once the FN settles in the ventral r6 derived territory it repels migrating PN neurons that express the SLIT receptors ROBO1 and 2 and switch from phase 1 (ventral migration) to phase 2 (rostral migration; see above) (Di Meglio et al., 2008; Geisen et al., 2008). The expression of *Robo2* is regulated by the *Hox2* paralogs, *Hoxa2* and *Hoxb2* (Geisen et al., 2008). Moreover, in *Hoxa2;Hoxb2* knockout mice (**Figure 4B**) PN neurons migrate prematurely to the ventral midline, similar to *Robo1;Robo2*, *Slit1;Slit2* and *Robo2;Slit2* mutant mice (**Figures 4D,G**; Di Meglio et al., 2008; Geisen et al., 2008). Ectopic PN neuron migration could also be observed in *Phox2b* mutant mice that do not develop the Slit1/2 expressing facial nucleus (**Figure 4F**; Geisen et al., 2008). Once beyond the influence of the FN, PN neurons are guided by Ntn1/Dcc signaling to their final destination lateral to the floorplate.

In addition to NTN/DCC and ROBO/SLIT signaling, several factors are involved in PN neuron migration. In mutants for *Unc5c*, a repulsive receptor of NTN1, PN neurons migrate ectopically (**Figure 4K**). While their ventral positioning is unaffected, some neurons migrate prematurely towards the midline at ectopic posterior positions. These defects can be rescued by overexpression of *Unc5c* in PN neurons suggesting a cell-autonomous role (Kim and Ackerman, 2011). The paralog *Unc5b* is also expressed in migrating PN neurons, however only in a subset. Overexpression of *Unc5b* results in anterior ectopic migration as well as lateral migratory arrest (**Figure 4J**; Di Meglio et al., 2013). A second repulsive guidance protein, DRAXIN, which interacts with DCC (Islam et al., 2009), was also suggested to play

a role in PN neuron migration. Although DRAXIN inhibits precerebellar neuron migration *in vitro*, no significant differences in PN neuron migration could be shown in *Draxin* knockout animals (Riyadh et al., 2014). DCC also cooperates with RIG1/ROBO3 to mediate NTN1 attraction (Zelina et al., 2014). In *Robo3* deficient mice, PN neurons fail to arrive at the midline and are instead arrested at a lateral position after phase 2 of migration, forming a disorganized ectopic cluster of cells (**Figure 4I**; Marillat et al., 2004; Zelina et al., 2014). The phenotype is reminiscent of the *Dcc* and *Ntn1* knockouts, however without a clear decrease in cell number. In summary, these results suggest that NTN1 and ROBO signaling are integrated in a complex manner throughout the migration of PN neurons. The ratio of repulsion vs. attraction is tightly regulated and balanced, resulting in the stereotypic migration along the AES.

Several other factors have been shown to influence PN neuron migration. In mouse mutants for the glycosyltransferase *LARGE*, the migration is stalled after phase 2 resembling the phenotype in *Robo3* mutants (Qu et al., 2006). Similarly, knockdown of *Calmodulin (Calm1)* resulted in aberrantly positioned PN neurons, and additionally, nucleogenesis was affected (Kobayashi et al., 2015). Cadherins, a group of adhesion molecules involved in collective cell migration (Theveneau and Mayor, 2012), have been shown to regulate the tangential migration of precerebellar neurons (Taniguchi et al., 2006). Lastly, the meninges are also involved in guiding migrating PN neurons (Zhu et al., 2009). The chemokine SDF1, ligand of the CXCR4 receptor is released from the meninges and is required for the marginal migration of the PN neurons directly beneath the meninges. Removal of the meninges or *Cxcr4* knockout induced submarginal migration and a far less confined migratory stream (**Figure 4L**; Zhu et al., 2009). Additionally, SDF1/CXCR4 signaling might contribute to the anterior migration of pontine neurons. *Cxcr4* null mutants show multiple ectopic posterior

pontine clusters (Zhu et al., 2009). Therefore, the SDF1/CXCR4 signaling pathway might either have an instructive role (*Sdf1* has higher expression levels anteriorly) and/or modulate the responsiveness of pontine neurons to other anterior guidance cues such as Netrins and Slits. Similarly, retinoic acid (RA) is also released from the meninges and increased RA levels have been suggested to induce defasciculation of the migratory stream and posterior ectopic migration (Yamamoto et al., 2003, 2005). However, due to the extensive effects of varying RA levels on several developmental processes, direct roles in PN guidance are difficult to pinpoint. Hence, SDF1 might not be the only non-cell- autonomous instructive signal from the meninges contributing to the migration of pontine neurons.

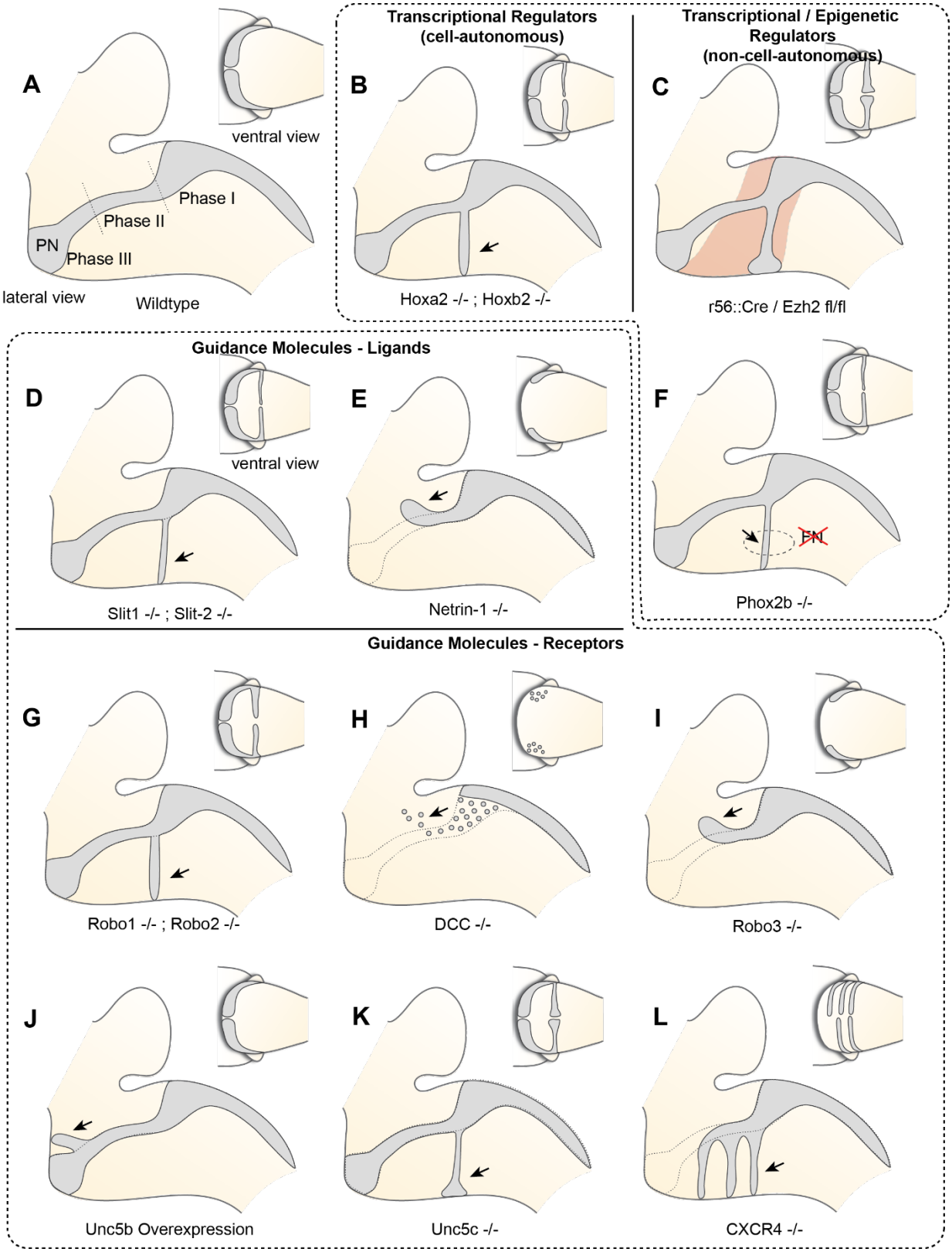


**Figure 4: Molecular mechanisms controlling pontine nuclei (PN) migration I**. The migration of PN neurons can be divided into three phases (Phase I-III). In the first phase (phase I) PN neurons migrate ventrally, switch then to a rostral direction (phase II), and

finally migrate to the ventral midline (phase III). Several cell-autonomous and non-cell autonomous factors including guidance molecules and upstream epigenetic and transcriptional regulators have been shown to influence all or distinct phases of PN migration.

But how is the expression of these guidance factors controlled? Besides the aforementioned transcription factors such as ATOH1 and PAX6, several other transcription factors have been shown to be not only essential for proper migration but also for PN neuron specification. HOXA2 and HOXB2 act upstream of *Robo2* in migrating PN neurons regulating their response to repulsion from the FN (Geisen et al., 2008), resulting in the rostroventral migratory route. The helix-loop-helix transcription factors NSCL-1 and NSCL-2 are strongly expressed in the AES (Schmid et al., 2007). Single null mutants have no PN neuron migration defects, whereas in *Nscl-1/Nscl-2* compound mutants the basal PN are absent and the RTN are strongly reduced (Schmid et al., 2007). *Dcc* was downregulated in *Nscl-1/Nscl-2* double mutants, suggesting that NSCL-1/NSCL-2 act upstream of *Dcc*, possibly explaining the increased apoptosis in double mutants. In mutants for the Nuclear Factor Ib (*Nfib*), the PN are greatly reduced and the migration is delayed, suggesting that early migrating PN neurons are more vulnerable to the knockout of *Nfib*. However, their targeting to the ventral pons is not disturbed (Kumbasar et al., 2009). Additionally, genes that are involved in post-transcriptional regulation have been proposed to control migration of precerebellar neurons including the RNA-binding protein *Csde1* for the PN (Kobayashi et al., 2013) and *Musashi1* (*Msi1*) for LRN and ECN (Kuwako et al., 2010).

**Nucleogenesis and patterning of the pontine nuclei**

The migration of PN neurons from lower rhombic lip to their target region in the ventral pons is followed by nucleogenesis (Altman and Bayer, 1987d; Kawauchi et al., 2006). During this process, PN neurons form a 3-dimensional aggregate bulging out of the ventral pons. In mice, PN nucleogenesis occurs between E14.5, when the first neurons arrive at their final destination, and E18.5, when nucleogenesis is close to completion (Shinohara et al., 2013). Various studies done in rodents provide a detailed analysis of the movement of neurons during nucleogenesis; however, the molecular mechanisms involved in the regulation of this process are poorly understood.

Timing plays an important role during PN nucleogenesis. Early born-early arriving neurons switch their migration mode from tangential to radial near the ventral midline (Watanabe and Murakami, 2009; Shinohara et al., 2013). Depending on the cellular behavior of neurons, this switch can be categorized into two types (**Figure 6**). The first category comprises neurons that pause their migration at the ventral midline and switch to radial migration (**Figure 6A**). Hereby, the soma of these neurons migrates orthogonal to the surface, leaving the leading process behind. The second category is composed of neurons that change their migratory direction without ceasing migration (Watanabe and Murakami, 2009). In both categories, migrating neurons grow a new short process or a bifurcation of the leading process, enabling the neuron to take up a new migratory route. This switch between tangential to radial migration is most apparent at E15.5 (Kawauchi et al., 2006). Interestingly, the ability to switch between tangential to radial migration was only seen in early born-early arriving PN neurons (Watanabe and Murakami, 2009; Shinohara et al., 2013). Late born PN neurons instead stack ventrally to early arriving neurons (Altman and Bayer, 1987d; Shinohara et al., 2013) resulting in an inside-out lamellae-like structure of the PN (**Figures 6B**, **7A**). Because early born PN

neurons are able to migrate dorsally and late born PN neurons are mostly located more ventrally, it was hypothesized that the RTN is populated mostly by early born neurons, whereas BPN is formed of both early and late born PN neurons (Altman and Bayer, 1987d; Shinohara et al., 2013).

In addition to the migration along the dorsoventral axis, migrations along the mediolateral and rostrocaudal axes can also be observed during PN nucleogenesis (Shinohara et al., 2013; **Figure 6**). Neurons enter the forming PN and migrate medially. However, some neurons migrate laterally (lateral migration), settling at a more distal position, eventually resulting in an expansion of the PN along the mediolateral axis. Both early born and late born PN neuron subsets can switch from medial to lateral migration. Migration along the rostrocaudal axis of the forming PN occurs rarely and mostly involves early born neurons. In summary, distinct neuron migratory patterns contribute to PN nucleogenesis, expansion and organization. The switch from tangential to radial migration contributes to nucleogenesis along the dorsoventral axis, whereas a switch from medial to lateral migration contributes to mediolateral expansion. Lastly, widening of the tangential migratory stream has a direct bearing on PN rostrocaudal expansion (Shinohara et al., 2013).

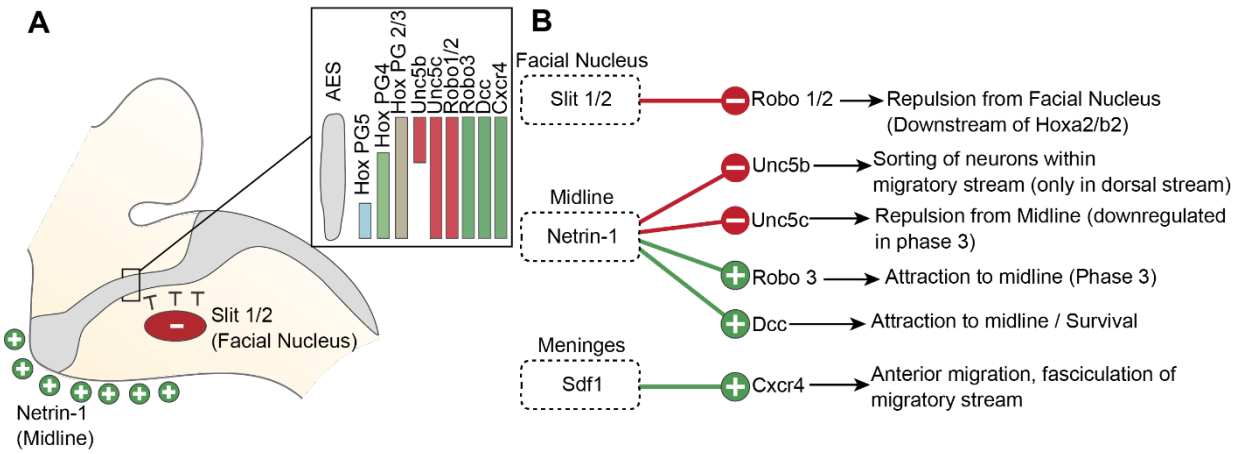

**Figure 5: Molecular mechanisms regulating pontine nuclei (PN) migration II**. Several guidance molecules and their receptors regulate the migration of PN neurons including Slit1/2, Robo1/2, Rig1/Robo3, Netrin-1, Dcc, Sdf1 and Cxcr3. Slits, released from the facial nucleus, repel rostrally migrating PN neurons, which express the receptors Robo 1 and 2. Robo2 expression is regulated by the *Hox* paralog group (PG) 2 genes, *Hoxa2* and *Hoxb2*. Ventral migration is guided by the ligand Netrin-1 that is released from the midline. A balance of expression of Dcc and Robo3, mediating attraction, and *Unc5b/c*, mediating repulsion, receptors controls the targeting to the ventral midline. The Unc5b receptor is expressed in the dorsal part of the migratory stream, contributing to maintain the position of rhombomere (r)6 derived PN neurons. *Hox* genes display dorsoventrally nested expression within the migratory stream. *Hox PG5* genes downregulate Unc5b expression in the ventral part of the migratory stream.

A few studies have investigated the molecular regulation of PN nucleogenesis and the maintenance of PN integrity. The transmembrane immunoglobulin superfamily molecule NEPH2 regulates the movement of neurons within the PN (Nishida et al., 2011). *Neph2* null mutants show disrupted intranuclear migration of PN neurons along the mediolateral axis. Most neurons in *Neph2* mutant are found to be stuck along the ventral midline. In mice lacking the homeobox transcription factor BARHL1/MBH2, PN are only a third of their normal size. *Barhl1* is expressed in all rhombic lip derivatives except inferior olivary nuclei throughout migration and nucleogenesis. The phenotype of *Barhl1* null mutants appears to be mainly due to a postnatal increase in apoptosis (Li et al., 2004). However, the downstream mechanisms are still unclear.

The process of PN nucleogenesis occurs primarily prenatally; yet, there is a dramatic increase in the PN size postnatally. The peak of postnatal growth of PN is between postnatal day 0 (P0) and P4. Interestingly, this growth is mainly a consequence of a large production of oligodendrocytes from the $Sox2^{+}/Olig2^{+}$ expressing progenitors present in the ventricular zone along the fourth ventricle, the midline domain and in the parenchyma (Lindquist et al., 2016).

**One stream to bring them all - the cryptic heterogeneity of the anterior extramural stream**

*Atoh1*-derived PN neurons migrate along the AES as a large, seemingly homogeneous, stream of cells. However, the AES may be composed of subsets of neurons bearing heterogeneous positional cell identities. Several factors may generate distinct subsets of PN neurons. One important factor of heterogeneity is their birthdate (Altman and Bayer, 1987d). As noted in the previous section, PN neurons are generated between E12.5 and E16.5 and nucleogenesis occurs until E18.5 (**Figure 7A**). The timing of the birth of a PN neuron defines its position along the dorsoventral axis (Altman and Bayer, 1987d), hence providing a source of distinct PN neuron subpopulation positional identity.

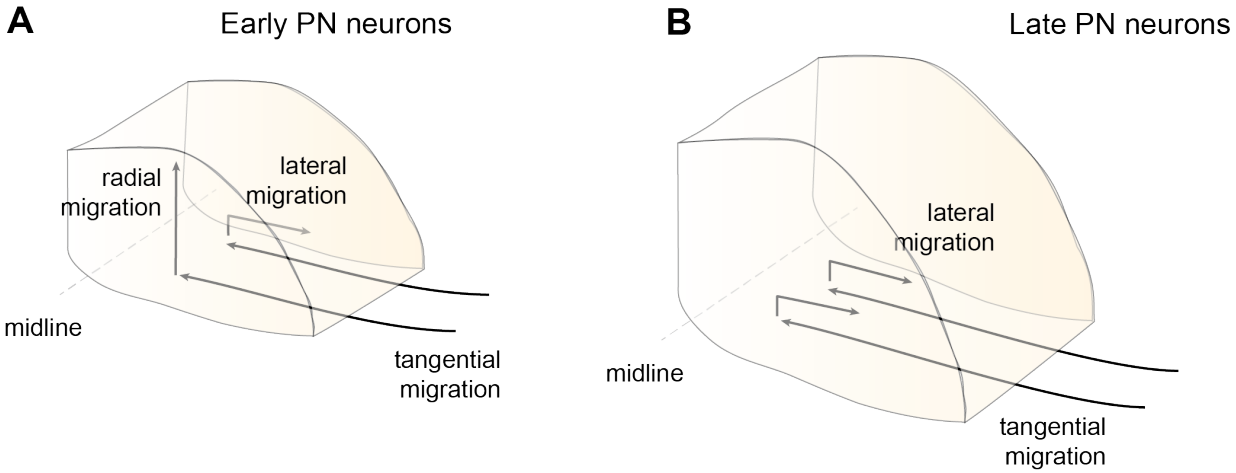


**Figure 6: Migration modes during pontine nuclei (PN) assembly**. After that the tangentially migrating PN neurons arrive at the ventral midline they switch their migratory mode and/or direction. Early arrived PN neurons partially migrate radially contributing to the core of the PN, including the neurons of the reticulotegmental nucleus (RTN), or switch their migration laterally under the surface. Late PN neurons rarely migrate radially, but mostly migrate laterally and stack onto progressively forming layers of PN neurons and therefore mainly contributing the basilar pontine nuclei (BPN) (modified after Shinohara et al., 2013).

PN neurons are also segregated into distinct subpopulations settling at different positions along the rostrocaudal axis of the forming nuclei (Di Meglio et al., 2013). PN neurons originate from r6–pr8 (**Figure 8**). Subsets of pontine neurons derived from different anteroposterior (AP) progenitor domains do not move freely in the migratory stream nor in the forming PN, but tend to remain dorsoventrally segregated during AES migration and settle in distinct anteroposterior domains in the PN (**Figures 7B**, **8B**). This was shown by fate mapping approaches using rhombomere specific Cre-expressing mouse drivers crossed with Cre-dependent floxed reporter lines (Di Meglio et al., 2013). Pontine neuron subsets derived from different AP rhombic lip progenitor domains also exhibit distinct expression profiles of HOX2–5 transcription factors. This molecular information is maintained throughout their tangential migration and nucleogenesis (**Figures 7B**, **8**). Pr8 derived neurons express *Hox5* genes, namely *Hoxa5*, *Hoxb5* and *Hoxc5*. *Hox5* expressing PN cells leave the rhombic lip at posterior positions, migrate in the most ventral part of the AES, and finally settle in the most posterior part of the nuclei (Di Meglio et al., 2013). But does the differential expression of *Hox* genes influence pontine neuron migratory behavior and/or PN circuit formation?

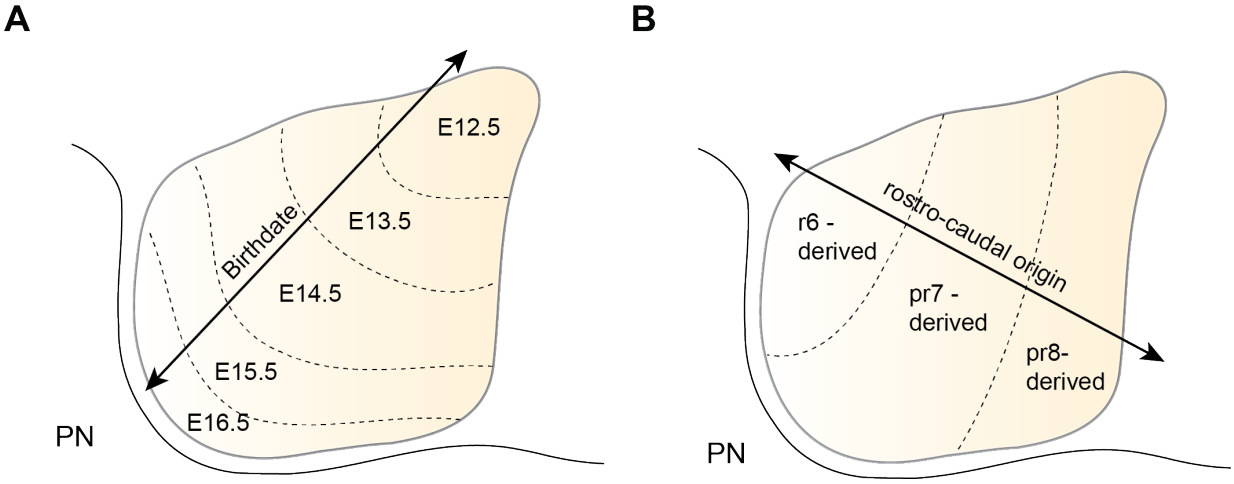


**Figure 7: Patterning of the pontine nuclei (PN) during nucleogenesis**. (A) During nucleogenesis, PN neurons populate the target region in an inside-out (dorsoventral) fashion with early born neurons building the inner core of the PN and late born neurons contributing to the outer shell of the PN. (B) The rostrocaudal order of PN neuron progenitors at the lower

rhombic lip is maintained by postmitotic PN neurons during tangential migration and nucleogenesis. Rhombomere (r)6 derived neurons position themselves in the most rostral part of the PN, pr8 derived in the most caudal part of the PN. pr: pseudo-rhombomere.

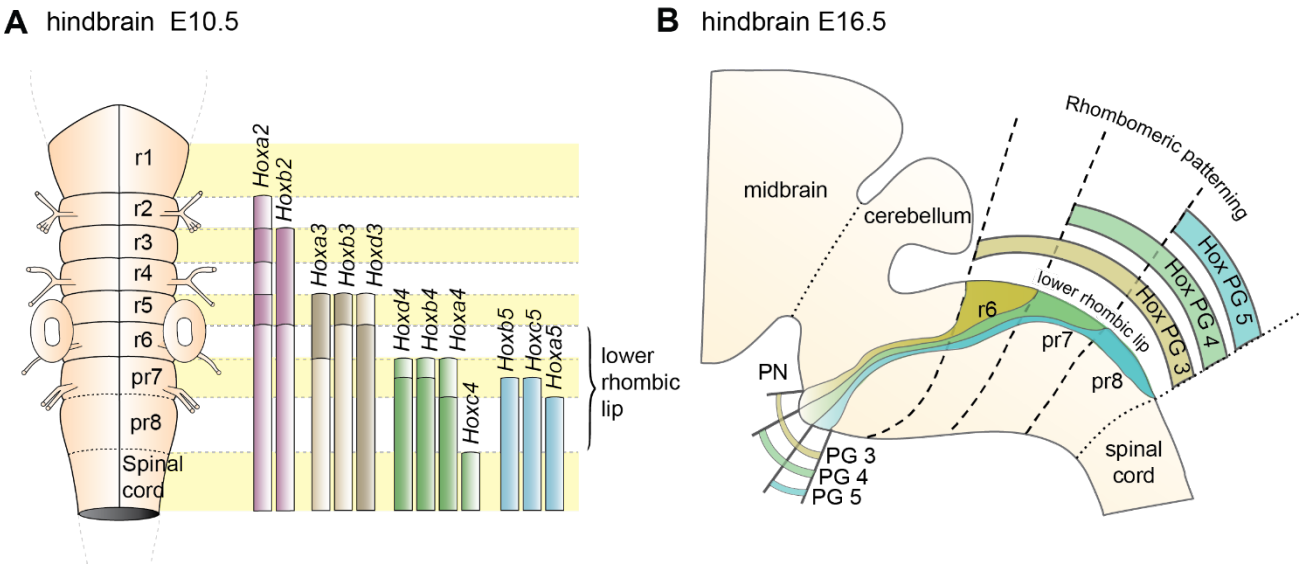


**Figure 8: Patterning of pontine nuclei (PN) progenitors along the rostrocaudal axis.** (A) The progenitors of the PN in the lower (caudal) rhombic lip are generated in rhombomere (r)6, pr7 and pr8 and are molecularly defined by the expression of *Hox* genes. r6 derived PN neurons express Hox paralog (PG) 2 and PG3 genes, pr7 derived neurons PG2-4 genes and pr8 derived neurons PG2-5 genes. (B) *Hox* expression is maintained throughout migration and PN assembly. Moreover, PN neuron subsets originated from r6 or pr7-8 remain segregated and keep their relative position throughout tangential migration and settling in the forming PN, with r6-derived neurons being positioned dorsally in the stream and rostrally in the mature PN.

In compound *Hoxa5;Hoxb5;Hoxc5* null mutants, high levels of *Unc5b* are expressed throughout the AES (Di Meglio et al., 2013). *Unc5b* is highly expressed in r6 derived PN neurons, but has low expression in pr8 derived PN neurons (**Figure 5A**). The lack of this expression gradient in compound *Hox5* knockout mice thus suggests that *Hox5* genes normally inhibit *Unc5b* expression in the ventral AES (Di Meglio et al., 2013). Moreover, *Unc5b* overexpression results in anterior ectopic migration and stalled migration lateral to the normal nucleus (Di Meglio et al., 2013). Additionally, overexpression of *Netrin 1* (*Ntn1*)

in the r5 and r6 derived migratory environment of the AES leads to premature migration of Unc5b negative cells to the midline generating ectopic PN (Di Meglio et al., 2013). Differential *Hox* expression in the AES may therefore provide PN subsets with distinct UNC5B-dependent responses to environmental guidance cues (NTN1) and thus contribute to maintaining neuronal position during migration and nucleogenesis (**Figure 4**). Interestingly, *Ntn1* expression is epigenetically controlled (Di Meglio et al., 2013). Transcriptional silencing mediated by the polycomb protein EZH2 maintains the ventral restriction of *Ntn1* expression at the midline. Loss of *Ezh2* results in spatial expansion of the *Ntn1* expression domain and ectopic migration of *Unc5b* negative cells (**Figure 4C**, Di Meglio et al., 2013).

In summary, migrating PN neuron subsets are regulated through a tightly balanced mix of repulsive and attractive cues. Anterior, r6 derived, PN neurons migrating in the dorsal part of the AES lack *Hox4* and *Hox5* expression and display high expression levels of *Unc5b*, thus resulting in stronger repulsion from the midline than $Hox4^{+};Hox5^{+};Unc5b^{low}$ expressing neurons in more ventral aspects of the AES (Di Meglio et al., 2013). If such a tightly balanced signaling system is challenged through genetic manipulations, three distinct phenotypes can be observed in which PN neurons are derailed from their stereotypic migratory pathways. Neurons can either: (a) prematurely migrate ectopically and take a more posterior pathway; or, (b) be stalled generating an ectopic cluster lateral to their normal position; or, (c) migrate ectopically towards a more anterior position. It is predicted that for (a) mostly pr8 derived *Hox5* expressing, ventrally migrating neurons are affected, while for (b) and (c) mostly dorsally migrating, *Hox5* negative neurons are affected (Di Meglio et al., 2013). Also, the reduction of PN size observed in several mutant lines might in fact be due to selective loss of rostrocaudal (or early/late born) PN neuron subsets.

**Molecular determinants of PN connectivity**

At the same time when PN neurons reach their final position, axonal branches project towards the cerebellum. Mossy fiber afferents from the PN will eventually synapse with the granule cells. Several cell- and non-cell-autonomous molecular factors have been identified in rodents to regulate PN neuron axon growth, target selection and synapse formation.

Most of the mossy fibers emerging from BPN neurons target the contralateral cerebellum. The position of the neurons within the BPN is thought to be a determinant of the laterality of axonal projections (Cicirata et al., 2005). *ZIC1*, a zinc finger transcription factor expressed in mossy fiber BPN neurons was identified to regulate BPN neuron position as well as axon laterality (DiPietrantonio and Dymecki, 2009). In *Zic1* mutants, a higher number of mossy fiber afferents innervated the ipsilateral cerebellum, thus suggesting a role of *ZIC1* in self autonomously regulating the laterality of BPN mossy fibers (DiPietrantonio and Dymecki, 2009). At high expression levels, *ZIC1* may act to suppress activity of RIG1/ROBO3, an axon guidance molecule regulating laterality of axonal projections (Renier et al., 2010) in addition to regulating neuronal migration (see above). Moreover, several axon guidance molecules are implicated in the pathfinding of axons to the cerebellum. The previously discussed UNC5C receptor controls not only migration but also axon guidance of PN fibers to the cerebellum. PN projections of *Unc5c* mutants turn caudally or rostrally instead of directly projecting laterally towards the cerebellum (Kim and Ackerman, 2011). Additionally, the axon guidance molecule, semaphorin 3A (SEMA3A) and its receptor component neuropilin-1 *(NPN-1)* are potentially involved in selective targeting of the BPN neurons in the cerebellum (Solowska et al., 2002). BPN neurons express *Npn-1*, while *Sema3A* is expressed in the cerebellum. However, the expression of both *Npn-1* and *Sema3A* varies across the BPN and in different cerebellar regions or lobules, respectively. Due to varying expression of *Npn-1* along the

rostrocaudal axis of the BPN, a graded repulsive responsiveness to SEMA3A was identified in the BPN, with higher levels of responsiveness to SEMA3A rostrally as compared to caudally. Thus, high Npn-1 expressing BPN mossy fibers may selectively avoid high Sema3A expressing cerebellar lobules resulting in topographic connectivity of BPN axons. Upstream of this graded expression could be the *Hox* genes that have nested expression patterns within the PN and could have a similar role as upstream regulators in the PN as shown in other hindbrain nuclei (Gavalas et al., 1997; Oury et al., 2006; Bechara et al., 2015).

In a gene expression analysis of BPN neurons during development of the pontocerebellar mossy fibers, markers of axon elongation (for example, GAP43) were downregulated during early postnatal period and there was a simultaneous upregulation of synaptic markers (Díaz et al., 2002). The upregulation of synaptic markers is induced by interaction of mossy fibers with granule cells in the cerebellar cortex. In BPN neurons of the *weaver* mouse mutant, synaptic marker genes fail to upregulate (Díaz et al., 2002).

A key aspect of synapse formation is the regulation of axonal growth and arborization. As the axons reach their targets, the growth of axon should be regulated. In the pontocerebellar system, *Cadherin7* is expressed in both granule neurons and mossy fiber pontine neurons, regulates axonal growth when mossy fibers reach the granule layer and also initiates synapse formation (Kuwako et al., 2014). Upon downregulation of *Cadherin7*, mossy fibers fail to stop at the inner granule cell layer and instead extend up to the molecular layer where they synapse with the Purkinje cells. Neuregulins, a group of signaling proteins having known roles in development and maintenance of the nervous system have also been implicated in the maturation of pontocerebellar afferents. Neuregulins, specifically NRGbeta1, are expressed at the synapses between mossy fibers and granule cells (Ozaki et al., 2000). The expression of membrane-anchored forms at the synapse suggests a role in junction formation.

Several other factors control growth, survival and differentiation of synapses within the granule cell layers. Among the first factors shown to influence the development of pontocerebellar mossy fibers are the neurotrophic factors BDNF and NT4/5 that increase survival and collateralization of BPN projections in rodents *in vitro* (Rabacchi et al., 1999a). WNT-7a is another signaling molecule released from cerebellar granule cells that controls mossy fiber development. WNT-7a is involved in mossy fiber synapse maturation (Hall et al., 2000). WNT-7a induces mossy fiber axonal remodeling, a process characterized by shortening of axons, axonal branching and increase in growth cone size, and synapsin 1 clustering in the mossy fiber terminals. Thus WNT-7a acts as a synapse-initiating factor in the pontocerebellar mossy fiber maturation.

Purkinje cells that are positioned adjacent to the granule cell layer play an important role for the development of the pontocerebellar fibers. Interestingly, during early postnatal periods, mossy fibers transiently contact Purkinje cells. However, as development proceeds, these synapses are eliminated. Several studies have identified molecular mechanisms regulating the growth of mossy fibers at the level of Purkinje cells. BMP4, a patterning molecule, is expressed in the Purkinje cells during early postnatal periods. In Purkinje cells in which BMP4 was conditionally deleted, the elimination of mossy fiber- Purkinje cell contacts were decreased by half suggesting a retrograde role of BMP4 in target specificity of the mossy fiber afferents (Kalinovsky et al., 2011). SEMA3A (also referred to as COLLAPSIN-1 or SEMAD) is another molecule expressed in cerebellar Purkinje cells. *In vitro* studies performed in chick and mouse indicated that SEMA3A, prevents mossy fiber afferents from innervating Purkinje cells by initiating collapse of growth cones (Rabacchi et al., 1999b). This effect of SEMA3A was restricted to only mossy fiber growth cones and no effect was seen on the climbing fibers (Rabacchi et al., 1999b).

**Function and basic connectivity of the PN**

The PN receive their major input from the cerebral cortex and most prominently project as mossy fibers to the granule cell layer of the cerebellum. Consequently, the PN have received most attention for their integral position in the cerebro- cerebellar communication. PN are hypothesized to serve as a first integrator of the information from cortical regions and adapt these signals for the use of the cerebellum (Schwarz and Thier, 1999). They are part of several closed loop systems, including the corticopontine–cerebellar–thalamic loop (Apps and Hawkes, 2009). Additionally, the PN not only project to the cerebellum, they also exhibit reciprocal connections with the deep cerebellar nuclei. Simplified models of PN function have suggested that PN neurons receive an ‘‘efference copy’’ of motor commands and process this information for the use of the cerebellum. In the cerebellum, motor plan (also referred to as ‘‘internal model’’), sensory feedback, and actual performance are compared and eventual arising discrepancies are fed back to the cortex to modify further motor movements (Ito, 2008; Grimaldi and Manto, 2012). This provides a functional framework for complex motor behaviors, where sequences of precise muscle contractions have to be executed. Also, it provides the structural basis of motor learning, during which cerebellar circuits are modified.

**The topography of the cortico-pontine projection: how much of the cortical organization is in the pontine nuclei?**

The majority of PN afferents arise in the cerebral cortex. Axons of cortical layer V neurons project through the cortico- fugal/cortico-spinal tract onto the PN (**Figures 9**, **10**). In rodents, this innervation is formed shortly after birth. Two days after the corticospinal tracts bypass the developing PN, fibers or collaterals from these axonal tracts start growing into the PN forming corticopontine fibers (Leergaard et al., 1995). Several experiments suggest that the innervation is triggered by the PN neurons, since ectopically migrating neurons are innervated as well (Zhu et al., 2009; Di Meglio et al., 2013).

Both BPN and RTN receive afferents from layer V neurons of the ipsilateral cortex. However, the cortical innervation of BPN is more prominent, compared to that of RTN. Several subcortical inputs to the PN have been described. These include inputs from the spinal cord, the superior and inferior colliculus, the mammillary body, the trigeminal nuclei and the dorsal column nuclei just to name a few (summarized in Paxinos, 2014). The cortical innervation of the PN has been studied intensively. Fibers originate from sensory (somatosensory, visual, and auditory) and motor cortices with additional contributions from the caudal temporal and perirhinal cortex (Cicirata et al., 2005). The RTN predominantly receive afferents from the cingular cortex with fewer contributions from the motor and sensory cortices. Interestingly, less overlap is observed in the cortical afferents terminating in the BPN, whereas the extent of overlap in the RTN is higher, which suggests stronger convergence of information from different cortical areas in the RTN (Brodal and Brodal, 1971).

A remarkable feature of the corticopontine projections is the precise pattern of their termination in the PN. Focal tracer injections in the cerebral cortex helped in delineating the projection pattern of corticopontine projections in rodents. An at least partially topographic

organization could be shown for the pathway from cerebral cortex to the pons (Brodal, 1968; Leergaard et al., 1995, 2000, 2004, 2006; Leergaard, 2003; Odeh et al., 2005; Leergaard and Bjaalie, 2007). Distinct regions in the cortex tend to project to relatively segregated regions in the PN, with only limited overlap, thus partially preserving the cortical spatial organization (**Figures 9**, **10**). Frontal cortex projects rostrally and medially in the PN, parietal cortex projects to central and caudal parts, temporal cortex to central and lateral regions and occipital cortex projects to lateral and rostral parts of the PN (Leergaard and Bjaalie, 2007). Although the projections are governed by a topographical pattern, convergent as well as divergent projections can be found (Mihailoff, 1983; Nikundiwe et al., 1994), the overall convergence of corticopontine to pontocerebellar neurons being 2:1 (Brodal and Bjaalie, 1992).

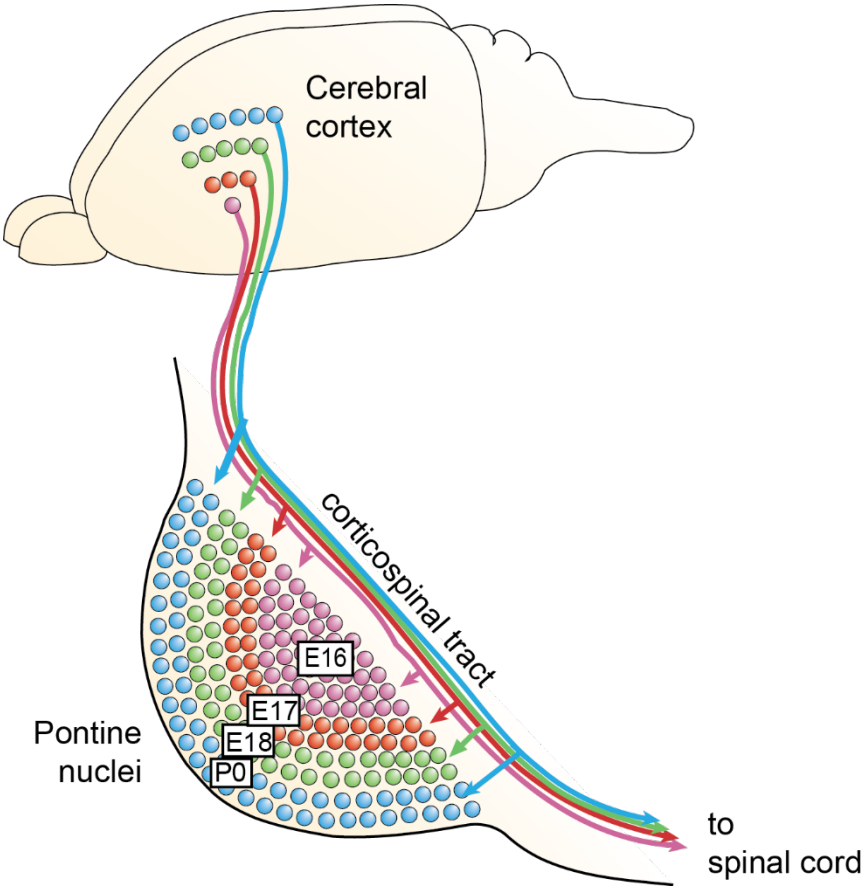

**Figure 9: The chrono-architectonic hypothesis of cortico-pontine circuit development.** During development, PN neurons settle in the pontine nuclei (PN) in a shell-like fashion according to their birthdate. Early born neurons form the center of the PN, later born neurons consecutively settle around the earlier born neurons forming concentric rings (Altman and Bayer, 1987d). Similarly, it has been suggested that collaterals of the corticospinal axons innervate the PN topographically at early postnatal stages in a shell-like fashion (Leergaard et al., 1995). This suggests that the birthdate of PN neurons can be linked to both nucleogenesis and spatial organization of cortical inputs (Altman and Bayer, 1997). Consequently, intrinsic differences in PN neurons born at different stages could have an instructive role for patterning the architecture of the PN as well as their innervation (Adapted with permission from Leergaard et al., 2000, Wiley).

The topography of corticopontine projections is also maintained within the representation of the somatosensory modality. Tactile information from the body is somatotopically mapped onto the primary somatosensory cortex. This information is projected to the PN largely maintaining the somatotopy of the information (Leergaard et al., 2006). In support of this, pontine neuron dendritic fields remain largely constrained within the area targeted by a single cortical region (Schwarz and Thier, 1995). It is noteworthy, however, that some PN neurons have large dendritic fields, receiving information from various cortical locations, therefore suggesting that integration of sensory information might happen already at the level of the PN (Schwarz and Thier, 1995).

The concentric ‘‘inside-out’’ temporal gradient of neuronal organization in the PN might correlate with patterned axonal input related to temporal maturational gradients of layer V cortical neurons—referred to as the chrono-architectonic hypothesis (Altman and Bayer, 1997). The earliest arriving corticopontine fibers grow into the core of PN, where the earliest born PN neurons have settled. Step by step, the PN are innervated in an inside-out fashion. Consequently, a causal link between birthdate/arrival of PN neurons and birthdate/arrival of projections at the PN was proposed (Altman and Bayer, 1987d, 1997; Leergaard et al., 1995; **Figures 9**, **10**). Also, cortical areas are broadly pre-patterned along the rostrocaudal axis by

the graded activity of homeobox transcription factors (O'Leary et al., 2007). It is noteworthy that rostrocaudal pre-patterning and regionalization is also observed in the developing PN as described before, thus intersecting spatial dimension to the temporal gradient model (**Figure 7**). Both timing and rostrocaudal information could generate a complex morphogenetic field that might contribute to the target selection of cortico-pontine and ponto-cerebellar fibers.

In contrast to most other precerebellar nuclei, PN also receive significant innervation from non-somatosensory cortices including the visual and auditory cortices—as shown in several mammalian species including rodents, rabbits, cats and monkeys. In particular, the RTN and the dorso-lateral pontine nucleus (DLPN) constitute a major relay for visual and visuomotor input into the cerebellum (Glickstein et al., 1980, 1994; Thielert and Thier, 1993). The DLPN has been particularly well analyzed. It receives major inputs from the visual cortex (Glickstein et al., 1980, 1994) and auditory cortex (Perales et al., 2006). The DLPN has been involved in optokinetic nystagmus including smooth- pursuit eye movements, ocular following, visually guided motor learning (Tziridis et al., 2009, 2012) and visually guided eye movements (May et al., 1988; Thier et al., 1988; Ono et al., 2003; Thier and Möck, 2006).

Several other subcortical and spinal cord regions are also known to provide input to the PN, however these projections account for only a small fraction of afferents to the PN. Subcortical structures projecting to the BPN have been broadly classified in two groups based on their projection pattern (Brodal and Bjaalie, 1992). The first group includes nuclei which project to BPN in a diffused manner. These nuclei include reticular formation, raphe nuclei, nucleus coeruleus and periaqueductal gray (summarized in Paxinos, 2014). The second group is composed of nuclei with at least partially topographic projections in the BPN. This group includes the superior colliculus, medial mammillary nucleus, trigeminal nucleus, dorsal column nuclei, the spinal cord, the pretectal nuclei, zona incerta and intracerebellar nuclei

(**Figure 10**; summarized in Paxinos, 2014). It is interesting to note that in the BPN, specific subcortical afferents overlap with cortical afferents arising from regions which are functionally related. One of the best examples are projections from dorsal column nuclei that topographically overlap with the afferents from limb specific somatosensory cortex (Kosinski et al., 1986).

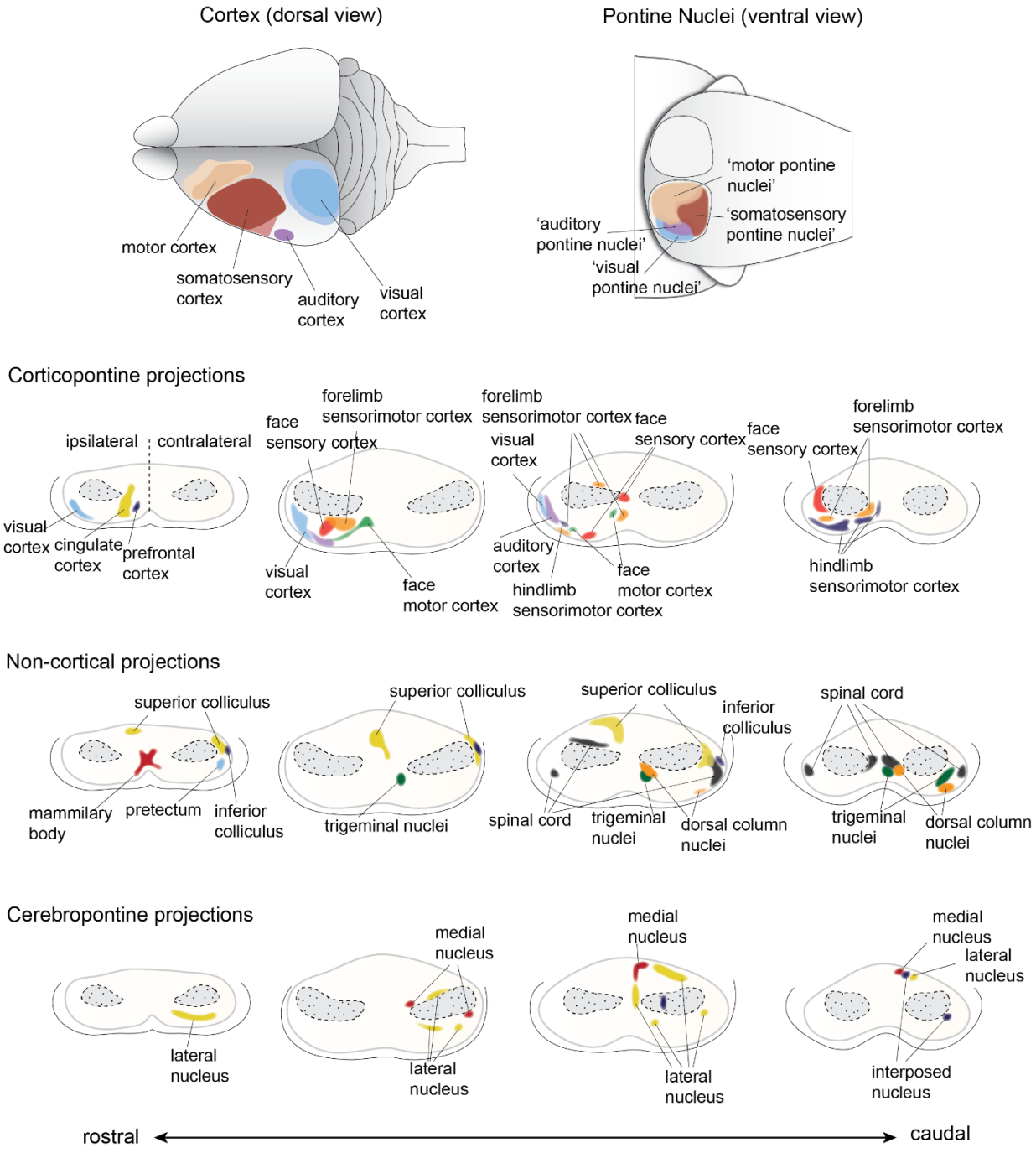

**Figure 10: Input innervations of the pontine nuclei (PN)**. Pontine nuclei mainly receive projections from the cortex and partially also from subcortical regions. Using dye tracings, innervation patterns from various cortical and subcortical areas were identified. Cortical projections mainly innervate the ipsilateral PN, while subcortical projections innervate both ipsilateral and contralateral PN. Simplified model of cortico-pontine connectivity have but forward the idea that the topography of cortical regions is roughly maintained in the PN (top panel), with auditory and visual cortex projecting to the dorso-lateral parts of the PN, motor cortex projecting to the rostral and medial areas and somatosensory cortex projecting to the caudal regions of the PN (Brodal, 1968; Leergaard, 2003; Leergaard and Bjaalie, 2007; Leergaard et al., 1995; 2000; 2004; 2006; Odeh et al., 2005). But, the cortical spatial organization is only partially maintained, several cortical areas innervate multiple areas in the PN. Additionally, subcortical areas including superior and inferior colliculus, spinal cord and trigeminal nuclei and pretectum, but also the cerebellar nuclei project onto the PN (Kosinski et al., 1986). Here, often projections from cortex and subcortical regions representing similar information target the same region of the PN (Figure modified from Paxinos, 2014).

**Ponto-cerebellar projections of pontine nuclei**

While a broad topographic organization of the cortico-pontine projections is well established and described in detail (Leergaard et al., 2006; Leergaard and Bjaalie, 2007), the logic behind the connectivity patterns from PN to the cerebellum has been debated for many decades (Apps and Hawkes, 2009). Projections from PN to cerebellum have been intensively studied in rats (Azizi et al., 1981; Mihailoff et al., 1981) and monkeys (Brodal, 1982) by performing retrograde tracing experiments. BPN and RTN project to multiple locations in both cerebellar vermis and hemispheres (Azizi et al., 1981; Mihailoff et al., 1981; Paxinos, 2014; **Figure 11**). There is evidence for a high degree of divergence and convergence of projections/terminations of single PN neurons or clusters of PN neurons. Divergence is suggested by the fact that neurons located in close by regions within BPN or RTN are labelled by distant cerebellar injection sites, convergence is put forward by the fact that restricted cerebellar injections result in the retrograde labelling of spatially distinct neuron

populations within BPN (Azizi et al., 1981; Mihailoff et al., 1981). A few single neurons can also project to multiple lobules (Bolstad et al., 2007). Therefore, the complexity of the cerebrocerebellar connectivity seems to arise from properties of the PN that do not simply relay information from the cortex but redistribute permutations of information from cortical sensory and motor input in a convergent and divergent manner to different areas of the cerebellum. Such connectivity patterns are essential for distributing information from discrete cortical regions to multiple lobules of the cerebellum. The cerebrocerebellar connectivity patterns have therefore both a partially topographic as well as a non-continuous or ‘‘fractured’’ organization.

PN mossy fibers have collateral branches targeting the deep cerebellar nuclei. Little overlap is observed between the termination zones of BPN and RTN neurons within cerebellar nuclei. BPN projects mostly to the lateroventral part of the nucleus lateralis and caudoventral part of the nucleus interpositus anterior. Projections from the RTN are mostly observed in the nucleus medialis and mediodorsal part of the nucleus lateralis (Cicirata et al., 2005). The number of cerebellar fibers arising from BPN are higher than those from RTN. The distinct connectivity of BPN and RTN cannot be explained on the basis of differences in the maturation of projection neurons in these nuclei as dendritic field, number of branching points, or the length of terminal dendrites of the neurons in BPN and RTN are similar (Schwarz et al., 1996). Although some differences were observed, such as larger somata and more primary dendrites in the projection neurons located dorsally than ventrally, these differences are more reflective of the dorsoventral positioning rather than nucleus-specific properties.

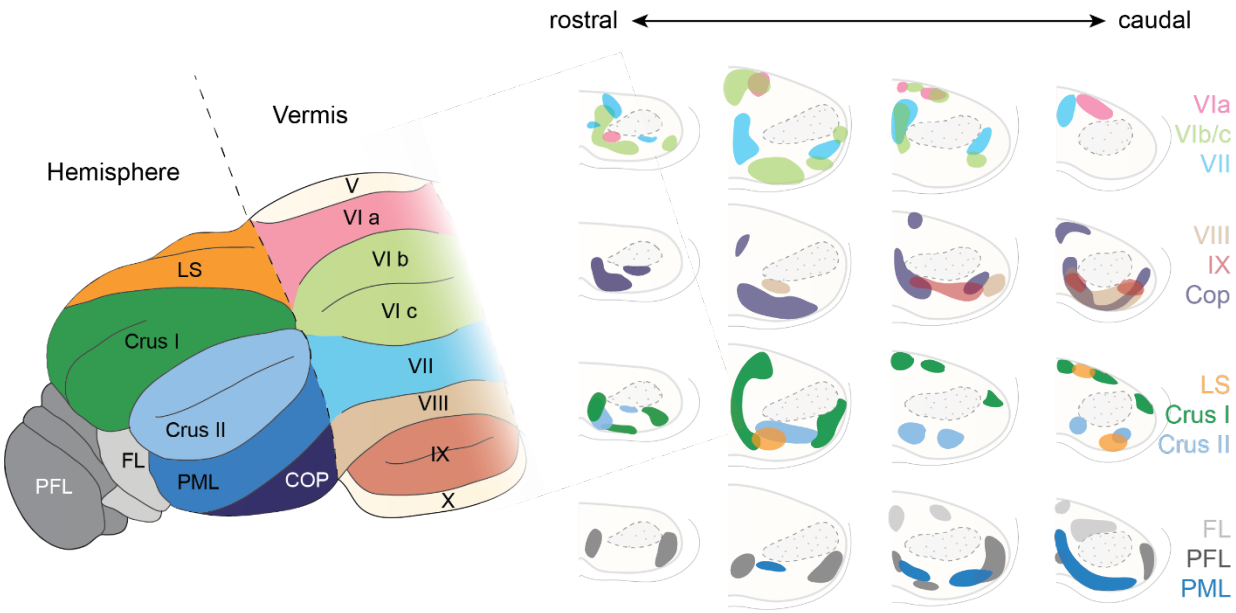


**Figure 11: Topography of the ponto-cerebellar projections**. The pontine nuclei (PN) project to lobules VI to IX of the vermis as well as to the cerebellar hemispheres including LS, Crus I and II, PML, COP, PFL and FL. Projections from the rostral and lateral regions of the PN, corresponding to the visual areas innervate mostly the PFL that are part of the vestibulocerebellum that are also strongly innervated by vestibular nuclei, whereas COP mostly receives projections from the rostral and dorsal region of the PN. Several cerebellar areas including lobe VIa or the flocculus are mainly innervated by the retinotegmental nuclei portion of the PN. The basal pontine nuclei strongly innervate Crus I and II, PML as well as in lobes VIb,c and VIII. In general ponto-cerebellar projections display strong overlap suggesting distribution of the information from a single region in the PN to various lobules in the cerebellum. LS, lobule simplex, PML, paramedian lobule, COP, copula, PFL, paraflocculus, FL, flocculus.

How the complex patterns of pontocerebellar connectivity are achieved is poorly understood. Most tracing data (Azizi et al., 1981; Mihailoff et al., 1981; Broch-Smith and Brodal, 1990) suggest that neither the temporal (inside-out) nor other spatial distribution of PN neurons might be major determinants for the establishment of the pontocerebellar connectivity patterns. Cells labelled by retrograde tracings of specific lobule do not cluster unambiguously along inside-out, mediolateral or rostrocaudal axes in the PN (Azizi et al., 1981; Mihailoff et al., 1981; Broch-Smith and Brodal, 1990). On the other hand, retrograde tracing experiments

performed in cats (Broch-Smith and Brodal, 1990; Nikundiwe et al., 1994) have shown that more than 70% of the neurons labelled after injections in the paraflocculus are located in the rostral half of the PN and have a lamellar-like organization (Nikundiwe et al., 1994). The paraflocculus projecting areas of the PN mainly get inputs from visual, parietal associative and to a lesser extent from primary and secondary sensory and primary motor cortical areas, but almost no input from secondary motor areas and prefrontal cortex (Broch-Smith and Brodal, 1990; Nikundiwe et al., 1994). Interestingly, it has been also shown that the pattern of cerebropontocerebellar projections converges with somatotopically equivalent projections from the inferior olive (Odeh et al., 2005), suggesting common organizational principles across precerebellar nuclei.

**Evolution of the pontine nuclei and cortico-ponto-cerebellar connectivity**

PN have been analyzed in mammals from rats (Mihailoff et al., 1978) to opossums (Mihailoff and King, 1975), cats (Hoddevik, 1975) and macaques (Glickstein et al., 1980). The PN are often considered as structures specific to mammals and have been poorly described in other amniotes such as reptiles and birds. If the structures found in amniotes are indeed PN homologous structures is debated. Two populations of PN, referred to as medial pontine nucleus and lateral pontine nucleus have been described in chicken (Brodal et al., 1950; Marín and Puelles, 1995). These two populations are located medially and laterally to the midline at the level of r3/r4 and originate at the posterior rhombic lip (Marín and Puelles, 1995). Birds neither have cortico-spinal tracts (Aboitiz et al., 2003) nor pronounced cerebellar hemispheres, their cerebella consisting almost entirely of the vermis (Sultan and Glickstein, 2007). Therefore, PN neurons lack the main input (cortex) as well as their main output areas (cerebellar hemispheres). Nonetheless, they share some striking similarities with two nuclei

that exist also in rodents, namely the RTN and the recently described interfascicular trigeminal nucleus (Fu et al., 2013). Both nuclei are strongly innervated by subcortical areas (and have only minor input from the cortex) and profusely project to the vermis in rodents (Azizi et al., 1981; Mihailoff et al., 1981; Fu et al., 2011). The mammalian RTN is for example involved in processing visual information and strongly innervated by subcortical afferents as e.g., from tectum (superior colliculus), by which it receives visual and oculomotor information (Thielert and Thier, 1993). Considering the importance of the visual and oculomotor system in amniotes in contrast to somatosensory and tactile information (Naumann et al., 2015), we speculate that a primitive mammalian ponto- cerebellar system might have processed only visual and vestibular information. Mammals as rodents and monkeys extensively use the somatosensory sense to experience their environment, especially by the use of whiskers (rodents and cats), lips and paws/hands (monkeys), which might explain the expansion of the cortico-ponto-cerebellar system and the stronger projections of somatosensory and motor areas.

Hence, the coevolution of cortex, PN and cerebellar hemispheres, the three components of the cortico-ponto- cerebellar circuit, may have played a pivotal role for the evolution of complex motor behaviors (including the corresponding sensory feedback), since all three areas increased dramatically in size throughout evolution. In humans, more than a third of the hindbrain is occupied by the PN, and both cortex and cerebellar hemispheres increased greatly in volume (the hemispheres are also referred to as cerebro- or neo-cerebellum). A further interesting observation on the evolution of the cortex is that the cortical area subdivisions well described in rodents, monkeys and humans (Rakic, 2009) are not as strictly topographically segregated in monotremes and marsupials, the sister groups of mammals (Lende, 1963, 1964; Krubitzer, 2007) and are absent in non-mammalian vertebrates (Aboitiz et al., 2003). Marsupials as the opossum and wallaby (Lende, 1963) and monotremes (Lende, 1964) have

a strong to almost complete overlap of somatosensory and motor areas in the cortex (Aboitiz et al., 2003).

The spatial segregation of distinct somatic motor and sensory representations came along with the increasing size of cortical areas as well as with the interpretation of sensory information and the control of motor behavior (Aboitiz et al., 2003; Rakic, 2009). Interestingly, spatial segregation is less obvious in the cerebellum (Apps and Hawkes, 2009), due to the functional role of the cerebellum as a major integrator of motor and sensory information. The PN evolved during early mammalian evolution, at a time when neocortex and neocerebellum (the hemispheres) evolved from the dorsal pallium and in the cerebellum, respectively. Cortex and cerebellum have a strikingly correlated volumetric evolution (Barton, 2002) further suggesting a strong link between the evolution of these two brain regions. It is also likely that the main structure connecting these two areas has an important function during the evolution of these two systems. From an evolutionary-developmental perspective, it might be postulated that the highly convergent and divergent circuitry between cortex and cerebellum are reminiscent of the cortical features of evolutionarily early mammals in which somatosensory and motor areas were partially overlapping, as it is still in the PN of more derived mammalian species. Hence, it is possible that the evolution of an increased connectivity with the cerebellum resulted in a gradual transfer of integrative computations that were performed in the cortex of ancestral mammals to the cerebellum of derived mammals. From an evolutionary standpoint this could explain the gradual decrease of sensory topography along the cortico-ponto- cerebellar pathway. It coincides with stronger divergence and convergence of connections transforming the somatotopically continuous sensory maps in the cortex over PN to the fractured somatotopy in the cerebellum, serving to integrate sensory- motor information.

**Conclusions and outstanding questions**

The PN are a suitable system to study processes of neuronal development from early specification to neuronal migration, axon guidance, target selection and synaptic refinement. Also, the PN can be considered as part of one of the most complex neuronal circuits within the brain—not only in terms of connectivity pattern but also function. Several questions remain that are of central importance for a better understanding of brain development and function. One of the most puzzling topics in developmental neuroscience is how complex circuitry emerges from homogenous cell populations. For the PN it has been suggested that both the rostrocaudal origin and the birthdate of PN neurons are determinants of their connectivity (Altman and Bayer, 1987d, 1997; Leergaard et al., 1995; Di Meglio et al., 2013). However, the molecular logic behind the complex input-output PN connectivity patterns has not been fully uncovered. For a better understanding of the molecular determinants of PN connectivity, a combination of tools and approaches will be necessary. First, approaches that combine connectivity pattern analysis with markers for birthdate, rostro- caudal origin and other available markers are necessary. Second, due to the complexity of the circuit, a focus on single PN neuron molecular identity and associated wiring will be required. Single-cell transcriptomics can help to understand the transcriptional diversity that in turn control differences in projection patterns and innervation among PN neurons. Also the wealth of transgenic lines that exist nowadays can be used in combination with *in utero* electroporation and transynaptic virus tracing (Wickersham et al., 2007) to analyze the connectivity and transcriptional profile of specific PN subsets. This includes rostrocaudal subsets that can be targeted using *Hox* gene enhancers driving Cre expression (Di Meglio et al., 2013), or PN neuron subsets with different birthdates that can be labeled using *in utero* electroporation at different embryonal stages or by *CreER*$^{T2}$ lines (Machold and Fishell, 2005). Also, the

evolutionary origin of the PN and cortico- ponto-cerebellar connectivity would be an exciting research focus. With the expanding toolset for gene editing in non-model organisms this might become feasible (Kratochwil and Meyer, 2015).

These are exciting times in developmental neuroscience, where we can expect great advances in understanding the molecular determinants of complex neural circuitry. The PN are a wonderful system that allows studying all developmental processes from progenitor specification to synapse formation.

**Acknowledgements**

We are grateful to T. Di Meglio for valuable comments on the manuscript. The Swiss National Science Foundation (P2BSP3_148629), the EU FP7 Marie Curie Zukunftskolleg Incoming Fellowship Program (grant no. 291784), the Deutsche Forschungsgemeinschaft (DFG; KR 4670/2-1), the Young Scholar Fund of the University of Konstanz and the Elite Program for Postdocs of the Baden-Württemberg Stiftung funded C.F.K. F.M.R. is supported by the Swiss National Science Foundation (31003A_149573) and ARSEP. All authors have been funded by the Novartis Research Foundation.

**Statement of contribution**: C.F.K., U.M., and F.M.R. conceived and discussed the topic, organization, and layout of the review article. CFK and UM wrote an initial draft of the manuscript and prepared the figures. FMR revised and finalized the article.

## 1.5 AIM OF THE THESIS

In the vertebrate brain, individual nuclei receive several inputs and in turn project to several other brain areas. In particular, nuclei are often organized in largely segregated sub-circuits with distinct input-output connectivity, often topographically organized, and carrying distinct information. How these complex wiring diagrams are established by intrinsic vs. extrinsic mechanisms is still poorly understood. Transcription factors are instrumental during development in establishing the subtype identity of distinct classes of neurons (e.g. neurotransmitter identity, cortical layer-specific identity, etc.). However, whether additional subsets of transcription factors are involved in orchestrating intra-nuclear sub-circuit diversification of neurons of similar subtype identity is unknown.

In mammals, the cerebellum is one main area of the brain involved in the control of motor activity. Motor and sensory information from the cortex is primarily relayed to the cerebellum via the mossy fiber precerebellar pontine nuclei (PN) present in the ventral hindbrain. PN receive topographically organized input from various cortical areas, including major motor and sensory areas, and 'relay' such information to several cerebellar lobules without an obvious topography. Virtually nothing is known about the molecular and cellular mechanisms underlying the logic of assembling these complex input-output sub-circuit patterns in the pontine nuclei.

The developing hindbrain is rostrocaudally segregated into progenitor cell compartments, or rhombomeres (r1-r8). Mouse pontine neurons are generated from a stripe of dorsal progenitors, the lower rhombic lip, in rhombomeres r6-r8. Recent studies from our lab showed that the pontine nuclei are assembled from topographically organised subsets of rhombic lip derived neurons settling along the rostrocaudal axis of the nuclei and expressing distinct subsets of Hox transcription factors. Hox paralogue group 2 (*Hox2*) and *Hox3* genes

are expressed throughout the pontine nuclei, whereas the expression of *Hox5* genes is restricted to the posterior PN (Di Meglio et al., 2013). Interestingly, unlike other *Hox* genes which are expressed at the progenitor level and maintained in postmitotic pontine neurons, *Hox5* genes are only induced postmitotically, thus defining a unique cluster of pontine neurons segregated at a specific posterior location in the nucleus. Thus, *Hox5*$^{+}$ neurons provide a suitable model to address the role of Hox5 genes in the diversification of cortico-ponto-cerebellar sub-circuits. In this thesis, I wish to address this broad question by focusing on two main aims.

**Aim 1 – To unravel the complex logic of the pontine input connectivity.**

To achieve this goal, we aim to understand the development of selected pontine neurons, which receive specific visual or somatosensory input from the cortex and relay this information to the cerebellum. It is already known that a topographic arrangement is maintained by the cortical afferents upon targeting the PN (Leergard et al., 2006 and 2007). Cortical fibers arising in the primary somatosensory cortex (S1) arborize in the caudal part of the PN whereas primary visual neurons project to the rostral region of the PN. Since neurons have a distinct *Hox* identity along the PN rostro-caudal axis, we wished to investigate the contribution of Hox factors in regulating cues for the topographic targeting of cortical afferents of specific PN neuron subsets.

To understand the input connectivity of PN neurons and the role of *Hox5* genes towards it, I first focused on identifying the role of *Hox5* genes in the formation of PN. By using *in utero* electroporation, I could overexpress *Hoxa5* gene specifically in the neurons born from IRL. I identified that *Hoxa5* gene expression drives PN neurons to a posterior location. Moreover,

I identified that the observed posterior displacement of *Hoxa5* overexpressing PN neurons could be in part explained by the downregulation of *Unc5b* expression.

By using trans-synaptic rabies virus tracing techniques, I showed that S1 cortical afferents are mono-synaptically connected with neurons in the caudal PN whereas V1 neurons connect to more anterior regions in the PN. By overexpressing *Hoxa5* in PN neurons and tracing their connectivity, I identified that *Hoxa5* expression in PN neurons is sufficient to select input from somatosensory limb specific cortical afferents while these neurons received reduced input from visual cortex. To further analyze the effect of *Hox5* gene expression on the topography of cortical afferents in PN, I overexpressed *Hoxa5* gene in PN neurons late during development by using tamoxifen dependent Cre plasmids in in-utero electroporation and then assessed the changes in PN neuron inputs. I focused mainly on the cortical inputs arising in the somatosensory cortex and visual cortex and overexpressed *Hoxa5* at E18.5, when PN nucleation is complete. Overexpression of *Hoxa5* at E18.5, resulted in *Hoxa5* overexpressing neurons spreading throughout the rostro-caudal extent of PN. These neurons showed no such preference in connecting with limb specific cortical regions. However, they still received significantly reduced input from the visual cortical region. By performing anterograde tracing from the cortex, I further showed that ectopic expression of *Hoxa5* in anterior PN neurons is sufficient to attract cortical somatosensory afferents to the anterior PN.

In summary, *Hoxa5* expression in randomly selected subsets of PN neurons is sufficient to integrate them in a specific connectivity sub-network relaying mainly somatosensory information while at the same time avoiding visual input.

**Aim 2 - To understand the involvement of *Hox* genes in the output connectivity of PN to the cerebellum.**

PN neurons send mossy fiber projection to the lateral hemispheres of the cerebellum but very little is known if different rostro-caudally defined (defined by Hox expression pattern) PN neuron subsets project to distinct target regions in the cerebellum. To understand the output connectivity of pontine neurons we used mouse lines labeling specific subsets of pontine neurons namely, *MafBCre::ERT2*, *ChAT::Cre* and *Hoxa5::CreERT2*, which specifically label Hoxa5 negative (*Mafb::CreERT2* and *ChAT::Cre*) and Hoxa5 positive (*Hoxa5::CreERT2*) subsets respectively in the precerebellar nuclei. We observed the projections in the cerebellar lobules by crossing these mouse lines with a reporter line. For tracing PN specific inputs from the *ChAT::Cre* and *Hoxa5::CreERT2* mouse lines, we electroporated lRL progenitors with a floxed EGFP construct. My results show that Hoxa5 expressing PN neurons project to multiple lobules of cerebellum involved in somatosensation while projections from Hoxa5 negative subsets in *Mafb::CreERT2* mostly localized to the paraflocculus, a lobule of cerebellum well known for its role in the visual system. Projections from *ChAT*$^{+}$ PN neurons were identified in the paraflocculus and to a lower extent also in lobules involved in somatosensation.

# CHAPTER 2: RESULTS

## 2.1 Postmitotic *Hoxa5* expression specifies pontine neuron positional identity and input connectivity of cortical afferent subsets. (Manuscript accepted in *Cell Reports*)


### Abstract

Cortical input is relayed to the cerebellum mainly via the precerebellar pontine nuclei. Cortical afferents are mapped in a topographic manner onto the pontine nucleus. However, very little is known about the molecular determinants of corticopontine circuit formation. We recently found that the pontine nucleus is composed of a heterogeneous population of neurons expressing distinct Hox genes (Di Meglio et al., Science 2013). Here, we asked whether Hox expression in pontine neurons is instructive to select topographic input from selected cortical afferents. In particular, we focused on the functional involvement of Hox paralogue group 5 (*Hox5*) genes. Hox5 genes are only expressed in a subset of migrating pontine neurons (Di Meglio et al., 2013). In the present study, we discovered how this spatial heterogeneity of pontine neurons is achieved.

We found that *Hox5* genes are not expressed in rhombic lip progenitors and only induced in posterior subsets of migrating postmitotic pontine neurons by local response to retinoic acid (RA) signalling. We further show *in vivo* that *Hox5* genes are poised for transcriptional induction but kept epigenetically silenced in rhombic lip progenitors by the Polycomb Repressive Complex 2, as assessed by *Ezh2* deletion. Only in posterior pontine neuron subsets, high levels of RA from meninges and the H3K27 demethylase JmjD3 are able to alleviate Ezh2-dependent chromatin repression and induce the expression of *Hox5* genes at the onset of their migration. We further show that both JmjD3 and Retinoic Acid

Receptor (RAR) directly bind to a Hoxa5 specific retinoic acid response enhancer and that response to RA induces 3D chromatin folding changes at Hox5 gene loci *in vivo*. Furthermore, we discovered that maintenance of *Hoxa5* expression throughout the migration of posterior precerebellar pontine neurons is a key determinant of their settling position in the forming pontine nucleus. In fact, ectopic expression of Hoxa5 in migrating anterior pontine neurons is sufficient to drive them to a posterior position in part by regulating the expression of the guidance molecule Unc5b.

Perhaps most importantly, we show, by transsynaptic rabies virus tracing, that Hoxa5 expressing pontine neurons preferentially connect with limb somatosensory cortical neurons. *Hoxa5* also provides an intrinsic cue to pontine neurons to repel visual cortical input and attract somatosensory cortical afferents, even when Hoxa5 is ectopically expressed in anterior pontine neurons after their migration and settling in the nucleus. Thus, Hoxa5 provides instructive cues to incoming cortical afferents, independently of the position of pontine neurons. We finally show that Hoxa5 expression in pontine neurons can regulate a unique transcriptional program, which could underlie specific connectivity of Hoxa5 expressing pontine neurons.

**Statement of contribution**: I designed and performed all the experiments to identify the role of *Hoxa5* in pontine neuron migration and shaping cortico-pontine connectivity.

# Postmitotic *Hoxa5* Expression Specifies Pontine Neuron Positional Identity and Input Connectivity of Cortical Afferent Subsets

Upasana Maheshwari[1,2,*], Dominik Kraus[1,2,*], Nathalie Vilain[1], Sjoerd J. B. Holwerda[1,3], Vanja Cankovic[1], Nicola A. Maiorano[1], Hubertus Kohler[1], Daisuke Satoh[1,4], Markus Sigrist[1,4], Silvia Arber[1,4], Claudius F. Kratochwil[1,5], Thomas Di Meglio[1,6], Sebastien Ducret[1], and Filippo M. Rijli[1,2,7]

[1]Friedrich Miescher Institute for Biomedical Research, Maulbeerstrasse 66, 4058 Basel, Switzerland

[2]University of Basel, 4051 Basel, Switzerland

[3]Present address: Novartis Institutes for Biomedical Research, Novartis Pharma AG, Basel, Switzerland

[4]Biozentrum, University of Basel, Kingelbergstrasse 70, 4056 Basel, Switzerland

[5]Present address: Chair in Zoology and Evolutionary Biology, Department of Biology, University of Konstanz, Konstanz, Germany

[6]Present address: Universidad Autónoma de Madrid, Centro de Biología Molecular, Cabrera 1, 28049 Madrid, Spain

*These authors have equally contributed to this work

[7]Correspondence : Filippo M. Rijli (filippo.rijli@fmi.ch)

## SUMMARY

The mammalian precerebellar pontine gray nucleus (PN) has a main role in relaying cortical information to the cerebellum. The molecular determinants establishing ordered connectivity patterns between cortical afferents and precerebellar neurons are largely unknown. We show that expression of Hox5 transcription factors is induced in specific subsets of postmitotic PN neurons at migration onset. *Hox5* induction is achieved by response to retinoic acid signaling resulting in Jmjd3-dependent derepression of Polycomb chromatin and 3D conformational changes. Hoxa5 drives neurons to settle posteriorly in the PN, where they are monosynaptically targeted by cortical neuron subsets mainly carrying limb somatosensation. Furthermore, *Hoxa5* postmigratory ectopic expression in PN neurons is sufficient to attract cortical somatosensory inputs irrespective of position and avoid visual afferents. Transcriptome analysis further suggests that Hoxa5 is involved in circuit formation. Thus, *Hoxa5* coordinates postmitotic specification, migration, settling position, and sub-circuit assembly of PN neuron subsets in the cortico-cerebellar pathway.

## INTRODUCTION

Neural circuit assembly sequentially involves neuronal fate specification, migration, and establishment of precise input-output axonal wiring and synaptic connectivity. Coordination among these processes is critical, especially when distant brain structures need to be topographically connected. Yet, molecular determinants able to coordinate these processes remain largely unknown.

The cerebral cortex and cerebellum are two major structures involved in sensorimotor coordination through extensive reciprocal connections (D'Angelo and Casali, 2012). Cerebro-cerebellar projections are mainly relayed through the mossy fiber projection

neurons of the precerebellar pontine gray nucleus (PN) (Allen and Tsukahara, 1974). In mice, PN neurons are generated in the caudal hindbrain between embryonic day 12.5 (E12.5) to E16.5 from the dorsal rhombomere (r) 6-8-derived *Wnt1*$^{+}$*/Atoh1*$^{+}$ progenitors of the lower rhombic lip (lRL) (Harkmark, 1954; Taber-Pierce, 1973; Tan and Le Douarin, 1991; Rodriguez and Dymecki, 2000; Wang et al., 2005; Farago et al., 2006; Di Meglio et al., 2013). From the lRL, PN neurons undergo a long-distance tangential migration forming the anterior extramural stream (AES) and settle in the rostral pons on both sides of the ventral midline (Altman and Bayer, 1987; Rodriguez and Dymecki, 2000).

Members of the Hox transcription factor family play important roles during hindbrain neuronal and circuit development (Philippidou and Dasen, 2013; Oury et al., 2006; Di Bonito et al., 2013; Bechara et al., 2015; Karmakar et al., 2017). In the precerebellar system, *Hox* expression molecularly defines specific subsets of rhombic lip progenitors and neurons migrating in the AES and settling in distinct rostrocaudal positions of the PN (Di Meglio et al., 2013). In particular, Hox paralogue group 5 (*Hox5*) expression defines neuron subsets migrating in ventral AES and settling in posterior PN; in dorsal AES, the *Unc5b* guidance receptor maintains positioning of *Hox5*-negative PN neurons which settle anteriorly in the PN, whereas *Unc5b* is downregulated in ventral AES by Hox5 factors (Di Meglio et al., 2013).

In the corticopontine pathway, axons from primary somatosensory (S1), visual (V1) or motor (M1) cortices mostly target centroposterior (S1), anterolateral (V1) or medial and rostral (M1) areas of PN, respectively, roughly preserving cortical area topographic organization (Wiesendanger and Wiesendanger, 1982; Mihailoff et al., 1984; O'Leary and Terashima, 1988; Leergaard et al., 2000b; Leergaard and Bjaalie, 2007). At the cellular level, an internal-external lamellar organization of cortical axon terminal fields might topographically match

an inside-out organization of PN neurons based on their birthdate (Altman and Bayer, 1987; Leergaard et al., 1995). Moreover, an intrinsic positional organization of PN neurons according to their rostro-caudal origin in the lRL is topographically maintained during AES migration and PN assembly (Di Meglio et al., 2013). However, the molecular basis of corticopontine connectivity is still poorly understood.

Here, we found that expression of Hox5 transcription factors is induced in subsets of postmitotic PN neurons from migration onset. Spatially restricted *Hox5* gene induction requires local response to retinoic acid (RA) signaling from the meninges, resulting in Jmjd3-dependent derepression of Polycomb chromatin and higher order chromatin conformational changes. Moreover, Hoxa5 expression in PN neurons is sufficient to drive them to posterior PN. By transsynaptic viral tracings we show that cortical neurons targeting Hoxa5-expressing neurons in posterior PN are enriched with limb somatosensory afferents. On the other hand, widespread Hoxa5 expression after neuronal migration is instructive to attract somatosensory and avoid visual cortical inputs, irrespective of neuron position in PN. Lastly, Hoxa5 expression in neuronal subsets regulates transcriptional sub-programs potentially underlying the specificity of their connectivity.

This comprehensive study elucidates how single Hox transcription factors may coordinate precerebellar neuron specification, migration, orderly settling in the PN, and topographic input connectivity from specific cortical neuron subsets. Moreover, these findings further our understanding of the molecular logic underlying sub-circuit assembly and diversification in the mammalian corticopontine pathway.

## RESULTS

### Hox5 Expression is Induced Postmitotically in Posterior Subsets of PN Neurons

In the precerebellar system, *Hox2-4* genes are expressed in mitotically active *Wnt1*$^{+}$ lRL progenitors (Rodriguez and Dymecki, 2000) as well as postmitotic *Barhl1*$^{+}$ neurons (Figure S1C-E; Bulfone et al., 2000; Geisen et al., 2008; Di Meglio et al., 2013). In E14.5 lRL, *Barhl1* and *Wnt1*, or the Wnt activity marker *Axin2* (Jho et al., 2002), display mutually exclusive expression patterns (Figure 1B-D), with Ki67$^{+}$ mitotic cells restricted to the *Wnt1*$^{+}$/*Barhl1*$^{-}$ inner lRL portion (Figure 1J). Unlike *Hox2-4* genes, *Hoxa5* and *Hoxb5* were mainly detected in *Barhl1*$^{+}$/*Ki67*$^{-}$ postmitotic neurons (Figure 1F',G', S1F-G). Moreover, *Hoxa5* levels appeared quite low at the onset of migration and more posteriorly induced than *Hoxb5* throughout PN neuron generation from E12.5 to E16.5 (Figure 1F', G', S1F-I).

To further support these findings, we analyzed the distribution of tdTomato$^{+}$ cells in *Hoxa5*$^{Cre\text{-}KI/tdTomato}$ (Figure 1H,H'; STAR Methods; Suppl. Table 1) as a proxy for endogenous *Hoxa5*. Consistent with endogenous *Hoxa5* expression, tdTomato$^{+}$ cells were barely present in the E14.5 *Wnt1*$^{+}$ mitotic domain, while tdTomato was detected in a few *Wnt1*$^{-}$ postmitotic neurons of posterior lRL (p-lRL) (arrows, Figure 1H'). Unlike Hoxb5, which was already detected in the *Barhl1*$^{+}$/*Ki67*$^{-}$ postmitotic domain of p-lRL (Figure 1K-L), accumulation of endogenous Hoxa5 protein was only evident in the AES. In addition, Hoxb4 also appeared to accumulate only in postmitotic neurons (Figure 1M), despite *Hoxb4* expression in both mitotic as well as postmitotic cells (Figure S1E). Hoxa5$^{+}$ and Hoxb5+ neurons migrated in ventral AES and settled posteriorly within the developing PN (Figure 1K-M, S1J-M; Di Meglio et al., 2013).

Thus, *Hox5* genes define specific neuron subsets in posterior PN, with *Hoxa5* specifying the most posterior subset. Moreover, Hox4 and Hox5 transcription factors are only postmitotically expressed and this may be a specific property of rhombic lip-derived precerebellar neurons.

**Spatially Restricted *Hox5* Expression in Posterior PN Neurons Requires Retinoic Acid Signaling**

RA is mainly synthesized by *Raldh2* in the meninges overlaying the lRL (Niederreither and Dolle, 2008; Zhang et al., 2003). At E14.5, we found a posterior-high to anterior-low expression of *Raldh2* (Figure 1I',I). Analysis of the $RARE^{lacZ}$ reporter mouse line, which provides a readout of endogenous RA response, revealed β-gal staining mostly in postmitotic lRL derived neurons (Figure 1E, S1P-S), which was ventrodorsally graded in the AES (Figure 1P). *Wnt1*/*Ki67*/β-gal stainings on E12.5-E15.5 $RARE^{lacZ}$ serial sections (Figure S1P-S) further indicated that the RA response induction is mainly restricted to the postmitotic lRL-derived neurons. Accordingly, β-gal staining and *Hoxb5* transcript distribution overlapped in posterior lRL-derived postmitotic PN neurons (Figure S1N,O).

To assess RA dependency of *Hox5* induction, we increased or decreased RA availability *in vivo*. We imaged transverse sections of the E14.5-E15.5 AES as this allows to directly visualize on each section the whole contribution of r6-r8 derived PN neurons dorsoventrally distributed in the AES (Di Meglio et al., 2013), and their RA response (Figure 1N). Exogenous RA administration at E11.5 (STAR Methods) resulted in dorsal expansion of the RA response and *Hoxa5* expression within the $RARE^{lacZ}$ AES (Figure 1P-U). Quantitative PCR (qPCR) also confirmed significant increase in *Hoxa5* expression levels in E18.5 RA-treated $Atoh1(45)^{tdTomato}$ PN neurons (Figure 1V; Suppl. Table 1) dissected and further isolated by fluorescence activated cell sorting (FACS) (Figure 1O). At this stage, migration is complete (Shinohara et al., 2013) and PN are prominent and relatively simple structures to dissect.

To assess the effect of decreased RA, we *in utero* electroporated lRL progenitors of $RARE^{lacZ}$ embryos at E13.5 with *GFP*, or the RA degrading enzyme *Cyp26b1*. Ectopic induction of

*Cyp26b1* resulted in strongly decreased responsiveness to endogenous retinoids (Figure S1T-T''). Moreover, *Hoxa5* expression was decreased in electroporated *Cyp26b1*$^{+}$ neurons, as assessed by both Hoxa5 immunohistochemistry (Figure 1W'',X'') and *Hoxa5* qPCR in GFP$^{+}$ PN neurons isolated by FACS (Figure 1Y).

In summary, *Hox5* genes are RA targets and their rostrocaudally restricted expression likely relies on higher endogenous RA activity experienced by posterior vs. anterior lRL-derived PN neurons.

### *Hox5* Transcriptional Induction in Pontine Neurons Requires Jmjd3 Demethylase

*Hox5* gene silencing in dorsal AES is maintained by Ezh2 (Di Meglio et al., 2013), a member of Polycomb Repressive Complex 2 (PRC2) which represses chromatin by trimethylation of histone H3 at lysine 27 (H3K27me3) (Margueron and Reinberg, 2011). In E14.5 lRL, *Ezh2* expression was stronger in the mitotic than postmitotic domain and displayed no obvious rostrocaudal bias (Figure S1A,A'). Conditional *Ezh2* depletion in *Wnt1*$^{+}$ lRL progenitors (*Wnt1*$^{Ezh2cKO}$; Suppl. Table 1) resulted in *Barlh1*$^{+}$ cells partially intermingling with the *Axin2*$^{+}$ domain, which appeared to be reduced (Figure 2A,C,F,H). Ectopic *Hoxa5* expression was induced, suggesting that *Hox5* gene loci are poised for transcriptional induction throughout the rostrocaudal extent of the lRL (Figure 2B,E,G,J).

To test whether H3K27me3 depletion is necessary for spatially regulated *Hox5* transcriptional induction, we generated null mutants of the H3K27 demethylase *Kdm6b*/*Jmjd3* (Agger et al., 2007; De Santa et al., 2007; Lan et al., 2007; Lee et al., 2007) (Figure S2A,B; STAR Methods). In E14.5 lRL, *Jmjd3* expression pattern was complementary to *Ezh2*, with low expression in *Axin2*$^{+}$ and high in *Barlh1*$^{+}$ cells, as assessed by β-gal staining in *Jmjd3*$^{+/lacZ}$ mice (Figure S1A,B; Suppl. Table 1). Heterozygous mutant mice were viable and fertile, whereas

*Jmjd3*$^{lacZ/lacZ}$ or *Jmjd3*$^{-/-}$ mutant fetuses died perinatally (Burgold et al., 2012). Nonetheless, E18.5 *Jmjd3* homozygous mutant PN were not grossly affected (Figure S2K, L), which allowed for prenatal analysis of *Hox5* gene induction.

In E14.5 *Jmjd3*$^{lacZ/lacZ}$ fetuses, *Hoxa5* was not induced in posterior lRL-derived PN neurons (Figure 2K), whereas the *Axin2* expression domain appeared to be expanded (Figure 2L). Normal *Raldh2* and *Cyp26b1* expression ruled out changes in endogenous RA synthesis or degradation (Figure S2D-F,H-J). *Jmjd3*-dependent regulation was specific to *Hox5* genes, as in *Jmjd3*$^{-/-}$ AES Hoxa5 expression was strongly impaired whereas Hoxb4 appeared unaffected (Figure 2M-P). Moreover, qPCR on E18.5 *Atoh1(45)*$^{tdTomato}$;*Jmjd3*$^{-/-}$ FACS-isolated PN neurons showed strong *Hoxa5* reduction while *Hoxb4* and *Hoxb3* levels were unchanged (Figure 2Q and Figure S2N-O).

Lastly, chromatin immunoprecipitation (ChIP) in E14.5 FACS-isolated cells from *Hoxa5*$^{tdTomato}$ mice (Suppl. Table 1; Figure 2R-S) revealed that both the retinoic acid receptor alpha (RARa) and Jmjd3 bound a previously identified Hoxa5 retinoic acid response enhancer (RARE) (Mahony et al., 2011, Figure 2T), indicating that *Hoxa5* is a direct RA transcriptional target.

In summary, *Jmjd3* is involved in alleviating *Ezh2*-dependent chromatin repression at the *Hox5* loci following transcriptional induction by RA and liganded RAR. Integration of local signaling and chromatin remodeling provides an *in vivo* template for spatially restricted, transcription factor mediated, induction of *Hox5* transcription in a specific subset of pontine neurons.

**A 3D Chromatin Switch at *Hox5* Loci is Induced by *In Vivo* Response to Retinoids**

To investigate the role of RA in driving spatially regulated transitions of higher order chromatin conformation at *Hox5* loci in hindbrain neurons, we carried out high-resolution circular chromosome conformation capture followed by high throughput sequencing (4C-Seq)(van de Werken et al., 2012). We collected E14.5 *Hox5*-negative fluorescent cells from *r5-6*$^{tdTomato}$ mice (Suppl. Table 1), *Hox5*-positive fluorescent cells from *Hoxa5*$^{tdTomato}$ mice, and *Hox*-negative control cells from cerebral cortex (CC), and used *Hoxa5* (Figure 3A-C, S3C) and *Hoxb5* (Figure S3D-G) promoters as view-points. In CC, both *Hoxa* and *Hoxb* clusters were organized into a single association domain (Figure S3C-D), correlating with their transcriptionally silent state in this tissue. In contrast, in rostrocaudally adjacent *Hox5*-negative and *Hox5*-positive hindbrain neuronal cell populations, *Hoxa5* or *Hoxb5* segregated into distinct 3D chromatin association domains, displaying opposite sets of interactions with either transcriptionally inactive or active *Hoxa* or *Hoxb* genes, respectively (Figure 3A and Figure S3E).

We then compared the 3D chromatin conformations of *Hoxa* and *Hoxb* clusters after exogenous RA treatment at E9.5. In CC and *Hox5*-positive cells, RA treatment did not result in chromatin topological changes as compared to untreated cells (Figure 3C and Figure S3C,D,G). In contrast, the chromatin interaction profiles in RA-treated *Hox5*-negative cells switched to a conformation similar to that normally displayed by the adjacent *Hox5*-positive cells, i.e. displaying less interactions with inactive and enhanced contacts with transcriptionally active *Hox* loci (Figures 3B and S3F).

In summary, chromatin conformation transitions at *Hox* loci can be induced in specific subpopulations of hindbrain neurons in a position-specific and context-dependent manner by their spatially restricted response to environmental RA (drawing in Figure 3D).

**Hoxa5 Expression is Sufficient to Drive Pontine Neuron Subsets into Posterior PN**

Hoxa5 is expressed in posterior subsets of PN neurons and maintained throughout migration and PN development. Thus, Hoxa5 could contribute to drive PN neurons to a posterior location in developing PN. To test this hypothesis, we ectopically expressed Hoxa5 by *in utero* electroporation of E14.5 $ROSA^{CAG\text{-}lsl\text{-}Hoxa5\text{-}KI/lsl\text{-}tdTomato}$ (Suppl. Table 1) lRL progenitors with *Cre*. Given the presence of a strong CAG promoter, the $ROSA^{CAG\text{-}lsl\text{-}Hoxa5\text{-}KI}$ line (STAR Methods) provides sustained Hoxa5 overexpression in a Cre-dependent manner. We compared the localization of *Cre* electroporated, $tdTomato^+$, neurons in control $ROSA^{lsl\text{-}tdTomato}$ and $ROSA^{CAG\text{-}lsl\text{-}Hoxa5\text{-}KI/lsl\text{-}tdTomato}$ E18.5 PN (Figure 4A-D). In controls, $tdTomato^+$ neurons were spread throughout the anteroposterior axis (Figure 4A), whereas in $ROSA^{CAG\text{-}lsl\text{-}Hoxa5\text{-}KI/lsl\text{-}tdTomato}$, anterior PN was devoided of $tdTomato^+$ neurons (Figure 4C,D). The posterior bias of Hoxa5 overexpressing PN neuron distribution was confirmed by quantification (Figure 4I).

To further support these results, we assessed the effect of Hoxa5 ectopic expression on the positioning of *Hox5*-negative PN neurons, using the tamoxifen (TM)-inducible $MafB^{tdTomato}$ line (Suppl. Table 1). Following TM treatment at E7.5, 3D reconstructions of E18.5 and P21 PN (Figure 4J, S4A) showed that $tdTomato^+$ cells selectively localized to anterolateral and anteriormost positions. Next, we crossed $MafB^{tdTomato}$ with the Cre-dependent *Hoxa5* overexpressing $ROSA^{lsl\text{-}Hoxa5\text{-}BAC}$ line and generated $MafB^{Hoxa5/tdTomato}$ mice (STAR Methods; Suppl. Table 1). In $MafB^{Hoxa5/tdTomato}$ E18.5 fetuses and P21 mice, ectopic *Hoxa5* expressing $tdTomato^+$ PN neurons lost their spatial restriction and spread towards posterior PN (Figure 4K, S4B).

***Unc5b* Overexpression Rescues Mispositioning of Ectopic Hoxa5 Expressing PN Neurons**

The *Unc5b* guidance receptor is required to maintain anterior lRL-derived PN neuron subsets in dorsal AES, whereas in ventral AES *Unc5b* is repressed by Hox5 factors (Di Meglio et al., 2013). Thus, the posterior misplacement of anterior lRL-derived PN neurons ectopically overexpressing Hoxa5 might be partially explained by *Unc5b* downregulation during migration. We quantified *Unc5b* expression by RNA-FISH (STAR Methods) in the whole E15.5 AES of *Cre* electroporated $ROSA^{CAG\text{-}lsl\text{-}Hoxa5\text{-}KI/lsl\text{-}tdTomato}$ and $ROSA^{lsl\text{-}tdTomato}$ as well as $MafB^{tdTomato}$ and $MafB^{Hoxa5/tdTomato}$ (Figure 4L-M', S4C-D). We found significant reduction of *Unc5b* levels in both *Cre* electroporated $ROSA^{CAG\text{-}lsl\text{-}Hoxa5\text{-}KI/lsl\text{-}tdTomato}$ and $MafB^{Hoxa5/tdTomato}$ AES (Figures 4N, S4E).

Next, we co-electroporated E14.5 lRL progenitors in $ROSA^{lsl\text{-}tdTomato}$ and $ROSA^{CAG\text{-}lsl\text{-}Hoxa5\text{-}KI/lsl\text{-}tdTomato}$ with *Unc5b* and *Cre*. Co-electroporated neurons overexpressing both Unc5b and Hoxa5 spread throughout the PN anteroposterior axis (Figure 4G,H), thus rescuing the mispositioning phenotype resulting from the only Hoxa5 overexpression. Rescue was also confirmed by quantification (Figure 4I).

In summary, ectopic Hoxa5 expression in lRL-derived neurons is sufficient to drive them into the posterior PN and this is in part achieved through *Unc5b* downregulation.

**Relative Rostrocaudal Position of PN Neurons is Predictive of Topographic Cortical Input**

To investigate monosynaptic targeting of cortical axons onto PN neurons and the relationship between rostrocaudal location of PN neurons and patterned cortical input, we carried out trans-synaptic tracing (Wickersham et al., 2007; Callaway and Luo, 2015) of cortical cells from PN neurons (Figure 5A,B). To selectively infect PN neuron terminals in cerebellum, we used the TVA/EnvA cell type-specific viral infection system (Beier et al.,

2011; Osakada and Callaway, 2013) combined with *in utero* electroporation. We unilaterally electroporated E14.5 lRL progenitors with *rabies virus glycoprotein* and viral receptor *TVA* plasmids. Electroporation at this stage allows PN progenitors to be specifically targeted, since all other precerebellar mossy fiber nuclei have been already generated from the lRL (Altman and Bayer, 1987). At P2, we injected the mCherry EnvA pseudotyped glycoprotein-deleted rabies virus, *EnvA-Rabies-ΔG-mCherry,* into the contralateral cerebellar hemisphere. Virus injection at this early stage resulted in widespread infection of the axon terminals of TVA-expressing neurons distributed throughout the rostrocaudal extent of PN (Figure 5C-E). Rabies glycoprotein expression in these PN neurons (referred to as $WT^{TVA/EnvA/RabiesG}$) further allowed trans-synaptic tracing of monosynaptically connected neurons from cortical areas (Figure 5D).

In $WT^{TVA/EnvA/RabiesG}$ P8 brains, the majority of monosynaptically connected mCherry$^+$ neurons were in the Ctip2$^+$ cortical layer V ipsilateral to the electroporated PN neurons, while vGluT2 labeling of incoming thalamocortical axon terminals readily identified barrel cortex layer IV (Figure S5A-C). In addition, we found some labelled neurons in the contralateral cortical layer V, and several subcortical structures (Figure S5D-O), supporting previous analyses of PN input using non-trans-synaptic tracers (Kolmac et al., 1998; Mihailoff et al., 1989; Swenson et al., 1984; Terenzi et al., 1995). No cortical neurons were transsynaptically labelled in non-electroporated animals (Figure 5C). 3D reconstruction of a representative whole cortex showed that cortical neurons projecting to PN are distributed in all major motor and sensory areas (Figure 5E',I; STAR Methods for area contour mapping).

To assess input connectivity of PN neuron subsets, we changed the placement of electroporation electrodes and selected anterior or posterior rhombic lip portions thereby targeting neuron subsets with anterior or posterior PN distributions, respectively (Figure 5F-

G). 3D reconstruction of the respective cortices revealed that monosynaptically connected neurons were regionally segregated (Figure 5F',G'). Transsynaptic tracing from neurons in anterior PN resulted in labeling cortical neurons mostly in visual and motor areas (Figure 5F',I). Conversely, neurons in posterior PN were mostly connected to somatosensory and motor areas (Figure 5G',I).

Thus, the relative rostrocaudal position of PN neurons can be broadly predictive of monosynaptic topographic regional input from cerebral cortex.

**Hoxa5 Expressing PN Neurons Are Preferentially Targeted by Subsets of Limb Somatosensory Cortical Neurons**

Posterior PN neurons are preferentially connected to somatosensory cortical neurons (Figure 5; Leergaard and Bjaalie, 2007). Therefore, Hoxa5 expression in posterior subsets of PN neurons might orchestrate somatosensory specific input connectivity. We *in utero* co-electroporated *GFP* and *Cre* in E14.5 fetuses of homozygous females for $Tau^{lsl\text{-}RabiesG}$ (STAR methods; Supp. Table 1), crossed with conditional *Hoxa5* overexpressing $ROSA^{CAG\text{-}lsl\text{-}Hoxa5KI}$ heterozygous males (Figure S6A), and subsequently injected the *SAD-ΔG-mCherry* rabies virus (Osakada and Callaway, 2013) into their contralateral cerebellar hemisphere at P2; $ROSA^{CAG\text{-}lsl\text{-}Hoxa5\text{-}KI};Tau^{lsl\text{-}RabiesG}$, *Cre* electroporated, PN neurons overexpressed both *Hoxa5* and *rabies glycoprotein*, whereas $Tau^{lsl\text{-}RabiesG}$ electroporated neurons expressed only the *rabies glycoprotein* and served as controls.

In control *Cre*-electroporated $Tau^{lsl\text{-}RabiesG}$ cortex, $mCherry^{+}$ neurons were distributed in different cortical areas, including primary visual (V1), somatosensory (S1) and motor (M1) (Figure 6A', A", A'") (see also Figure 5). In contrast, *Cre*-electroporated $ROSA^{CAG\text{-}lsl\text{-}Hoxa5\text{-}KI};Tau^{lsl\text{-}RabiesG}$ PN neurons were preferentially distributed in posterior PN (Figure 6A,B),

supporting our previous findings (Figure 4), and received significantly reduced monosynaptic input from V1 (Figure 6B',B''',D, S5P), while no significant change was observed for S1 or M1 input (Figure 6B',B'',C,F, S5P).

In addition to regional representation of distinct cortical areas in the PN, the S1 sensory body representation is also generally mapped in a topographic manner onto the central-posterior PN. Namely, axons from S1 whisker (barrel) or face mapping regions project rostrally to limb-specific cortical projections, which project more posteriorly in PN, thus preserving cortical topography (Brodal, 1968; Mihailoff et al., 1978; Wiesendanger and Wiesendanger, 1982; Kosinski et al., 1986; Panto et al., 1995; Leergaard et al., 2000b). Quantification of $mCherry^{+}$ neurons in forelimb, hindlimb, and barrel S1 cortex in *Cre*-electroporated $Tau^{lsl\text{-}RabiesG}$ and $ROSA^{CAG\text{-}lsl\text{-}Hoxa5\text{-}KI};Tau^{lsl\text{-}RabiesG}$ brains showed that Hoxa5 expressing neurons were preferentially innervated by limb rather than barrel somatosensory cortical axon input (Figure 6E).

**Hoxa5 Expression Instructs Cortical Somatosensory at the Expense of Visual Inputs Irrespective of PN Neuron Position**

The enrichment of limb somatosensory and paucity of visual cortical inputs synapsing with Hoxa5 expressing PN neurons could be expected by their posterior position in the PN. To distinguish an additional Hoxa5 role, besides driving neurons to posterior PN, in selecting specific subsets of cortical inputs irrespective of neuron position, we modified our transsynaptic tracing strategy (Figure S6B). Expression of *rabies glycoprotein* only, or both *rabies glycoprotein* and Hoxa5 was induced in postmigratory, E14.5 *in utero CreERT2*-electroporated, $Tau^{lsl\text{-}RabiesG}$ or $ROSA^{CAG\text{-}lsl\text{-}Hoxa5\text{-}KI};Tau^{lsl\text{-}RabiesG}$ PN neurons, respectively, by

administering tamoxifen at E18.5; the *SAD-ΔG-mCherry* rabies virus was then injected in contralateral cerebellum at P2.

Unlike Hoxa5 overexpression at premigratory stage causing a posterior bias of Hoxa5$^{+}$ neuron position in PN (Figure 4, 6B), no rostrocaudal positional bias was observed at P8 for *ROSA*$^{CAG\text{-}lsl\text{-}Hoxa5\text{-}KI}$*;Tau*$^{lsl\text{-}RabiesG}$ *CreERT2*-electroporated neurons (Figure 6G-I). Hoxa5 overexpressing neurons in *ROSA*$^{CAG\text{-}lsl\text{-}Hoxa5\text{-}KI}$*;Tau*$^{lsl\text{-}RabiesG}$ received reduced input from V1 as compared to *Tau*$^{lsl\text{-}RabiesG}$ controls (Figure 6G', G''', H', H''',K, S5Q). As V1 axon collaterals only enter the rostral portion of PN (Mihailoff et al., 1984; O'Leary and Terashima, 1988), this finding strongly suggests that anteriorly located PN neurons ectopically expressing Hoxa5 inhibit their targeting by V1 axon collaterals. On the other hand, we observed no significant change in the fraction of monosynaptically connected neurons from S1 and M1 (Figure 6G'', H'', J, L), suggesting that Hoxa5 expressing neurons can be targeted by S1 axon collaterals irrespective of position in PN.

We next carried out cortical axon tracing using anterograde AAV (Figure S6C). E14.5 *CreERT2*-electroporated *ROSA*$^{lsl\text{-}tdTomato}$ and *ROSA*$^{CAG\text{-}lsl\text{-}Hoxa5\text{-}KI/lsl\text{-}tdTomato}$ served as control and experimental sets, respectively. TM was administered at E18.5 At P5, we injected AAV1.hSyn.eGFP (Harris et al., 2012) in S1 to trace cortical inputs to PN. Upon postmigratory Hoxa5 overexpression throughout the PN rostrocaudal extent, we observed increased S1 axon terminals in anterior PN (Figure 6M'',N'',O), strongly indicating that Hoxa5-expressing neurons are instructive for attracting somatosensory input.

In summary, Hoxa5 has successive roles in developing PN neurons. Early Hoxa5 expression in migrating neurons guides them to posterior PN; Hoxa5-expressing subsets will thus have higher probability to be targeted by topographically arranged somatosensory afferents of the corticospinal tract. We further reveal that Hoxa5 expression in randomly

selected subsets of anterior PN neurons after their migration is instructive to integrate them in a specific connectivity sub-network relaying mainly somatosensory information while avoiding visual input.

**Transcriptional Programs of Hoxa5 Expressing PN Neurons**

To identify genes potentially involved in circuit formation downstream *Hox5* genes, we carried out RNA sequencing (RNA-Seq) and comparative transcriptome analysis on the whole PN as well as distinct subsets of PN neurons, isolated by FACS from Cre-dependent reporter expressing lines. We used the *Atoh1(45)::Cre* driver, since in *Atoh1(45)$^{tdTomato}$* mice tdTomato expression is only detected in postmitotic lRL derived neurons starting at migration onset and distributed throughout the AES at E14.5 and PN at P0 (Figure S7A-D).

We compared RNA-seq datasets of PN neurons isolated from E18.5 *Atoh1(45)$^{tdTomato}$* and *Hoxa5$^{tdTomato}$* animals (Figure 7A, B) and identified 637 differentially expressed genes (FC > 1.5; FDR < 0.07), amongst which 456 (72%) were up- and 181 (28%) down-regulated (Figure 7E). As expected, *Hoxa5*, *Hoxb5* and *Hoxc5* were enriched in the *Hoxa5$^{tdTomato}$* vs. *Atoh1(45)$^{tdTomato}$* samples.

We next compared the RNA-seq profiles of *Atoh1(45)$^{tdTomato}$* and *Atoh1(45)$^{Hoxa5}$* (Supp. Table 1) E18.5 PN neurons (Figure 7C). In *Atoh1(45)$^{Hoxa5}$*, both GFP (as a proxy for Hoxa5 overexpression) and Hoxa5 were readily detected in PN neurons at P0 (Figure 7D, S7O). We found 736 genes differentially expressed, with 306 (42 %) being up- and 430 (58 %) down-regulated in the *Atoh1(45)$^{Hoxa5}$* vs. *Atoh1(45)$^{tdTomato}$* samples, respectively (Figure 7F). No other *Hox5* paralogue gene showed significant changes in their expression, indicating that Hoxa5 does not cross-regulate *Hox5* paralogues in PN neurons.

We next asked which genes were similarly expressed in *Hoxa5*$^{tdTomato}$ vs. *Atoh1(45)*$^{tdTomato}$ (i.e. endogenous *Hox5* expressing) and *Atoh1(45)*$^{Hoxa5}$ vs. *Atoh1(45)*$^{tdTomato}$ (i.e. *Hoxa5* overexpressing) neuron subsets. We found a highly significant genome-wide correlation ($r = 0.18$; $p < 0.0001$) between endogenous and overexpressing Hoxa5 PN subpopulations, respectively (Figure 7J). We found 145 genes whose expression pattern was shared, of which 107 (74%) were up- and 38 (26%) down-regulated in both populations (Figure 7G-H). On the other hand, when comparing *Atoh1(45)*$^{tdTomato}$ (whole PN) vs. *Hoxa5*$^{tdTomato}$ or *Atoh1(45)*$^{tdTomato}$ vs. *Atoh1(45)*$^{Hoxa5}$ many genes were differentially regulated in both comparisons (Figure 7I). Gene Ontology (GO) analysis revealed genes critical for biological processes involved in topographic circuit formation, such as cell adhesion, axon guidance, as well as chemotaxis (Figure 7I).

To uncover Hox5-dependent rostrocaudal molecular gradients within the developing PN, we next analysed the expression pattern of differentially expressed genes in *Atoh1(45)*$^{tdTomato}$ vs. *Atoh1(45)*$^{Hoxa5}$ RNA-seq assays. We screened the Allen Mouse Brain Atlas (Lein et al., 2007) (http://mouse.brain-map.org) and Allen Developing Mouse Brain Atlas (http://developingmouse.brain-map.org) for wild type expression of *Epha3, Pcdh19, Peg10, Cdhr1, Ephb1, Nrp1, Sfrp4, chl1, St18,* and *Sox11* (Figure S7E-N). These genes displayed rostrocaudally graded or spatially restricted expression supporting our experimental approach. We additionally assessed expression of a further set of differentially expressed genes, namely *Crabp1, Nrp2, Slit3, Clb1, Lmo3,* and *SST*. *Crabp1* and *SST* were downregulated (Figure S7Q-R), while *Nrp2*, *Slit3*, *Clb1* and *Lmo3* were up-regulated upon Hoxa5 overexpression (Figure S7S-V) thus validating them as Hoxa5 downstream targets in PN neurons.

In summary, comparative transcriptome analysis revealed the existence of molecular gradients within the PN in part regulated by Hoxa5, potentially contributing to specification and connectivity.

## DISCUSSION

During brain development, a stereotypic sequence of neuronal specification, ordered migration, establishment of axonal wiring, and synaptic connectivity need to be tightly regulated in space and time to achieve meaningful topographic circuit assembly. Yet, whether and how individual transcription factors are able to collectively coordinate these successive processes remain still largely unknown. Here, we used a comprehensive genetic approach coupled with *in utero* electroporation and *in vivo* transsynaptic tracing and showed that Hox5 transcription factors are involved in coordinating the specification and orderly positioning of distinct precerebellar neuron subsets in the developing PN, and orchestrating their topographic input connectivity from distinct cortical neuron subsets in position dependent and independent manners.

Rostrocaudal specification of neuronal identities requires Hox activity (Studer et al., 1996; Gavalas et al., 1997; Gavalas et al., 1998; Davenne et al., 1999; Dasen et al., 2003; Oury et al., 2006; Narita and Rijli, 2009; Tumpel et al., 2009; Philippidou and Dasen, 2013; Bechara et al., 2015). *Hox* spatiotemporal regulation in progenitor and/or postmitotic neurons involves an interplay between local signaling, dynamic chromatin changes, and transcriptional output. How these processes are integrated *in vivo* during cell fate specification is poorly understood. Here, we found that the response to RA of postmitotic PN neurons is spatially graded such that only posterior rhombic lip derived neurons are able to respond (Figure 1). *Hox5* gene induction is spatially restricted to these posterior RA responsive subsets. In pontine neurons,

*Hoxa5* and *Hoxb5* display distinct spatial expression limits in the lRL (Figure S1), which may reflect distinct responses to rostrocaudal RA levels from meninges. Dynamic patterns of transcription and associated chromatin changes at *Hox5* loci have been investigated during RA-mediated ES cell differentiation (Kashyap et al., 2011; Mazzoni et al., 2013; De Kumar et al., 2015). Indeed, *Hoxa5* and *Hoxb5* respond to RA through specific RAREs (Chen et al., 2007) and display distinct transcriptional responses, implemented through different mechanisms involving elongation of paused RNA polymerase II (PolII) or rapid recruitment of PolII and transcriptional initiation (Lin et al., 2011; De Kumar et al., 2015).

RA-dependent *Hox5* transcriptional output is accompanied by region-specific chromatin regulation along the rostrocaudal axis (Figure 2). In *Ezh2* null mutants, similarly to wild type mice treated with exogenous RA, *Hox5* genes are derepressed throughout the AES (Di Meglio et al., 2013), indicating increased sensitivity of *Ezh2*-depleted neurons to endogenous RA levels along the rostrocaudal axis. Thus, the *Ezh2*/H3K27me3 repressive mark may attenuate the transcriptional response of *Hox5* genes to endogenous RA, setting a threshold which can only be overcome in the posterior rhombic lip due to higher endogenous RA levels. *Ezh2*/H3K27me3 depletion is not by itself sufficient for strong *Hox5* induction which requires RA-induced transcriptional response. In *Ezh2* mutants, *Hox5* genes are not ectopically induced in the $Axin2^{+}$/$Wnt1^{+}$ mitotic progenitor compartment, which appears reduced in *Ezh2* null mutants (Figure 2). Moreover, the $Wnt1^{+}$ rhombic lip appears to be unresponsive to RA signalling from the meninges as assessed in $RARE^{lacZ}$ reporter mice (Figures 1 and S1). A mutually negative regulation has been shown between Wnt signalling, that maintains intestinal stem cells, and RA-induced HOXA5 which drives their differentiation (Ordonez-Moran et al., 2015), suggesting that a similar mechanism might be at work for *Hox5* expression in $Wnt1^{+}$ lRL mitotic domain.

H3K27me3 depletion at developmentally regulated genes, including *Hox* genes, requires UTX and/or Jmjd3 demethylases (Burchfield et al., 2015). *Jmjd3*, in particular, is involved in the regulation of neurogenesis (Ramadoss et al., 2012; Jiang et al., 2013; Kartikasari et al., 2013). However, little is known about how specific demethylases contribute to spatially restricted specification of neuronal subtype identity *in vivo* in response to rostrocaudal signals. We show that *Jmjd3* expression levels are strongly enhanced in pontine postmitotic neurons from the onset of migration (Figure S1) and that *Jmjd3* is necessary to achieve optimal RA-induced *Hox5* transcriptional levels at the onset and during migration (Figure 2). Together with RARa, Jmjd3 is recruited to directly bind a *Hoxa5* RARE, in keeping with a role of Jmjd3 at neural enhancers and promoters (Park et al., 2014), suggesting that it directly contributes to switching from poised to active enhancer state.

Lastly, *Hox* cluster higher order chromatin conformation is dynamic during development and differentiation (Noordermeer et al., 2011; Chambeyron and Bickmore, 2004; Ferraiuolo et al., 2010; Rousseau et al., 2014). However, the role of environmental signals in driving region-specific chromatin changes at *Hox* clusters during neuronal development remains poorly understood. We found that RA signalling is instructive for topographic transitions of *Hox* cluster chromatin 3D conformation along the hindbrain rostrocaudal axis (Figure 3).

Establishment of topographic maps require multiple processes including prenatal interactions of molecular gradient cues, axonal and dendritic remodeling, and experience dependent refinement during early postnatal critical periods (Cang and Feldheim, 2013). In the developing corticopontine circuit, somatosensory cortical axon collaterals target a broad centrocaudal region in PN and are further refined to attain the adult regional targeting pattern in the PN (Mihailoff et al., 1984). In contrast, visual cortical neuron axon collaterals only target the anterior PN (Stanfield and O'Leary, 1985; O'Leary and Terashima, 1988). At a larger

scale, pontine neuron dendritic fields remain constrained within the area targeted by a single cortical region (Schwarz and Thier, 1995; Schwarz et al., 2005), leading to the suggestion that regional cortical topography is largely preserved in PN. When cortical input from somatosensory or motor cortex is removed, then cortical visual axon collaterals can innervate posterior PN neurons (O'Leary et al., 1991). This suggests that distinct post-synaptic PN neuron subsets may provide both permissive and instructive cues which ultimately contribute to determine the topography and specificity of pre-synaptic cortical afferent targeting.

By transsynaptic tracing, we provide here direct demonstration that broad regional topography of cortical connectivity is maintained in PN. A main finding is that the settling position of pontine neurons along the PN rostrocaudal axis can be broadly predictive of input from distinct sensory cortical areas. For instance, pontine neurons in the centrocaudal PN display enriched somatosensory, at the expense of visual, cortical input (Figure 5). At a finer scale, clusters of corticopontine projections mapping the same body part distributed within inside-out concentric layers or 'lamellae', generating multiple somatosensory body maps in centrocaudal PN (Leergaard and Bjaalie, 1995; Leergaard et al., 2000a; Leergaard et al., 2000b ; Leergaard et al., 2004). This organisation was speculated to relate to the inside-out gradient of pontine neuron birthdating (Altman and Bayer, 1987) and temporal internal-to-external corticopontine projection pattern observed in newborns and further refined through adult stages (Leergaard et al., 1995). However, temporal and maturational gradients cannot fully explain the complexity of the fine-grained somatotopic connectivity pattern between cortical input and pontine neuron targets. One possibility is that both the position and specific intrinsic molecular programs of post-synaptic PN neurons contribute to this complex cortico-pontine input connectivity pattern.

The contributions of neuronal settling position versus intrinsic molecular identity in the establishment of complex input-output wiring diagrams is beginning to emerge during the assembly of spinal motor circuits (Jessell et al., 2011; Surmeli et al., 2011; Tripodi et al., 2011; Levine et al., 2012; Bikoff et al., 2016; Baek et al., 2017). Similarly, in the developing neocortex, certain transcription factors can concomitantly regulate neuronal migration and final position with the acquisition of laminar subtype identity and connectivity (Kwan et al., 2008). In this study, we investigated whether similar principles might apply during cortico-pontine circuit development. We found that Hoxa5 is required to couple both positional information and intrinsic molecular identity to determine specific cortical somatosensory afferent connectivity in the PN. Because of their final posterior position in the PN, Hoxa5$^{+}$ neurons have higher probability to connect to somatosensory than visual cortical input (Figures 5-6). On the other hand, we additionally found that Hoxa5$^{+}$ neurons preferentially connect with limb, rather than face/whisker, somatosensory cortical neurons (Figures 5-6). This suggested that Hoxa5 expression, in addition to driving neurons to posterior PN, could be sufficient to instruct a molecular program selecting cortical input specificity. To uncouple this potential additional role of Hoxa5 irrespective of PN neuron position, we overexpressed Hoxa5 after PN neuron migration and settling. We found that post-migratory neurons ectopically expressing Hoxa5 throughout the PN rostrocaudal axis preferentially connect to somatosensory (S1) and avoid visual (V1) cortical neurons (Figure 6). Moreover, anteriorly located ectopically Hoxa5 expressing PN neurons were able to ectopically attract S1 somatosensory axons (Figure 6).

It is noteworthy that Hoxa5 expression in pontine neurons is sufficient to restrict targeting by V1 cortical axons and bias the input of S1 axons towards limb, rather than face, representations. Other *Hox* paralogue group genes, i.e. *Hox2-4* genes, might provide

molecular and positional identities to PN neurons to acquire their main input. In this respect, *Hoxa2* ectopic expression in the brainstem dorsal principal trigeminal nucleus (dPrV) was sufficient to attract peripheral whisker-related sensory afferents and generate ectopic barrelettes, at the expense of mandibular somatosensory input (Bechara et al., 2015). Within the centrocaudal somatosensory PN, pontine neuron subsets might therefore establish Hox-dependent transcriptional sub-programs to determine the specificity of innervation of distinct subsets of incoming cortical somatosensory axons. Indeed, downstream of Hoxa5 several genes are involved in axon refinement and pathfinding (Figure 7), potentially assisting in cortico-pontine connectivity.

Lastly, a main limitation of this study is that it primarily relies on gain-of-function data. On the other hand, it is highly likely that the effects of single *Hox5* gene deletions would be largely compensated *in vivo* by functional redundancy from the other paralogues. Thus, rather than studying unique and shared functions of individual Hox5 paralogue genes in conditional compound mutant precerebellar neurons, which would have been technically unfeasible in the mouse, we used here a comprehensive genetic, cellular, and molecular *in vivo* approach to show that a single Hox5 factor is sufficient to regulate specific aspects of precerebellar neuron specification, migration, and connectivity.

In conclusion, we provide here critical insights into the developmental mechanisms establishing cortico-pontine somatosensory maps and improve our understanding of the molecular logic underlying Hox-dependent sub-circuit specialization during development.

**ACKNOWLEDGEMENTS**

We are grateful to D. Saur for mouse line, E. Callaway for viruses, B. Roska for electroporation plasmids, P. Bovolenta, P. Dollé, and A. Chédotal for in situ hybridization

probes, K. Karmakar for help with setting up trans-synaptic rabies tracing experiment, D. Machlab for position weight matrix of Hoxa5 RARE, S. Jin and R. Nitschke for providing and teaching the LIC macro for tile recording with Zeiss Zen 2010 software. We thank FMI imaging, genomics, and animal facilities for excellent technical support, T. Roloff for RNA sequencing. TDM was an EMBO LT Fellowship recipient. NM was funded by Marie Curie IEF (FP7-PEOPLE-2013). Work in FMR laboratory was supported by the Swiss National Science Foundation (31003A_149573 and 31003A_175776), and Novartis Research Foundation.

**AUTHOR CONTRIBUTIONS**

U.M., D.K., N.V., S.J.B.H., V.K., and T.D.M. carried out the experiments and analysis. H.K. carried out FACS. N.M. prepared *EnvA-Rabies-*Δ*G-mCherry* virus. S.D. generated transgenic mouse lines. D.S., M.S., and S.A. generated the $Tau^{lsl\text{-}RabiesG}$ mouse line. C. F. K. established the transsynaptic virus tracing approach. F.M.R. supervised the project and contributed to designing experiments and data analysis. F.M.R., U.M., and D.K. wrote the manuscript. All authors commented on the manuscript.

## FIGURES

### Figure 1

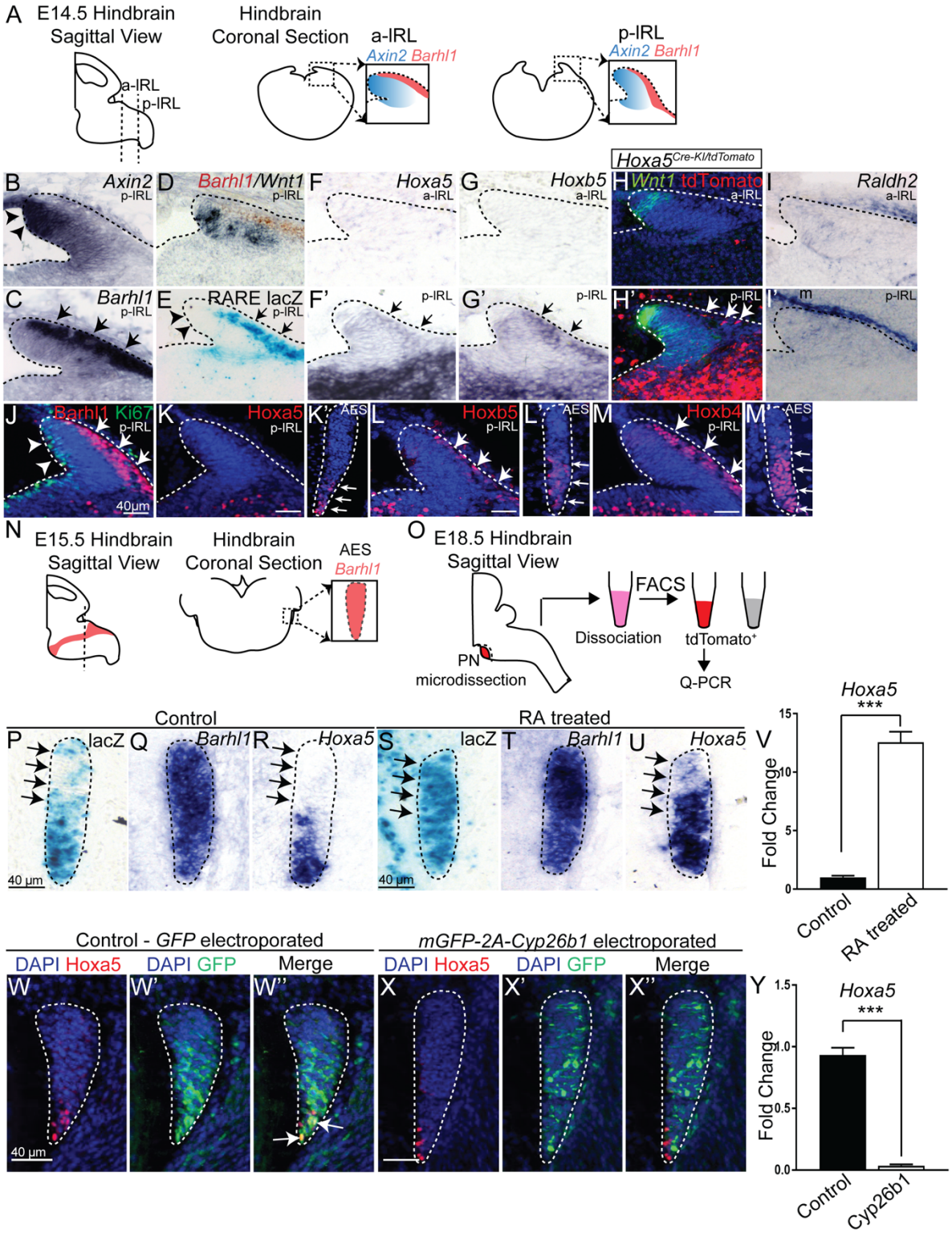

**Figure 1: *Hox5* genes are induced in a subset of lower rhombic lip derived PN neurons and require RA signaling**

**(A)** Drawing illustrating anterior (a-lRL) and posterior (p-lRL) lower rhombic lip at E14.5. **(B-I)** E14.5 wild type coronal sections showing in situ hybridization for (B) *Axin 2*, (C) *Barhl1*, (D) *Barhl1* (red) and *Wnt1* (blue), labeling postmitotic precerebellar neurons (arrows) and progenitor domain (arrowheads), respectively, (E) $RARE^{lacz}$ β-gal stained coronal section showing strong endogenous retinoid activity in postmitotic p-lRL (arrows, postmitotic neurons and arrowheads, progenitors), (F-F') *Hoxa5* and (G-G') *Hoxb5*, expressed in postmitotic neurons of p-lRL (arrows in F' and G') not a-lRL, (H-H') *Wnt1* (green) and tdTomato immunohistochemistry (IHC) (red) in $Hoxa5^{Cre\text{-}KI/tdTomato}$, labeling mitotic domain and *Hoxa5*-driven Cre activity, respectively. tdTomato signal is only detected in postmitotic neurons in p-lRL (arrows), (I-I') *Raldh2*, showing lower expression in meninges overlying a-lRL (I) than p-lRL (I'). **(J-M)** E14.5 wild type coronal sections showing IHC for (J) Barhl1 (red) and Ki67 (green), labeling postmitotic neurons and mitotically active progenitors, respectively, (K-K') Hoxa5, (L-L') Hoxb5, and (M-M') Hoxb4 in plRL (K,L,M) and in anterior extramural stream (AES) (K',L'M'). Hoxa5 is only detected in AES (arrows, K') whereas Hoxb5 and Hoxb4 in both postmitotic neurons and AES (L-L',M-M'). **(N-O)** Drawings illustrating AES (N) and collection and isolation of PN neurons by FACS for qPCR assay (O). **(P-U)** E15.5 untreated $RARE^{lacz}$ coronal sections (P-R), or RA treated at E11.5 (S-U), stained with β-gal (P,S), or in situ hybridized with *Barhl1* (Q,T) and *Hoxa5* (R,U) (arrows, dorsal AES). **(V)** qPCR on FACS isolated PN neurons from E18.5 control or RA treated $Atoh1(45)^{tdTomato}$ (n=3, p-value < 0.0001). **(W-X)** E15.5 $RARE^{lacz}$ coronal sections *in utero* electroporated at E13.5 with *GFP* (W-W'') or *Cyp26b1* (X-X"), showing expression of Hoxa5 (W,X), GFP (W',X'); arrows indicate GFP and Hoxa5 co-expression in W'', not detected in X''. **(Y)** qPCR on FACS isolated neurons from control or *Cyp26b1* electroporated PN (n=3, p-value < 0.001). Data presented as mean + SD. See also Figure S1.

**Figure 2**

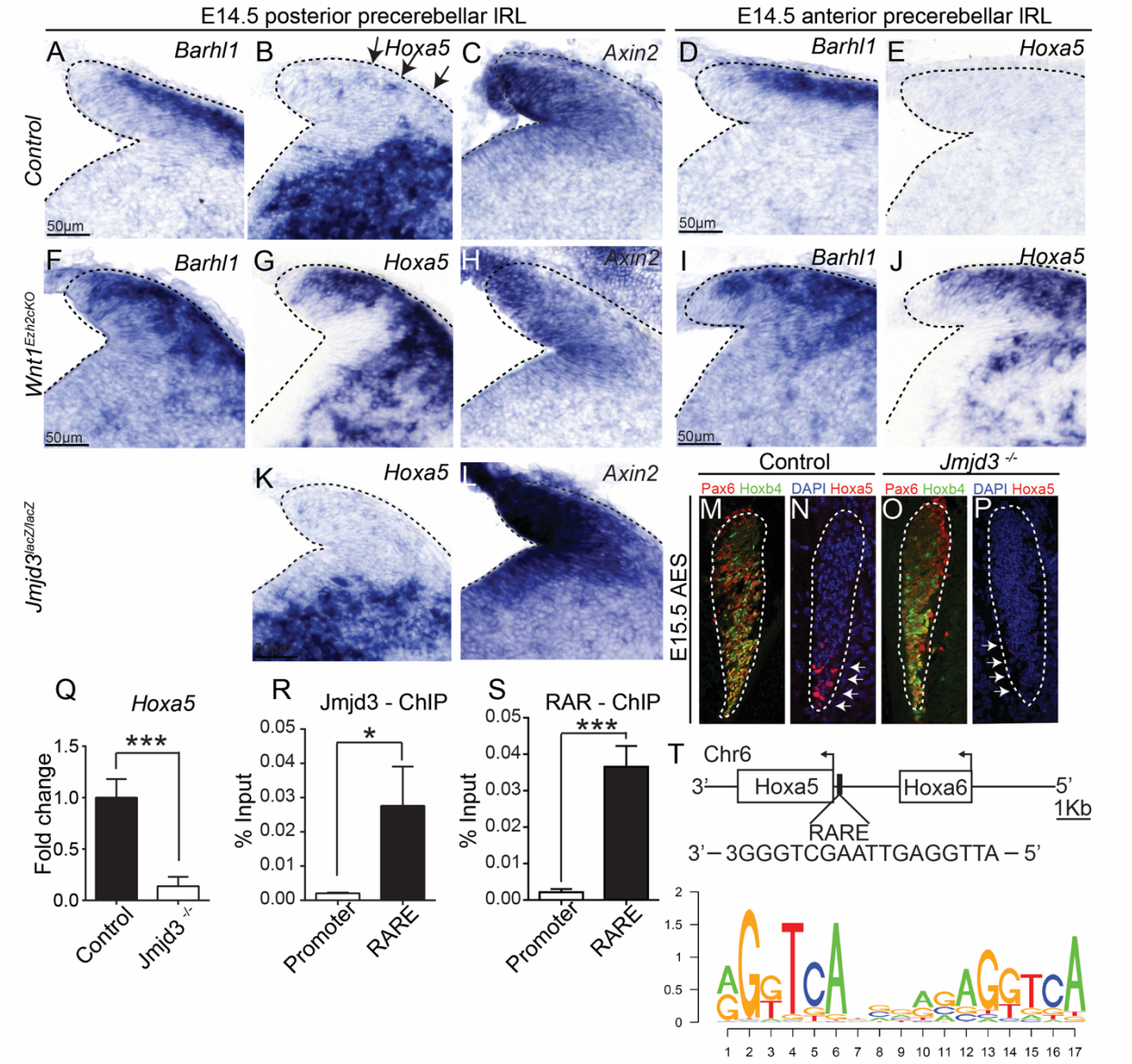


**Figure 2: *Hox5* transcriptional induction in PN neurons requires Jmjd3**

(**A-L**) E14.5 coronal sections of wild type (A-E), *Wnt1*$^{Ezh2cKO}$ (F-J), *Jmjd3*$^{lacZ/lacZ}$ (K-L) showing expression of *Barhl1* (A, D, F, I), *Hoxa5* (B, E, G, J, K), and *Axin2* (C, H, L). In *Wnt1*$^{Ezh2cKO}$, *Hoxa5* ectopically expands in a- and p-lRL postmitotic domains (G, J), correlating with increased *Barhl1* (F, I) and reduced *Axin2* expression (H); conversely, in *Jmjd3*$^{lacZ/lacZ}$, *Axin2* expression is expanded (L) and *Hoxa5* is not induced in postmitotic neurons (K). (**M-P**) Pax6 and Hoxb4 (M,O) or Hoxa5 (N,P) expression on E15.5 AES of control (M-N) or *Jmjd3*$^{-/-}$ (O-P), showing strongly decreased Hoxa5 levels in *Jmjd3*$^{-/-}$ AES (arrows) while no change is observed for Hoxb4. (**Q**) qPCR on FACS isolated PN neurons from E18.5 control and *Atoh1(45)*$^{tdTomato}$;*Jmjd3*$^{-/-}$ (n=3, p-value < 0.001). (**R-S**) ChIP-qPCR showing that Jmjd3 (R) and retinoic acid receptor (RAR) (S) bind to Hoxa5 RARE enhancer but not promoter in E14.5 hindbrain cells. (**T**) Drawing illustrating position and sequence of the RARE with respect to *Hoxa5* and *Hoxa6* and JASPAR position weight matrix of Hoxa5 RARE. Data presented as mean + S.D. See also Figure S2.

**Figure 3**

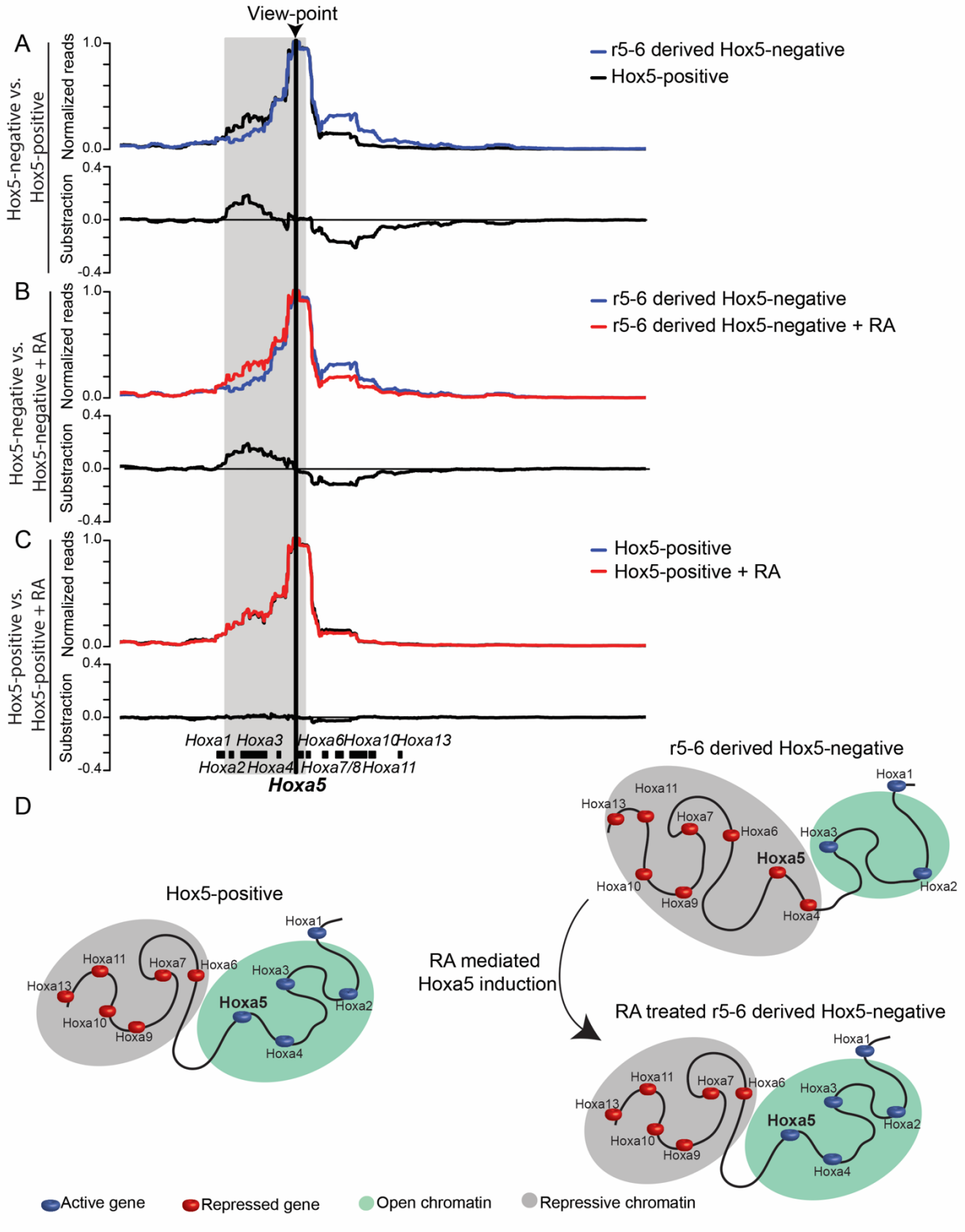
View-point
A
Hox5-negative vs. Hox5-positive
Normalized reads
Substraction
r5-6 derived Hox5-negative
Hox5-positive
B
Hox5-negative vs. Hox5-negative + RA
r5-6 derived Hox5-negative
r5-6 derived Hox5-negative + RA
C
Hox5-positive vs. Hox5-positive + RA
Hox5-positive
Hox5-positive + RA
Hoxa1 Hoxa3 Hoxa6 Hoxa10 Hoxa13
Hoxa2 Hoxa4 Hoxa7/8 Hoxa11
Hoxa5
D
r5-6 derived Hox5-negative
Hox5-positive
RA mediated Hoxa5 induction
RA treated r5-6 derived Hox5-negative
Hoxa1
Hoxa2
Hoxa3
Hoxa4
Hoxa5
Hoxa6
Hoxa7
Hoxa9
Hoxa10
Hoxa11
Hoxa13
Active gene
Repressed gene
Open chromatin
Repressive chromatin

**Figure 3: RA signaling regulates higher order chromatin configuration at *Hox5* gene loci**

(**A-C**) Contact profiles of E14.5 r5-6-derived *Hox5*-negative and *Hox5*-positive hindbrain cells using the *Hoxa5* promoter as viewpoint (arrowhead) within a 400kb window spanning the *Hoxa* cluster with or without RA treatment at E9.5. Substractions of the respective comparisons are depicted below normalized reads. (A) Rostrocaudal differences in association frequency of *Hoxa5* promoter with active or inactive domains within the *Hoxa* cluster. Exogenous RA leads to a 3D reorganization of chromatin conformation *in vivo* at the *Hoxa5* locus in *Hox5*-negative (B) but not *Hox5*-positive samples (C). Note that RA-treated *Hox5*-negative (B) and untreated *Hox5*-positive (C) profiles are similar. **(D)** Model of rostrocaudal RA-dependent chromatin reorganisation at *Hoxa* cluster *in vivo*. See also Figure S3.

**Figure 4**

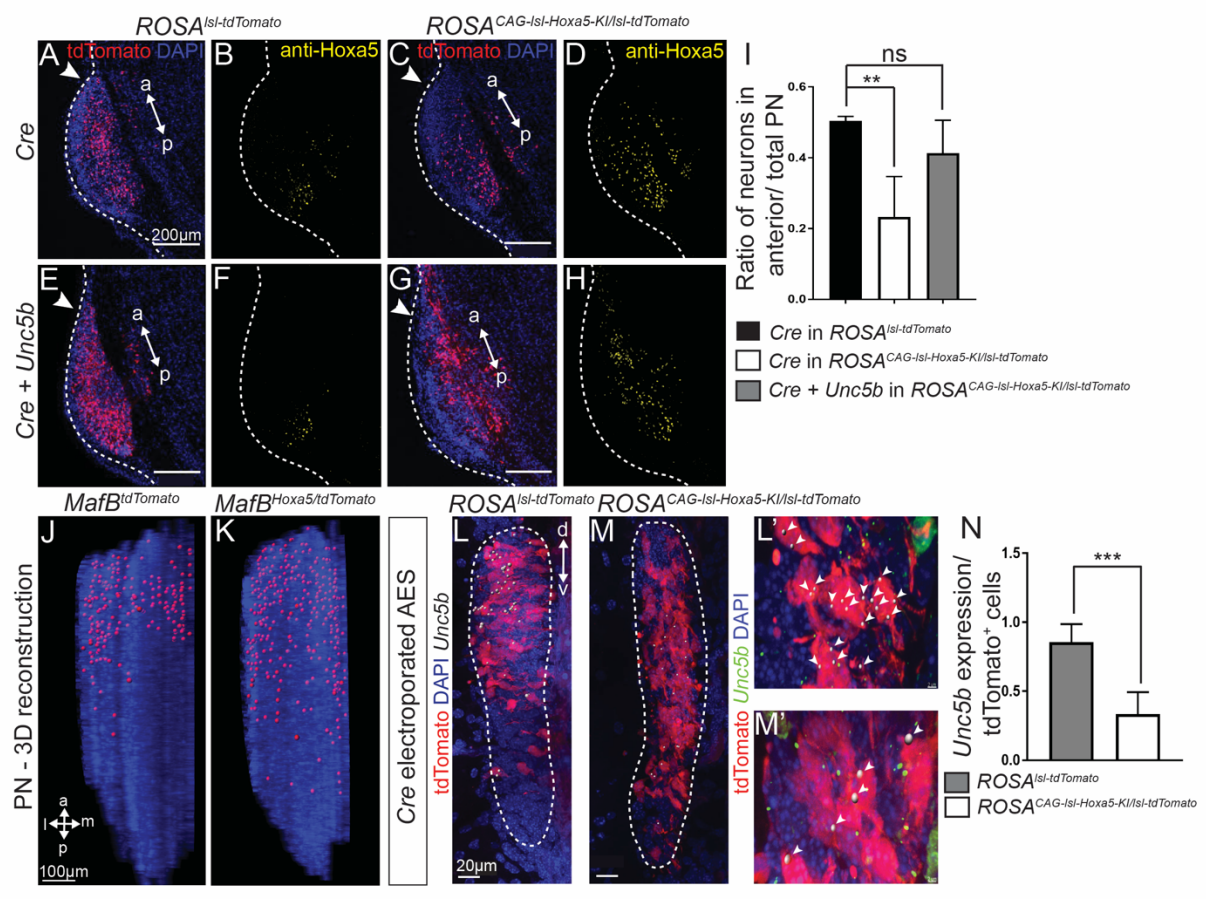


**Figure 4: Hoxa5 ectopic expression downregulates *Unc5b* and drives neurons to posterior PN**

**(A-H)** E18.5 PN sagittal sections of *ROSA*$^{lsl\text{-}tdTomato}$ (A,B,E,F) and *ROSA*$^{CAG\text{-}lsl\text{-}Hoxa5\text{-}KI/lsl\text{-}tdTomato}$ (C,D,G,H) electroporated at E14.5 with *Cre* (A-D) or *Cre* and *Unc5b* (E-H). *Cre* electroporated *ROSA*$^{lsl\text{-}tdTomato}$ tdTomato$^{+}$ PN neurons spread rostrocaudally (arrowhead, anterior PN) (A,E), whereas *ROSA*$^{CAG\text{-}lsl\text{-}Hoxa5\text{-}KI/lsl\text{-}tdTomato}$ Hoxa5-overexpressing tdTomato$^{+}$ neurons are mainly in posterior PN (C); co-electroporated tdTomato$^{+}$ neurons spread throughout the anteroposterior extent of the PN (G), rescuing the posterior mispositioning of (C); (D,H) overexpression of Hoxa5 protein in *Cre* and *Cre* plus *Unc5b* electroporated *ROSA*$^{CAG\text{-}lsl\text{-}Hoxa5\text{-}KI/lsl\text{-}tdTomato}$ neurons. **(I)** Bar graph of ratio of anterior-to-total tdTomato$^{+}$ PN neurons (n=4 for *Cre*, n=3 for *Cre* and *Unc5b*, p-value = 0.005). **(J-K)** 3D reconstruction of E18.5 *Mafb*$^{tdTomato}$ (J) and *MafB*$^{Hoxa5/tdTomato}$ (K) PN; tdTomato$^{+}$ neurons are indicated as red spots. *Mafb*$^{tdTomato}$ neurons localize to anterolateral PN (J); upon ectopic Hoxa5 expression, neurons lose their spatial restriction and spread more posteriorly. **(L-M)** E15.5 AES, whole (L,M) or partial (L',M'), of E13.5 *Cre*-electroporated *ROSA*$^{lsl\text{-}tdTomato}$ (L,L') and *ROSA*$^{CAG\text{-}lsl\text{-}Hoxa5\text{-}KI/lsl\text{-}tdTomato}$ (M,M'), showing tdTomato$^{+}$ neurons and *Unc5b* RNA-FISH. *Unc5b*-tdTomato$^{+}$ colocalization (arrowheads) is detected by IMARIS and marked as a spot. Reduced *Unc5b* expression is observed upon Hoxa5 ectopic expression. **(N)** Bar graph of *Unc5b* expression per tdTomato$^{+}$ cells in E15.5 AES (n=6 for *ROSA*$^{lsl\text{-}tdTomato}$, n=5 for

*ROSA*$^{CAG\text{-}lsl\text{-}Hoxa5\text{-}KI/lsl\text{-}tdTomato}$, p-value = 0.0002). Data presented as mean + S.D. a-anterior, p-posterior. See also Figure S4.

**Figure 5**

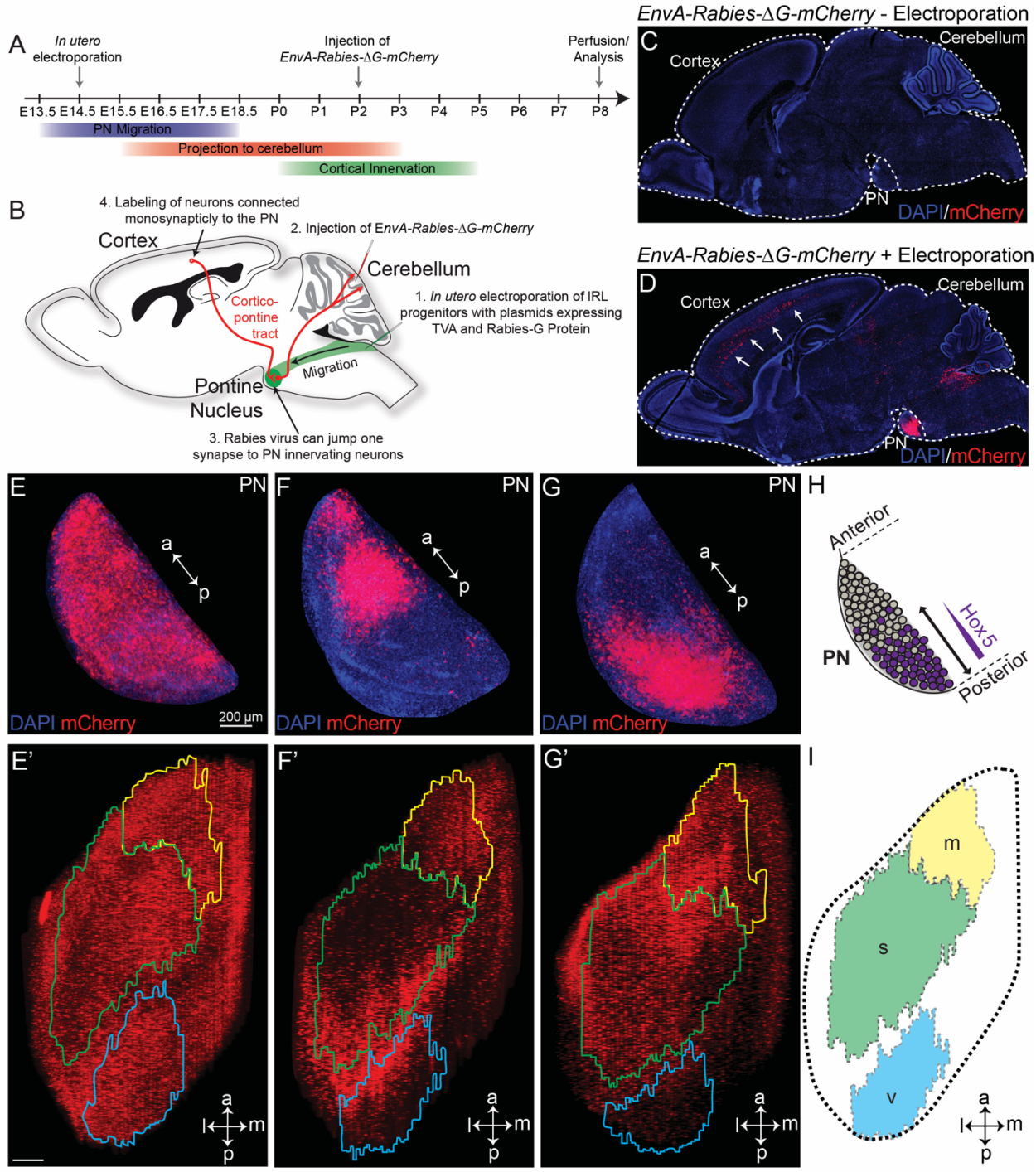


**Figure 5: Rostrocaudal position of PN neurons is predictive of cortical input connectivity**

(**A, B**) Diagrams of experimental design for transsynaptic tracing from PN neurons. (**C, D**) P8 brain sagittal sections showing mCherry$^+$ neuron distributions following cerebellar *EnvA-Rabies-ΔG-mCherry* virus injection and infection of PN neurons, non-electroporated (C) or *in utero* co-electroporated with *Rabies-glycoprotein* and *TVA* at E14.5 (D). Only in co-electroporated PN

neurons *EnvA-Rabies-ΔG-mCherry* virus transynaptically traces monosynaptically connected cortical neurons (arrows in D). (**E-G**) 3D reconstructions of P8 $WT^{TVA/EnvA/RabiesG}$ PN (E-G) and respective ipsilateral cortices (E'-G') showing infected neuron distribution after electroporation of whole (E-E'), anterior (F-F'), or posterior lRL (G-G'); single red spots are single $mCherry^{+}$ neurons. Color-coded contours label different cortical areas. Anterior PN neurons receive inputs mainly from visual and motor cortex (F,F'), whereas posterior PN neurons mainly from somatosensory and motor cortex (G,G'). (**H**) Diagram of *Hox5* (purple) expression in PN. (**L**) Diagram of different color-coded 3D reconstructed cortical areas as in F'. V, primary visual cortex (blue); S, primary somatosensory cortex (green); M, primary motor cortex (yellow); a, anterior; p, posterior; m, medial; l, lateral. See also Figure S5.

**Figure 6**

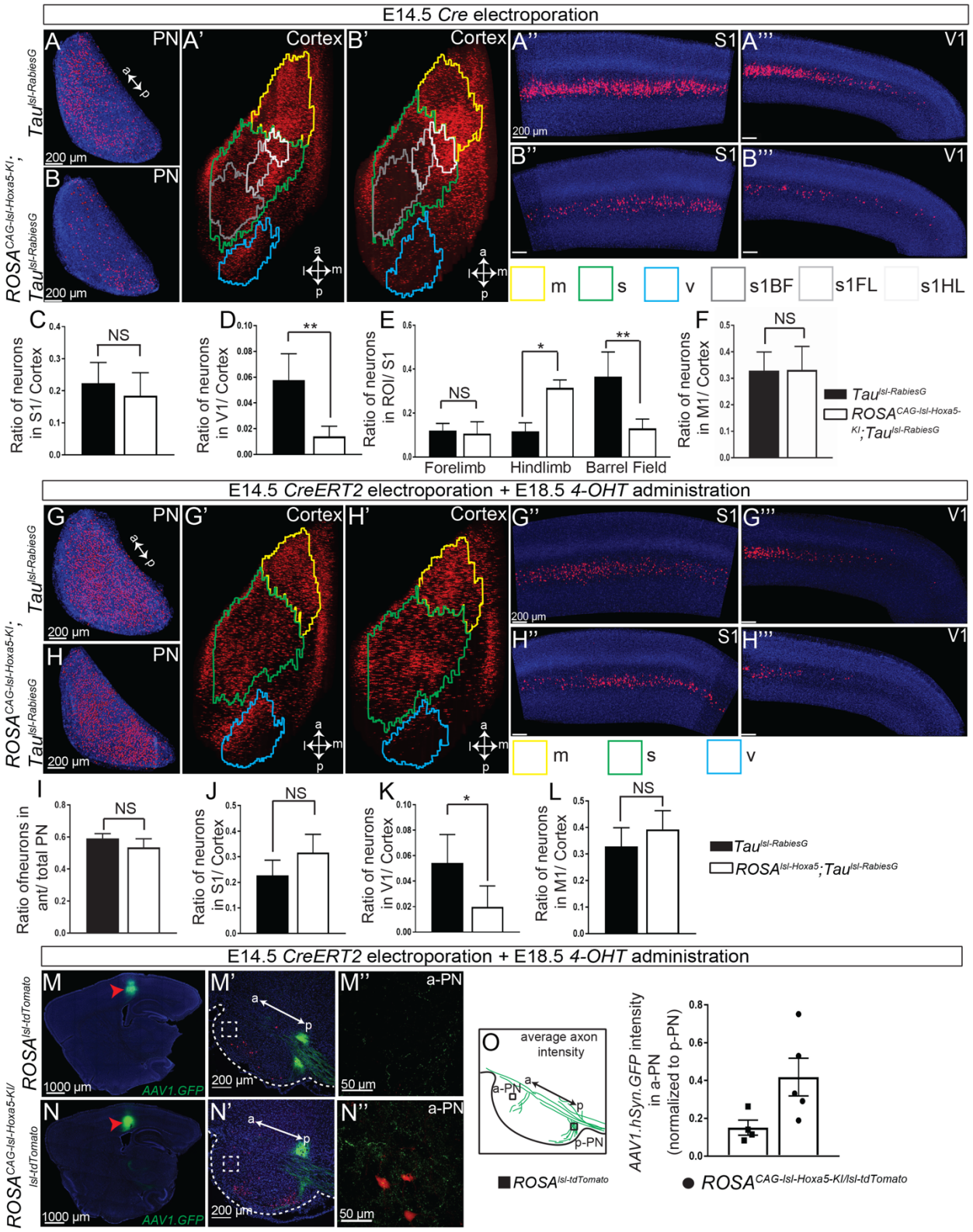
E14.5 Cre electroporation
A PN
A' Cortex
B' Cortex
A'' S1
A''' V1
B PN
B'' S1
B''' V1
200 µm
ROSA CAG-lsl-Hoxa5-KI ; Tau lsl-RabiesG
m
s
v
s1BF
s1FL
s1HL
C
Ratio of neurons in S1/ Cortex
NS
D
Ratio of neurons in V1/ Cortex
**
E
Ratio of neurons in ROI/ S1
NS
*
**
Forelimb
Hindlimb
Barrel Field
F
Ratio of neurons in M1/ Cortex
NS
Tau lsl-RabiesG
ROSA CAG-lsl-Hoxa5-KI ; Tau lsl-RabiesG
E14.5 CreERT2 electroporation + E18.5 4-OHT administration
G PN
G' Cortex
H' Cortex
G'' S1
G''' V1
H PN
H'' S1
H''' V1
I
Ratio ofneurons in ant/ total PN
NS
J
Ratio of neurons in S1/ Cortex
NS
K
Ratio of neurons in V1/ Cortex
*
L
Ratio of neurons in M1/ Cortex
NS
Tau lsl-RabiesG
ROSA lsl-Hoxa5 ; Tau lsl-RabiesG
E14.5 CreERT2 electroporation + E18.5 4-OHT administration
M
M'
M''
a-PN
N
N'
N''
ROSA lsl-tdTomato
ROSA CAG-lsl-Hoxa5-KI/ lsl-tdTomato
1000 µm
AAV1.GFP
200 µm
50 µm
O
average axon intensity
a-PN
p-PN
ROSA lsl-tdTomato
AAV1.hSyn.GFP intensity in a-PN (normalized to p-PN)
ROSA CAG-lsl-Hoxa5-KI/lsl-tdTomato

**Figure 6: Hoxa5 expression is sufficient to organize input connectivity of PN neurons**

(**A-B**) P8 sagittal sections of E14.5 *Cre*-electroporated $Tau^{lsl\text{-}RabiesG}$ (A) and $ROSA^{CAG\text{-}lsl\text{-}Hoxa5\text{-}KI}$;$Tau^{lsl\text{-}RabiesG}$ (B) showing distribution of electroporated neurons in PN (GFP+, in red) (A,B), and transsynaptically traced mCherry$^+$ neurons in distinct areas of respective ipsilateral cortices (A',B'), and S1 and V1 (A'',A''',B'',B'''), following P2 cerebellar injection of *SAD-ΔG-mCherry* virus. (**C-F**) Bar graph of fraction of mCherry$^+$ neurons in S1 (C), V1 (D), within distinct S1 regions (E), and M1 (F) (n=7 for $Tau^{lsl\text{-}RabiesG}$, n=5 for $ROSA^{CAG\text{-}lsl\text{-}Hoxa5\text{-}KI}$;$Tau^{lsl\text{-}RabiesG}$) (p-values are 0.348 (C), 0.001 (D), 0.974 (E, Forelimb), <0.0001 (E, hindlimb), <0.0001 (E, barrel field), 0.955 (F), respectively). Posteriorly biased, Hoxa5 overexpressing, PN neurons receive reduced input from V1 and barrel S1, and enriched input from hindlimb S1. **(G-H)** P8 sagittal sections of E14.5 *CreERT2* electroporated $Tau^{lsl\text{-}RabiesG}$ (G) and $ROSA^{CAG\text{-}lsl\text{-}Hoxa5\text{-}KI}$;$Tau^{lsl\text{-}RabiesG}$ (H) showing distribution of PN electroporated neurons (GFP+, in red) and transsynaptically traced mCherry$^+$ neurons in distinct areas of respective ipsilateral cortices (G',H'), and S1 and V1 (G'',G''',H'',H'''), following tamoxifen-induced *CreERT2*-mediated Hoxa5 and Rabies-glycoprotein ectopic activation at E18.5 and P2 cerebellar injection of *SAD-ΔG-mCherry*. **(I-L)** Bar graph of fraction of mCherry$^+$ neurons in anterior PN (I), S1 (J), V1 (K), and M1 (L) (n=4 for $Tau^{lsl\text{-}RabiesG}$, n=7 for $ROSA^{CAG\text{-}lsl\text{-}Hoxa5\text{-}KI}$;$Tau^{lsl\text{-}RabiesG}$) (p-values are 0.089 (I), 0.063 (J), 0.016 (K), 0.214 (L), respectively). Irrespective of their rostrocaudal position, postmigratory PN neurons ectopically overexpressing Hoxa5 are still targeted by S1, but receive reduced V1 inputs. **(M-N)** P18 sagittal sections of E14.5 *CreERT2*-electroporated $ROSA^{lsl\text{-}tdTomato}$ and $ROSA^{CAG\text{-}lsl\text{-}Hoxa5\text{-}KI/lsl\text{-}tdTomato}$ cortically injected with *AAV1.hSyn.eGFP* at P5 after tamoxifen-induced CreERT2 activation at E18.5. (M,N) Whole cortex sections indicating injection site (red arrowhead), (M',N') PN sagittal sections showing cortical axon bundles (green) and tdTomato$^+$ electroporated neurons (red), (M'',N'') higher magnification of a-PN neurons from inset in M' and N'. S1 afferents project to p-PN, with very few collaterals present in a-PN (M''); upon postmigratory Hoxa5 ectopic expression, S1 input targeting the a-PN is increased (N''). (O) Quantification of the S1 projections in a-PN in tamoxifen-treated *AAV1.hSyn.eGFP* injected, *CreERT2*-electroporated $ROSA^{lsl\text{-}tdTomato}$ and $ROSA^{CAG\text{-}lsl\text{-}Hoxa5\text{-}KI/lsl\text{-}tdTomato}$. Bar graph of ratio of GFP signal intensity in a-PN normalized to p-PN (p-value= 0.058). Each point represents quantification from individual animals. Data presented as mean + SD. PN and cortex representations are 3-D reconstructions. S1 and V1 images are 3-D reconstructions of a stack of 5 consecutive sagittal sections. Contour color and legend: m, motor (yellow); s, somatosensory (green); v, visual (blue); S1BF, primary somatosensory barrel field (dark grey); S1FL, S1 forelimb (light grey); S1HL, S1 hindlimb (white). a, anterior; p, posterior; m, medial; l, lateral; S1, primary somatosensory cortex; V1, primary visual cortex; M1, primary motor cortex. See also Figures S5 and S6.

**Figure 7**

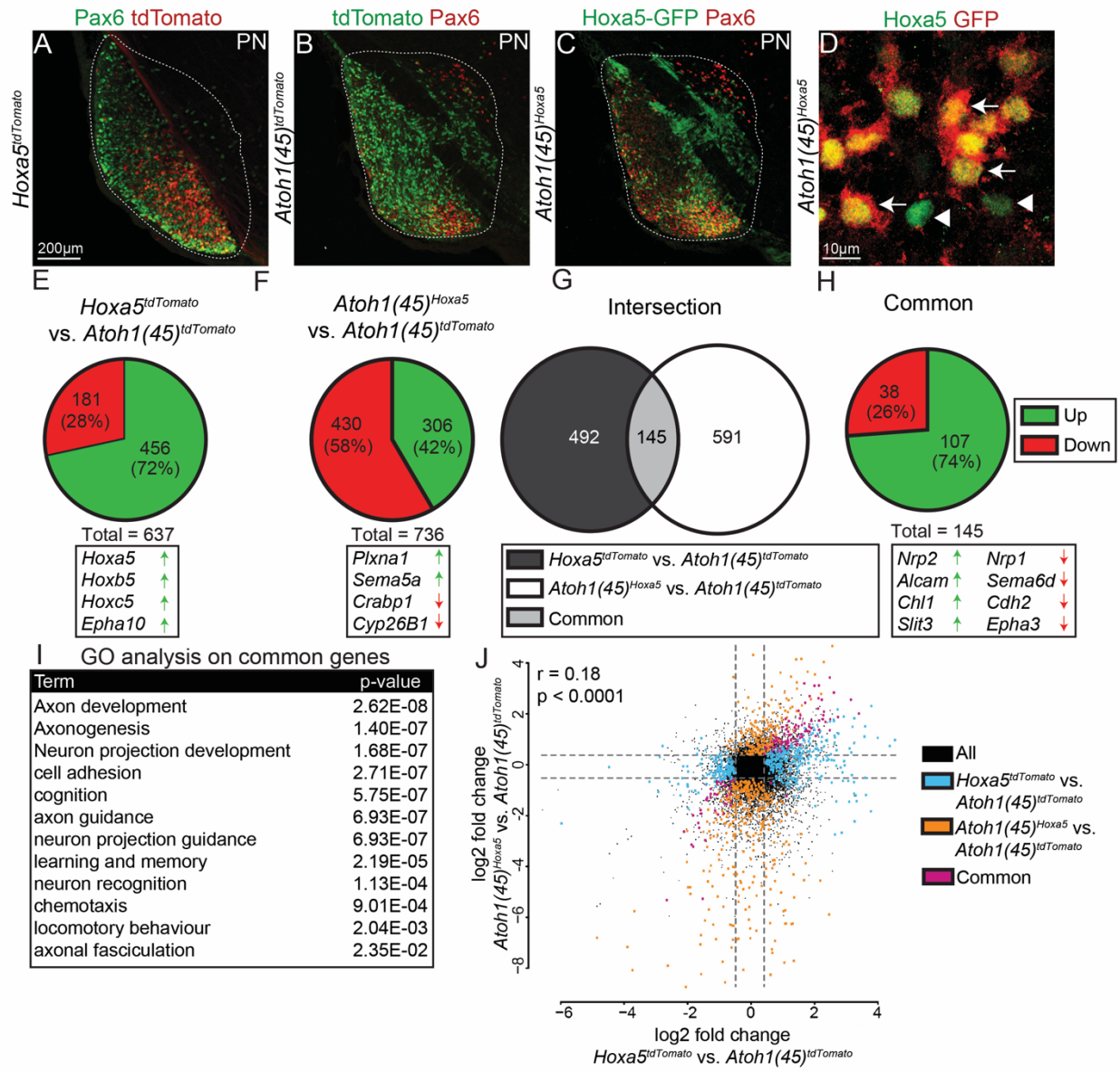


**Figure 7: Transcriptional programs of *Hoxa5* expressing PN neurons**

(**A-C**) E18.5 PN sagittal sections showing Pax6 (green) and tdTomato (red) expression in *Hoxa5*$^{tdTomato}$ (A) and *Atoh1(45)*$^{tdTomato}$ (B) and Pax6 (red) and GFP (green) in *Atoh1(45)*$^{Hoxa5}$ (C). (**D**) Higher magnification of PN neurons in *Atoh1(45)*$^{Hoxa5}$ showing co-expression of Hoxa5 (green) and GFP (red) (arrows). A few Hoxa5$^{+}$/GFP$^{-}$ cells were also seen (arrowheads). (**E-H**) Pie charts showing genes regulated in *Hoxa5*$^{+}$ (E) Hoxa5-overexpressing (F) as well as commonly regulated genes (H), as assessed by E18.5 RNA-seq of PN neurons FACS isolated from *Atoh1(45)*$^{tdTomato}$, *Hoxa5*$^{tdTomato}$, and *Atoh1(45)*$^{Hoxa5}$ (FC > 1.5; FDR < 0.07). Examples of genes and their regulation are in the boxes below the respective pie charts. (**G**) Venn diagram showing the intersection between *Hoxa5*$^{tdTomato}$ vs. *Atoh1(45)*$^{tdTomato}$ and *Atoh11(45)*$^{Hoxa5}$ vs. *Atoh1(45)*$^{tdTomato}$ RNA-seq comparisons. (**I**) Gene Ontology analysis of commonly regulated genes. (**J**) Scatter plot showing significant correlation between the

*Hoxa5*$^{tdTomato}$ vs. *Atoh1(45)*$^{tdTomato}$ and *Atoh11(45)*$^{Hoxa5}$ vs. *Atoh1(45)*$^{tdTomato}$ RNA-seq comparisons ($r = 0.19$; R squared = 0.036; p-value < 0.0001). Data presented as mean + SD. See also Figure S7.

## MATERIAL AND METHODS

### Animals

All animal procedures were performed in accordance with institutional guidelines and were approved by the Veterinary Department of the Kanton Basel-Stadt

### Generation of the *Atoh1(45)::Cre* line

The original goal was to create a *Atoh1::CreERT2* line. Due to Cre activity in the absence of tamoxifen for one of the founders (#45), this line was used as a normal Cre line and renamed *Atoh1(45)::Cre*. In these transgenic mice, the *Cre* is driven by a 1.7 kb enhancer of *Atoh1* (Helms et al., 2000*)*. The enhancer was subcloned into the vector pKS-ß-globin-CreERT2-SV40pA, created by replacing the *LacZ* gene of the pKS-ß-globin-lacZ vector (BGZ40) (Studer et al., 1996) with a CreERT2 cassette (Santagati et al., 2005) using homologous recombination. The enhancer was amplified by PCR from genomic DNA using the following primers: 5'AGT TGT GCC TGT CTA AGG TC 3' and 5'ATC TAC TAG TGC TCT GGC TTC TGT AAA CTC 3'. The PCR band was purified and inserted 5' of the ß-globin promoter using restriction sites SacII and SpeI, thus generating a construct consisting of the enhancer, a ß-globin minimal promoter and CreERT2 encoding sequence. The construct was linearized, purified and microinjected into the pronuclei of mouse zygotes. Founders were identified by PCR (907bp fragment) using the following primers: 5'AGT GGA GAA TGG GTT AAA TCC 3' and 5'ATC AGT GCG TTC GAA CGC TA 3'.

**Generation of the *Jmjd3* knock-in line**

The knock-in mouse strain *JmjD3*$^{lacZ}$ was created from ES cell clone (EPD0330_7_F03, Kdm6b$^{tm1(KOMP)Wtsi}$) obtained from the NCRR-NIH supported KOMP Repository (www.komp.org) and generated by the CSD consortium for the NIH funded Knockout Mouse Project (KOMP). Methods used on the CSD targeted alleles have been published in Testa et al., 2004. The ES cells were aggregated with morula-stage embryos obtained from inbred (C57BL/6 x DBA/2) F1 mice. Germline transmission of the Kdm6b$^{tm1(KOMP)Wtsi}$ allele was obtained and heterozygous mice were viable and fertile. The mice were genotyped by PCR (359bp wild type and 572bp mutant fragments) with the following primers: wild type forward, 5' CCT TAG AGA GAG CAG AGT TC 3'; wild type reverse, 5' TGG TTT CCG ACT GCT GTG TG 3'; mutant reverse, 5' CTG TCC CTC TCA CCT TCT AC 3'. The in-frame *LacZ* expression cassette was flanked by two flip sites, which allowed its Flippase mediated removal.

**Generation of the *ROSA26::(lox-stop-lox)Hoxa5-IRES-GFP BAC transgenic line***

The generation of the conditional *Hoxa5* overexpression BAC transgenic line was a two-step process. First we generated a BAC ROSA26::(lox-stop-lox)galK-IRES-GFP, used it as an entry for further constructs and allowing us the introduction of different cDNAs between the lox-stop-lox sequence and the IRES-GFP by using BAC recombineering and galK negative selection (Warming et al., 2005). Then we used this strategy to replace the *galK* gene by a codon optimized DNA sequence encoding for the Hoxa5 protein. The original BAC clone RP23-401D9 containing the ROSA26 locus was obtained from BACPAC Resources Center (Children's Hospital Oakland Research Institute, Oakland, Calif., USA) and was used as a template for bacterial recombination. To prevent any further interactions,

the LoxP511 and the LoxP sites located in the backbone vector of this BAC were removed respectively by recombination of an ampicillin resistance gene and by using the galK positive/negative selection (Warming et al., 2005). The final BAC *ROSA26::(lox-stop-lox)Hoxa5-IRES-GFP* (consisting of a splice acceptor, a lox-PGK-Neo-3xpA(stop)-lox cassette, a codon optimized *Hoxa5*, an IRES-GFP-pA) and all the intermediate constructs were tested by PCR, restriction enzyme digestion and sequencing for correct recombination and removals of the lox/galK sequences. The purified BAC was linearized by PI-SceI digestion prior to microinjection into pronuclei of mouse zygotes. Founders were identified by PCR (220bp fragment) using the following primers: 5' TGC AGC CCA AGC TAG CTT AT 3' and 5' TCT CTG AAC TGC TCG GAC AC 3'.

**Generation of the *ROSA26::CAG(lox-stop-lox)3xFlag-Hoxa5-IRES-GFP* knock-in line**

The conditional Hoxa5 overexpression mouse line was generated by homologous recombination in the ROSA26 locus using the targeting vector pR26-CAG-lsl-3xflagHoxa5-IRES-GFP, consisting of a CAG promoter, a lox-stop-lox cassette, a codon optimized *Hoxa5* tagged with a 3xFlag, an IRES-GFP, a WPRE element, a bGH poly(A) and a PGK-Neo cassette. To generate this vector, we used the vector pR26-CAG-lsl-Kir (kind gift from Guillermina López-Bendito and derived from the plasmid Ai27 (Madisen et al., 2012); Addgene Plasmid #34630), in which we replaced the insert located between the two FseI restriction sites by the cassette 3xflagHoxa5-IRES-GFP (PCR amplified from the BAC *ROSA26::(lox-stop-lox)Hoxa5-IRES-GFP* and cloned into the TOPO vector pCRII (Invitrogen) with insertion of a 3xFlag tag). The final targeting vector pR26-CAG-lsl-3xflagHoxa5-IRES-GFP was linearized with PvuI and electroporated into the E14 ES cell line. The positive ES cell clones selected by G418 resistance and screened by PCR were

aggregated with morula-stage embryos obtained from inbred (C57BL/6 x DBA/2) F1 mice. Germline transmission of the *ROSA26::CAG(lox-stop-lox)3xFlag-Hoxa5-IRES-GFP* allele was obtained. Heterozygous and homozygous mice were viable and fertile. The mice were genotyped by PCR (603-bp wild type and 325-bp mutant fragments) with the following primers: wild type forward, 5' AAA GTC GCT CTG AGT TGT TAT 3'; wild type reverse, 5' GGA GCG GGA GAA ATG GAT ATG 3'; mutant reverse, 5' GGC CAT TTA CCG TAA GTT ATG 3'.

**Generation of the *Tau::(lox-stop-lox)Rabies-glycoprotein-IRES-nls-LacZ***

The Tau::(lox-stop-lox)Rabies-glycoprotein-IRES-nls-LacZ mouse line was generated by inserting a cassette encoding (lox-stop-lox)Rabies-glycoprotein-IRES-nls-LacZ into exon 2 of the Tau locus using a strategy described previously (Hippenmeyer et al., 2005).

**Generation of *Hoxa5::Cre* knock-in line**

We generated a targeting construct *pHoxa5-Cre-FRT-Neo-FRT* consisting of a Cre cassette and a SV40 poly A signal derived from the plasmid pN21-Cre (Di Meglio et al., 2003) followed by cassette *FRT–PGK–NeobpA–FRT* from the plasmid PL451 (Liu et al., 2003), flanked by 5' and 3' homology arms corresponding to 1125 bases upstream and 1619 bases starting 45 bases downstream of the *Hoxa5* ATG codon respectively. This construct, initially prepared for homologous recombination in mouse embryonic stem cells, was used to produce a linear double stranded (ds) DNA template for mouse zygote injection in combination with the CRISPR/Cas9 system. The targeting construct was digested by the restriction enzyme PspOMI and gel purified to obtain a linear 5,5 kb dsDNA template

composed by the cassette Cre-SV40polyA-FRT-Neo-FRT flanked by 5' and 3' homology arms of 0.98 kb and 1.5 kb respectively.

We designed a single guide (sg)RNA, produced by Integrated DNA Technologies (IDT), to target *Hoxa5* at the following protospacer sequence: TTTTGCGGTCGCTATCCAAA.

For zygote injection, sgRNA (50 ng/µl), cas9 mRNA (100 ng/µl) and the linear dsDNA template (45 ng/µl) were mixed in 0.1 TE buffer (10 mM Tris-HCl pH 7.4, 0.1 mM EDTA pH 8.0) and microinjected into the pronuclei of B6CF2 mouse zygotes. Knock-in founder was identified by PCR and Southern-Blot. Germline transmission of the *Hoxa5::Cre(FRT-neo-FRT)* allele was confirmed and in vivo Flp-mediated excision of the PGK-*neo* cassette was obtained by mating the *Hoxa5::Cre(FRT-neo-FRT)* mice to the ACTB:FLPe deleter. The mice were genotyped by PCR (317bp wild type and 581bp mutant fragments) with the primers described in key resource table.

**Other mouse lines used in this study**

*RARE::lacZ* (Rossant et al., 1991), *ACTB::Flip* (Rodriguez et al., 2000), *Wnt1::Cre* (Danielian et al., 1998), *r5-6::Cre*, *Hoxa5::Cre*, *MafB::CreERT2* (Di Meglio et al., 2013), *Ezh2*$^{fl/fl}$ (Puschendorf et al., 2008), and *ROSA26::(lox-stop-lox)TVA-IRES-LacZ* (Seidler et al., 2008) lines were as described. *ROSA26::(lox-stop-lox)tdTomato* (Madisen et al., 2010) mice were obtained from The Jackson Laboratory, USA.

### *In vivo* treatment

Retinoic acid (RA) was dissolved in DMSO and administered to pregnant mice by intraperitoneal injection (30mg/Kg at E11.5 or 60mg/kg at E9.5). Tamoxifen was dissolved in corn oil (10mg/ml stock solution) and was administered by oral gavage at E7.5 (1mg) to *Mafb::CreERT2* mice. For activation of Cre from *ERT2CreERT2* plasmid, 1mg of 4-Hydroxytamoxifen (4-OHT) (dissolved in 50µL Ethanol, diluted to 500µL with corn oil) was administered to pregnant mice orally at E18.5. For oral gavage, disposable plastic feeding tubes were used.

### *In utero* electroporation

*In utero* electroporation was performed on embryos at E13.5 or E14.5 as described previously (Taniguchi et al., 2006). Plasmids used for electroporation were diluted to 1.5mg/ml in 1x phosphate buffer (PBS). Plasmids used in this study were as follows: *pCX-eGFP* (Okada et al., 2007), *pCX-rabies-glycoprotein-WPRE*, *pCAG-mGFP-2a-Cyp26b1*, *pAAV-EF1a-TVA-WPRE* (kind gift from Botond Roska), *pCAG-Cre*, *pCAG-ERT2CreERT2* (addgene, Plasmid #13777; Matsuda et al., 2007), *pCAG-Unc5b*

### Histological analysis, immunostaining, and *in situ* hybridization

Prenatal brains were dissected if necessary and fixed in 4% PFA diluted in 1xPBS from 30 minutes at room temperature to overnight at 4°C. Postnatal animals were perfused with 4% PFA diluted in 1xPBS for 10 minutes and post fixed in 4% PFA diluted in 1xPBS overnight at 4°C. For cryostat sections, tissues were cryoprotected in 20% sucrose (Sigma) / 1xPBS and embedded in 7.5% gelatin (Sigma) / 10% sucrose / 1xPBS before being frozen at -80°C. Cryostat sections (25-30 µm) were cut (Microm HM560) in coronal and sagittal orientations.

Vibratome sections (50-80 μm) were prepared from postnatal brains after embedding in 4% agarose (Promega) / 0.1 M phosphate buffer (pH7.4). Immunohistochemistry was performed as described before (Geisen et al., 2008) using following primary antibodies: rabbit anti-Pax6 (Millipore; AB2237; 1/1000), rabbit anti-Hoxa5 (Sigma; HPA029319; 1/100), rabbit anti-RFP (Rockland, 600-401-379, 1/1000), rabbit anti-Barhl1 (Sigma; HPA004809; 1/200), rat anti-Hoxb4 (developed by A. Gould and R. Krumlauf; obtained from the Developmental Studies Hybridoma Bank developed under the auspices of the NICHD and maintained by The University of Iowa, Department of Biology, Iowa City, IA 52242; 1/100), chicken anti-GFP (Invitrogen, A10262, 1/500), mouse anti-Phospho Histone H3 (Cell Signalling; 6G3; 1/100) and chicken anti-mcherry (Novus Biologicals; NBP2-25158; 1/500) followed by species-specific fluorochrome-coupled secondary antibody staining (Alexa Fluor 488, 546, or 647, Invitrogen, 1/500). Nuclei were stained with DAPI (Invitrogen, 1/10000). Simple and double *in situ* hybridisations were performed as described previously (Geisen et al., 2008). The following probes were used: *Barhl1, Wnt1, Axin2* (a kind gift from Paola Bovolenta)*, Hoxa2, Hoxa3, Hoxa4, Hoxb4, Hoxb5, Hoxa5, Ezh2, Cyp26b1, Raldh2, Chl1, Alcam1, Nrp1, and Nrp2, Robo3*. X-Galactosidase staining was performed as previously described (Geisen et al., 2008).

**Fluorescent activated Cell Sorting (FACS)**

Regions of interested were micro-dissected in 1xPBS at the desired stage and incubated for 5 – 10 minutes in activated dissociation solution (HBSS, 2.5mM Cystein, 0.5mM EDTA, 10mM HEPES, 1mg/ml Papain (Roche)) at 37°C. Samples were rinsed five times in HBSS / 10% FBS. Single cell suspension was achieved through mechanical dissociation of tissue

with Pasteur pipettes. Fluorescent cells were collected by FACS (FACSCalibur, Becton Dickson) in appropriate solutions for analysis.

**Quantitative PCR (qPCR)**

100 cells isolated by FACS were directly sorted into the reverse transcription (RT) buffer (1x CellsDirect One-Step qPCR Kit (Invitrogen, 11753-100), SuperScript III RT Platinum Taq Mix, Primer mix (50nM final concentration)). RT was done for 15 minutes at 50°C flowed by inactivation of the reverse transcriptase and activation of the Taq at 95°C for 2 minutes. 18 cycles (95°C 15 seconds, 60°C 4 minutes) of pre-amplification of specific targets were done on a standard thermal cycler. Unincorporated primers were removed by Exonuclease I treatment (NEB, M0293S, 1U/µl) for 30 minutes at 37°C. The final product was diluted 10-fold with DNA Suspension Buffer (TEKnova, T0221). qPCR was carried out with StepOne Real Time PCR System (Applied Biosystems) with the primers described below. Calculations were done using the delta delta cycle threshold (ddCt) model using Ssu72 as an endogenous control.

Hoxb3_F: GGCCTCAATCACCTTTCCCA

Hoxb3_R: CAGGGTCCATGATGCTGGTT

Hoxb4_F: GCAAAGAGCCCGTCGTCTA

Hoxb4_R: GGCGTAATTGGGGTTTACCG

Hoxa5_F: CCCCAGATCTACCCCTGGATG

Hoxa5_R: TGGGCCACCTATATTGTCGTG

Ssu72_F: GGTGTGCTCGAGTAACCAGAA

Ssu72_R: CAAAGGAGCGGACACTGAAAC

**Chromatin immunoprecipitation (ChIP)**

Micro-dissected tissue samples were dissociated to single cells. Cells were cross-linked for 15 min in 1% PFA/1xPBS solution and subsequently lysed in cell lysis buffer (5mM PIPES pH8.0, 85mM KCl, 0.5% NP40, and protease inhibitors) for 10 min on ice. Nuclei were spin down at 2500g for 5 min at 4°C and finally lysed in nuclei lysis buffer (50mM Tris-HCl pH8.0, 10mM EDTA, 1% SDS and protease inhibitors). Following 15 min of lysis on a tube shaker at 4°C, samples were sonicated on Covaris and centrifuged at 22000g for 15 min at 4°C. Chromatin preparation was diluted 10x with IP Dilution Buffer (0.01% SDS, 1.1% Triton-X 100, 1.2mM EDTA, 16.7mM Tris-HCl pH8.0, 167 mM NaCl, and protease inhibitors) and used for IP. For IP, chromatin preparations were incubated overnight with primary antibodies against H3K27me3 (Millipore, 17-622, 1µg), H3K4me3 (Millipore, 17-614, 1µg), RAR (Santa Cruz, sc-773, 1µg), or Jmjd3 (Abcam, ab38113, 1µg) on a tube roller at 4°C. 50 µl of protein G magnetic beads were added and the incubation continued for 2 h. Beads were washed 3 times with 1ml of 0.02% Tween20/TBS solution. Precipitated material was eluted twice for 15min with 100µl of 1% SDS/ 100 mM sodium hydrogencarbonate (NaHCO3) solution at 65ºC on a thermal shaker. 20µl of 5M NaCl was added to the elute and the cross-links reversed by incubating for 6 h at 65ºC. DNA was purified using Min-elute PCR purification kit (Qiagen). qPCR for amplification of genomic regions of interest was described as above with the following primer pairs.

Hoxa2_promoter_F: CGCCTGCAGTCATTAACAAA

Hoxa2_promoter_R: TCCCACTCTGCTCCTTTCTC

Hoxa5_promoter_F: CACCCAAATATGGGGTACGA

Hoxa5_promoter_R: CCCCATTAGTGCACGAGTTT

Hoxb5_promoter_F: CAGCCACGGTAATTCTCCAT

Hoxb5_promoter_R: TATTTGAGGCAAAGCCAAGC

Hoxa9_promoter_F: TCACCTCGCCTAGTTTCTGG

Hoxa9_promoter_R: GGAGGGAGGGGAGTAACAAA

Hoxa5_RARE_F: ATTGCATTTCCCTCGCAGTTCC

Hoxa5_RARE_R: GCTGACGGCCTCACAATTGG

Negative_control_region_F: ATGCCCCTCAGCTATCACAC

Negative_control_region_R: GGACAGACATCTGCCAAGGT

**4C template preparation**

4C template was prepared as described in (van de Werken et al., 2012) with modifications. Briefly, cells were dissociated (30' @ 37°C in 0.25% trypsin; 1mg/ml collagenase type II; 5mM EDTA). Cells were fixed using 2% formaldehyde/10%FCS/PBS for 10' at RT. Cells were lysed for 10' on ice (50mM Tris-HCl pH 7.5, 150mM NaCl, 5mM EDTA, 0.5% NP40 substitute, 1% Triton-X100, 1X proteinase inhibitors). Chromatin was digested in the context of the nucleus using the restriction enzymes NlaIII, followed by ligation. Ligated chromatin was de-crosslinked in the presence of proteinase K at 65°C O/N and subsequently treated with RNase A. Genomic DNA was extracted by beads purification and subsequently digested O/N using the restriction enzymes Csp6I and ligated under diluted conditions (16°C, O/N) favoring intra-molecular ligations. Genomic DNA was cleaned up using bead purification.

**4C PCR, mapping and analysis of 4C data**

The 4C PCR was performed as described in (van de Werken et al., 2012) using the primers below and sequencing was done on the Illumina HiSeq. Reads were mapped, allowing no mismatches, to a database of 4C-seq fragment-ends generated from the mm10/NCBI m38 version of the mouse genome. Interaction profiles shown are produced using all fragments (blind and non-blind) calculating a running mean with a window of 31 fragments. The profiles are normalized to the total amount of reads in cis.

| **Primer Name** | **Primer sequence** | **Tissue** |
|---|---|---|
| Hoxa5_Fw | AAGGATCGAAATAGCTCATG | Cortex WT |
| Hoxa5_Fw_TTG | TTGAAGGATCGAAATAGCTCATG | Cortex RA |
| Hoxa5_Fw_TCA | TCAAAGGATCGAAATAGCTCATG | r8 WT |
| Hoxa5_Fw_GAC | GACAAGGATCGAAATAGCTCATG | r8 RA |
| Hoxa5_Fw_CTT | CTTAAGGATCGAAATAGCTCATG | r5-6 WT |
| Hoxa5_Fw_AGT | AGTAAGGATCGAAATAGCTCATG | r5-6 RA |
| Hoxa5_Rev | AAACGCACTGAAGCACTACT | |
| Hoxb5_Fw | AAAGACATTGAAGGAACATG | Cortex WT |
| Hoxb5_Fw_GTA | GTAAAAGACATTGAAGGAACATG | Cortex RA |
| Hoxb5_Fw_GAC | GACAAAGACATTGAAGGAACATG | r8 WT |
| Hoxb5_Fw_CTT | CTTAAAGACATTGAAGGAACATG | r8 RA |
| Hoxb5_Fw_AGT | AGTAAAGACATTGAAGGAACATG | r5-6 WT |
| Hoxb5_Fw_AAG | AAGAAAGACATTGAAGGAACATG | r5-6 RA |
| Hoxb5_Rev | TAGATCCCCAAAGAGACTCA | |

**RNA sequencing analysis**

All samples were run in triplicates with three embryos per replicate. 2000 cells per sample were isolated by FACS, directly sorted into lysis buffer and snap frozen to -80°C. RNA was extracted using the PicoPure RNA Isolation Kit (Applied Biosystems) and retro-transcribed. cDNA was amplified from total RNA using the Ovation RNA Amplification System (NuGEN). Libraries were prepared using the Total RNA Sequencing TotalScript Kit (Epicenter) and sequencing was performed using Hi-Seq 2500 Illumina solid sequencer. Data analysis was performed using the Bioconductor QuasR Package (Gaidatzis et al., 2015). The cut-off for low abundant transcripts was set to 1 count per million reads in control samples. Gene Ontology analysis was performed using the GO Enrichment Analysis tool powered by PANTHER (http://geneontology.org/page/go-enrichment-analysis).

**Virus production and tracing experiments**

EnvA-Rabies-ΔG-mCherry (a kind gift of E. Callaway) or SAD-ΔG-mCherry viruses were produced in B19G2 and BHK-EnvA2 cells stably expressing the rabies-glycoprotein and viral titers were determined as described elsewhere (Wickersham et al., 2010). Multiple injections per animal were targeted to the cerebellar hemisphere contralateral to the electroporated PN at P2. Pups were perfused at P8. Brains were dissected out and fixed in 4% PFA overnight at 4°C. Vibratome sectioning was performed to obtain brain slices which were subsequently stained with DAPI and imaged on Zeiss Axioscan Z1, analysis was done using Fiji and IMARIS (Bitplane). AAV1.hSyn.GFP.WPRE.bGH (Penn Vectors) was used for anterograde tracing from cortex. Stereotaxic injection (Kopf Instruments) was performed on isoflurane anaesthetized P5 animals using picospitzer (Parker). Coordinates to target S1 cortex used bregma as a reference point for anterior-posterior (-0.58), medio-lateral (1.5-1.8)

and dorso-ventral (1.0 -1.5) coordinates. The injection was targeted to the hemisphere ipsilateral to electroporated PN. Mice were perfused at P18 and dissected brains were processed for vibratome sectioning and immunohistochemistry. Only mice with confirmed anatomical precision to the target region and efficient electroporation were included in further analysis. Imaging was done on Zeiss LSM 700.

**RNA-FISH**

Fluorescent *in situ* hybridisation (FISH) was performed using the RNAscope Multiplex Fluorescent Kit (Advanced Cell Diagnostics (ACD), ref: 320850) according to the protocol described in Laumonnerie et al., 2015. Targeted sequences were: Mm-*Unc5b*-C1, nucleotides 3531 – 4791 of accession number NM_029770.2 and Mm-*Barhl1*-C3, nucleotide 821 – 2282 of accession number NM_019446.4 . A probe against the gene encoding POL2RA, a protein expressed in mammalian cells, was used as a positive control, and a probe against *Escherichia coli dapB* (not expressed in mammalian cells) was used as a negative control (data not shown). Imaging was done on Nikon Ti2-E Eclipse spinning disk, image analysis was done using Fiji and IMARIS (Bitplane).

**Imaging and picture processing**

Chromogenic staining was examined by classical wide-field or binocular microscope (Nikon). Dual chromogenic and fluorescent imaging was done on a Zeiss LSM 700 confocal microscope. Imaging of fluorescent signals was performed using an Axio imager Z2 upright microscope coupled to a LSM700 Zeiss laser scanning confocal 5x (NA 0.25), 10x (NA 0.45), 20x (NA 0.8),40x (NA 1.3) or 63X (NA 1.4) lens. Stitching of whole-mounts was performed using Zen software or Xuvtools (http://www.xuvtools.org). For 3D reconstructions the whole

brain was sliced in 50µm sections and imaged with an Axio Scan.Z1 using a 10x (NA 0.45) lens. Regions of interest in consecutive images were aligned using TrakEM2 as incorporated into the Fiji software (http://fiji.sc/wiki/index.php/Fiji). Reconstructions were visualized using Bitplane IMARIS. Counting of neuronal cell bodies in different regions of the CNS was done with Imaris Spot detection tool.

**Statistical analysis**

Graphs were generated and statistical analysis was done with GraphPad Prism software. All results are presented as the mean ± S.D. Statistical significance was accepted at the $p<0.05$ level ($p<0.05$ = *, $p<0.01$ = **, $p<0.001$ = ***). Statistical significance was assessed by nonpaired, two-tailed Student's t-test for the comparison of two unmatched groups, ordinary one-way ANOVA followed by Bonferroni's multiple comparisons test for more than two unmatched groups, and by ordinary two-way ANOVA followed by Bonferroni's multiple comparisons test for analysis with two factors. Comparison of RNA-seq datasets was done using Pearson correlation coefficient analysis.

## SUPPLEMENTAL MATERIAL

| Nomenclature | Genotype |
|---|---|
| *Hoxa5$^{Cre\text{-}KI/tdTomato}$* | Hoxa5::Cre (Knock-in); ROSA::(lox-stop-lox)tdTomato |
| *ROSA$^{lsl\text{-}tdTomato}$* | ROSA::(lox-stop-lox)tdTomato |
| *RARE$^{lacZ}$* | RARE::LacZ |
| *Atoh1(45)$^{tdTomato}$* | Atoh1(45)::Cre; ROSA::(lox-stop-lox)tdTomato |
| *Wnt1$^{Ezh2cKO}$* | Wnt1::Cre; Ezh2$^{fl/fl}$ |
| *Jmjd3$^{lacZ/lacZ}$* | homozygous lacZ Knock-in of Jmjd3 locus |
| *Jmjd3$^{+/-}$* | Jmjd3$^{lacZ/+}$ crossed with ACTB:FLPe deleter to remove the targeting cassette |
| *Atoh1(45)$^{tdTomato}$;Jmjd3$^{-/-}$* | Atoh1(45)::Cre; ROSA::(lox-stop-lox)tdTomato; Jmjd3$^{-/-}$ |
| *Hoxa5$^{tdTomato}$* | Hoxa5::Cre (BAC transgenic); ROSA::(lox-stop-lox)tdTomato |
| *r5-6$^{tdTomato}$* | r5-6::Cre; ROSA::(lox-stop-lox)tdTomato |
| *ROSA$^{lsl\text{-}Hoxa5\text{-}BAC}$* | *ROSA::(lox-stop-lox)Hoxa5-IRES-GFP* (BAC transgenic) |
| *ROSA$^{CAG\text{-}lsl\text{-}Hoxa5\text{-}KI}$* | *ROSA::CAG(lox-stop-lox)Hoxa5-IRES-GFP* (Knock-in) |
| *ROSA$^{CAG\text{-}lsl\text{-}Hoxa5\text{-}KI/lsl\text{-}tdTomato}$* | ROSA::CAG(lox-stop-lox)Hoxa5-IRES-GFP (Knock-in); ROSA::(lox-stop-lox)tdTomato |
| *MafB$^{tdTomato}$* | MafB::CreERT2; ROSA::(lox-stop-lox)tdTomato |
| *MafB$^{Hoxa5/tdTomato}$* | MafB::CreERT2; ROSA::(lox-stop-lox)Hoxa5-IRES-GFP (BAC transgenic); ROSA::(lox-stop-lox)tdTomato |
| *WT$^{TVA/EnvA/RabiesG}$* | CD1 electroporated at E14.5 with plasmids expressing *TVA* and *Rabies-Glycoprotein*, injected with *EnvA-Rabies-ΔG-mCherry* |
| *Tau$^{lsl\text{-}RabiesG}$* | Tau::(lox-stop-lox)Rabies-glycoprotein-IRES-LacZ |
| *ROSA$^{CAG\text{-}lsl\text{-}Hoxa5\text{-}KI}$;Tau$^{lsl\text{-}RabiesG}$* | ROSA::CAG(lox-stop-lox)Hoxa5-IRES-GFP (Knock-in); Tau::(lox-stop-lox)Rabies-glycoprotein-IRES-LacZ |
| *Atoh1(45)$^{Hoxa5}$* | Atoh1(45)::Cre; ROSA::CAG(lox-stop-lox)Hoxa5-IRES-GFP (Knock-in) |

Table S1: List of mouse lines used and their nomenclature. Related to Figures 1, 2, 4, 5, 6 and 7.

**Figure S1**

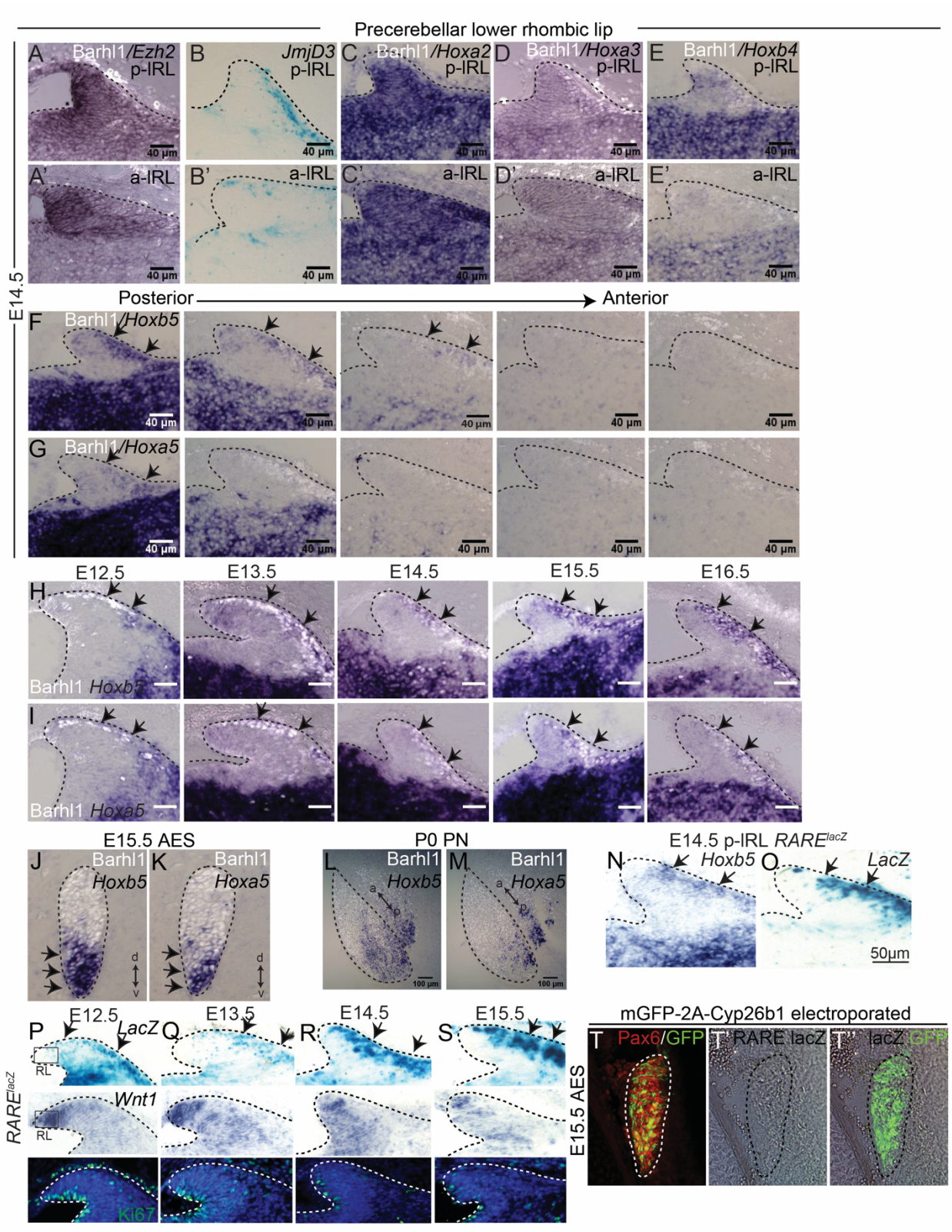
Precerebellar lower rhombic lip
A Barhl1/Ezh2 p-IRL
B JmjD3 p-IRL
C Barhl1/Hoxa2 p-IRL
D Barhl1/Hoxa3 p-IRL
E Barhl1/Hoxb4 p-IRL
A' a-IRL
B' a-IRL
C' a-IRL
D' a-IRL
E' a-IRL
E14.5
Posterior
Anterior
F Barhl1/Hoxb5
G Barhl1/Hoxa5
40 µm
E12.5
E13.5
E14.5
E15.5
E16.5
H Barhl1 Hoxb5
I Barhl1 Hoxa5
E15.5 AES
J Barhl1 Hoxb5
K Barhl1 Hoxa5
d
v
P0 PN
L Barhl1 Hoxb5
M Barhl1 Hoxa5
a
p
100 µm
E14.5 p-IRL RARE lacZ
N Hoxb5
O LacZ
50µm
P LacZ
Q
R
S
RL
Wnt1
Ki67
RARE lacZ
mGFP-2A-Cyp26b1 electroporated
T Pax6/GFP
T' RARE lacZ
T'' lacZ GFP
E15.5 AES

**Figure S1: *Hox* gene expression pattern at different stages and role of RA in regulating *Hox5* gene expression. Related to Figure 1.**

**(A-E)** E14.5 wild type coronal sections showing in situ hybridization (ISH) for *Ezh2* **(**A,A'), *Hoxa2* (C,C'), *Hoxa3* (D,D'), and *Hoxb4* (E,E') coupled with immunohistochemistry (IHC) for Barhl1 (white), in posterior (A-E) and anterior (A'-E') lRL; *Hox2-4* genes are expressed in progenitor as well as postmitotic domains, while expression of *Ezh2* is stronger in progenitor domain. (B) $Jmjd3^{LacZ/+}$ β-gal stained coronal sections showing *Jmjd3* expression in posterior (B) and anterior (B') lRL. Unlike *Ezh2*, *Jmjd3* is expressed in the postmitotic precerebellar neurons. **(F-G)** ISH for *Hoxb5* (F) and *Hoxa5* (G) coupled with IHC for Barhl1 (white) through the anteroposterior lRL. Both *Hoxa5* and *Hoxb5* are expressed in posterior postmitotic neurons; *Hoxa5* expression is lower and restricted to more posterior lRL than *Hoxb5* (arrows in F and G). **(H-M)** ISH for *Hoxb5* (H,J,L) and *Hoxa5 (*I,K,M*)* coupled with IHC for Barhl1 (white) in E12.5 to E16.5 lRL (H-I), E15.5 AES (J-K) and P0 PN (L-M). Expression of *Hoxa5* and *Hoxb5* is mostly induced in postmitotic $Barhl1^{+}$ precerebellar neurons (arrows in H and I), remains posterior in AES (J,K) and PN (L,M). **(N-O)** E14.5 $RARE^{lacZ}$ coronal section showing ISH for *Hoxb5* (N) and β-gal staining (O). Expression of Hoxb5 was observed mostly in RA responsive postmitotic precerebellar neurons. **(P-S)** $RARE^{lacz}$ coronal sections showing β-gal staining, *Wnt1* ISH and Ki67 IHC (in green) at E12.5 (P), E13.5 (Q), E14.5 (R) and E15.5 (S). β-gal staining is mostly seen in postmitotic precerebellar neurons (arrows) while Ki67 staining is observed in the cells around ventricles. Most endogenous RA responsive cells are negative for *Wnt1* expression (square box, P). **(T)** E15.5 $RARE^{lacZ}$ AES in utero electroporated with *Cyp26b1* plasmid at E13.5, showing IHC for GFP/Pax6 (T), and β-gal staining (T'). Expression of RARE is greatly reduced upon ectopic expression of *Cyp26b1*.

**Figure S2**

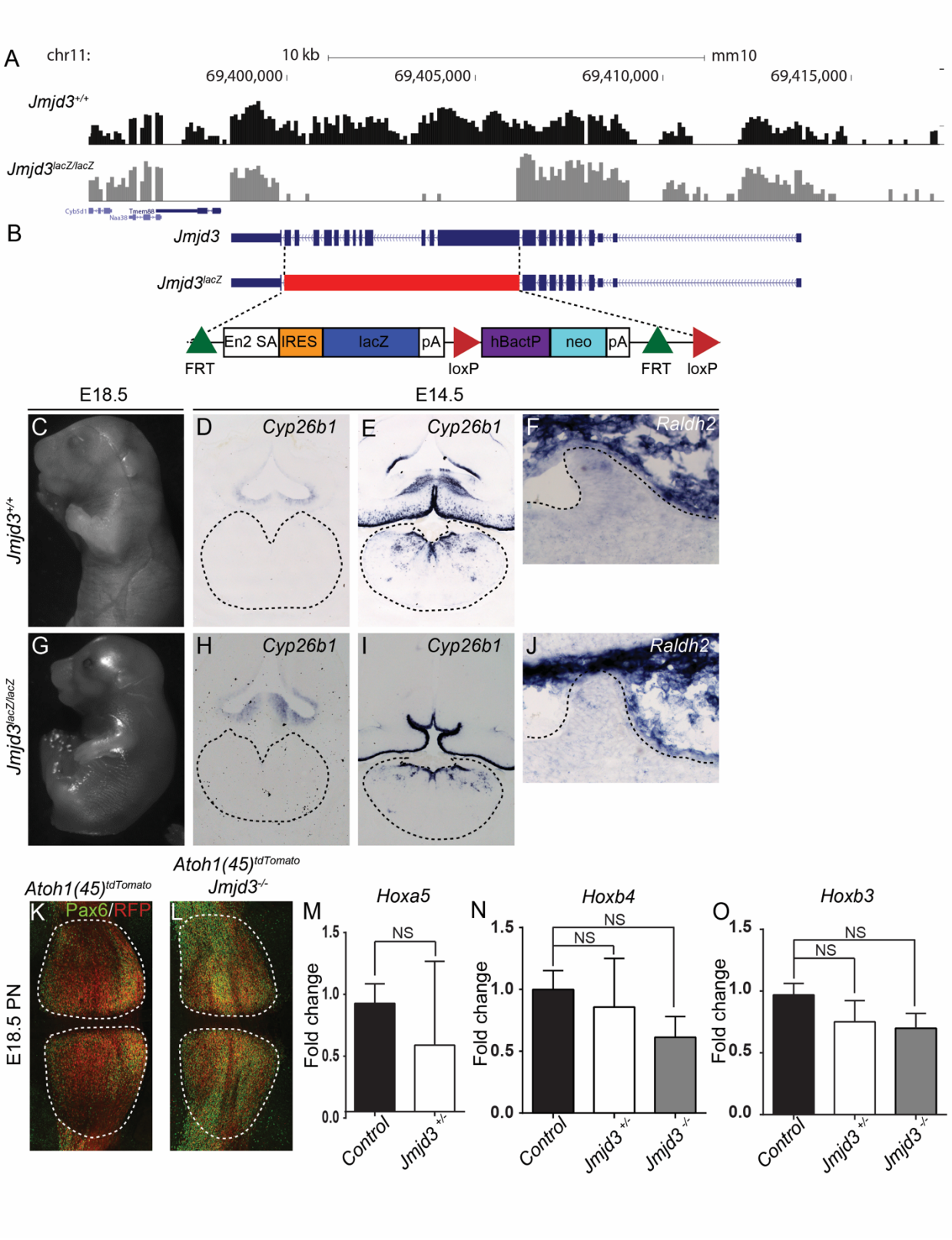


**Figure S2: Role of Jmjd3 in the regulation of *Hox5* gene expression. Related to Figure 2.**

(**A**) RNA-seq profiles of the *Jmjd3* in control and *Jmjd3*$^{lacZ/lacZ}$ confirming the deletion of Exons 2-13 in *Jmjd3*$^{lacZ/lacZ}$. (**B**) Schematic drawing of the construct used for generation of *Jmjd3*$^{lacZ}$ mice. (**C,G**) Whole mount images of E18.5 control and *Jmjd3*$^{lacZ/lacZ}$ embryos. **(D-J)** E14.5 control (D-F) and *Jmjd3*$^{lacZ/lacZ}$ (H-J) coronal sections showing ISH for *Cyp26b1* (D,E,H,I), and *Raldh2* (F,J); no change in the expression of *Cyp26b1* or *Raldh2* was observed in *Jmjd3*$^{LacZ/LacZ}$. (**K-L**) Whole mount images of E18.5 *Atoh1(45)*$^{tdTomato}$ and *Atoh1(45)*$^{tdTomato}$;*Jmjd3*$^{-/-}$ PN showing IHC for Pax6 (green) and RFP (for tdTomato, red). (**M-O**) qPCR for *Hoxa5* (M), *Hoxb4* (N) and *Hoxb3* (O) on FACS isolated neurons from E18.5 *Atoh1(45)*$^{tdTomato}$, *Atoh1(45)*$^{tdTomato}$;*Jmjd3*$^{+/-}$ or *Atoh1(45)*$^{tdTomato}$;*Jmjd3*$^{-/-}$ PN (M, n = 3, p = 0.4286) (N, n = 3, p = 0.999 (*Jmjd3*$^{+/-}$), p = 0.3002 (*Jmjd3*$^{-/-}$)) (O, n=3, p= 0.083 (*Jmjd3*$^{+/-}$), p=0.062 (*Jmjd3*$^{-/-}$)). Data presented as mean + SD.

**Figure S3**

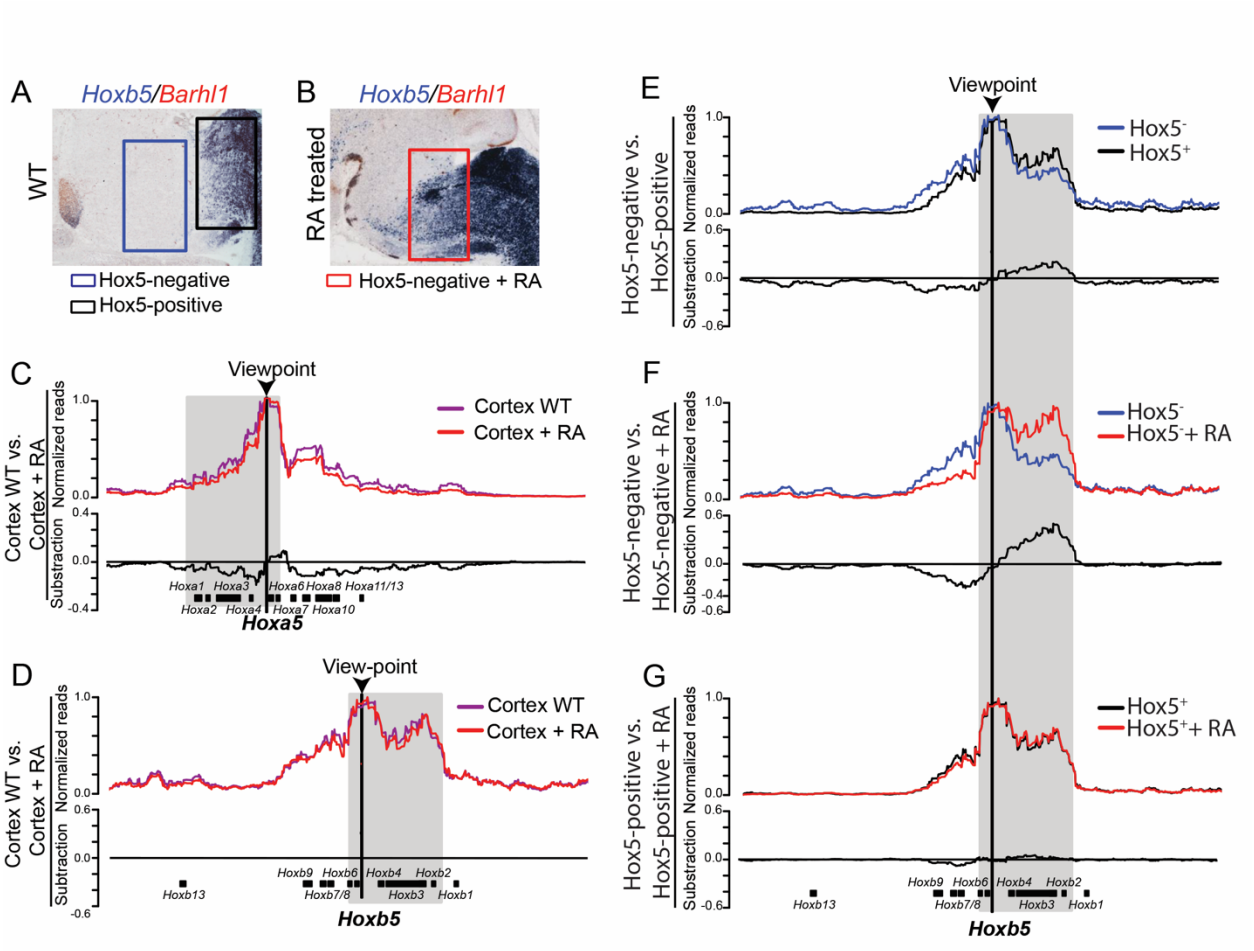


**Figure S3: Epigenetic and higher order chromatin conformational changes upon RA induced onset of *Hox5* expression *in vivo*. Related to Figure 3.**

(**A, B**) E18.5 sagittal sections of control (A) or E9.5 RA treated embryo (B) showing in situ hybridization (ISH) for *Barhl1 and Hoxb5* in hindbrain. Exogenous amounts of RA induce *Hoxb5* expression in previously *Hoxb5* negative hindbrain tissue (compare blue box in A to red box in B). **(C-E)** E14.5 Contact profile of CC population looking from the *Hoxa5* promoter as a viewpoint (arrow head) within a 400kB window spanning the *Hoxa* cluster (C) and of CC (D), Hox5-negative (E,F) and Hox5-positive populations (E,G) looking from *Hoxb5* promoter as a view point within *Hoxb* cluster with or without RA treatment. The substractions of the respective comparisons are depicted below the traces with the normalized reads. Exogenous amounts of RA leads to reorganization of the chromatin conformation *in vivo* at the *Hoxb5* locus in Hox5-negative (F) but not in CC or Hox5-positive cells (D,G) and *Hoxa5* locus in CC (C).

**Figure S4**

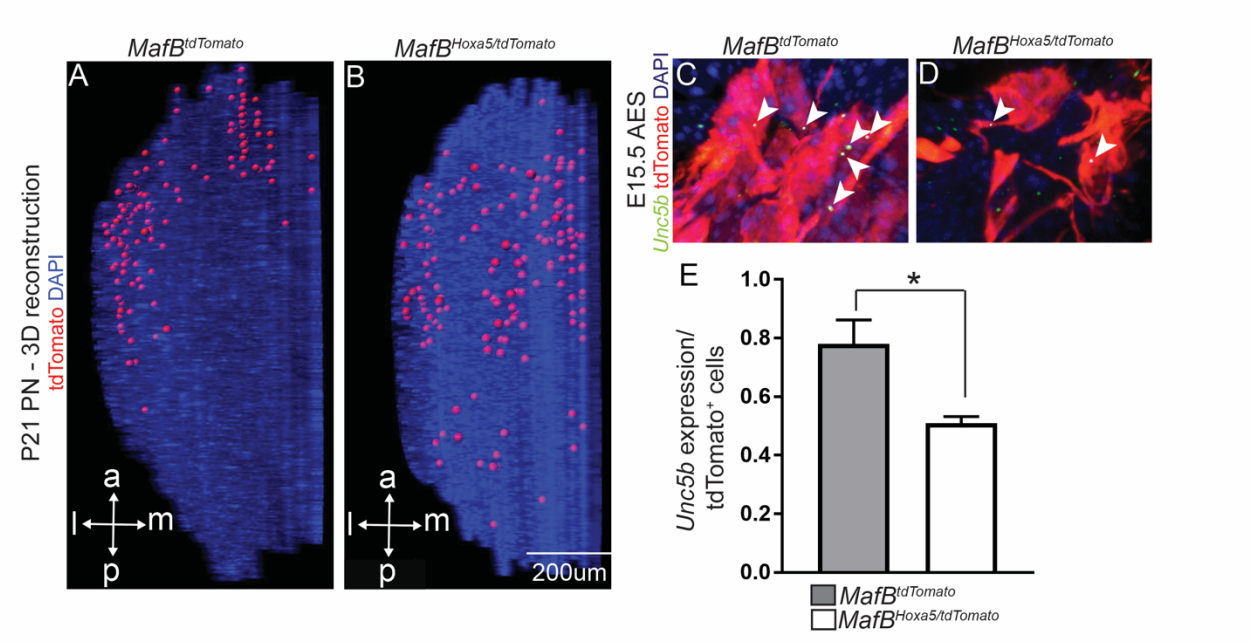


**Figure S4: Effect of ectopic expression of Hoxa5 on pontine neuron position and Unc5b expression. Related to Figure 4.**

**(A-B)** 3D reconstruction of P21 *Mafb*$^{tdTomato}$ (A) and *Mafb*$^{Hoxa5/tdTomato}$ (B) PN. *Mafb*$^{tdTomato}$ neurons mostly localize to anterolateral PN (A); upon ectopic *Hoxa5* expression, neurons lose their spatial restriction and spread more posteriorly (B). (**C-D**) Part of E15.5 AES of *Mafb*$^{tdTomato}$ (C) and *Mafb*$^{Hoxa5/tdTomato}$ (D) showing tdTomato+ neurons and *Unc5b* RNA-FISH (green). *Unc5b*-tdTomato$^{+}$ colocalization (arrowheads) was detected by IMARIS and marked as a spot (white spots) **(E)** Bar graph of *Unc5b* RNA expression per tdTomato$^{+}$ cells in E15.5 AES of *Mafb*$^{tdTomato}$ and *Mafb*$^{Hoxa5/tdTomato}$ (n=2, p = 0.0461). Data presented as mean + S.D.

**Figure S5**

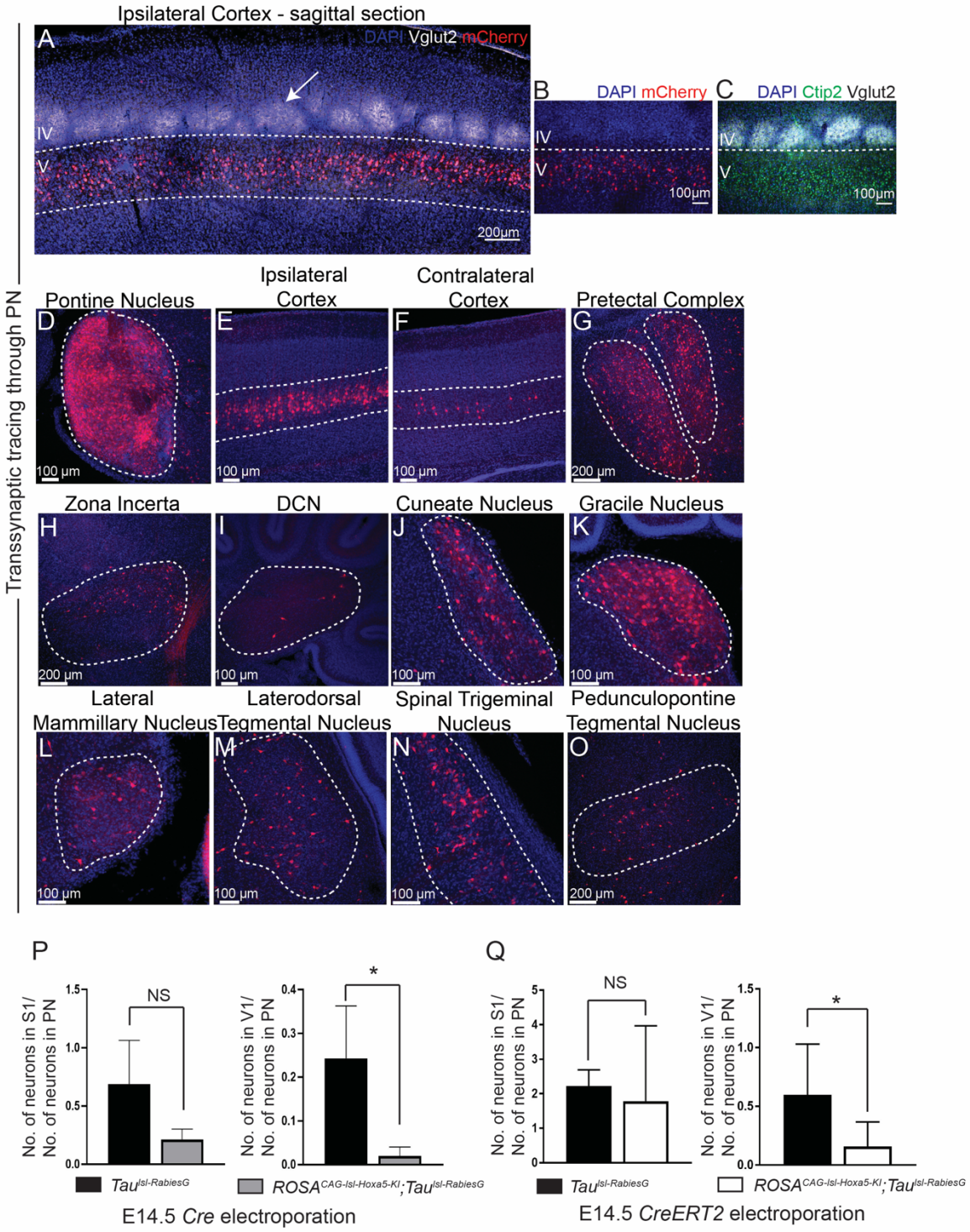


**Figure S5: Input connectivity of PN neurons as revealed by trans-synaptic Rabies tracings. Related to Figures 5 and 6.**

(**A-C**) Sagittal sections through a transsynaptically traced P8 mouse brain showing immunohistochemistry (IHC) for (A)Vglut2 (white) and mCherry (red), labelling

thalamocortical axon terminals present in cortical layer IV (arrow) and monosynaptically traced mCherry+ neurons in cortical layer V, respectively, (B) mCherry only, and (C) Ctip2 (green), labelling cortical layer V neurons, and Vglut2 (white). The monosynaptically traced cortical neurons are present in the layer V of the cortex. **(D-O)** Sagittal sections through a transsynaptically traced P8 mouse brain showing infected, $mCherry^{+}$, neurons in ipsilateral PN (D) and monosynaptically traced neurons in ipsilateral (E), contralateral cortex (F), pretectal complex (G), zona incerta (H), deep-cerebellar nuclei (I), cuneate nucleus (J), gracile nucleus (K), lateral mammillary nucleus (L), laterodorsal tegmental nucleus (M), spinal trigeminal nucleus (N), and pedunculopontine tegmental nucleus (O). **(P-Q)** Bar graphs of ratio of $mCherry^{+}$ neurons in S1 and V1 per electroporated PN neuron in Cre (P) or CreERT2 (Q) electroporated $Tau^{lsl\text{-}RabiesG}$ and $ROSA^{CAG\text{-}lsl\text{-}Hoxa5\text{-}KI};Tau^{lsl\text{-}RabiesG}$ (P, n=4 for $Tau^{lsl\text{-}RabiesG}$ , n=3 for $ROSA^{CAG\text{-}lsl\text{-}Hoxa5\text{-}KI};Tau^{lsl\text{-}RabiesG}$, p value=0.0259 for V1, 0.0896 for S1) (Q, n=4 for $Tau^{lsl\text{-}RabiesG}$ , n=7 for $ROSA^{CAG\text{-}lsl\text{-}Hoxa5\text{-}KI};Tau^{lsl\text{-}RabiesG}$, p value= 0.0453 for V1 and 0.7044 for S1). Data presented as mean + S.D.

**Figure S6**

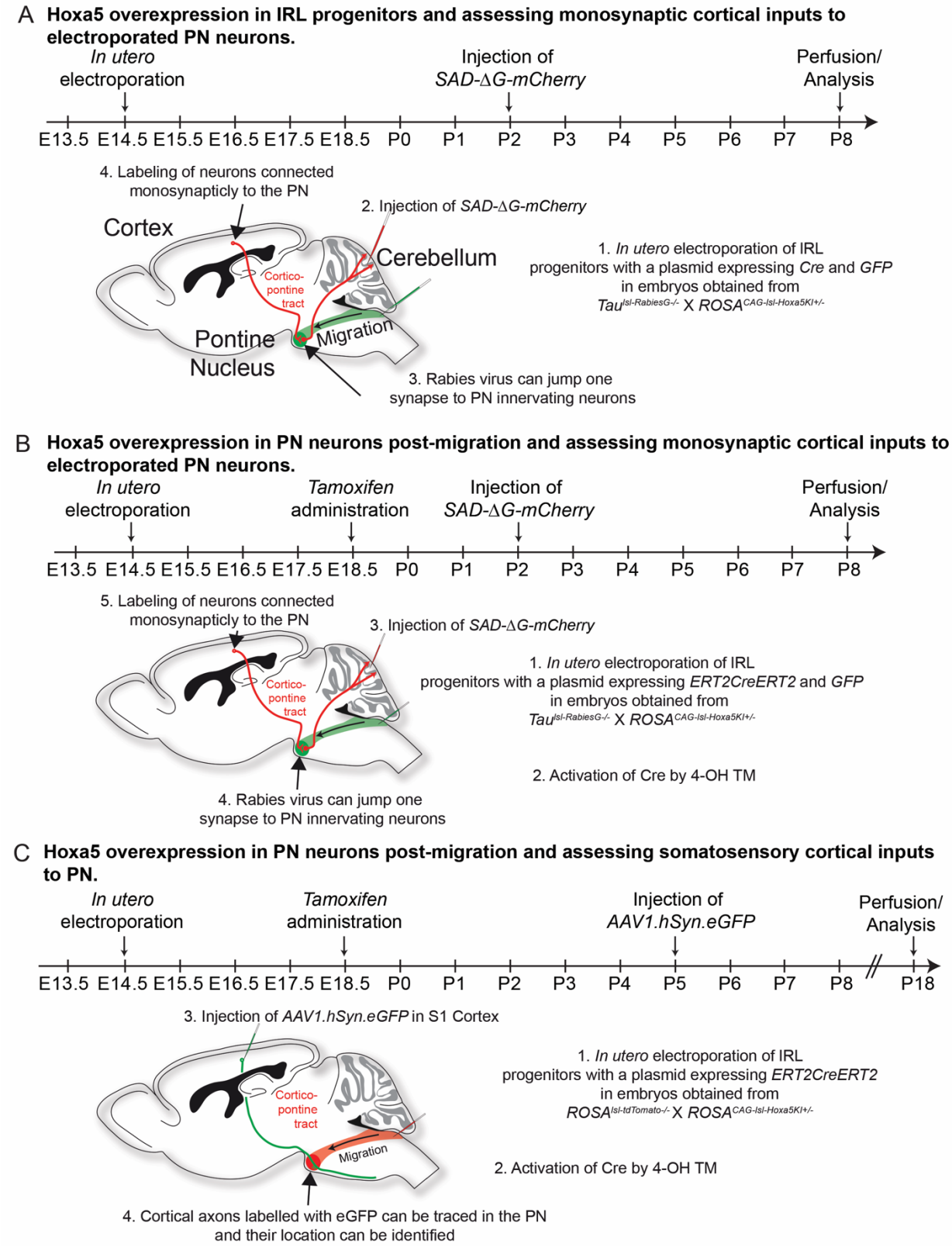
A Hoxa5 overexpression in IRL progenitors and assessing monosynaptic cortical inputs to electroporated PN neurons.
In utero electroporation
Injection of SAD-ΔG-mCherry
Perfusion/ Analysis
E13.5 E14.5 E15.5 E16.5 E17.5 E18.5 P0 P1 P2 P3 P4 P5 P6 P7 P8
4. Labeling of neurons connected monosynapticly to the PN
2. Injection of SAD-ΔG-mCherry
Cortex
Cerebellum
Cortico-pontine tract
Pontine Nucleus
Migration
1. In utero electroporation of IRL progenitors with a plasmid expressing Cre and GFP in embryos obtained from Tau lsl-RabiesG-/- X ROSA CAG-lsl-Hoxa5KI+/-
3. Rabies virus can jump one synapse to PN innervating neurons
B Hoxa5 overexpression in PN neurons post-migration and assessing monosynaptic cortical inputs to electroporated PN neurons.
In utero electroporation
Tamoxifen administration
Injection of SAD-ΔG-mCherry
Perfusion/ Analysis
E13.5 E14.5 E15.5 E16.5 E17.5 E18.5 P0 P1 P2 P3 P4 P5 P6 P7 P8
5. Labeling of neurons connected monosynapticly to the PN
3. Injection of SAD-ΔG-mCherry
Cortico-pontine tract
1. In utero electroporation of IRL progenitors with a plasmid expressing ERT2CreERT2 and GFP in embryos obtained from Tau lsl-RabiesG-/- X ROSA CAG-lsl-Hoxa5KI+/-
2. Activation of Cre by 4-OH TM
4. Rabies virus can jump one synapse to PN innervating neurons
C Hoxa5 overexpression in PN neurons post-migration and assessing somatosensory cortical inputs to PN.
In utero electroporation
Tamoxifen administration
Injection of AAV1.hSyn.eGFP
Perfusion/ Analysis
E13.5 E14.5 E15.5 E16.5 E17.5 E18.5 P0 P1 P2 P3 P4 P5 P6 P7 P8 P18
3. Injection of AAV1.hSyn.eGFP in S1 Cortex
Cortico-pontine tract
Migration
1. In utero electroporation of IRL progenitors with a plasmid expressing ERT2CreERT2 in embryos obtained from ROSA lsl-tdTomato-/- X ROSA CAG-lsl-Hoxa5KI+/-
2. Activation of Cre by 4-OH TM
4. Cortical axons labelled with eGFP can be traced in the PN and their location can be identified

**Figure S6: Experimental design for tracing connectivity of Hoxa5 expressing PN neurons from conditional Hoxa5 overexpressing mouse line. Related to Figure 6.**

(**A, B**) Schematic illustration of the experimental design to initiate transsynaptic rabies spread from PN neurons after overexpression of *Hoxa5* in lRL progenitors (A) or in PN neurons post migration (B). **(C)** Schematic illustration of the experimental design for anterograde tracing of somatosensory cortical input to PN neurons with or without overexpression of Hoxa5 in PN neurons post-migration.

**Figure S7**

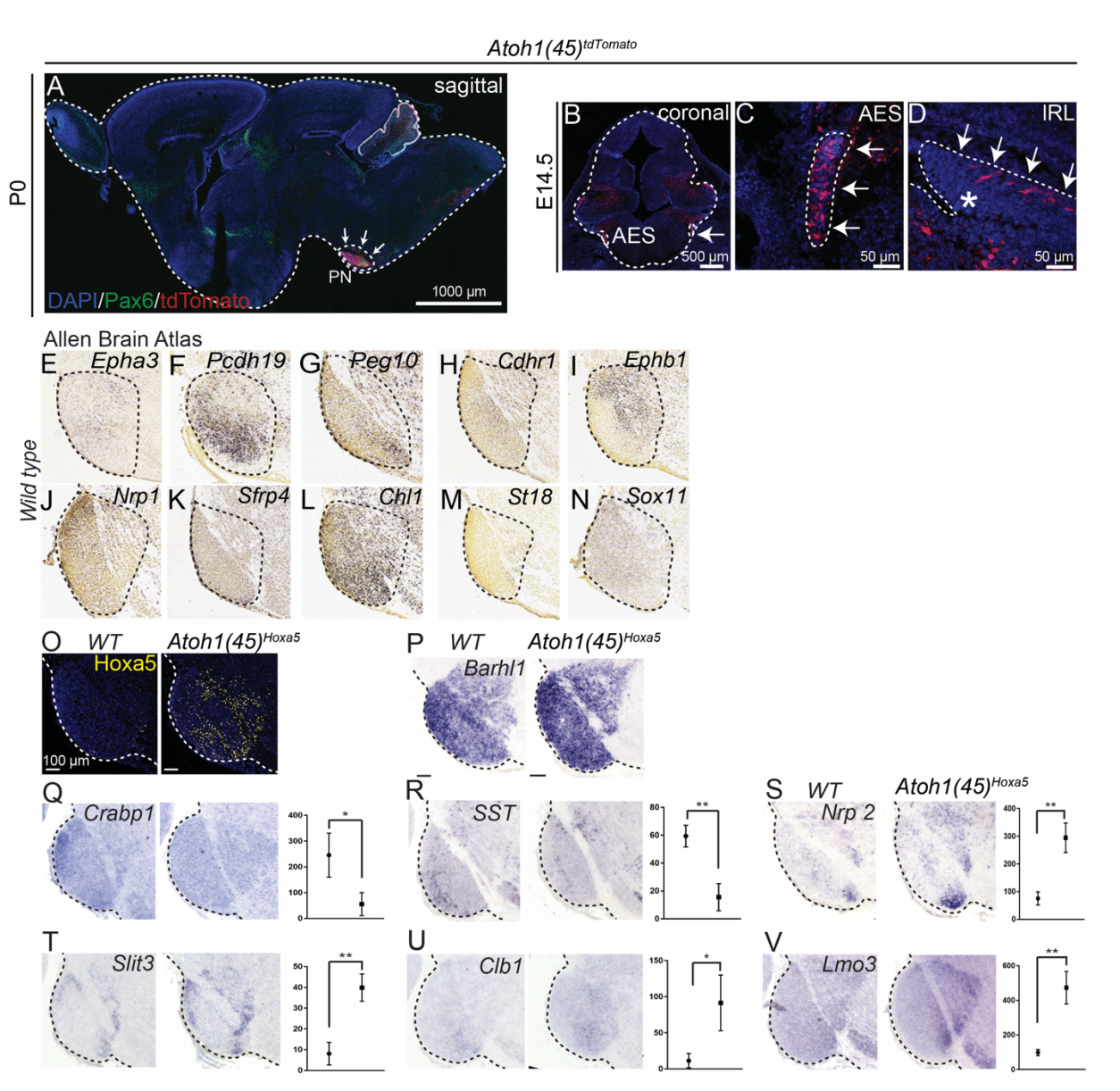


**Figure S7: Characterization of *Atoh1(45)::Cre* transgenic mouse line and validation of RNAseq data. Related to Figure 7.**

(**A**) E18.5 *Atoh1(45)*$^{tdTomato}$ sagittal section showing immunohistochemistry (IHC) for Pax6 (green), and tdTomato (red), labeling of RL derived neuronal populations including PN, cerebellum and other precerebellar nuclei, and *Atoh1*$^{+}$ cells in this mouse line, respectively. (**B-D**) E14.5 *Atoh1(45)*$^{tdTomato}$ coronal section showing specific labeling of RL derived neuronal populations (B), tdTomato$^{+}$ cells in the AES (C) and *Cre* activity selectively in random postmitotic lRL neurons at the onset of migration (D). (**E-N**) E18.5 WT sagittal sections from Allen brain atlas showing in situ hybridizations (ISH) for *Epha3* (E), *Pcdh19*

(F), *Peg10* (G), *Cdhr1* (H), *Ephb1* (I), *Nrp1* (J), *Sfrp4* (K), *Chl1* (L), *St18* (M), and *Sox11* (N) showing differential expression of candidate genes along the anteroposterior axis of PN. (**O**) WT and *Atoh1(45)$^{Hoxa5}$* P0 PN sagittal sections showing IHC for Hoxa5 (yellow); upon overexpression of Hoxa5 in *Atoh1(45)$^{Hoxa5}$*, the expression of Hoxa5 can be observed in selected neurons throughout PN. **(P-V)** E18.5 WT and *Atoh1(45)$^{Hoxa5}$* PN sagittal sections showing expression of *Barhl1* (P), *Crabp1* (Q), *Somatostatin* (R), *Neuropilin 2* (S), *Slit3* (T), *Calbindin 1* (U), and *Lmo3* (V). *Barhl1* expression was used to determine PN structure. Respective graphs represent changes in the expression as seen from RNAseq data. Data are presented as mean + SD. Image credit: Allen Institute for Brain Science. © 2015 Allen Institute for Brain Science. Allen Developing Mouse Brain Atlas [Internet]. Available from: http://developingmouse.brain-map.org and © 2015 Allen Institute for Brain Science. Allen Mouse Brain Atlas [Internet]. Available from: http://mouse.brain-map.org.

## 2.2 Establishing ponto-cerebellar connectivity


### Abstract

The entire PN projects as mossy fibers to different parts of the cerebellum. PN mossy fibers largely target the granule cells in the contralateral cerebellar cortex, and to a much lower extend to the ipsilateral cerebellar cortex (Herrero et al., 2002; Rosina and Provini, 1984). PN mossy fibers mostly target the lobules of cerebellar hemispheres including simple lobule (SL), CrusI, CrusII, paramedian lobule (PML), paraflocculus (PF) and to a very less extent flocculus. PN neurons can send projections to different lobules within a hemisphere and also to different folia within a lobule, mostly to *Zebrin* positive stripes (Mihailoff, 1983; Bjaalie and Brodal, 1997; Biswas et al., 2019). Unlike a continuous map that is formed between the cortex and the PN, the projections from PN to the cerebellum are fractured (Shambes et al., 1978). Different body parts are thus represented in several discrete spots in the cerebellum and the spatial relationship between different body parts is not necessarily faithfully recapitulated. Although much work has been done to understand the projection pattern of PN neurons in the cerebellum, the molecular logic behind this complex connectivity is not yet defined. Here, we show that the molecular identity of PN neurons could be critical to define the projections irrespective of their position along the A-P axis. Different PN neurons can express different combinations of *Hox* genes, with posterior neurons having the most complex combinations. It is this combination that may underlie the ability of PN neurons to project to multiple lobules. PN neurons from *Mafb::CreERT2* mouse line are derived from the r6 and positioned anteriorly in the PN. These neurons project mostly to the paraflocculus, with only a small fraction of projections to the other lobules. On the contrary, PN neurons from *Hoxa5::CreERT2* mouse line project to multiple lobules of the cerebellum. These

neurons are derived from r8 and are more likely to express different combinations of *Hox2*, *Hox3*, *Hox4* and *Hox5* genes. PN neurons derived from *ChAT::Cre* mouse line settle in between *Mafb::CreERT2* and *Hoxa5::CreERT2* labelled neurons with some overlap with the *Mafb::CreERT2* labelled neurons. These neurons also project heavily to paraflocculus, similar to *Mafb*$^{+}$ but also project to some lobules involved in somatosensation.

Although we are still far from understanding the complex molecular logic behind the transformation of continuous cortico-pontine maps to fractured ponto-cerebellum maps, we believe that this preliminary work provides the basis to start understanding this problem. Here we show that *Hox* expression provides intrinsic information in pontine neuron subsets to target specific cerebellar lobules providing a molecular framework for corticocerebellar map transformation.

**Statement of contribution:** I performed the experiments and did the analysis. Claudius Kratochwil first described the positioning of r6 derived PN neurons and their projection to the cerebellum in *Mafb::CreERT2* mouse line. *Mafb::CreERT2* and *Hoxa5::CreERT2* were generated and characterized by Sebastien Ducret.

**RESULT**

To characterize the projection pattern of subsets of PN neurons to the cerebellum, we used three different mouse lines, namely *Mafb::CreERT2*, *ChAT::Cre* and *Hoxa5::CreERT2*, crossed with a *ROSA-lox-stop-lox-tdTomato* reporter mouse line, thereby genetically defining different subsets of PN neurons. Each of these mouse lines also label hindbrain structures other than PN, which may also contribute to cerebellar projections. We, therefore, electroporated the lRL progenitors of $ChATCre^{tdTomato}$ and $Hoxa5CreERT2^{tdTomato}$ fetuses with a floxed GFP construct, *pCAG::lox-GFP_pA-lox*, to specifically label PN neurons and their projections. Due to very early and transient expression of Mafb in the hindbrain, it was not possible to perform *in utero* electroporation in this mouse line.

Projection analysis at P21 revealed that $MafBCreERT2^{tdTomato}$ mossy fiber terminals were mostly restricted to the PF, with additionally a few terminals in Crus1, Crus2, paramedian (PML) and floculus (FL) lobules (Figure 8A). $ChATCre^{tdTomato}$ mossy fiber terminals were also mostly present in the PF, with additional terminals in the PML and COP (Figure 8B). We next mapped the projection pattern of Hoxa5 expressing PN neurons. In the hemispheres, labeled $Hoxa5CreERT2^{tdTomato}$ mossy fiber axon terminals mostly targeted cerebellar lobules involved in the processing of somatosensory information including simple lobule (SL), CrusI, CrusII paramedian, and to a lesser extent copula (COP) (Figure 8C). $Hoxa5CreERT2^{tdTomato}$ mossy fiber axon terminals were also identified in the PF, although to a lesser extent.

In summary, the molecular identity of PN neurons may underlie their ability to target different lobules of the cerebellum.

**Figure 8**

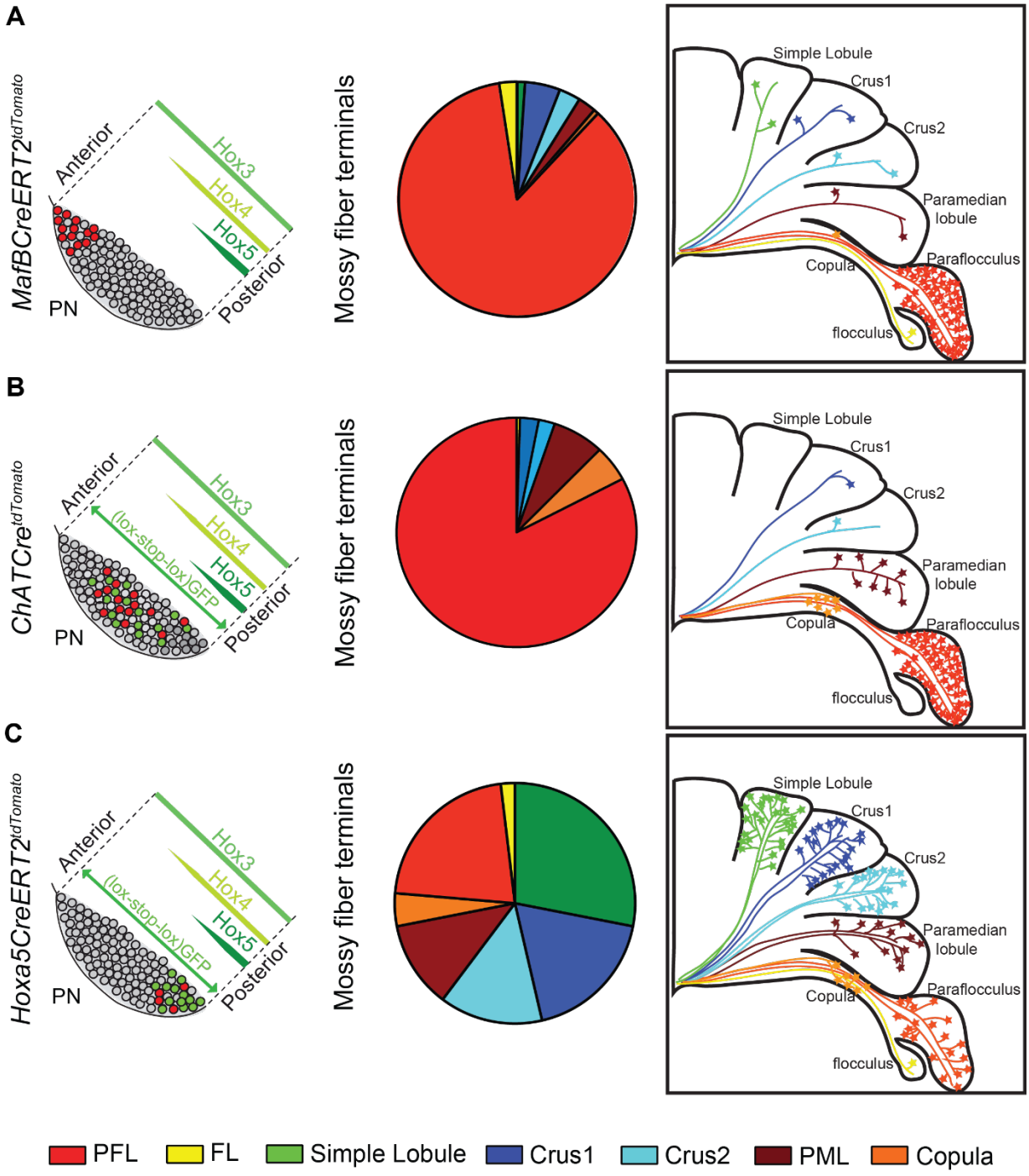


**Figure 8: Establishing ponto-cerebellar connectivity**. Schematic illustration to describe the position of labelled neurons in the PN and pie chart for their cerebellar projection pattern in **(A)** *MafbCreERT2*$^{tdTomato}$, **(B)** *ChATCre*$^{tdTomato}$, and **(C)** *Hoxa5CreERT2*$^{tdTomato}$ mouse line. While *Hoxa5* negative subsets labelled by *ChATCre*$^{tdTomato}$ and *MafbCreERT2*$^{tdTomato}$ projects heavily to the PF (A,B), projections from *Hoxa5* positive subsets are present in multiple lobules of the cerebellar hemisphere (C). n=3 animals per genotype. Projections presented as mean.

## Material and Methods

### *In utero* electroporation and activation of tamoxifen

In utero electroporation was performed as described before. Briefly, pCAG::lox-GFP_PA-lox plasmid was electroporated in the lRL progenitors of *ChATCre*$^{tdTomato}$ and *Hoxa5CreERT2*$^{tdTomato}$ fetuses at E14.5. Additionally, *Hoxa5CreERT2*$^{tdTomato}$animals received intra-gastric injection of Tamoxifen (Sigma; T5648-5G) dissolved in corn oil (1mg/ml stock solution) at P1, P2 and P3. Tamoxifen (10mg/ml stock) was administered by oral gavage at E7.5 (1mg) to *MafbCreERT2*$^{tdTomato}$ mice.

### Immunostaining and image analysis

Deeply anaesthetized P21 animals were subjected to trans-cardial perfusion using 4% PFA in PBS. Brains were dissected out and further fixed in 4% PFA overnight at 4°C. Brain samples were sectioned using vibratome (60µm thick) and processed for immunofluorescence staining for GFP as described above. Z-stack images of the cerebellum were acquired on Axio scan Z1 microscope using a 10X lens. GFP labelled mossy fiber rosettes in *ChATCre*$^{tdTomato}$ and *Hoxa5CreERT2*$^{tdTomato}$, and tdTomato labelled mossy fiber rosettes in *MafCreERT2*$^{tdTomato}$ cerebellum were identified and quantified using Bitplane IMARIS spot detection tool.

### 2.2.1 Discussion

While the somatotopic organization of the S1 cortical map is largely preserved in centrocaudal PN (Leergard, 2007) the granule cell layer of the cerebellar hemispheres contains discontinuous, or 'fractured', body representations (Shambes et al., 1978). Each lobule contains a distinct mosaic of body part representations (defined as patches, zones or microzones; Apps and Hawkes, 2009), and each body part is represented multiple times across the cerebellar hemispheres and lobules. Retrograde labelling from upper lip representing zones in both Crus IIa and PML lobules showed that projecting neurons have overlapping spatial distributions in centrocaudal PN, corresponding to the targeting area of upper lip related S1 cortical afferents (Leergard et al., 2006). Considerable overlapping of spatial distributions was also observed for PN neurons projecting to forelimb representing zones of SL and PML (Herrero et al., 2002). One possibility to explain these targeting patterns is extensive axon branching of individual mossy fiber neurons (Wu et al., 1999). However, while pontine neuron axon branching may occur within lobules, only a small fraction of pontocerebellar neurons branch to target multiple lobules (Herrero et al., 2002; Odeh et al., 2005). Thus, for a given 'lamellar' subspace in the centrocaudal PN innervated by a specific subset of S1 afferents, PN neurons holding similar somatosensory representations but projecting to different lobules are likely intermingled.

The molecular logic of such a complex targeting pattern underlying somatosensory map transformation between PN and cerebellum is unknown. Here we show that the heterogeneity in the molecular identity of PN neurons along the A-P axis is important for orchestrating the cerebellar projection pattern. *Mafb*$^{+}$ PN neurons are positioned along the antero-ventral region, which receives visual input and project mostly to the PF, lobule known for its role in the visual circuit. While *Hoxa5*$^{+}$ PN neurons are positioned along to caudo-medial region,

receive somatosensory input and project to most lobules of the cerebellar hemisphere involved in somatosensation. *ChAT*$^{+}$ neurons, which are spread between the Mafb and Hoxa5 population, projects considerably to the PF, but also to PML and COP, suggesting a role of *ChAT*$^{+}$ PN neurons in both visual and somatosensory circuits. It is interesting to note that in the posterior PN, Hox-dependent neuronal identity may be relatively heterogeneous at the single cell level, due to the potential to express several combinations of Hox2-5 paralogue genes. As discussed earlier, heterogeneity could be further enhanced by Hox5 paralogue-specific RA-dependent induction in postmitotic PN neuron subsets. While neurons in adjacent position would share the similar S1 input, adjacent PN neurons may express distinct Hox combinations generating different lobular targeting patterns. Further work will be required to support such a hypothesis.

Finally, while expression of *Hoxa5* in PN neurons may be important for their input connectivity (Result 2.1), it might not be sufficient to determine their specific cerebellar targeting pattern which could be rather specified by the individual *Hox* transcription profile of PN neurons. In this respect, ectopic expression of *Hoxa2* in the brainstem dorsal principal trigeminal nucleus (PrV) was sufficient to drive topographically directed axonal targeting to the thalamic barreloid area, normally targeted by Hoxa2-expressing ventral PrV axons (Bechara et al., 2015).

At any rate, our findings provide the first evidence of an intrinsic Hox-dependent molecular program underlying specific pontocerebellar mossy fiber targeting patterns of PN neuron subsets.

# CHAPTER 3: CONCLUSIONS AND OUTLOOK

The results and techniques presented in this thesis provide a framework to understand and analyze the development of pontine nuclei and its integration in the cortico-ponto-cerebellar circuit. This study highlights the role of *Hox5* genes at multiple steps during the development of pontine nuclei and its circuitry.

Here we have shown that, unlike other *Hox* genes expressed in lRL progenitors and postmitotic neurons during the development of PN, *Hox5* genes are induced only in the postmitotic PN neurons. This spatial restriction of Hox5 gene expression is a result of an interplay between retinoic acid, PcG member Ezh2 and H3K27 demethylase JmjD3. We have also shown that among the members of Hox PG5, *Hoxa5* and *Hoxb5* have different expression domains, with the expression of *Hoxa5* restricted to most posterior r8 derived PN neurons. Thereby, defining subsets of PN neurons based on their Hox expression.

We have shown that *in-utero* electroporation is a great tool to target and manipulate developing PN neurons, without effecting other precerebellar nuclei. By combining *in-utero* electroporation and mouse genetics, we could show that expression of Hoxa5 in migrating PN neurons is critical for their positioning in the PN. Ectopic expression of Hoxa5 in migrating PN neurons can lead to posteriorizing of PN neurons. This is due to the downregulation of guidance receptor *Unc5b*. We further show that overexpression of Unc5b in migrating PN neurons ectopically expressing Hoxa5 is sufficient to override the posteriorizing effect of Hoxa5.

By combining in-utero electroporation, mouse genetics and trans-synaptic rabies virus tracing, we could identify the input connectivity of subsets of PN neurons. Moreover, we

could identify the role of Hoxa5 in shaping the input connectivity of PN neurons. We show that expression of *Hoxa5* is not only sufficient to position PN neurons to posterior position but to also attract limb somatosensory cortical input and avoid visual cortical input.

Finally, in this thesis, we show that PN neurons can have different cerebellar projections based on their molecular identity. *MafB*$^{+}$ anterior PN neurons project mostly to the PF lobule, while *Hoxa5*$^{+}$ posterior PN neurons project to multiple lobules of the cerebellum, thereby transforming continuous cortical somatosensory maps to fractured maps in the cerebellum.

Although this work highlights the role of Hox transcription factors in formation of cortico-ponto-cerebellar maps, much more work is needed to completely understand the molecular logic behind this complex circuitry. We found in our RNAseq experiment that almost all relevant classes of guidance molecules including Netrins (Ntng1), Slits (Slit3), Ephrins (Efna3, Efnab3), Semaphorins (Sema6a, Sema6d, Plxna4, Nrp1, Nrp2), cell adhesion molecules (Cdh2, Cdh23, Pcdh9, Pcdh19) and other signaling molecules such as NGFs, FGFs and Wnts are differentially expressed along the PN rostrocaudal axis (Figure 7, Result 2.1). However, how these guidance cues could be involved in the PN circuit formation is still unclear. It is interesting to note that several guidance cues were identified to be partially dependent on *Hoxa5* expression. Further analysis of *Hoxa5* dependent guidance cues could give insights on downstream effectors of Hoxa5 in orchestrating PN neurons connectivity.

We have addressed the sufficiency of Hoxa5 in attracting somatosensory specific inputs to the PN, however if Hoxa5 is necessary for attracting limb somatosensory input to the PN is still unclear. *Hox* genes of the same paralogous group are known to show

redundancy in their functions, however conditional deletion of *Hoxa2* in the brainstem was sufficient to change the input-output connectivity of PrV (Oury et al., 2006). It would be therefore interesting to analyse the input connectivity on PN nucleus after conditional deletion of *Hoxa5* in PN neurons.

Here we have proposed that the combination of *Hox* genes in PN neurons underlie their complex output connectivity. Identifying the molecular heterogeneity of genetically defined PN neuron subsets with different cerebellar projection patterns (*ChAT::Cre*, *Mafb::CreERT2*, *Hoxa5::CreERT2* compared with *Atoh1(45)::Cre*) will further extend our knowledge about the molecular mechanisms controlling the connectivity of specific pontine nuclei modules. It is well known that the activity of neurons, in turn, shape their connectivity. PN neurons start projecting to the cerebellum early during development, however they receive cortical inputs only postnatally. PN mossy fiber projections undergo pruning during early post-natal stages. Involvement of activity of PN neurons or their cortical input connectivity in the cerebellar map formation can be investigated.

Finally, in this study we have investigated only cortical inputs to the PN, while PN receive projections from several sub-cortical regions as well. Involvement of Hox genes in shaping sub-cortical input connectivity will further increase our understanding of the role of Hox genes in circuit formation. Projections from forelimb and hindlimb somatosensory cortical regions are present in discrete regions of the PN, with hindlimb sensorimotor fibers distributed caudal to forelimb projections. Similar somatotopy is also observed in the pontine afferents from dorsal column nuclei, with graciloPontine fibers distributed caudally to cuneopontine fibers (Kosinski et al., 1986). Projections from forelimb sensory cortical region and cuneate nucleus as well as from hindlimb sensory cortical region and gracile

nucleus overlap partially in the pontine nucleus. Investigation of these projections at a single neuron level as well as the involvement of Hoxa5 in shaping the overlapping projections from hindlimb cortical region and gracile nucleus will further add to our knowledge on PN connectivity.

# REFERENCES


Aboitiz, F., Morales, D., and Montiel, J. (2003). The evolutionary origin of the mammalian isocortex: Towards an integrated developmental and functional approach. *Behavioral and Brain Sciences* 26, 535–552. doi:10.1017/S0140525X03000128.

Abu-Abed, S., Dolle, P., Metzger, D., Beckett, B., Chambon, P., and Petkovich, M. (2001). The retinoic acid-metabolizing enzyme, CYP26A1, is essential for normal hindbrain patterning, vertebral identity, and development of posterior structures. Genes Dev *15*, 226-240.

Agger, K., Cloos, P.A., Christensen, J., Pasini, D., Rose, S., Rappsilber, J., Issaeva, I., Canaani, E., Salcini, A.E., and Helin, K. (2007). UTX and JMJD3 are histone H3K27 demethylases involved in HOX gene regulation and development. Nature *449*, 731-734.

Akam, M. (1987). The molecular basis for metameric pattern in the Drosophila embryo. Development *101*, 1-22.

Alcántara, S., Ruiz, M., De Castro, F., Soriano, E., and Sotelo, C. (2000). Netrin 1 acts as an attractive or as a repulsive cue for distinct migrating neurons during the development of the cerebellar system. *Development* 127, 1359–1372. Available at: https://dev.biologists.org/content/127/7/1359.long.

Allen, G.I., and Tsukahara,N. (1974). Cerebrocerebellar communication systems. Physiological Reviews *54*, 957-1006.

Alonso, C.R. (2012). A complex 'mRNA degradation code' controls gene expression during animal development. Trends Genet *28*, 78-88.

Altman, J., and Bayer, S. A. (1987a). Development of the precerebellar nuclei in the rat: I. The precerebellar neuroepithelium of the rhombencephalon. *J. Comp. Neurol.* 257, 477–489. doi:10.1002/cne.902570402.

Altman, J., and Bayer, S. A. (1987b). Development of the precerebellar nuclei in the rat: II. The intramural olivary migratory stream and the neurogenetic organization of the inferior olive. *J. Comp. Neurol.* 257, 490–512. doi:10.1002/cne.902570403.

Altman, J., and Bayer, S. A. (1987c). Development of the precerebellar nuclei in the rat: III. The posterior precerebellar extramural migratory stream and the lateral reticular and external cuneate nuclei. *J. Comp. Neurol.* 257, 513–528. doi:10.1002/cne.902570404.

Altman, J., and Bayer, S. A. (1987d). Development of the precerebellar nuclei in the rat: IV. The anterior precerebellar extramural migratory stream and the nucleus reticularis tegmenti pontis and the basal pontine gray. *J. Comp. Neurol.* 257, 529–552. doi:10.1002/cne.902570405.

Altman, J., and Bayer, S. A. (1997). *Development of the cerebellar system: in relation to its evolution, structure, and functions*. CRC Press.

Alvarez-Buylla, A., Garcia-Verdugo, J.M., and Tramontin, A.D. (2001). A unified hypothesis on the lineage of neural stem cells. Nat Rev Neurosci *2*, 287-293.

Apps, P. R., and Hawkes, R. (2009). Cerebellar cortical organization: a one-map hypothesis. *Nat. Rev. Neurosci.* 10, 670–681. doi:10.1038/nrn2698.

Arai, Y., Funatsu, N., Numayama-Tsuruta, K., Nomura, T., Nakamura, S., and Osumi, N. (2005). Role of Fabp7, a downstream gene of Pax6, in the maintenance of neuroepithelial cells during early embryonic development of the rat cortex. J Neurosci *25*, 9752-9761.

Auclair, F., Valdes, N., and Marchand, R. (1996). Rhombomere-specific origin of branchial and visceral motoneurons of the facial nerve in the rat embryo. J Comp Neurol *369*, 451-461.

Azizi, S. A., Mihailoff, G. A., Burne, R. A., and Woodward, D. J. (1981). The pontocerebellar system in the rat: An HRP study. I. Posterior vermis. *J. Comp. Neurol.* 197, 543–558. doi:10.1002/cne.901970402.

Backer, S., Sakurai, T., Grumet, M., Sotelo, C., and Bloch-Gallego, E. (2002). Nr-CAM and TAG-1 are expressed in distinct populations of developing precerebellar and cerebellar neurons. *Neuroscience* 113, 743–748. doi:10.1016/S0306-4522(02)00221-X.

Bartel, D.P. (2009). MicroRNAs: target recognition and regulatory functions. Cell *136*, 215-233.

Barton, R. A. (2002). How did brains evolve? *Nature* 415, 134–135. doi:10.1038/415134a.

Bechara, A., Laumonnerie, C., Vilain, N., Kratochwil, C. F., Cankovic, V., Maiorano, N. A., et al. (2015). Hoxa2 Selects Barrelette Neuron Identity and Connectivity in the Mouse Somatosensory Brainstem. *Cell Rep* 13, 783–797. doi:10.1016/j.celrep.2015.09.031.

Beier, K.T., Samson, M.E., Matsuda, T., and Cepko, C.L. (2011). Conditional expression of the TVA receptor allows clonal analysis of descendents from Cre-expressing progenitor cells. Dev Biol *353*, 309-320.

Bel-Vialar, S., Itasaki, N., and Krumlauf, R. (2002). Initiating Hox gene expression: in the early chick neural tube differential sensitivity to FGF and RA signaling subdivides the HoxB genes in two distinct groups. Development *129*, 5103-5115.

Bell, E., Wingate, R.J., and Lumsden, A. (1999). Homeotic transformation of rhombomere identity after localized Hoxb1 misexpression. Science *284*, 2168-2171.

Bikoff, J.B., Gabitto, M.I., Rivard, A.F., Drobac, E., Machado, T.A., Miri, A., Brenner-Morton, S., Famojure, E., Diaz, C., Alvarez, F.J.*, et al.* (2016). Spinal Inhibitory Interneuron Diversity Delineates Variant Motor Microcircuits. Cell *165*, 207-219.

Biswas, M. S., Luo, Y., Sarpong, G. A., Sugihara, I. (2019). Divergent projections of single pontocerebellar axons to multiple cerebellar lobules in the mouse. *J. Comp. Nurol.* 2019;1-20. doi:10.1002/cne.24662

Bolstad, I., Leergaard, T. B., and Bjaalie, J. G. (2007). Branching of individual somatosensory cerebropontine axons in rat: evidence of divergence. 212, 85–93. doi:10.1007/s00429-007-0145-1.

Bouvier, J., Thoby-Brisson, M., Renier, N., Dubreuil, V., Ericson, J., Champagnat, J., Pierani, A., Chedotal, A., and Fortin, G. (2010). Hindbrain interneurons and axon guidance signaling critical for breathing. Nat Neurosci *13*, 1066-1074.

Brankatschk, M., and Dickson, B.J. (2006). Netrins guide Drosophila commissural axons at short range. Nat Neurosci *9*, 188-194.

Broch-Smith, T., and Brodal, P. (1990). Organization of the cortico-ponto-cerebellar pathway to the dorsal paraflocculus. An experimental study with anterograde and retrograde transport of WGA-HRP in the cat. *Arch Ital Biol* 128, 249–271. Available at: http://architalbiol.org/aib/article/view/128249/822.

Brodal, A., and Brodal, P. (1971). The organization of the nucleus reticularis tegmenti pontis in the cat in the light of experimental anatomical studies of its cerebral cortical afferents. *Exp Brain Res* 13, 90–110. doi:http://link.springer.com/article/10.1007/BF00236432.

Brodal, A., Kristiansen, K., and Jansen, J. (1950). Experimental demonstration of a pontine homologue in birds. *J. Comp. Neurol.* 92, 23–69. doi:10.1002/cne.900920104.

Brodal, P. (1968). The corticopontine projection in the cat I. Demonstration of a somatotopically organized projection from the primary sensorimotor cortex. *Exp Brain Res* 5, 210–234. doi:10.1007/BF00238665.

Brodal, P. (1978). The corticopontine projection in the rhesus monkey. Origin and principles of organization. Brain *101*, 251-283.

Brodal, P. (1982). Further observations on the cerebellar projections from the pontine nuclei and the nucleus reticularis tegmenti pontis in the rhesus monkey. *J. Comp. Neurol.* 204, 44–55. doi:10.1002/cne.902040106.

Brodal, P., and Bjaalie, J. G. (1992). Organization of the pontine nuclei. *Neuroscience Research*. doi:10.1016/0168-0102(92)90092-Q.

Brose, K., Bland, K.S., Wang, K.H., Arnott, D., Henzel, W., Goodman, C.S., Tessier-Lavigne, M., and Kidd, T. (1999). Slit proteins bind Robo receptors and have an evolutionarily conserved role in repulsive axon guidance. Cell *96*, 795-806.

Bulfone, A., Menguzzato, E., Broccoli, V., Marchitiello, A., Gattuso, C., Mariani, M., Consalez, G.G., Martinez, S., Ballabio, A., and Banfi, S. (2000). Barhl1, a gene belonging to a new subfamily of mammalian homeobox genes, is expressed in migrating neurons of the CNS. Hum Mol Genet *9*, 1443-1452.

Burchfield, J.S., Li, Q., Wang, H.Y., and Wang, R.F. (2015). JMJD3 as an epigenetic regulator in development and disease. Int J Biochem Cell Biol *67*, 148-157.

Burgold, T., Voituron, N., Caganova, M., Tripathi, P.P., Menuet, C., Tusi, B.K., Spreafico, F., Bevengut, M., Gestreau, C., Buontempo, S.*, et al.* (2012). The H3K27 demethylase JMJD3 is required for maintenance of the embryonic respiratory neuronal network, neonatal breathing, and survival. Cell Rep *2*, 1244-1258.

Callaway, E.M., and Luo, L. (2015). Monosynaptic Circuit Tracing with Glycoprotein-Deleted Rabies Viruses. J Neurosci *35*, 8979-8985.

Cang, J., and Feldheim, D.A. (2013). Developmental mechanisms of topographic map formation and alignment. Annu Rev Neurosci *36*, 51-77.

Carpenter, E.M., Goddard, J.M., Chisaka, O., Manley, N.R., and Capecchi, M.R. (1993). Loss of Hox-A1 (Hox-1.6) function results in the reorganization of the murine hindbrain. Development *118*, 1063-1075.

Chamberlin, N.L., Du, B., de Lacalle, S., and Saper, C.B. (1998). Recombinant adeno-associated virus vector: use for transgene expression and anterograde tract tracing in the CNS. Brain Res *793*, 169-175.

Chambeyron, S., and Bickmore, W.A. (2004). Chromatin decondensation and nuclear reorganization of the HoxB locus upon induction of transcription. Genes Dev *18*, 1119-1130.

Chatonnet, F., Wrobel, L.J., Mezieres, V., Pasqualetti, M., Ducret, S., Taillebourg, E., Charnay, P., Rijli, F.M., and Champagnat, J. (2007). Distinct roles of Hoxa2 and Krox20 in the development of rhythmic neural networks controlling inspiratory depth, respiratory frequency, and jaw opening. Neural Dev *2*, 19.

Chen, J., and Ruley, H.E. (1998). An enhancer element in the EphA2 (Eck) gene sufficient for rhombomere-specific expression is activated by HOXA1 and HOXB1 homeobox proteins. J Biol Chem *273*, 24670-24675.

Chen, H., Zhang, H., Lee, J., Liang, X., Wu, X., Zhu, T., Lo, P.K., Zhang, X., and Sukumar, S. (2007). HOXA5 acts directly downstream of retinoic acid receptor beta and contributes to retinoic acid-induced apoptosis and growth inhibition. Cancer Res *67*, 8007-8013.

Chen, S.Y., and Cheng, H.J. (2009). Functions of axon guidance molecules in synapse formation. Curr Opin Neurobiol *19*, 471-478.

Cheng, Y.C., Amoyel, M., Qiu, X., Jiang, Y.J., Xu, Q., and Wilkinson, D.G. (2004). Notch activation regulates the segregation and differentiation of rhombomere boundary cells in the zebrafish hindbrain. Dev Cell *6*, 539-550.

Chisaka, O., Musci, T.S., and Capecchi, M.R. (1992). Developmental defects of the ear, cranial nerves and hindbrain resulting from targeted disruption of the mouse homeobox gene Hox-1.6. Nature *355*, 516-520.

Colamarino, S.A., and Tessier-Lavigne, M. (1995). The role of the floor plate in axon guidance. Annu Rev Neurosci *18*, 497-529.

Cicirata, F., Serapide, M. F., Parenti, R., and Pantò, M. R. (2005). The basilar pontine nuclei and the nucleus reticularis tegmenti pontis subserve distinct cerebrocerebellar pathways. *Progress in Brain Research*. doi:10.1016/S0079-6123(04)48021-2.

Cooke, J., Moens, C., Roth, L., Durbin, L., Shiomi, K., Brennan, C., Kimmel, C., Wilson, S., and Holder, N. (2001). Eph signalling functions downstream of Val to regulate cell sorting and boundary formation in the caudal hindbrain. Development *128*, 571-580.

Cooke, J.E., Kemp, H.A., and Moens, C.B. (2005). EphA4 is required for cell adhesion and rhombomere-boundary formation in the zebrafish. Curr Biol *15*, 536-542.

Cordes, S.P., and Barsh, G.S. (1994). The mouse segmentation gene kr encodes a novel basic domain-leucine zipper transcription factor. Cell *79*, 1025-1034.

Crossley, P.H., and Martin, G.R. (1995). The mouse Fgf8 gene encodes a family of polypeptides and is expressed in regions that direct outgrowth and patterning in the developing embryo. Development *121*, 439-451.

D'Angelo, E., and Casali, S. (2012). Seeking a unified framework for cerebellar function and dysfunction: from circuit operations to cognition. Front Neural Circuits *6*, 116.

Damm, K., Heyman, R.A., Umesono, K., and Evans, R.M. (1993). Functional inhibition of retinoic acid response by dominant negative retinoic acid receptor mutants. Proc Natl Acad Sci U S A *90*, 2989-2993.

Danielian, P. S., Muccino, D., Rowitch, D. H., Michael, S. K., and McMahon, A. P. (1998). Modification of gene activity in mouse embryos in utero by a tamoxifen-inducible form of Cre recombinase. *Curr. Biol.* 8, 1323–S2. doi:10.1016/S0960-9822(07)00562-3.

Dasen, J.S., Liu, J.P., and Jessell, T.M. (2003). Motor neuron columnar fate imposed by sequential phases of Hox-c activity. Nature *425*, 926-933.

Davenne, M., Maconochie, M.K., Neun, R., Pattyn, A., Chambon, P., Krumlauf, R., and Rijli, F.M. (1999). Hoxa2 and Hoxb2 control dorsoventral patterns of neuronal development in the rostral hindbrain. Neuron *22*, 677-691.

Davis, A.A., and Temple, S. (1994). A self-renewing multipotential stem cell in embryonic rat cerebral cortex. Nature *372*, 263-266.

De Kumar, B., Parrish, M.E., Slaughter, B.D., Unruh, J.R., Gogol, M., Seidel, C., Paulson, A., Li, H., Gaudenz, K., Peak, A.*, et al.* (2015). Analysis of dynamic changes in retinoid-induced transcription and epigenetic profiles of murine Hox clusters in ES cells. Genome Res.

De Santa, F., Totaro, M.G., Prosperini, E., Notarbartolo, S., Testa, G., and Natoli, G. (2007). The histone H3 lysine-27 demethylase Jmjd3 links inflammation to inhibition of polycomb-mediated gene silencing. Cell *130*, 1083-1094.

Deiner, M.S., Kennedy, T.E., Fazeli, A., Serafini, T., Tessier-Lavigne, M., and Sretavan, D.W. (1997). Netrin-1 and DCC mediate axon guidance locally at the optic disc: loss of function leads to optic nerve hypoplasia. Neuron *19*, 575-589.

Dent, E.W., and Gertler, F.B. (2003). Cytoskeletal dynamics and transport in growth cone motility and axon guidance. Neuron *40*, 209-227.

Di Bonito, M., Narita, Y., Avallone, B., Sequino, L., Mancuso, M., Andolfi, G., Franze, A.M., Puelles, L., Rijli, F.M., and Studer, M. (2013). Assembly of the auditory circuitry by a Hox genetic network in the mouse brainstem. PLoS Genet *9*, e1003249.

Di Meglio, T., and Rijli, F. M. (2013). Transcriptional Regulation of Tangential Neuronal Migration in the Vertebrate Hindbrain. *Cellular Migration and Formation of Neuronal Connections*, 377–404. doi:10.1016/B978-0-12-397266-8.00033-8.

Di Meglio, T., Kratochwil, C. F., Vilain, N., Loche, A., Vitobello, A., Yonehara, K., et al. (2013). Ezh2 orchestrates topographic migration and connectivity of mouse precerebellar neurons. *Science* 339, 204–207. doi:10.1126/science.1229326.

Di Meglio, T., Nguyen-Ba-Charvet, K. T., Tessier-Lavigne, M., Sotelo, C., and Chedotal, A. (2008). Molecular Mechanisms Controlling Midline Crossing by Precerebellar Neurons. 28, 6285–6294. doi:10.1523/JNEUROSCI.0078-08.2008.

DiPietrantonio, H. J., and Dymecki, S. M. (2009). Zic1 levels regulate mossy fiber neuron position and axon laterality choice in the ventral brain stem. *Neuroscience* 162, 560–573. doi:10.1016/j.neuroscience.2009.02.082.

Dolle, P., Lufkin, T., Krumlauf, R., Mark, M., Duboule, D., and Chambon, P. (1993). Local alterations of Krox-20 and Hox gene expression in the hindbrain suggest lack of rhombomeres 4 and 5 in homozygote null Hoxa-1 (Hox-1.6) mutant embryos. Proc Natl Acad Sci U S A *90*, 7666-7670.

Douarin, N. L., and Kalcheim, C. (1999). The neural crest. Book

Duboule, D. (1992). The vertebrate limb: a model system to study the Hox/HOM gene network during development and evolution. Bioessays *14*, 375-384.

Dupe, V., Davenne, M., Brocard, J., Dolle, P., Mark, M., Dierich, A., Chambon, P., and Rijli, F.M. (1997). In vivo functional analysis of the Hoxa-1 3' retinoic acid response element (3'RARE). Development *124*, 399-410.

Dupe, V., and Lumsden, A. (2001). Hindbrain patterning involves graded responses to retinoic acid signalling. Development *128*, 2199-2208.

Dymecki, S. M., and Tomasiewicz, H. (1998). Using Flp-Recombinase to Characterize Expansion ofWnt1-Expressing Neural Progenitors in the Mouse. *Dev. Biol.* 201, 57–65. doi:10.1006/dbio.1998.8971.

Díaz, E., Ge, Y., Yang, Y. H., Loh, K. C., Serafini, T. A., Okazaki, Y., et al. (2002). Molecular Analysis of Gene Expression in the Developing Pontocerebellar Projection System. *Neuron* 36, 417–434. doi:10.1016/S0896-6273(02)01016-4.

Engelkamp, D., Rashbass, P., Seawright, A., and van Heyningen, V. (1999). Role of Pax6 in development of the cerebellar system. *Development* 126, 3585–3596. Available at: http://dev.biologists.org/content/126/16/3585.long.

Erzurumlu, R.S., Murakami, Y., and Rijli, F.M. (2010). Mapping the face in the somatosensory brainstem. Nat Rev Neurosci *11*, 252-263.

Farago, A. F., Awatramani, R. B., and Dymecki, S. M. (2006). Assembly of the brainstem cochlear nuclear complex is revealed by intersectional and subtractive genetic fate maps. *Neuron* 50, 205–218. doi:10.1016/j.neuron.2006.03.014.

Fazeli, A., Dickinson, S. L., Hermiston, M. L., Tighe, R. V., Steen, R. G., Small, C. G., et al. (1997). Phenotype of mice lacking functional Deleted in colorectal cancer (Dcc) gene. *Nature* 386, 796–804. doi:10.1038/386796a0.

Feldheim, D.A., and O'Leary, D.D. (2010). Visual map development: bidirectional signaling, bifunctional guidance molecules, and competition. Cold Spring Harb Perspect Biol *2*, a001768.

Ferraiuolo, M.A., Rousseau, M., Miyamoto, C., Shenker, S., Wang, X.Q., Nadler, M., Blanchette, M., and Dostie, J. (2010). The three-dimensional architecture of Hox cluster silencing. Nucleic Acids Res *38*, 7472-7484.

Ferretti, E., Cambronero, F., Tumpel, S., Longobardi, E., Wiedemann, L.M., Blasi, F., and Krumlauf, R. (2005). Hoxb1 enhancer and control of rhombomere 4 expression: complex interplay between PREP1-PBX1-HOXB1 binding sites. Mol Cell Biol *25*, 8541-8552.
Fishell, G., and Kriegstein, A.R. (2003). Neurons from radial glia: the consequences of asymmetric inheritance. Curr Opin Neurobiol *13*, 34-41.

Frank, D., and Sela-Donenfeld, D. (2019). Hindbrain induction and patterning during early vertebrate development. Cell Mol Life Sci *76*, 941-960.

Fraser, S., Keynes, R., and Lumsden, A. (1990). Segmentation in the chick embryo hindbrain is defined by cell lineage restrictions. Nature *344*, 431-435.

Frohman, M.A., Martin, G.R., Cordes, S.P., Halamek, L.P., and Barsh, G.S. (1993). Altered rhombomere-specific gene expression and hyoid bone differentiation in the mouse segmentation mutant, kreisler (kr). Development *117*, 925-936.

Fu, Y., Tvrdik, P., Makki, N., Machold, R., Paxinos, G., and Watson, C. (2013). The interfascicular trigeminal nucleus: A precerebellar nucleus in the mouse defined by retrograde neuronal tracing and genetic fate mapping. *J. Comp. Neurol.* 521, 697–708. doi:10.1002/cne.23200.

Fu, Y., Tvrdik, P., Makki, N., Paxinos, G., and Watson, C. (2011). Precerebellar Cell Groups in the Hindbrain of the Mouse Defined by Retrograde Tracing and Correlated with Cumulative Wnt1-Cre Genetic Labeling. *The Cerebellum* 10, 570–584. doi:10.1007/s12311-011-0266-1.

Gaidatzis, D., Lerch, A., Hahne, F., and Stadler, M.B. (2015). QuasR: quantification and annotation of short reads in R. Bioinformatics *31*, 1130-1132.

Garcia-Dominguez, M., Gilardi-Hebenstreit, P., and Charnay, P. (2006). PIASxbeta acts as an activator of Hoxb1 and is antagonized by Krox20 during hindbrain segmentation. EMBO J *25*, 2432-2442.

Garel, S., Garcia-Dominguez, M., and Charnay, P. (2000). Control of the migratory pathway of facial branchiomotor neurones. *Development* 127, 5297–5307. doi:10.1038/386838a0.

Gaufo, G.O., Flodby, P., and Capecchi, M.R. (2000). Hoxb1 controls effectors of sonic hedgehog and Mash1 signaling pathways. Development *127*, 5343-5354.

Gaufo, G.O., Thomas, K.R., and Capecchi, M.R. (2003). Hox3 genes coordinate mechanisms of genetic suppression and activation in the generation of branchial and somatic motoneurons. Development *130*, 5191-5201.

Gavalas, A., Davenne, M., Lumsden, A., Chambon, P., and Rijli, F. M. (1997). Role of Hoxa-2 in axon pathfinding and rostral hindbrain patterning. *Development* 124, 3693–3702. Available at: http://dev.biologists.org/content/124/19/3693.long.

Gavalas, A., and Krumlauf, R. (2000). Retinoid signalling and hindbrain patterning. Curr Opin Genet Dev *10*, 380-386.

Gavalas, A., Studer, M., Lumsden, A., Rijli, F.M., Krumlauf, R., and Chambon, P. (1998). Hoxa1 and Hoxb1 synergize in patterning the hindbrain, cranial nerves and second pharyngeal arch. Development *125*, 1123-1136.

Geisen, M. J., Di Meglio, T., Pasqualetti, M., Ducret, S., Brunet, J.-F., Chedotal, A., et al. (2008). Hox paralog group 2 genes control the migration of mouse pontine neurons through slit-robo signaling. *PLoS Biol.* 6, e142. doi:10.1371/journal.pbio.0060142.

Geisler, S.J., and Paro, R. (2015). Trithorax and Polycomb group-dependent regulation: a tale of opposing activities. Development *142*, 2876-2887.

Gesemann, M., Litwack, E.D., Yee, K.T., Christen, U., and O'Leary, D.D. (2001). Identification of candidate genes for controlling development of the basilar pons by differential display PCR. Mol Cell Neurosci *18*, 1-12.

Giudicelli, F., Gilardi-Hebenstreit, P., Mechta-Grigoriou, F., Poquet, C., and Charnay, P. (2003). Novel activities of Mafb underlie its dual role in hindbrain segmentation and regional specification. Dev Biol *253*, 150-162.

Glickstein, M., Cohen, J. L., Dixon, B., Gibson, A., Hollins, M., Labossiere, E., et al. (1980). Corticopontine visual projections in macaque monkeys. *J. Comp. Neurol.* 190, 209–229. doi:10.1002/cne.901900202.

Glickstein, M., Gerrits, N., Kralj-Hans, I., Mercier, B., Stein, J., and Voogd, J. (1994). Visual pontocerebellar projections in the macaque. *J. Comp. Neurol.* 349, 51–72. doi:10.1002/cne.903490105.

Glover, J.C., Renaud, J.S., and Rijli, F.M. (2006). Retinoic acid and hindbrain patterning. J Neurobiol *66*, 705-725.

Goddard, J.M., Rossel, M., Manley, N.R., and Capecchi, M.R. (1996). Mice with targeted disruption of Hoxb-1 fail to form the motor nucleus of the VIIth nerve. Development *122*, 3217-3228.

Godsave, S.F., and Durston, A.J. (1997). Neural induction and patterning in embryos deficient in FGF signaling. Int J Dev Biol *41*, 57-65.

Gotz, M., and Huttner, W.B. (2005). The cell biology of neurogenesis. Nat Rev Mol Cell Biol *6*, 777-788.

Gould, A., Itasaki, N., and Krumlauf, R. (1998). Initiation of rhombomeric Hoxb4 expression requires induction by somites and a retinoid pathway. Neuron *21*, 39-51.

Gould, A., Morrison, A., Sproat, G., White, R.A., and Krumlauf, R. (1997). Positive cross-regulation and enhancer sharing: two mechanisms for specifying overlapping Hox expression patterns. Genes Dev *11*, 900-913.

Graham, A., Papalopulu, N., and Krumlauf, R. (1989). The murine and Drosophila homeobox gene complexes have common features of organization and expression. Cell *57*, 367-378.

Grimaldi, G., and Manto, M. (2012). Topography of cerebellar deficits in humans. *Cerebellum* 11, 336–351. doi:10.1007/s12311-011-0247-4.

Guidato, S., Prin, F., and Guthrie, S. (2003). Somatic motoneurone specification in the hindbrain: the influence of somite-derived signals, retinoic acid and Hoxa3. Development *130*, 2981-2996.

Guthrie, S. (1996). Patterning the hindbrain. Curr Opin Neurobiol *6*, 41-48.

Guthrie, S., Butcher, M., and Lumsden, A. (1991). Patterns of cell division and interkinetic nuclear migration in the chick embryo hindbrain. J Neurobiol *22*, 742-754.

Guthrie, S., and Lumsden, A. (1991). Formation and regeneration of rhombomere boundaries in the developing chick hindbrain. Development *112*, 221-229.

Guthrie, S., Muchamore, I., Kuroiwa, A., Marshall, H., Krumlauf, R., and Lumsden, A. (1992). Neuroectodermal autonomy of Hox-2.9 expression revealed by rhombomere transpositions. Nature *356*, 157-159.

Hall, A. C., Lucas, F. R., and Salinas, P. C. (2000). Axonal Remodeling and Synaptic Differentiation in the Cerebellum Is Regulated by WNT-7a Signaling. *Cell* 100, 525–535. doi:10.1016/S0092-8674(00)80689-3.

Hanashima, C., Shen, L., Li, S.C., and Lai, E. (2002). Brain factor-1 controls the proliferation and differentiation of neocortical progenitor cells through independent mechanisms. J Neurosci *22*, 6526-6536.

Harding, K., Wedeen, C., McGinnis, W., and Levine, M. (1985). Spatially regulated expression of homeotic genes in Drosophila. Science *229*, 1236-1242.

Harris, J.A., Oh, S.W., and Zeng, H. (2012). Adeno-associated viral vectors for anterograde axonal tracing with fluorescent proteins in nontransgenic and cre driver mice. Curr Protoc Neurosci *Chapter 1*, Unit 1 20 21-18.

Hatanaka, Y., Zhu, Y., Torigoe, M., Kita, Y., and Murakami, F. (2016). From migration to settlement: the pathways, migration modes and dynamics of neurons in the developing brain. *Proc. Jpn. Acad., Ser. B, Phys. Biol. Sci.* 92, 1–19. doi:10.2183/pjab.92.1.

Hatten, M. E. (1999). Central nervous system neuronal migration. *Annu. Rev. Neurosci.* 22, 511–539. doi:10.1146/annurev.neuro.22.1.511.

Helms, A.W., Abney, A.L., Ben-Arie, N., Zoghbi, H.Y., and Johnson, J.E. (2000).

Autoregulation and multiple enhancers control Math1 expression in the developing nervous system. Development *127*, 1185-1196.

Herrero, L., Pardoe, J., and Apps, R. (2002). Pontine and lateral reticular projections to the c1 zone in lobulus simplex and paramedian lobule of the rat cerebellar cortex. Cerebellum *1*, 185-199.

Heyman, I., Faissner, A., and Lumsden, A. (1995). Cell and matrix specialisations of rhombomere boundaries. Dev Dyn *204*, 301-315.

Hippenmeyer, S., Vrieseling, E., Sigrist, M., Portmann, T., Laengle, C., Ladle, D.R., and Arber, S. (2005). A developmental switch in the response of DRG neurons to ETS transcription factor signaling. PLoS Biol *3*, e159.

Hoddevik, G. H. (1975). The pontocerebellar projection onto the paramedian lobule in the cat: an experimental study with the use of horseradish peroxidase as a tracer. *Brain Res.* 95, 291–307. Available at: http://www.sciencedirect.com/science/article/pii/0006899375901080.

Hong, K., Hinck, L., Nishiyama, M., Poo, M.M., Tessier-Lavigne, M., and Stein, E. (1999). A ligand-gated association between cytoplasmic domains of UNC5 and DCC family receptors converts netrin-induced growth cone attraction to repulsion. Cell *97*, 927-941.

Hunt, P., Gulisano, M., Cook, M., Sham, M.H., Faiella, A., Wilkinson, D., Boncinelli, E., and Krumlauf, R. (1991). A distinct Hox code for the branchial region of the vertebrate head. Nature *353*, 861-864.

Hurley, I., Hale, M.E., and Prince, V.E. (2005). Duplication events and the evolution of segmental identity. Evol Dev *7*, 556-567.

Irving, C., and Mason, I. (2000). Signalling by FGF8 from the isthmus patterns anterior hindbrain and establishes the anterior limit of Hox gene expression. Development *127*, 177-186.

Islam, S. M., Shinmyo, Y., Okafuji, T., Su, Y., Bin Naser, I., Ahmed, G., et al. (2009). Draxin, a Repulsive Guidance Protein for Spinal Cord and Forebrain Commissures. *Science* 323, 388–393. doi:10.1126/science.1165187.

Ito, M. (2008). Control of mental activities by internal models in the cerebellum. *Nat Rev Neurosci* 9, 304–313. doi:10.1038/nrn2332.

Jacob, J., and Guthrie, S. (2000). Facial visceral motor neurons display specific rhombomere origin and axon pathfinding behavior in the chick. J Neurosci *20*, 7664-7671.

Jessell, T.M., Surmeli, G., and Kelly, J.S. (2011). Motor neurons and the sense of place. Neuron *72*, 419-424.

Jho, E.H., Zhang, T., Domon, C., Joo, C.K., Freund, J.N., and Costantini, F. (2002). Wnt/beta-catenin/Tcf signaling induces the transcription of Axin2, a negative regulator of the signaling pathway. Mol Cell Biol *22*, 1172-1183.

Jiang, W., Wang, J., and Zhang, Y. (2013). Histone H3K27me3 demethylases KDM6A and KDM6B modulate definitive endoderm differentiation from human ESCs by regulating WNT signaling pathway. Cell Res *23*, 122-130.

Kaas, J.H. (1997). Topographic maps are fundamental to sensory processing. Brain Res Bull *44*, 107-112.

Kageyama, R., Shimojo, H., and Ohtsuka, T. (2019). Dynamic control of neural stem cells by bHLH factors. Neurosci Res *138*, 12-18.

Kalinovsky, A., Boukhtouche, F., Blazeski, R., Bornmann, C., Suzuki, N., Mason, C. A., et al. (2011). Development of Axon-Target Specificity of Ponto-Cerebellar Afferents. *PLoS Biol.* 9, e1001013. doi:10.1371/journal.pbio.1001013.

Karmakar, K., Narita, Y., Fadok, J., Ducret, S., Loche, A., Kitazawa, T., Genoud, C., Di Meglio, T., Thierry, R., Bacelo, J.*, et al.* (2017). Hox2 Genes Are Required for Tonotopic Map Precision and Sound Discrimination in the Mouse Auditory Brainstem. Cell Rep *18*, 185-197.

Kandel, E. R., Schwartz, J. H., Jessel, T. M., Siegelbaum, S. A., Hudspeth, A. J. Principles of neural science. V Edition.

Kartikasari, A.E., Zhou, J.X., Kanji, M.S., Chan, D.N., Sinha, A., Grapin-Botton, A., Magnuson, M.A., Lowry, W.E., and Bhushan, A. (2013). The histone demethylase Jmjd3 sequentially associates with the transcription factors Tbx3 and Eomes to drive endoderm differentiation. Embo J *32*, 1393-1408.

Kashyap, V., Gudas, L.J., Brenet, F., Funk, P., Viale, A., and Scandura, J.M. (2011). Epigenomic reorganization of the clustered Hox genes in embryonic stem cells induced by retinoic acid. J Biol Chem *286*, 3250-3260.

Kaufman, T.C., Lewis, R., and Wakimoto, B. (1980). Cytogenetic Analysis of Chromosome 3 in DROSOPHILA MELANOGASTER: The Homoeotic Gene Complex in Polytene Chromosome Interval 84a-B. Genetics *94*, 115-133.

Kawauchi, D., Taniguchi, H., Watanabe, H., Saito, T., and Murakami, F. (2006). Direct visualization of nucleogenesis by precerebellar neurons: involvement of ventricle-directed, radial fibre-associated migration. *Development* 133, 1113–1123. doi:10.1242/dev.02283.

Keino-Masu, K., Masu, M., Hinck, L., Leonardo, E.D., Chan, S.S., Culotti, J.G., and Tessier-Lavigne, M. (1996). Deleted in Colorectal Cancer (DCC) encodes a netrin receptor. Cell *87*, 175-185.

Keleman, K., and Dickson, B.J. (2001). Short- and long-range repulsion by the Drosophila Unc5 netrin receptor. Neuron *32*, 605-617.

Kennedy, T.E., Serafini, T., de la Torre, J.R., and Tessier-Lavigne, M. (1994). Netrins are diffusible chemotropic factors for commissural axons in the embryonic spinal cord. Cell *78*, 425-435.

Kessel, M., and Gruss, P. (1991). Homeotic transformations of murine vertebrae and concomitant alteration of Hox codes induced by retinoic acid. Cell *67*, 89-104.

Keynes, R., and Krumlauf, R. (1994). Hox genes and regionalization of the nervous system. Annu Rev Neurosci *17*, 109-132.

Kheradmand, A., and Zee, D.S. (2011). Cerebellum and ocular motor control. Front Neurol *2*, 53.

Kim, C.H., Oda, T., Itoh, M., Jiang, D., Artinger, K.B., Chandrasekharappa, S.C., Driever, W., and Chitnis, A.B. (2000). Repressor activity of Headless/Tcf3 is essential for vertebrate head formation. Nature *407*, 913-916.

Kim, D., and Ackerman, S. L. (2011). The UNC5C netrin receptor regulates dorsal guidance of mouse hindbrain axons. *Journal of Neuroscience* 31, 2167–2179. doi:10.1523/JNEUROSCI.5254-10.2011.

Kidd, T., Bland, K.S., and Goodman, C.S. (1999). Slit is the midline repellent for the robo receptor in Drosophila. Cell *96*, 785-794.

Kidd, T., Brose, K., Mitchell, K.J., Fetter, R.D., Tessier-Lavigne, M., Goodman, C.S., and Tear, G. (1998). Roundabout controls axon crossing of the CNS midline and defines a novel subfamily of evolutionarily conserved guidance receptors. Cell *92*, 205-215.

Kiecker, C., and Niehrs, C. (2001). A morphogen gradient of Wnt/beta-catenin signalling regulates anteroposterior neural patterning in Xenopus. Development *128*, 4189-4201.

Klein, R. (2004). Eph/ephrin signaling in morphogenesis, neural development and plasticity. Curr Opin Cell Biol *16*, 580-589.

Kobayashi, H., Kobayashi, H., Kawauchi, D., Hashimoto, Y., Ogata, T., and Murakami, F. (2013). The control of precerebellar neuron migration by RNA-binding protein Csde1. 253, 292–303. doi:10.1016/j.neuroscience.2013.08.055.

Kobayashi, H., Saragai, S., Naito, A., Ichio, K., Kawauchi, D., and Murakami, F. (2015). Calm1 signaling pathway is essential for the migration of mouse precerebellar neurons. *Development* 142, 375–384. doi:10.1242/dev.112680.

Koentges, G., and Matsuoka, T. (2002). Evolution. Jaws of the fates. Science *298*, 371-373.

Kolmac, C.I., Power, B.D., and Mitrofanis, J. (1998). Patterns of connections between zona incerta and brainstem in rats. J Comp Neurol *396*, 544-555.

Kolodkin, A.L., and Tessier-Lavigne, M. (2011). Mechanisms and molecules of neuronal wiring: a primer. Cold Spring Harb Perspect Biol *3*.

Kosinski, R. J., Neafsey, E. J., and Castro, A. J. (1986). A comparative topographical analysis of dorsal column nuclear and cerebral cortical projections to the basilar pontine gray in rats. *J. Comp. Neurol.* 244, 163–173. doi:10.1002/cne.902440204.

Kratochwil, C. F. (2013). Transcriptional and epigenetic regulation of neuronal migration and circuitry development in the murine hindbrain. doi:10.5451/unibas-006137308.

Kratochwil, C. F., and Meyer, A. (2015). Closing the genotype-phenotype gap: Emerging technologies for evolutionary genetics in ecological model vertebrate systems. *Bioessays* 37, 213–226. doi:10.1002/bies.201400142.

Kratochwil, C.F., Maheshwari, U., and Rijli, F.M. (2017). The Long Journey of Pontine Nuclei Neurons: From Rhombic Lip to Cortico-Ponto-Cerebellar Circuitry. Front Neural Circuits *11*, 33.

Kratochwil, C. F., and Rijli, F. M. (2014). The Cre/Lox system to assess the development of the mouse brain. *Methods Mol. Biol.* 1082, 295–313. doi:10.1007/978-1-62703-655-9_20.

Krubitzer, L. (2007). The magnificent compromise: cortical field evolution in mammals. *Neuron* 56, 201–208. doi:10.1016/j.neuron.2007.10.002.

Krumlauf, R. (1993). Mouse Hox genetic functions. Curr Opin Genet Dev *3*, 621-625.

Krumlauf, R., Marshall, H., Studer, M., Nonchev, S., Sham, M.H., and Lumsden, A. (1993). Hox homeobox genes and regionalisation of the nervous system. J Neurobiol *24*, 1328-1340.

Kumbasar, A., Plachez, C., Gronostajski, R. M., Richards, L. J., and Litwack, E. D. (2009). Absence of the transcription factor Nfibdelays the formation of the basilar pontine and other mossy fiber nuclei. *J. Comp. Neurol.* 513, 98–112. doi:10.1002/cne.21943.

Kuwako, K.-I., Kakumoto, K., Imai, T., Igarashi, M., Hamakubo, T., Sakakibara, S.-I., et al. (2010). Neural RNA-binding protein Musashi1 controls midline crossing of precerebellar neurons through posttranscriptional regulation of Robo3/Rig-1 expression. *Neuron* 67, 407–421. doi:10.1016/j.neuron.2010.07.005.

Kuwako, K.-I., Nishimoto, Y., Kawase, S., Okano, H. J., and Okano, H. (2014). Cadherin-7 Regulates Mossy Fiber Connectivity in the Cerebellum. *Cell Rep* 9, 311–323. doi:10.1016/j.celrep.2014.08.063.

Kwan, K.Y., Lam, M.M., Krsnik, Z., Kawasawa, Y.I., Lefebvre, V., and Sestan, N. (2008). SOX5 postmitotically regulates migration, postmigratory differentiation, and projections of subplate and deep-layer neocortical neurons. Proc Natl Acad Sci U S A *105*, 16021-16026.

Landsberg, R. L., Awatramani, R. B., Hunter, N. L., Farago, A. F., DiPietrantonio, H. J., Rodriguez, C. I., et al. (2005). Hindbrain Rhombic Lip Is Comprised of Discrete Progenitor Cell Populations Allocated by Pax6. *Neuron* 48, 933–947. doi:10.1016/j.neuron.2005.11.031.

Laumonnerie, C., Bechara, A., Vilain, N., Kurihara, Y., Kurihara, H., and Rijli, F. M. (2015). Facial whisker pattern is not sufficient to instruct a whisker-related topographic map in the mouse somatosensory brainstem. Development *142*, 3704-3712.

Lan, F., Bayliss, P.E., Rinn, J.L., Whetstine, J.R., Wang, J.K., Chen, S., Iwase, S., Alpatov, R., Issaeva, I., Canaani, E*., et al.* (2007). A histone H3 lysine 27 demethylase regulates animal posterior development. Nature *449*, 689-694.

Lee, M.G., Villa, R., Trojer, P., Norman, J., Yan, K.P., Reinberg, D., Di Croce, L., and Shiekhattar, R. (2007). Demethylation of H3K27 regulates polycomb recruitment and H2A ubiquitination. Science *318*, 447-450.

Lee, D., and Shin, C. (2012). MicroRNA-target interactions: new insights from genome-wide approaches. Ann N Y Acad Sci *1271*, 118-128.

Leergaard, T. B. (2003). Clustered and laminar topographic patterns in rat cerebro-pontine pathways. 206, 149–162. doi:10.1007/s00429-002-0272-7.

Leergaard, T.B., Alloway, K.D., Mutic, J.J., and Bjaalie, J.G. (2000a). Three-dimensional topography of corticopontine projections from rat barrel cortex: correlations with corticostriatal organization. J Neurosci *20*, 8474-8484.

Leergaard, T.B., Lyngstad, K.A., Thompson, J.H., Taeymans, S., Vos, B.P., De Schutter, E., Bower, J.M., and Bjaalie, J.G. (2000b). Rat somatosensory cerebropontocerebellar pathways: spatial relationships of the somatotopic map of the primary somatosensory cortex are preserved in a three-dimensional clustered pontine map. J Comp Neurol *422*, 246-266.

Leergaard, T. B., Alloway, K. D., Pham, T. A. T., Bolstad, I., Hoffer, Z. S., Pettersen, C., et al. (2004). Three-dimensional topography of corticopontine projections from rat sensorimotor cortex: comparisons with corticostriatal projections reveal diverse integrative organization. *J. Comp. Neurol.* 478, 306–322. doi:10.1002/cne.20289.

Leergaard, T. B., and Bjaalie, J. G. (2007). Topography of the complete corticopontine projection: from experiments to principal Maps. *Front Neurosci* 1, 211–223. doi:10.3389/neuro.01.1.1.016.2007.

Leergaard, T. B., Lakke, E. A. J. F., and Bjaalie, J. G. (1995). Topographical organization in the early postnatal projection: A carbocyanine dye and 3-D computer reconstruction study in the rat. *J. Comp. Neurol.* 361, 77–94. doi:10.1002/cne.903610107.

Leergaard, T. B., Lillehaug, S., De Schutter, E., Bower, J. M., and Bjaalie, J. G. (2006). Topographical organization of pathways from somatosensory cortex through the pontine nuclei to tactile regions of the rat cerebellar hemispheres. *Eur. J. Neurosci.* 24, 2801–2812. doi:10.1111/j.1460-9568.2006.05150.x.

Lein, E.S., Hawrylycz, M.J., Ao, N., Ayres, M., Bensinger, A., Bernard, A., Boe, A.F., Boguski, M.S., Brockway, K.S., Byrnes, E.J.*, et al.* (2007). Genome-wide atlas of gene expression in the adult mouse brain. Nature *445*, 168-176.

Leonardo, E.D., Hinck, L., Masu, M., Keino-Masu, K., Fazeli, A., Stoeckli, E.T., Ackerman, S.L., Weinberg, R.A., and Tessier-Lavigne, M. (1997). Guidance of developing axons by netrin-1 and its receptors. Cold Spring Harb Symp Quant Biol *62*, 467-478.
Lende, R. A. (1963). Cerebral Cortex: A Sensorimotor Amalgam in the Marsupialia. *Science* 141, 730–732. doi:10.1126/science.141.3582.730.

Lende, R. A. (1964). Representation in the cerebral cortex of a primitive mammal. Sensorimotor, visual and auditory fields in the echidna (*Tachzglossus aculeatus*). *J. Neurophysiol.* 27, 37–48.

Levine, A.J., Lewallen, K.A., and Pfaff, S.L. (2012). Spatial organization of cortical and spinal neurons controlling motor behavior. Curr Opin Neurobiol *22*, 812-821.

Lewis, A. E., Vasudevan, H. N., O'Neill, A. K., Soriano, P., and Bush, J. O. (2013). The widely used Wnt1-Cre transgene causes developmental phenotypes by ectopic activation of Wnt signaling. *Dev. Biol.* 379, 229–234. doi:10.1016/j.ydbio.2013.04.026.

Lewis, E.B. (1978). A gene complex controlling segmentation in Drosophila. Nature *276*, 565-570.

Lewis, R.A., Kaufman, T.C., Denell, R.E., and Tallerico, P. (1980a). Genetic Analysis of the Antennapedia Gene Complex (Ant-C) and Adjacent Chromosomal Regions of DROSOPHILA MELANOGASTER. I. Polytene Chromosome Segments 84b-D. Genetics *95*, 367-381.

Lewis, R.A., Wakimoto, B.T., Denell, R.E., and Kaufman, T.C. (1980b). Genetic Analysis of the Antennapedia Gene Complex (Ant-C) and Adjacent Chromosomal Regions of DROSOPHILA MELANOGASTER. II. Polytene Chromosome Segments 84A-84B1,2. Genetics *95*, 383-397.

Li, H.S., Chen, J.H., Wu, W., Fagaly, T., Zhou, L., Yuan, W., Dupuis, S., Jiang, Z.H., Nash, W., Gick, C.*, et al.* (1999). Vertebrate slit, a secreted ligand for the transmembrane protein roundabout, is a repellent for olfactory bulb axons. Cell *96*, 807-818.

Li, S., Qiu, F., Xu, A., Price, S. M., and Xiang, M. (2004). Barhl1 Regulates Migration and Survival of Cerebellar Granule Cells by Controlling Expression of the Neurotrophin-3 Gene. 24, 3104–3114. doi:10.1523/JNEUROSCI.4444-03.2004.

Lin, C., Garrett, A.S., De Kumar, B., Smith, E.R., Gogol, M., Seidel, C., Krumlauf, R., and Shilatifard, A. (2011). Dynamic transcriptional events in embryonic stem cells mediated by the super elongation complex (SEC). Genes Dev *25*, 1486-1498.

Lindquist, R. A., Guinto, C. D., Rodas-Rodriguez, J. L., Fuentealba, L. C., Tate, M. C., Rowitch, D. H., et al. (2016). Identification of proliferative progenitors associated with prominent postnatal growth of the pons. *Nature Communications* 7, 11628. doi:10.1038/ncomms11628.

Liu, Z., Li, H., Hu, X., Yu, L., Liu, H., Han, R., et al. (2008). Control of Precerebellar Neuron Development by Olig3 bHLH Transcription Factor. 28, 10124–10133. doi:10.1523/JNEUROSCI.3769-08.2008.

Llambi, F., Causeret, F., Gallego, E. B., and Mehlen, P. (2001). Netrin-1 acts as a survival factor via its receptors UNC5H and DCC. *The EMBO Journal* 20, 2715–2722. doi:10.1093/emboj/20.11.2715.

Lowery, L.A., and Van Vactor, D. (2009). The trip of the tip: understanding the growth cone machinery. Nat Rev Mol Cell Biol *10*, 332-343.

Lufkin, T., Dierich, A., LeMeur, M., Mark, M., and Chambon, P. (1991). Disruption of the Hox-1.6 homeobox gene results in defects in a region corresponding to its rostral domain of expression. Cell *66*, 1105-1119.

Lumsden, A., and Krumlauf, R. (1996). Patterning the vertebrate neuraxis. Science *274*, 1109-1115.

Lyuksyutova, A.I., Lu, C.C., Milanesio, N., King, L.A., Guo, N., Wang, Y., Nathans, J., Tessier-Lavigne, M., and Zou, Y. (2003). Anterior-posterior guidance of commissural axons by Wnt-frizzled signaling. Science *302*, 1984-1988.

Machold, R., and Fishell, G. (2005). Math1 Is Expressed in Temporally Discrete Pools of Cerebellar Rhombic-Lip Neural Progenitors. *Neuron* 48, 17–24. doi:10.1016/j.neuron.2005.08.028.

Maconochie, M., Nonchev, S., Morrison, A., and Krumlauf, R. (1996). Paralogous Hox genes: function and regulation. Annu Rev Genet *30*, 529-556.

Maconochie, M.K., Nonchev, S., Studer, M., Chan, S.K., Popperl, H., Sham, M.H., Mann, R.S., and Krumlauf, R. (1997). Cross-regulation in the mouse HoxB complex: the expression of Hoxb2 in rhombomere 4 is regulated by Hoxb1. Genes Dev *11*, 1885-1895.

Madisen, L., Mao, T., Koch, H., Zhuo, J.M., Berenyi, A., Fujisawa, S., Hsu, Y.W., Garcia, A.J., 3rd, Gu, X., Zanella, S.*, et al.* (2012). A toolbox of Cre-dependent optogenetic transgenic mice for light-induced activation and silencing. Nat Neurosci *15*, 793-802.

Madisen, L., Zwingman, T.A., Sunkin, S.M., Oh, S.W., Zariwala, H.A., Gu, H., Ng, L.L., Palmiter, R.D., Hawrylycz, M.J., Jones, A.R.*, et al.* (2010). A robust and high-throughput Cre reporting and characterization system for the whole mouse brain. Nat Neurosci *13*, 133-140.

Mahony, S., Mazzoni, E.O., McCuine, S., Young, R.A., Wichterle, H., and Gifford, D.K. (2011). Ligand-dependent dynamics of retinoic acid receptor binding during early neurogenesis. Genome Biol *12*, R2.
Margueron, R., and Reinberg, D. (2011). The Polycomb complex PRC2 and its mark in life. Nature *469*, 343-349.

Mallo, M., and Alonso, C.R. (2013). The regulation of Hox gene expression during animal development. Development *140*, 3951-3963.

Manzanares, M., Bel-Vialar, S., Ariza-McNaughton, L., Ferretti, E., Marshall, H., Maconochie, M.M., Blasi, F., and Krumlauf, R. (2001). Independent regulation of initiation and maintenance phases of Hoxa3 expression in the vertebrate hindbrain involve auto- and cross-regulatory mechanisms. Development *128*, 3595-3607.

Manzanares, M., Nardelli, J., Gilardi-Hebenstreit, P., Marshall, H., Giudicelli, F., Martinez-Pastor, M.T., Krumlauf, R., and Charnay, P. (2002). Krox20 and kreisler co-operate in the transcriptional control of segmental expression of Hoxb3 in the developing hindbrain. EMBO J *21*, 365-376.

Manzanares, M., Trainor, P.A., Nonchev, S., Ariza-McNaughton, L., Brodie, J., Gould, A., Marshall, H., Morrison, A., Kwan, C.T., Sham, M.H.*, et al.* (1999). The role of kreisler in segmentation during hindbrain development. Dev Biol *211*, 220-237.

Margueron, R., and Reinberg, D. (2011). The Polycomb complex PRC2 and its mark in life. Nature *469*, 343-349.

Marillat, V., Sabatier, C., Failli, V., Matsunaga, E., Sotelo, C., Tessier-Lavigne, M., et al.

(2004). The Slit Receptor Rig-1/Robo3 Controls Midline Crossing by Hindbrain Precerebellar Neurons and Axons. *Neuron* 43, 69–79. doi:10.1016/j.neuron.2004.06.018.

Mark, M., Lufkin, T., Dolle, P., Dierich, A., LeMeur, M., and Chambon, P. (1993a). Roles of Hox genes: what we have learnt from gain of function and loss of function mutations in the mouse. C R Acad Sci III *316*, 995-1008.

Mark, M., Lufkin, T., Vonesch, J.L., Ruberte, E., Olivo, J.C., Dolle, P., Gorry, P., Lumsden, A., and Chambon, P. (1993b). Two rhombomeres are altered in Hoxa-1 mutant mice. Development *119*, 319-338.

Marshall, H., Morrison, A., Studer, M., Popperl, H., and Krumlauf, R. (1996). Retinoids and Hox genes. FASEB J *10*, 969-978.

Marshall, H., Nonchev, S., Sham, M.H., Muchamore, I., Lumsden, A., and Krumlauf, R. (1992). Retinoic acid alters hindbrain Hox code and induces transformation of rhombomeres 2/3 into a 4/5 identity. Nature *360*, 737-741.

Marshall, H., Studer, M., Popperl, H., Aparicio, S., Kuroiwa, A., Brenner, S., and Krumlauf, R. (1994). A conserved retinoic acid response element required for early expression of the homeobox gene Hoxb-1. Nature *370*, 567-571.

Marillat, V., Sabatier, C., Failli, V., Matsunaga, E., Sotelo, C., Tessier-Lavigne, M., and Chedotal, A. (2004). The slit receptor Rig-1/Robo3 controls midline crossing by hindbrain precerebellar neurons and axons. Neuron *43*, 69-79.

Marín, F., and Puelles, L. (1995). Morphological Fate of Rhombomeres in Quail/Chick Chimeras: A Segmental Analysis of Hindbrain Nuclei. *European Journal of Neuroscience* 7, 1714–1738. doi:10.1111/j.1460-9568.1995.tb00693.x.

Matsuda, T., and Cepko, C.L. (2007). Controlled expression of transgenes introduced by in vivo electroporation. Proc Natl Acad Sci U S A *104*, 1027-1032.

Maves, L., Jackman, W., and Kimmel, C.B. (2002). FGF3 and FGF8 mediate a rhombomere 4 signaling activity in the zebrafish hindbrain. Development *129*, 3825-3837.

Mazzoni, E.O., Mahony, S., Peljto, M., Patel, T., Thornton, S.R., McCuine, S., Reeder, C., Boyer, L.A., Young, R.A., Gifford, D.K.*, et al.* (2013). Saltatory remodeling of Hox chromatin in response to rostrocaudal patterning signals. Nat Neurosci *16*, 1191-1198.

May, J. G., Keller, E. L., and Suzuki, D. A. (1988). Smooth-pursuit eye movement deficits with chemical lesions in the dorsolateral pontine nucleus of the monkey. *J. Neurophysiol.* 59, 952–977. Available at: http://jn.physiology.org/content/59/3/952.long.

McIntyre, D.C., Rakshit, S., Yallowitz, A.R., Loken, L., Jeannotte, L., Capecchi, M.R., and Wellik, D.M. (2007). Hox patterning of the vertebrate rib cage. Development *134*, 2981-2989.

McKay, I.J., Muchamore, I., Krumlauf, R., Maden, M., Lumsden, A., and Lewis, J. (1994). The kreisler mouse: a hindbrain segmentation mutant that lacks two rhombomeres. Development *120*, 2199-2211.

Mihailoff, G. A. (1983). Intra- and interhemispheric collateral branching in the rat pontocerebellar system, a fluorescence double-label study. *Neuroscience* 10, 141–160. doi:10.1016/0306-4522(83)90088-X.

Mihailoff, G.A., Adams, C.E., and Woodward, D.J. (1984). An autoradiographic study of the postnatal development of sensorimotor and visual components of the corticopontine system. J Comp Neurol *222*, 116-127.

Mihailoff, G. A., and King, J. S. (1975). The basilar pontine gray of the opossum: A correlated light and electron microscopic analysis. *J. Comp. Neurol.* 159, 521–551. doi:10.1002/cne.901590406.

Mihailoff, G. A., Burne, R. A., and Woodward, D. J. (1978). Projections of the sensorimotor cortex to the basilar pontine nuclei in the rat: an autoradiographic study. *Brain Res.* doi:10.1016/0006-8993(78)90867-3.

Mihailoff, G.A., Kosinski, R.J., Azizi, S.A., and Border, B.G. (1989). Survey of noncortical afferent projections to the basilar pontine nuclei: a retrograde tracing study in the rat. J Comp Neurol *282*, 617-643.

Mihailoff, G. A., Burne, R. A., Azizi, S. A., Norell, G., and Woodward, D. J. (1981). The pontocerebellar system in the rat: An HRP study. II. Hemispheral components. *J. Comp. Neurol.* 197, 559–577. doi:10.1002/cne.901970403.

Moazed, D., and O'Farrell, P.H. (1992). Maintenance of the engrailed expression pattern by Polycomb group genes in Drosophila. Development *116*, 805-810.

Moore, S.W., Tessier-Lavigne, M., and Kennedy, T.E. (2007). Netrins and their receptors. Adv Exp Med Biol *621*, 17-31.

Morriss-Kay, G.M., Murphy, P., Hill, R.E., and Davidson, D.R. (1991). Effects of retinoic acid excess on expression of Hox-2.9 and Krox-20 and on morphological segmentation in the hindbrain of mouse embryos. EMBO J *10*, 2985-2995.

Murphy, P., Davidson, D.R., and Hill, R. E. (1989). Segment-specific expression of a homeobox-containing gene in the mouse hindbrain. Nature *341*, 156-159.

Murthy, V.N. (2011). Olfactory maps in the brain. Annu Rev Neurosci *34*, 233-258.

Narita, Y., and Rijli, F.M. (2009). Hox genes in neural patterning and circuit formation in the mouse hindbrain. Curr Top Dev Biol *88*, 139-167.

Niederreither, K., and Dolle, P. (2008). Retinoic acid in development: towards an integrated view. Nat Rev Genet *9*, 541-553.

Niederreither, K., McCaffery, P., Drager, U.C., Chambon, P., and Dolle, P. (1997). Restricted expression and retinoic acid-induced downregulation of the retinaldehyde dehydrogenase type 2 (RALDH-2) gene during mouse development. Mech Dev *62*, 67-78.

Nieto, M.A., Bradley, L.C., and Wilkinson, D.G. (1991). Conserved segmental expression of Krox-20 in the vertebrate hindbrain and its relationship to lineage restriction. Dev Suppl *Suppl 2*, 59-62.

Nikundiwe, A. M., Bjaalie, J. G., Bjaalie, J. G., and Brodal, P. (1994). Lamellar organization of pontocerebellar neuronal populations. A multi-tracer and 3-D computer reconstruction study in the cat. *Eur. J. Neurosci.* 6, 173–186. doi:10.1111/j.1460-9568.1994.tb00259.x.

Nishida, K., Nakayama, K., Yoshimura, S., and Murakami, F. (2011). Role of Neph2 in pontine nuclei formation in the developing hindbrain. *Molecular and Cellular Neuroscience* 46, 662–670. doi:10.1016/j.mcn.2011.01.007.

Noordermeer, D., Leleu, M., Splinter, E., Rougemont, J., De Laat, W., and Duboule, D. (2011). The dynamic architecture of Hox gene clusters. Science *334*, 222-225.

Nonchev, S., Maconochie, M., Vesque, C., Aparicio, S., Ariza-McNaughton, L., Manzanares, M., Maruthainar, K., Kuroiwa, A., Brenner, S., Charnay, P.*, et al.* (1996a). The conserved role of Krox-20 in directing Hox gene expression during vertebrate hindbrain segmentation. Proc Natl Acad Sci U S A *93*, 9339-9345.

Nonchev, S., Vesque, C., Maconochie, M., Seitanidou, T., Ariza-McNaughton, L., Frain, M., Marshall, H., Sham, M.H., Krumlauf, R., and Charnay, P. (1996b). Segmental expression of Hoxa-2 in the hindbrain is directly regulated by Krox-20. Development *122*, 543-554.

O'Leary, D. D. M., Chou, S.-J., and Sahara, S. (2007). Area Patterning of the Mammalian Cortex. *Neuron* 56, 252–269. doi:10.1016/j.neuron.2007.10.010.

O'Leary, D.D., Heffner, C.D., Kutka, L., Lopez-Mascaraque, L., Missias, A., and Reinoso, B.S. (1991). A target-derived chemoattractant controls the development of the corticopontine projection by a novel mechanism of axon targeting. Dev Suppl *Suppl 2*, 123-130.

O'Leary, D.D., and Terashima, T. (1988). Cortical axons branch to multiple subcortical targets by interstitial axon budding: implications for target recognition and "waiting periods". Neuron *1*, 901-910.

Odeh, F., Ackerley, R., Bjaalie, J. G., and Apps, P. R. (2005). Pontine maps linking somatosensory and cerebellar cortices are in register with climbing fiber somatotopy. *Journal of Neuroscience* 25, 5680–5690. doi:10.1523/JNEUROSCI.0558-05.2005.

Okada, T., Keino-Masu, K., and Masu, M. (2007). Migration and nucleogenesis of mouse precerebellar neurons visualized by in utero electroporation of a green fluorescent protein gene. *Neuroscience Research* 57, 40–49. doi:10.1016/j.neures.2006.09.010.

Ono, S., Das, V. E., and Mustari, M. J. (2003). Role of the dorsolateral pontine nucleus in short-term adaptation of the horizontal vestibuloocular reflex. *J. Neurophysiol.* 89, 2879–2885. doi:10.1152/jn.00602.2002.

Ordonez-Moran, P., Dafflon, C., Imajo, M., Nishida, E., and Huelsken, J. (2015). HOXA5 Counteracts Stem Cell Traits by Inhibiting Wnt Signaling in Colorectal Cancer. Cancer Cell *28*, 815-829.

Osakada, F., and Callaway, E.M. (2013). Design and generation of recombinant rabies virus vectors. Nat Protoc *8*, 1583-1601.

Oury, F., Murakami, Y., Renaud, J.-S., Pasqualetti, M., Charnay, P., Ren, S.-Y., et al. (2006). Hoxa2- and Rhombomere-Dependent Development of the Mouse Facial Somatosensory Map. *Science* 313, 1408–1413. doi:10.1126/science.1130042.

Ozaki, M., Tohyama, K., Kishida, H., Buonanno, A., Yano, R., and Hashikawa, T. (2000). Roles of neuregulin in synaptogenesis between mossy fibers and cerebellar granule cells. *Journal of Neuroscience Research* 59, 612–623. doi:10.1002/(SICI)1097-4547(20000301)59:5<612::AID-JNR4>3.0.CO;2-V.

Packer, A.I., Crotty, D.A., Elwell, V.A., and Wolgemuth, D.J. (1998). Expression of the murine Hoxa4 gene requires both autoregulation and a conserved retinoic acid response element. Development *125*, 1991-1998.

Pasini, A., Henrique, D., and Wilkinson, D.G. (2001). The zebrafish Hairy/Enhancer-of-split-related gene her6 is segmentally expressed during the early development of hindbrain and somites. Mech Dev *100*, 317-321.

Palstra, R.J., Tolhuis, B., Splinter, E., Nijmeijer, R., Grosveld, F., and de Laat, W. (2003). The beta-globin nuclear compartment in development and erythroid differentiation. Nat Genet *35*, 190-194.

Panto, M.R., Cicirata, F., Angaut, P., Parenti, R., and Serapide, F. (1995). The projection from the primary motor and somatic sensory cortex to the basilar pontine nuclei. A detailed electrophysiological and anatomical study in the rat. J Hirnforsch *36*, 7-19.

Park, D.H., Hong, S.J., Salinas, R.D., Liu, S.J., Sun, S.W., Sgualdino, J., Testa, G., Matzuk, M.M., Iwamori, N., and Lim, D.A. (2014). Activation of neuronal gene expression by the JMJD3 demethylase is required for postnatal and adult brain neurogenesis. Cell Rep *8*, 1290-1299.

Pata, I., Studer, M., van Doorninck, J.H., Briscoe, J., Kuuse, S., Engel, J.D., Grosveld, F., and Karis, A. (1999). The transcription factor GATA3 is a downstream effector of Hoxb1 specification in rhombomere 4. Development *126*, 5523-5531.

Patel, N.S., Rhinn, M., Semprich, C.I., Halley, P.A., Dolle, P., Bickmore, W.A., and Storey, K.G. (2013). FGF signalling regulates chromatin organisation during neural differentiation via mechanisms that can be uncoupled from transcription. PLoS Genet *9*, e1003614.

Pattyn, A., Vallstedt, A., Dias, J.M., Samad, O.A., Krumlauf, R., Rijli, F.M., Brunet, J.F., and Ericson, J. (2003). Coordinated temporal and spatial control of motor neuron and serotonergic neuron generation from a common pool of CNS progenitors. Genes Dev *17*, 729-737.

Paxinos, G. (2014). *The Rat Nervous System*. Academic Press.

Penn, A.A., and Shatz, C.J. (1999). Brain waves and brain wiring: the role of endogenous and sensory-driven neural activity in development. Pediatr Res *45*, 447-458.

Perales, M., Winer, J. A., and Prieto, J. J. (2006). Focal projections of cat auditory cortex to the pontine nuclei. *J. Comp. Neurol.* 497, 959–980. doi:10.1002/cne.20988.

Philippidou, P., and Dasen, J.S. (2013). Hox genes: choreographers in neural development, architects of circuit organization. Neuron *80*, 12-34.

Pierce, E. T. (1966). Histogenesis of the nuclei griseum pontis, corporis pontobulbaris and reticularis tegmenti pontis (Bechterew) in the mouse an autoradiographic study. *J. Comp. Neurol.* 126, 219–239. doi:10.1002/cne.901260205.

Popperl, H., Bienz, M., Studer, M., Chan, S.K., Aparicio, S., Brenner, S., Mann, R.S., and Krumlauf, R. (1995). Segmental expression of Hoxb-1 is controlled by a highly conserved autoregulatory loop dependent upon exd/pbx. Cell *81*, 1031-1042.

Porter, F.D., Drago, J., Xu, Y., Cheema, S.S., Wassif, C., Huang, S.P., Lee, E., Grinberg, A., Massalas, J.S., Bodine, D.*, et al.* (1997). Lhx2, a LIM homeobox gene, is required for eye, forebrain, and definitive erythrocyte development. Development *124*, 2935-2944.

Prince, V.E., Holley, S.A., Bally-Cuif, L., Prabhakaran, B., Oates, A.C., Ho, R.K., and Vogt, T.F. (2001). Zebrafish lunatic fringe demarcates segmental boundaries. Mech Dev *105*, 175-180.

Puschendorf, M., Terranova, R., Boutsma, E., Mao, X., Isono, K., Brykczynska, U., Kolb, C., Otte, A.P., Koseki, H., Orkin, S.H.*, et al.* (2008). PRC1 and Suv39h specify parental asymmetry at constitutive heterochromatin in early mouse embryos. Nat Genet *40*, 411-420.

Qu, Q., Crandall, J. E., Luo, T., McCaffery, P. J., and Smith, F. I. (2006). Defects in tangential neuronal migration of pontine nuclei neurons in the Largemyd mouse are associated with stalled migration in the ventrolateral hindbrain. *Eur. J. Neurosci.* 23, 2877–2886. doi:10.1111/j.1460-9568.2006.04836.x.

Rabacchi, S. A., Kruk, B., Hamilton, J., Carney, C., Hoffman, J. R., Meyer, S. L., et al. (1999a). BDNF and NT4/5 promote survival and neurite outgrowth of pontocerebellar mossy fiber neurons. *J. Neurobiol.* 40, 254–269. doi:10.1002/(SICI)1097-4695(199908)40:2<254::AID-NEU11>3.0.CO;2-4.

Rabacchi, S. A., Solowska, J. M., Kruk, B., Luo, Y., Raper, J. A., and Baird, D. H. (1999b). Collapsin-1/semaphorin-III/D is regulated developmentally in Purkinje cells and collapses pontocerebellar mossy fiber neuronal growth cones. *Journal of Neuroscience* 19, 4437–4448. doi:10.1016/0925-4773(96)00525-4.

Ramadoss, S., Chen, X., and Wang, C.Y. (2012). Histone demethylase KDM6B promotes epithelial-mesenchymal transition. J Biol Chem *287*, 44508-44517.

Rakic, P. (2009). Evolution of the neocortex: a perspective from developmental biology. *Nat. Rev. Neurosci.* 10, 724–735. doi:10.1038/nrn2719.

Ray, R. S., and Dymecki, S. M. (2009). Rautenlippe Redux—toward a unified view of the precerebellar rhombic lip. *Curr. Opin. Cell Biol.* 21, 741–747. doi:10.1016/j.ceb.2009.10.003.

Renier, N., Schonewille, M., Giraudet, F., Badura, A., Tessier-Lavigne, M., Avan, P., et al. (2010). Genetic Dissection of the Function of Hindbrain Axonal Commissures. *PLoS Biol.* 8, e1000325. doi:10.1371/journal.pbio.1000325.

Riyadh, M. A., Shinmyo, Y., Ohta, K., and Tanaka, H. (2014). Inhibitory effects of draxin on axonal outgrowth and migration of precerebellar neurons. *Biochemical and Biophysical Research Communications* 449, 169–174. doi:10.1016/j.bbrc.2014.05.013.

Rodriguez, C. I., and Dymecki, S. M. (2000). Origin of the Precerebellar System. *Neuron* 27, 475–486. doi:10.1016/S0896-6273(00)00059-3.

Rodriguez, C.I., Buchholz, F., Galloway, J., Sequerra, R., Kasper, J., Ayala, R., Stewart, A.F., and Dymecki, S.M. (2000). High-efficiency deleter mice show that FLPe is an alternative to Cre-loxP. Nat Genet *25*, 139-140.

Rose, M.F., Ren, J., Ahmad, K.A., Chao, H.T., Klisch, T.J., Flora, A., Greer, J.J., and Zoghbi, H.Y. (2009). Math1 is essential for the development of hindbrain neurons critical for perinatal breathing. Neuron *64*, 341-354.

Rosina, A., and Provini, L. (1984). Pontocerebellar system linking the two hemispheres by intracerebellar branching. Brain Res *296*, 365-369.

Rossel, M., and Capecchi, M.R. (1999). Mice mutant for both Hoxa1 and Hoxb1 show extensive remodeling of the hindbrain and defects in craniofacial development. Development *126*, 5027-5040.

Rossant, J., Zirngibl, R., Cado, D., Shago, M., and Giguere, V. (1991). Expression of a retinoic acid response element-hsplacZ transgene defines specific domains of transcriptional activity during mouse embryogenesis. Genes Dev *5*, 1333-1344.

Rousseau, M., Crutchley, J.L., Miura, H., Suderman, M., Blanchette, M., and Dostie, J. (2014). Hox in motion: tracking HoxA cluster conformation during differentiation. Nucleic Acids Res *42*, 1524-1540.
Ruiz i Altaba, A., and Melton, D.A. (1989). Interaction between peptide growth factors and homoeobox genes in the establishment of antero-posterior polarity in frog embryos. Nature *341*, 33-38.

Sakai, Y., Meno, C., Fujii, H., Nishino, J., Shiratori, H., Saijoh, Y., Rossant, J., and Hamada, H. (2001). The retinoic acid-inactivating enzyme CYP26 is essential for establishing an uneven distribution of retinoic acid along the anterio-posterior axis within the mouse embryo. Genes Dev *15*, 213-225.

Salinas, P.C., and Zou, Y. (2008). Wnt signaling in neural circuit assembly. Annu Rev Neurosci *31*, 339-358.

Santagati, F., Minoux, M., Ren, S.Y., and Rijli, F.M. (2005). Temporal requirement of Hoxa2 in cranial neural crest skeletal morphogenesis. Development *132*, 4927-4936.

Schneider-Maunoury, S., Seitanidou, T., Charnay, P., and Lumsden, A. (1997). Segmental and neuronal architecture of the hindbrain of Krox-20 mouse mutants. Development *124*, 1215-1226.

Schmid, T., Krüger, M., and Braun, T. (2007). NSCL-1 and -2 control the formation of precerebellar nuclei by orchestrating the migration of neuronal precursor cells. *J Neurochem* 102, 2061–2072. doi:10.1111/j.1471-4159.2007.04694.x.

Schwarz, C., and Thier, P. (1995). Modular organization of the pontine nuclei: dendritic fields of identified pontine projection neurons in the rat respect the borders of cortical afferent fields. *Journal of Neuroscience* 15, 3475–3489. Available at: http://www.jneurosci.org/content/15/5/3475.full.

Schwarz, C., and Thier, P. (1999). Binding of signals relevant for action: towards a hypothesis of the functional role of the pontine nuclei. *Trends in Neurosciences* 22, 443–451. doi:10.1016/S0166-2236(99)01446-0.

Schwarz, C., Schwarz, C., Thier, P., and Thier, P. (1996). Comparison of projection neurons in the pontine nuclei and the nucleus reticularis tegmenti pontis of the rat. *J. Comp. Neurol.* 376, 403–419. doi:10.1002/(SICI)1096-9861(19961216)376:3<403::AID-CNE4>3.0.CO;2-6.

Schwarz, C., Horowski, A., Mock, M., and Thier, P. (2005). Organization of tectopontine terminals within the pontine nuclei of the rat and their spatial relationship to terminals from the visual and somatosensory cortex. J Comp Neurol *484*, 283-298.

Seidler, B., Schmidt, A., Mayr, U., Nakhai, H., Schmid, R.M., Schneider, G., and Saur, D. (2008). A Cre-loxP-based mouse model for conditional somatic gene expression and knockdown in vivo by using avian retroviral vectors. Proc Natl Acad Sci U S A *105*, 10137-10142.

Serafini, T., Colamarino, S.A., Leonardo, E.D., Wang, H., Beddington, R., Skarnes, W.C., and Tessier-Lavigne, M. (1996). Netrin-1 is required for commissural axon guidance in the developing vertebrate nervous system. Cell *87*, 1001-1014.

Serafini, T., Kennedy, T.E., Galko, M.J., Mirzayan, C., Jessell, T.M., and Tessier-Lavigne, M. (1994). The netrins define a family of axon outgrowth-promoting proteins homologous to C. elegans UNC-6. Cell *78*, 409-424.

Sham, M.H., Vesque, C., Nonchev, S., Marshall, H., Frain, M., Gupta, R.D., Whiting, J., Wilkinson, D., Charnay, P., and Krumlauf, R. (1993). The zinc finger gene Krox20 regulates HoxB2 (Hox2.8) during hindbrain segmentation. Cell *72*, 183-196.

Shambes, G.M., Gibson, J.M., and Welker, W. (1978). Fractured somatotopy in granule cell tactile areas of rat cerebellar hemispheres revealed by micromapping. Brain Behav Evol *15*, 94-140.

Shen, K., and Cowan, C.W. (2010). Guidance molecules in synapse formation and plasticity. Cold Spring Harb Perspect Biol *2*, a001842.

Shinohara, M., Zhu, Y., and Murakami, F. (2013). Four-dimensional analysis of nucleogenesis of the pontine nucleus in the hindbrain. *J. Comp. Neurol.* 521, 3340–3357. doi:10.1002/cne.23353.

Simon, H., and Lumsden, A. (1993). Rhombomere-specific origin of the contralateral vestibulo-acoustic efferent neurons and their migration across the embryonic midline. Neuron *11*, 209-220.

Solowska, J. M., Mazurek, A., Weinberger, L., and Baird, D. H. (2002). Pontocerebellar axon guidance: neuropilin-1- and semaphorin 3A-sensitivity gradients across basilar pontine nuclei and semaphorin 3A variation across cerebellum. *Mol. Cell. Neurosci.* 21, 266–284. doi:10.1006/mcne.2002.1187.

Sotelo, C. (2004). Cellular and genetic regulation of the development of the cerebellar system. Prog Neurobiol *72*, 295-339.

Sotelo, C., and Chedotal, A. (2013). Hindbrain tangential migration. *Cellular Migration and Formation of Neuronal Connections*. doi:10.1016/B978-0-12-397266-8.00032-6.

Stanfield, B.B., and O'Leary, D.D. (1985). The transient corticospinal projection from the occipital cortex during the postnatal development of the rat. J Comp Neurol *238*, 236-248.

Studer, M., Gavalas, A., Marshall, H., Ariza-McNaughton, L., Rijli, F.M., Chambon, P., and Krumlauf, R. (1998). Genetic interactions between Hoxa1 and Hoxb1 reveal new roles in regulation of early hindbrain patterning. Development *125*, 1025-1036.

Studer, M., Lumsden, A., Ariza-McNaughton, L., Bradley, A., and Krumlauf, R. (1996). Altered segmental identity and abnormal migration of motor neurons in mice lacking Hoxb-1. Nature *384*, 630-634.

Sultan, F., and Glickstein, M. (2007). The cerebellum: Comparative and animal studies. *The Cerebellum* 6, 168–176. doi:10.1080/14734220701332486.

Surmeli, G., Akay, T., Ippolito, G.C., Tucker, P.W., and Jessell, T.M. (2011). Patterns of spinal sensory-motor connectivity prescribed by a dorsoventral positional template. Cell *147*, 653-665.

Swenson, R.S., Kosinski, R.J., and Castro, A.J. (1984). Topography of spinal, dorsal column nuclear, and spinal trigeminal projections to the pontine gray in rats. J Comp Neurol *222*, 301-311.

Taneja, R., Thisse, B., Rijli, F.M., Thisse, C., Bouillet, P., Dolle, P., and Chambon, P. (1996). The expression pattern of the mouse receptor tyrosine kinase gene MDK1 is conserved through evolution and requires Hoxa-2 for rhombomere-specific expression in mouse embryos. Dev Biol *177*, 397-412.

Taniguchi, H., Kawauchi, D., Nishida, K., and Murakami, F. (2006). Classic cadherins

regulate tangential migration of precerebellar neurons in the caudal hindbrain. *Development* 133, 1923–1931. doi:10.1242/dev.02354.

Terenzi, M.G., Zagon, A., and Roberts, M.H. (1995). Efferent connections from the anterior pretectal nucleus to the diencephalon and mesencephalon in the rat. Brain Res *701*, 183-191.

Testa, G., Schaft, J., van der Hoeven, F., Glaser, S., Anastassiadis, K., Zhang, Y., Hermann, T., Stremmel, W., and Stewart, A.F. (2004). A reliable lacZ expression reporter cassette for multipurpose, knockout-first alleles. Genesis *38*, 151-158.

Theil, T., Frain, M., Gilardi-Hebenstreit, P., Flenniken, A., Charnay, P., and Wilkinson, D.G. (1998). Segmental expression of the EphA4 (Sek-1) receptor tyrosine kinase in the hindbrain is under direct transcriptional control of Krox-20. Development *125*, 443-452.

Theveneau, E., and Mayor, R. (2012). Neural crest delamination and migration: from epithelium-to-mesenchyme transition to collective cell migration. *Dev. Biol.* 366, 34–54. doi:10.1016/j.ydbio.2011.12.041.

Thielert, C. D., and Thier, P. (1993). Patterns of projections from the pontine nuclei and the nucleus reticularis tegmenti pontis to the posterior vermis in the rhesus monkey: A study using retrograde tracers. *J. Comp. Neurol.* 337, 113–126. doi:10.1002/cne.903370108.

Thier, P., and Möck, M. (2006). The oculomotor role of the pontine nuclei and the nucleus reticularis tegmenti pontis. *Prog. Brain Res.* 151, 293–320. doi:10.1016/S0079-6123(05)51010-0.

Thier, P., Koehler, W., and Buettner, U. W. (1988). Neuronal activity in the dorsolateral pontine nucleus of the alert monkey modulated by visual stimuli and eye movements. *Exp Brain Res* 70, 496–512. doi:10.1007/BF00247598.

Tomás-Roca, L., Corral-San-Miguel, R., Aroca, P., Puelles, L., and Marín, F. (2016). Crypto-rhombomeres of the mouse medulla oblongata, defined by molecular and morphological features. *Brain Struct Funct* 221, 815–838. doi:10.1007/s00429-014-0938-y.

Tran, T.S., Kolodkin, A.L., and Bharadwaj, R. (2007). Semaphorin regulation of cellular morphology. Annu Rev Cell Dev Biol *23*, 263-292.

Tripodi, M., Stepien, A.E., and Arber, S. (2011). Motor antagonism exposed by spatial segregation and timing of neurogenesis. Nature *479*, 61-66.
Tumpel, S., Wiedemann, L.M., and Krumlauf, R. (2009). Hox genes and segmentation of the vertebrate hindbrain. Curr Top Dev Biol *88*, 103-137.

Tziridis, K., Dicke, P. W., and Thier, P. (2009). The Role of the Monkey Dorsal Pontine Nuclei in Goal-Directed Eye and Hand Movements. *Journal of Neuroscience* 29, 6154–6166. doi:10.1523/JNEUROSCI.0581-09.2009.

Tziridis, K., Dicke, P. W., and Thier, P. (2012). Pontine reference frames for the sensory guidance of movement. *Cereb. Cortex* 22, 345–362. doi:10.1093/cercor/bhr109.

van de Werken, H.J., Landan, G., Holwerda, S.J., Hoichman, M., Klous, P., Chachik, R., Splinter, E., Valdes-Quezada, C., Oz, Y., Bouwman, B.A.*, et al.* (2012). Robust 4C-seq data analysis to screen for regulatory DNA interactions. Nat Methods *9*, 969-972.

Vesque, C., Maconochie, M., Nonchev, S., Ariza-McNaughton, L., Kuroiwa, A., Charnay, P., and Krumlauf, R. (1996). Hoxb-2 transcriptional activation in rhombomeres 3 and 5 requires an evolutionarily conserved cis-acting element in addition to the Krox-20 binding site. EMBO J *15*, 5383-5396.

Voiculescu, O., Taillebourg, E., Pujades, C., Kress, C., Buart, S., Charnay, P., and Schneider-Maunoury, S. (2001). Hindbrain patterning: Krox20 couples segmentation and specification of regional identity. Development *128*, 4967-4978.

Walshe, J., Maroon, H., McGonnell, I.M., Dickson, C., and Mason, I. (2002). Establishment of hindbrain segmental identity requires signaling by FGF3 and FGF8. Curr Biol *12*, 1117-1123.

Wandell, B.A., and Winawer, J. (2011). Imaging retinotopic maps in the human brain. Vision Res *51*, 718-737.

Wang, K.H., Brose, K., Arnott, D., Kidd, T., Goodman, C.S., Henzel, W., and Tessier-Lavigne, M. (1999). Biochemical purification of a mammalian slit protein as a positive regulator of sensory axon elongation and branching. Cell *96*, 771-784.

Wang, V. Y., Rose, M. F., and Zoghbi, H. Y. (2005). Math1 Expression Redefines the Rhombic Lip Derivatives and Reveals Novel Lineages within the Brainstem and Cerebellum. *Neuron* 48, 31–43. doi:10.1016/j.neuron.2005.08.024.

Wang, Z., Han, N., Racey, P. A., Ru, B., and He, G. (2010). A comparative study of prenatal development in Miniopterus schreibersii fuliginosus, Hipposideros armiger and H. pratti. *BMC Dev. Biol.* 10, 10. doi:10.1186/1471-213X-10-10.

Warming, S., Costantino, N., Court, D.L., Jenkins, N.A., and Copeland, N.G. (2005). Simple and highly efficient BAC recombineering using galK selection. Nucleic Acids Res *33*, e36.

Watanabe, H., and Murakami, F. (2009). Real time analysis of pontine neurons during initial stages of nucleogenesis. *Neuroscience Research* 64, 20–29. doi:10.1016/j.neures.2009.01.007.

Watari, N., Kameda, Y., Takeichi, M., and Chisaka, O. (2001). Hoxa3 regulates integration of glossopharyngeal nerve precursor cells. Dev Biol *240*, 15-31.

Wickersham, I. R., Lyon, D. C., Barnard, R. J. O., Mori, T., Finke, S., Conzelmann, K.-K., et al. (2007). Monosynaptic restriction of transsynaptic tracing from single, genetically targeted neurons. *Neuron* 53, 639–647. doi:10.1016/j.neuron.2007.01.033.

Wickersham, I.R., Sullivan, H.A., and Seung, H.S. (2010). Production of glycoprotein-deleted rabies viruses for monosynaptic tracing and high-level gene expression in neurons. Nat Protoc *5*, 595-606.

Wiesendanger, R., and Wiesendanger, M. (1982). The corticopontine system in the rat. I. Mapping of corticopontine neurons. J Comp Neurol *208*, 215-226.

Wilkinson, D.G., Bhatt, S., Cook, M., Boncinelli, E., and Krumlauf, R. (1989). Segmental expression of Hox-2 homoeobox-containing genes in the developing mouse hindbrain. Nature *341*, 405-409.

Wingate, R. (2005). Math-Map(ic)s. *Neuron* 48, 1–4. doi:10.1016/j.neuron.2005.09.012.

Wizenmann, A., and Lumsden, A. (1997). Segregation of rhombomeres by differential chemoaffinity. Mol Cell Neurosci *9*, 448-459.

Xu, Q., Mellitzer, G., Robinson, V., and Wilkinson, D.G. (1999). In vivo cell sorting in complementary segmental domains mediated by Eph receptors and ephrins. Nature *399*, 267-271.

Yamada, M., Seto, Y., Taya, S., Owa, T., Inoue, Y. U., Inoue, T., et al. (2014). Specification of spatial identities of cerebellar neuron progenitors by ptf1a and atoh1 for proper production of GABAergic and glutamatergic neurons. *J. Neurosci.* 34, 4786–4800. doi:10.1523/JNEUROSCI.2722-13.2014.

Yamada, M., Terao, M., Terashima, T., Fujiyama, T., Kawaguchi, Y., Nabeshima, Y.-I., et al. (2007). Origin of Climbing Fiber Neurons and Their Developmental Dependence on Ptf1a. 27, 10924–10934. doi:10.1523/JNEUROSCI.1423-07.2007.

Yamamoto, M., Fujinuma, M., Hirano, S., Hayakawa, Y., Clagett-Dame, M., Zhang, J., et al. (2005). Retinoic acid influences the development of the inferior olivary nucleus in the rodent. *Dev. Biol.* 280, 421–433. doi:10.1016/j.ydbio.2005.02.007.

Yamamoto, M., Zhang, J., Smith, D., Hayakawa, Y., and McCaffery, P. (2003). A critical period for retinoic acid teratogenesis and loss of neurophilic migration of pontine nuclei neurons. *Mech. Dev.* 120, 701–709. doi:10.1016/S0925-4773(03)00047-9.

Yazdani, U., and Terman, J.R. (2006). The semaphorins. Genome Biol *7*, 211.

Yoshikawa, S., McKinnon, R.D., Kokel, M., and Thomas, J.B. (2003). Wnt-mediated axon guidance via the Drosophila Derailed receptor. Nature *422*, 583-588.

Yee, K. T., Simon, H. H., Tessier-Lavigne, M., and O'Leary, D. D. M. (1999). Extension of Long Leading Processes and Neuronal Migration in the Mammalian Brain Directed by the Chemoattractant Netrin-1. *Neuron* 24, 607–622. doi:10.1016/S0896-6273(00)81116-2.

Zallen, J.A., Yi, B.A., and Bargmann, C.I. (1998). The conserved immunoglobulin superfamily member SAX-3/Robo directs multiple aspects of axon guidance in C. elegans. Cell *92*, 217-227.

Zelina, P., Blockus, H., Zagar, Y., Péres, A., Friocourt, F., Wu, Z., et al. (2014). Signaling Switch of the Axon Guidance Receptor Robo3 during Vertebrate Evolution. *Neuron* 84, 1258–1272. doi:10.1016/j.neuron.2014.11.004.

Zhang, F., Nagy Kovacs, E., and Featherstone, M.S. (2000). Murine hoxd4 expression in the CNS requires multiple elements including a retinoic acid response element. Mech Dev *96*, 79-89.

Zhang, L.I., and Poo, M.M. (2001). Electrical activity and development of neural circuits. Nat Neurosci *4 Suppl*, 1207-1214.

Zhang, M., Kim, H.J., Marshall, H., Gendron-Maguire, M., Lucas, D.A., Baron, A., Gudas, L.J., Gridley, T., Krumlauf, R., and Grippo, J.F. (1994). Ectopic Hoxa-1 induces rhombomere transformation in mouse hindbrain. Development *120*, 2431-2442.

Zhang, J., Smith, D., Yamamoto, M., Ma, L., and McCaffery, P. (2003). The meninges is a source of retinoic acid for the late-developing hindbrain. J Neurosci *23*, 7610-7620.

Zhu, Y., Matsumoto, T., Mikami, S., Nagasawa, T., and Murakami, F. (2009). SDF1/CXCR4 signalling regulates two distinct processes of precerebellar neuronal migration and its depletion leads to abnormal pontine nuclei formation. *Development* 136, 1919–1928. doi:10.1242/dev.032276.

# ACKNOWLEDGEMENTS

I would like to thank my Ph.D. supervisor Prof. Filippo Rijli for his guidance and support throughout these years. I would also like to thank him for believing in me, for enlightening discussions over the results, on scientific and non-scientific topics and for the freedom to perform all the experiments. I would like to thank my thesis committee members: Prof. Peter Scheiffele and Prof. Botond Roska for their helpful comments and suggestions.

I would like to express my gratitude to Nathalie Vilain and Sebastien Ducret, for their constant support, for being excellent colleagues and for always keeping me in happy mood.

I am grateful to all present members of Rijli lab, Maryline Minoux, Taro Kitazawa, Onkar Joshi, Yousra Ben Zuari, Leslie Bargsted, Dania Machlab, Sandra Kessler, Huanhuan Li, Guoliang Lyu as well as to past members, Thomas Di Meglio, Kajari Karmakar, Nicola Maiorano, Sjoerd Holwerda, Vanja Cankovic, Ahmad Bechara and Alberto Loche for all the scientific discussions, after lab drinks, for the fun time and for being wonderful people. Finally, I would like to thank Dominik Kraus for introducing me to the project and for being a great person to work with.

None of the presented work would have been possible without the great support provided by all the facilities at FMI, especially Steve, Laurent, Jan and Raphael from FAIM, members of animal facility, media kitchen, Augustyn and Sandrine from histology. A special thanks to Elida, for taking care of all administrative work and for being a wonderful listener, Gabi and Isabella for their great help with reservations and meeting registrations.

Last, but not the least, I would like to thank my husband for his constant support, my parents for being my strength my friends for keeping me on track and entertained and my mice for their sacrifice.

# CURRICULUM VITAE

**Upasana Maheshwari**
**Doctoral Student**
**Friedrich Miescher Institute for Biomedical Research, Basel, Switzerland**

## PERSONAL INFORMATION

| | |
|---|---|
| Address | Hammerstrasse 196, CH-4057 Basel |
| Telephone | +41 (0) 76 681 82 24 |
| E-Mail address | upasana.maheshwari@fmi.ch; 13.upasana@gmail.com |
| Date of birth | 13.10.1989 |
| Nationality | Indian |

## EDUCATION

2014-Present **Ph.D. in Neurobiology**
*Ph.D. Supervisor: Prof. Dr. F. M. Rijli, Friedrich Miescher Institute for Biomedical Research (FMI), Basel, Switzerland*
*Topic: "Role of Hox genes in sub-circuit diversification during cortico-ponto-cerebellar map formation."*
*Detailed summary attached*

2011-2014 **Masters in Biological Sciences**
*Masters Supervisor: Prof. Shubha Tole, Tata Institute for Fundamental Research (TIFR), Mumbai, India*
*Topic: "Cell fate specification in the developing cortex: Identifying the targets of Lhx2"*

2007-2010 **Bachelor in Science, Biological Science (Hons.)**
Sri Venkateswara College, University of Delhi, Delhi, India

## ADDITIONAL RESEARCH PROJECTS

Jan 2011- Mar 2011 Evaluation of phytochemical constituents, antibacterial activities, cytopathic and cytotoxic effects of extracts of indigenous plant species.
Institute of Biotechnology, G.B. Pant University, Uttarakhand, India

May 2009- Jun 2009 To synthesize Zinc Oxide (ZnO) nanoparticles by wet chemical route and to study their characteristics
Department of Physics, University of Delhi, Delhi, India

## PUBLICATIONS

- **Maheshwari U.***, Kraus D.*, Vilain N., Holwerda S. J. B., Cankovic V., Maiorano N., Kohler H., Satoh D., Sigrist M., Arber S., Kratochwil C. F., Meglio T. D., Ducret S., Rijli F. M. "Postmitotic *Hoxa5* expression specifies pontine neuron positional identity and input connectivity of cortical afferent subsets." (Manuscript accepted, *Cell Reports*). * Equal contribution.
- Coughlan E.*, Garside V.*, Wong S. F. L., Liang H., Kraus D., Karmakar K., **Maheshwari U.**, Rijli F. M., Bourne J., McGlinn E. A Hox code defines spinocerebellar neuron subtype regionalisation. ***bioRxiv***. doi: https://doi.org/10.1101/640243. (Manuscript under revision, *Cell Reports*). * Equal contribution.
- Muralidharan B., Keruzore M., Pradhan S. J., Roy B., Shetty A. S., Kinare V., D'Souza L., **Maheshwari U.**, Karmodiya K., Suresh A., Galande S., Bellefroid E. J., Tole S. "Dmrt5, a novel neurogenic factor, reciprocally regulates Lhx2 to control the neuron-glia cell-fate switch in the developing hippocampus." ***Journal of Neuroscience* (2017)**. doi:10.1523/JNEUROSCI.1535-17.2017
- Kratochwil C. F., **Maheshwari U.**, Rijli F. M. "The long journey of pontine nuclei neurons: from rhombic lip to cortico-ponto-cerebellar circuitry." ***Frontiers in Neural Circuits* (2017)**. doi: 10.3389/fncir.2017.00033
- Muralidharan B., Khatri Z., **Maheshwari U.**, Gupta R., Roy B., Pradhan S. J., Karmodiya K., Padmanabhan H., Shetty A. S., Balaji C., Kolthur-Seetharam U., Macklis J. D., Galande S., Tole S. "Lhx2 interacts with the NURD complex and regulates cortical neuron subtype determinants Fezf2 and Sox11." ***Journal of Neuroscience* (2017)**. doi:10.1523/JNEUROSCI.2836-16.2016
- Shetty A. S., Godbole G., **Maheshwari U.**, Padmanabhan H., Chaudhary R., Muralidharan B., Hou P. S., Monuki E. S., Kuo H. C., Rema V., Tole S. "Lhx2 regulates a cortex-specific mechanism for barrel formation." ***Proceedings of the National Academy of Science (USA)* (2013).** doi:10.1073/pnas.1311158110.
- Kannan D., Mehra R. S., Dubey S., Tiwari S., **Maheshwari U.**, Bisht V. S. "Evaluation of phytochemical constituents, antibacterial activities, cytopathic and cytotoxic effects of extracts of *Tylophora indica, Curcuma amada* and *Urtica dioica.*" ***Journal of Recent Advances in Applied Sciences* (2013).** 28:01-11

## PRESENTATIONS

- AMeeGus Ph.D. symposium, 27th-31st May 2017, Portugal. Poster presentation- Development of Cortico-ponto-cerebellar sensorimotor circuit.
- 21st Biennial meeting of the international society of developmental neuroscience (ISDN 2016), 11th-14th May 2016, France. Oral presentation- Development of the Cortico-ponto-cerebellar sensorimotor circuit.
- EMBO practical course on development neurobiology: from worms to mammals, 21st June- 4th July 2015, MRC London, United Kingdom. Poster presentation- Studying the development of the Cortico-ponto-cerebellar somatosensory circuit.
- Annual meeting of the Indian Society of Developmental Biologists, 1st-4th December 2013, India. Poster presentation- Understanding the mechanisms of cell fate determination in the developing cortex: Role of Lhx2.

## SCHOLARSHIPS

- Scholarship "International Ph.D. program" funded by Friedrich Miescher Institute for Biomedical Research, Basel, Switzerland.
- Scholarship "Masters in Biological Science program" funded by Tata Institute for Fundamental Research, Mumbai, India.